



University of
Zurich ^{UZH}



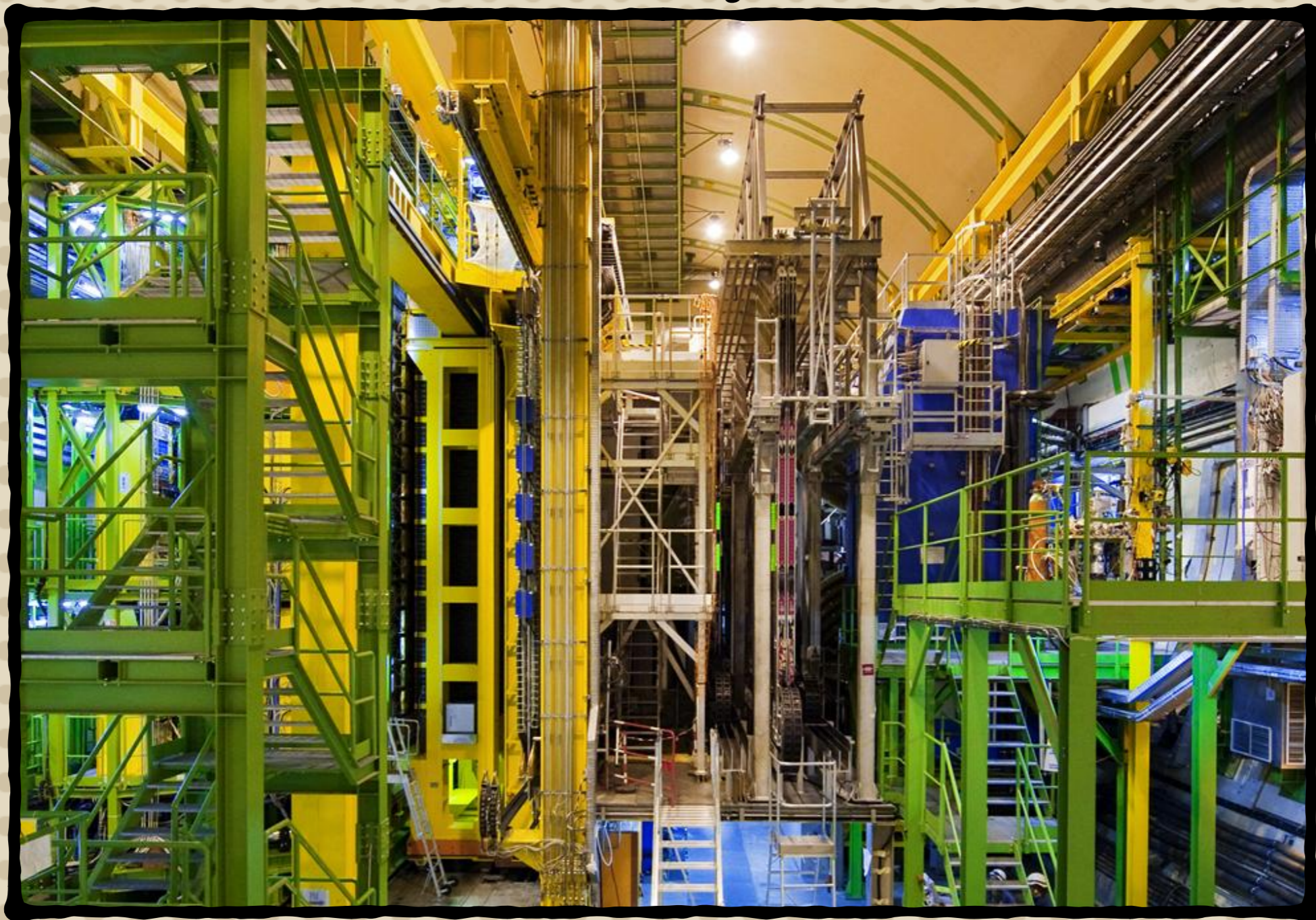
Flavour anomalies in b -hadron decays

Nico Serra
Universität Zürich

Università La Sapienza (Roma)
23 Maggio 2016

- **Introduction**
- **Flavour anomalies in $b \rightarrow sll$ transitions**
 - **Experimental measurements**
 - **Model independent interpretations**
 - **Lepton Flavour Universalities in $b \rightarrow sll$**
 - **Future Prospects**
- **Lepton Flavour Universality test in $b \rightarrow clv$**
 - **Experimental measurements**
 - **Model independent Interpretations**
 - **Future Prospects**

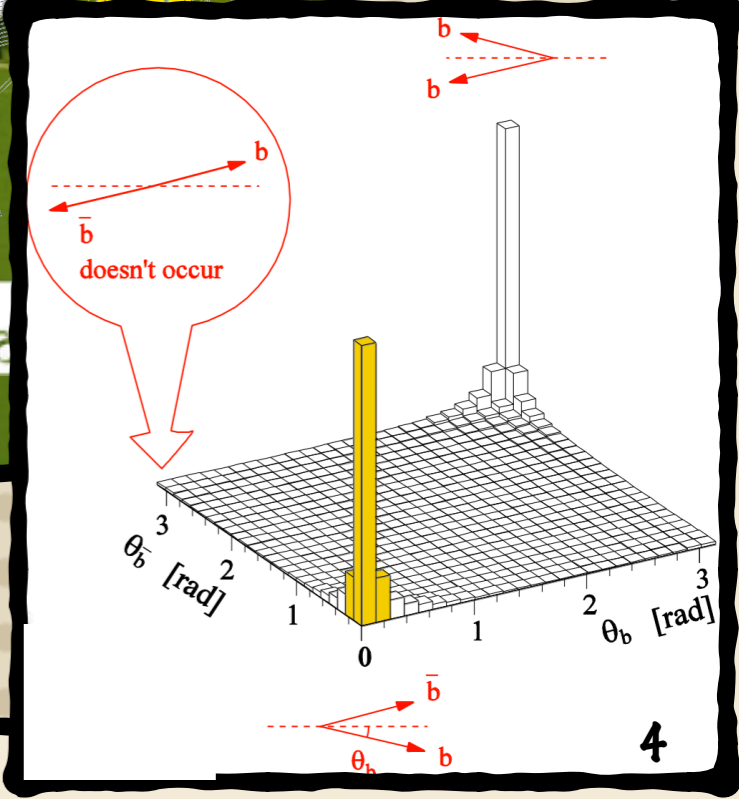
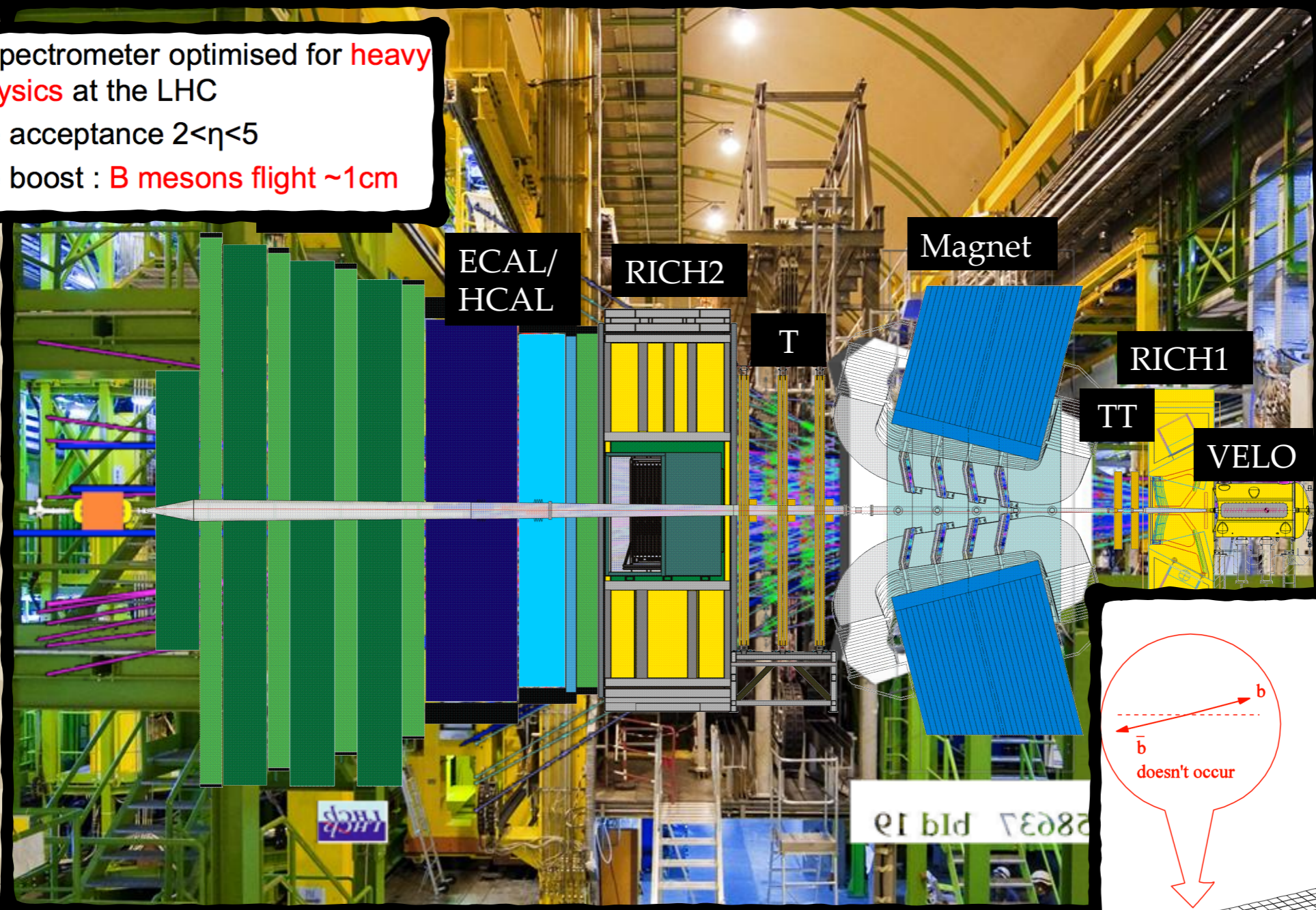
The LHCb experiment



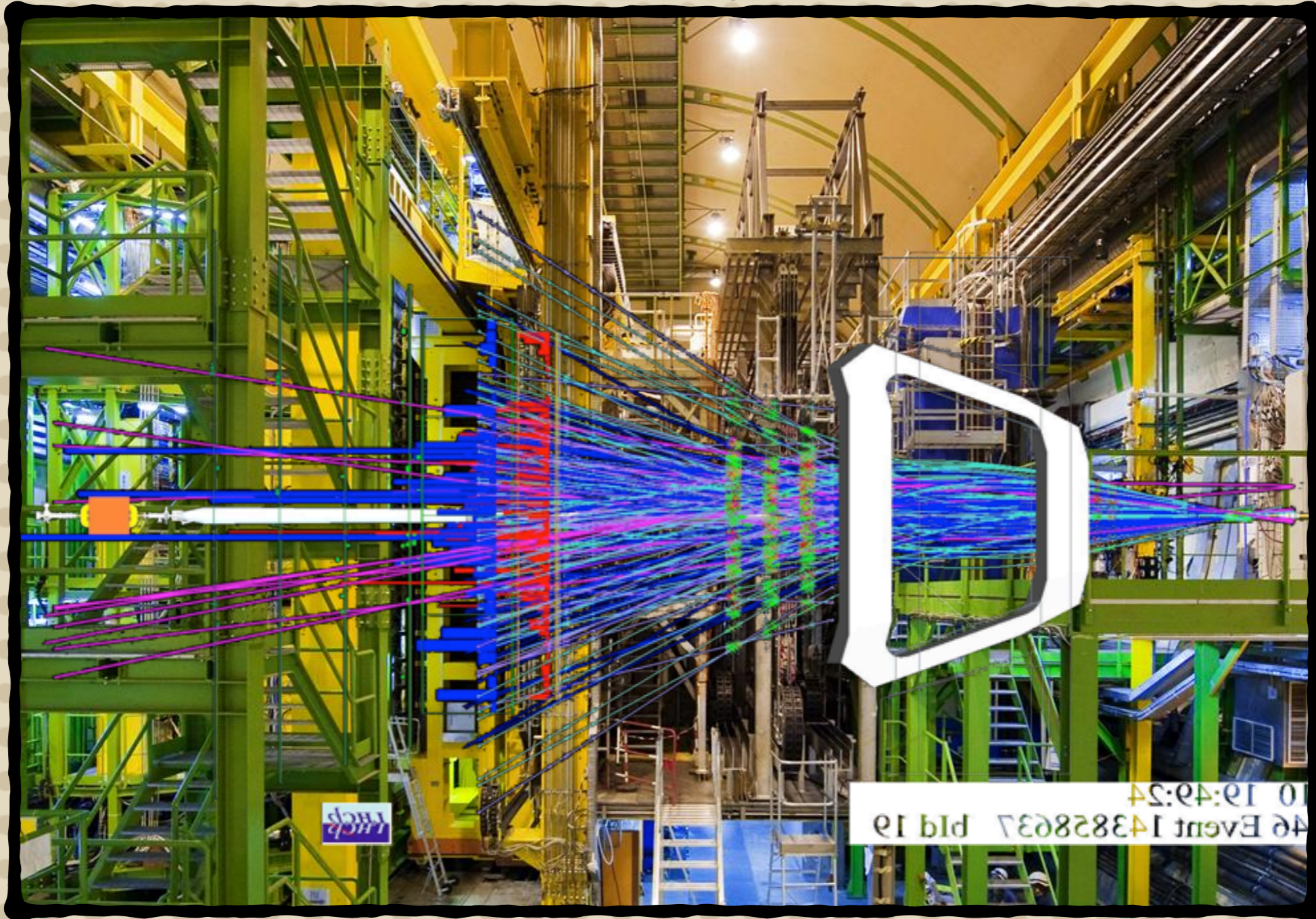
The LHCb experiment

Forward spectrometer optimised for **heavy flavour physics** at the LHC

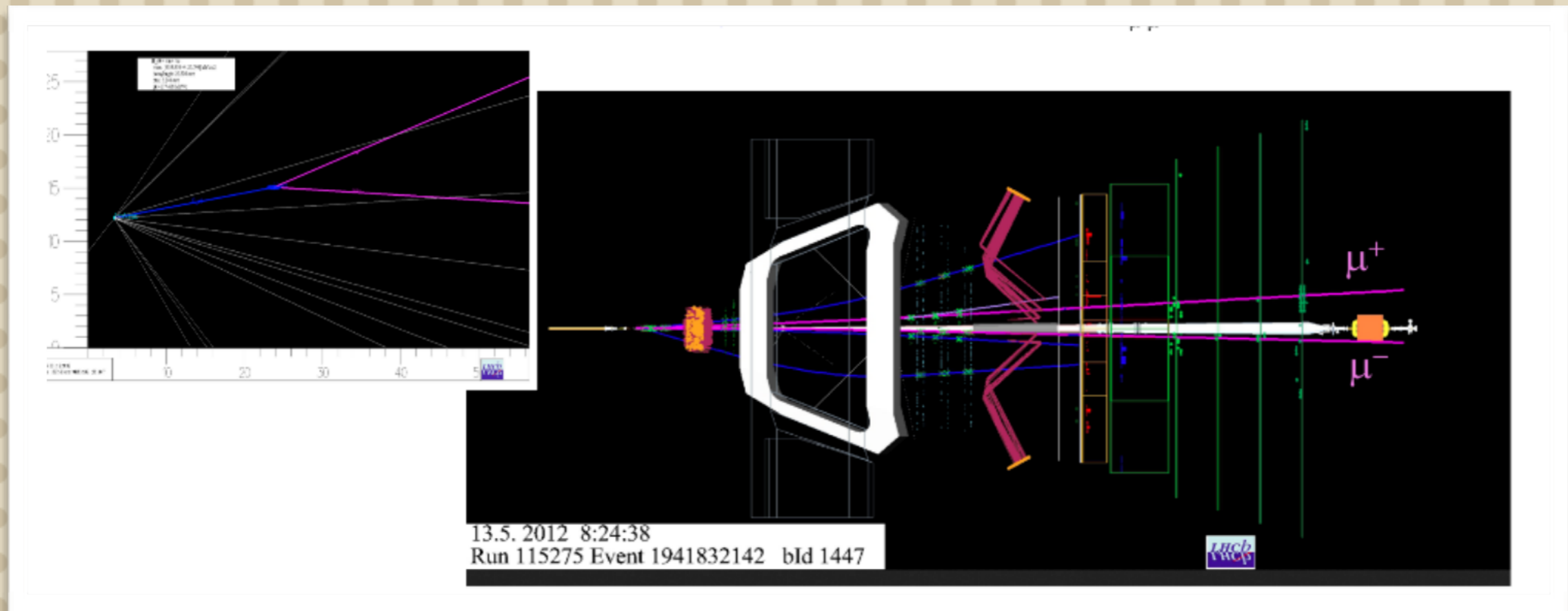
- Large acceptance $2 < \eta < 5$
- Large boost : **B mesons flight $\sim 1\text{cm}$**



The LHCb experiment



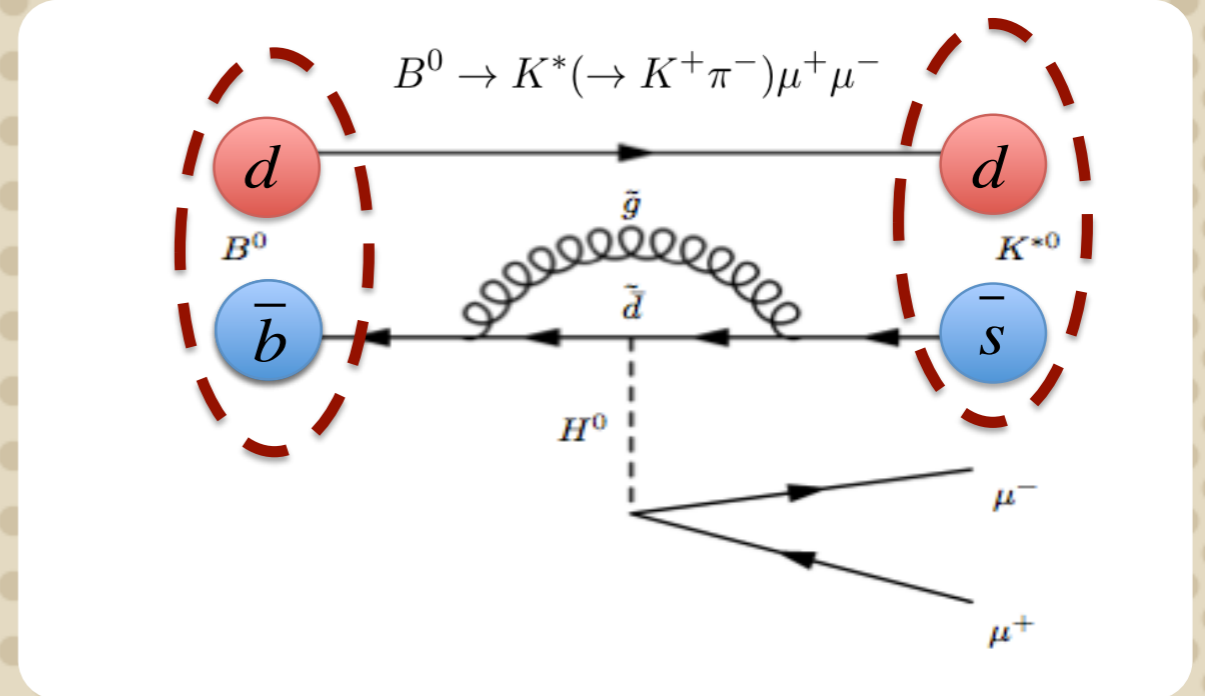
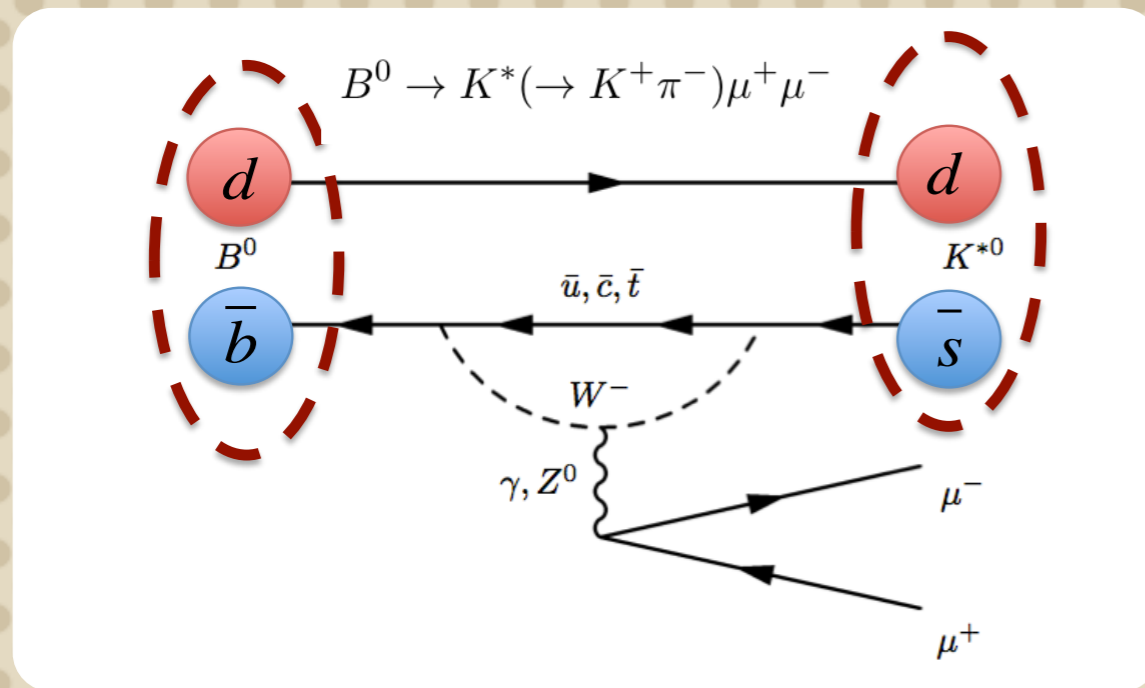
The LHCb experiment



Key features to identify b-hadron decays

- Secondary Vertex resolution (20 μ m IP resolution)
- Particle identification capabilities (1-3% $\pi \rightarrow \mu$ misID)
- Momentum Resolution ($\Delta p/p$ about 0.5%)

Weak Hamiltonian



- FCNC suppressed in the SM
- New heavy particle can contribute with competing diagrams

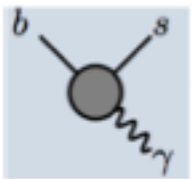
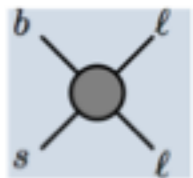
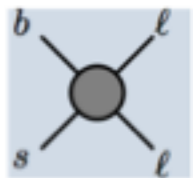
$$A(i \rightarrow f) = \langle f | H_{eff} | i \rangle = -\frac{4G_F}{\sqrt{2}} V_{tb} V_{ts}^* \sum_j (C_j \langle f | O_j | i \rangle + C'_j \langle f | O'_j | i \rangle) + \sum_i C_i^{NP} \langle f | O_i^{NP} | i \rangle$$

- C_i are short distance Wilson coefficients
- $\langle f | O_i | i \rangle$ long distance hadronization (form-factors)

Weak Hamiltonian

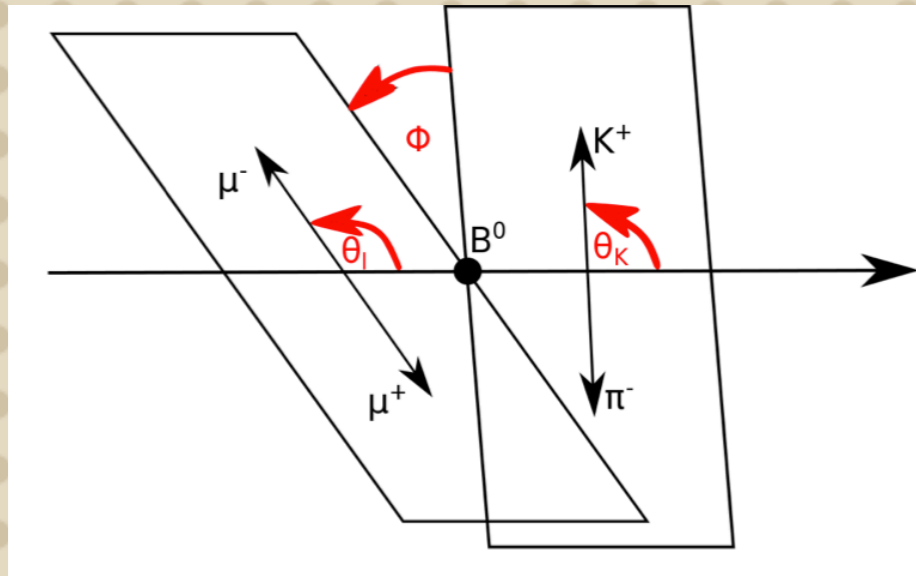
$$A(i \rightarrow f) = \langle f | H_{eff} | i \rangle = -\frac{4G_F}{\sqrt{2}} V_{tb} V_{ts}^* \sum_j (C_j \langle f | O_j | i \rangle + C'_j \langle f | O'_j | i \rangle) + \sum_i C_i^{NP} \langle f | O_i^{NP} | i \rangle$$

- Allows to separate short and long distance contributions
- Allows to classify the NP contributions
- Combine information from different decays

Operator O_i	$B \rightarrow K^{*0} \gamma$	$B \rightarrow K^{*0} \mu^+ \mu^-$	$B \rightarrow \mu^+ \mu^-$
 $O_7 \sim m_b (\bar{s}_L \sigma_{\mu\nu} b_R) F_{\mu\nu}$	✓	✓	
 $O_9 \sim (\bar{s} b)_{V-A} (\bar{l} l)_V$		✓	
 $O_{10} \sim (\bar{s} b)_{V-A} (\bar{l} l)_A$		✓	✓
$O_{S,P} \sim (\bar{s} b)_{S+P} (\bar{l} l)_{S,P}$			✓

Angular analysis of $B \rightarrow K^* \mu \mu$

The decay is described by three angles θ_ℓ , θ_K , ϕ and the dimuon invariant mass q^2



- Observables of interest:
 - F_L (longitudinal polarization fraction of the K^*)
 - The forward-backward asymmetry A_{FB}
 - The observables S_i
- Bilinear combination of the transversity amplitudes A_i
- Depend on Form-factors and Wilson coefficients

$$\frac{1}{\Gamma} \frac{d^3(\Gamma + \bar{\Gamma})}{d \cos \theta_\ell d \cos \theta_K d \phi} = \frac{9}{32\pi} \left[\frac{3}{4} (1 - F_L) \sin^2 \theta_K + F_L \cos^2 \theta_K + \frac{1}{4} (1 - F_L) \sin^2 \theta_K \cos 2\theta_\ell \right. \\ \left. - F_L \cos^2 \theta_K \cos 2\theta_\ell + S_3 \sin^2 \theta_K \sin^2 \theta_\ell \cos 2\phi + S_4 \sin 2\theta_K \sin 2\theta_\ell \cos \phi + \right. \\ \left. S_5 \sin 2\theta_K \sin \theta_\ell \cos \phi + \frac{4}{3} A_{FB} \sin^2 \theta_K \cos \theta_\ell + S_7 \sin 2\theta_K \sin \theta_\ell \sin \phi + \right. \\ \left. S_8 \sin 2\theta_K \sin 2\theta_\ell \sin \phi + S_9 \sin^2 \theta_K \sin^2 \theta_\ell \sin 2\phi \right]$$

Amplitudes

- The decay is described by six complex amplitudes $A_{0,\parallel,\perp}^{L,R}$
- Correspond to different transversity state of the K^*
- and different (left- and right-handed) chiralities of the dimuon system

$$F_L = \frac{A_0^2}{A_{\parallel}^2 + A_{\perp}^2 + A_0^2} = 1 - F_T$$

$$S_3 = \frac{1}{2} \frac{A_{\perp}^{L2} - A_{\parallel}^{L2}}{A_{\parallel}^2 + A_{\perp}^2 + A_0^2} + L \rightarrow R$$

$$S_4 = \frac{1}{\sqrt{2}} \frac{\Re(A_0^{L*} A_{\parallel}^L)}{A_{\parallel}^2 + A_{\perp}^2 + A_0^2} + L \rightarrow R$$

$$S_5 = \sqrt{2} \frac{\Re(A_0^{L*} A_{\perp}^L)}{A_{\parallel}^2 + A_{\perp}^2 + A_0^2} - L \rightarrow R$$

$$A_{FB} = \frac{8}{3} \frac{\Re(A_{\perp}^{L*} A_{\parallel}^L)}{A_{\parallel}^2 + A_{\perp}^2 + A_0^2} - L \rightarrow R$$

$$S_7 = \sqrt{2} \frac{\Im(A_0^{L*} A_{\parallel}^L)}{A_{\parallel}^2 + A_{\perp}^2 + A_0^2} + L \rightarrow R$$

$$S_8 = \frac{1}{\sqrt{2}} \frac{\Im(A_0^{L*} A_{\perp}^L)}{A_{\parallel}^2 + A_{\perp}^2 + A_0^2} + L \rightarrow R$$

$$S_9 = \frac{\Im(A_{\perp}^{L*} A_{\parallel}^L)}{A_{\parallel}^2 + A_{\perp}^2 + A_0^2} - L \rightarrow R$$

$$\bullet \Gamma = |A_{\parallel}|^2 + |A_0|^2 + |A_{\perp}|^2$$

• Let's see how the amplitudes depend on Wilson coefficients and form factors

Amplitudes

$$A_{\perp}^{L,R} \propto [(C_9^{eff} + C_9^{eff'}) \mp (C_{10}^{eff} + C_{10}^{eff'})] \frac{V(q^2)}{m_B + m_{K^*}} + \frac{2m_b}{q^2} (C_7^{eff} + C_7^{eff'}) T_1(q^2)$$

$$A_{\parallel}^{L,R} \propto [(C_9^{eff} - C_9^{eff'}) \mp (C_{10}^{eff} - C_{10}^{eff'})] \frac{A_1(q^2)}{m_B + m_{K^*}} + \frac{2m_b}{q^2} (C_7^{eff} - C_7^{eff'}) T_2(q^2)$$

$$A_0^{L,R} \propto [(C_9^{eff} - C_9^{eff'}) \mp (C_{10}^{eff} - C_{10}^{eff'})] \times [(m_B^2 - m_{K^*}^2 - q^2)(m_B + m_{K^*} A_1(q^2) - \lambda \frac{A_2(q^2)}{m_B + m_{K^*}})] +$$

$$2m_b (C_7^{eff} + C_7^{eff'}) [(m_B^2 + 3m_{K^*}^2 - q^2) T_2(q^2) - \frac{\lambda}{m_B^2 - m_{K^*}^2} T_3(q^2)]$$

"Clean" observables

At low q^2 and first order

$$A_0^{L,R} \propto [C_{9\mp 10}^+ A_{12} + C_7^+ T_{23}]$$

$$A_{\parallel}^{L,R} \propto [C_{9\mp 10}^- A_1 + C_7^- T_2]$$

$$A_{\perp}^{L,R} \propto [C_{9\mp 10}^- V + C_7^- T_1]$$

$$R_1 = \frac{T_1}{V} \sim 1$$

$$R_2 = \frac{T_2}{A_1} \sim 1$$

$$R_3 = \frac{T_{23}}{A_{12}} \sim \frac{q^2}{m_B^2}$$

$$A_{\perp}^{L,R} = \sqrt{2} N m_B (1 - \hat{s}) \left[(C_9^{\text{eff}} + C_9^{\text{eff}'}) \mp (C_{10} + C'_{10}) + \frac{2\hat{m}_b}{\hat{s}} (C_7^{\text{eff}} + C_7^{\text{eff}'}) \right] \xi_{\perp}(E_{K^*})$$

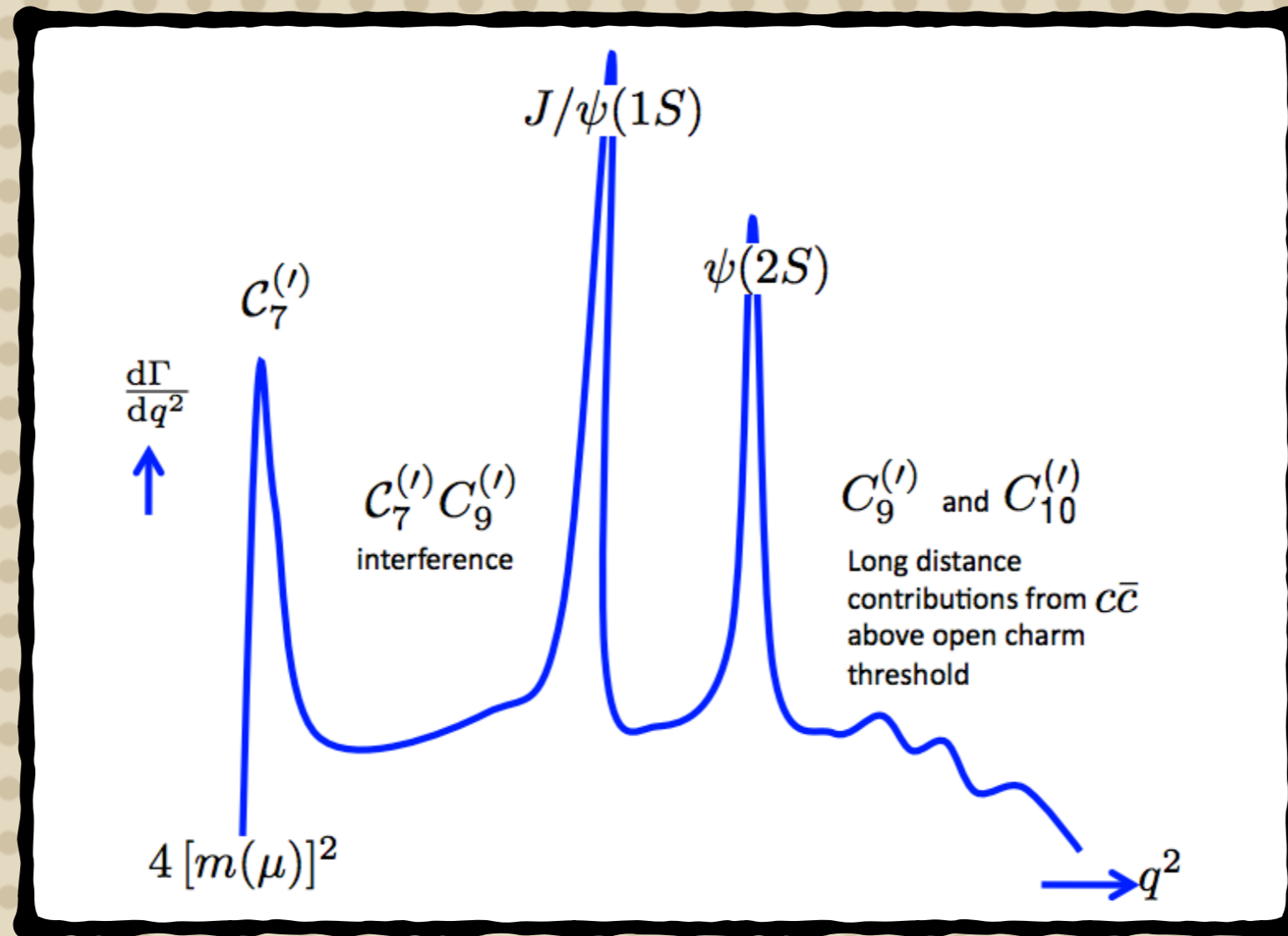
$$A_{\parallel}^{L,R} = -\sqrt{2} N m_B (1 - \hat{s}) \left[(C_9^{\text{eff}} - C_9^{\text{eff}'}) \mp (C_{10} - C'_{10}) + \frac{2\hat{m}_b}{\hat{s}} (C_7^{\text{eff}} - C_7^{\text{eff}'}) \right] \xi_{\perp}(E_{K^*})$$

$$A_0^{L,R} = -\frac{N m_B (1 - \hat{s})^2}{2\hat{m}_{K^*} \sqrt{\hat{s}}} \left[(C_9^{\text{eff}} - C_9^{\text{eff}'}) \mp (C_{10} - C'_{10}) + 2\hat{m}_b (C_7^{\text{eff}} - C_7^{\text{eff}'}) \right] \xi_{\parallel}(E_{K^*})$$

We now build ratios such that the same combination of FF appears in the numerator and in the denominator

$$P'_5 \propto \frac{\Re(A_0 A_{\perp})}{\sqrt{|A_0|^2 \times |A_{\perp}|^2}}$$

the q^2 distribution



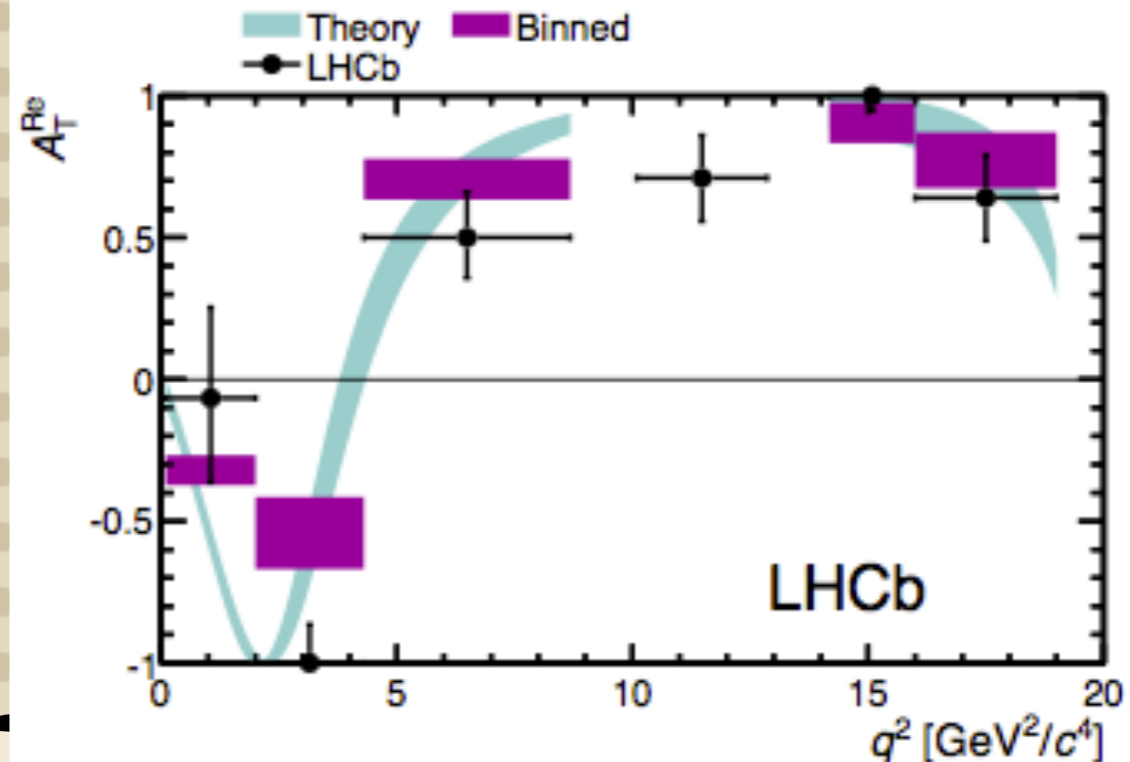
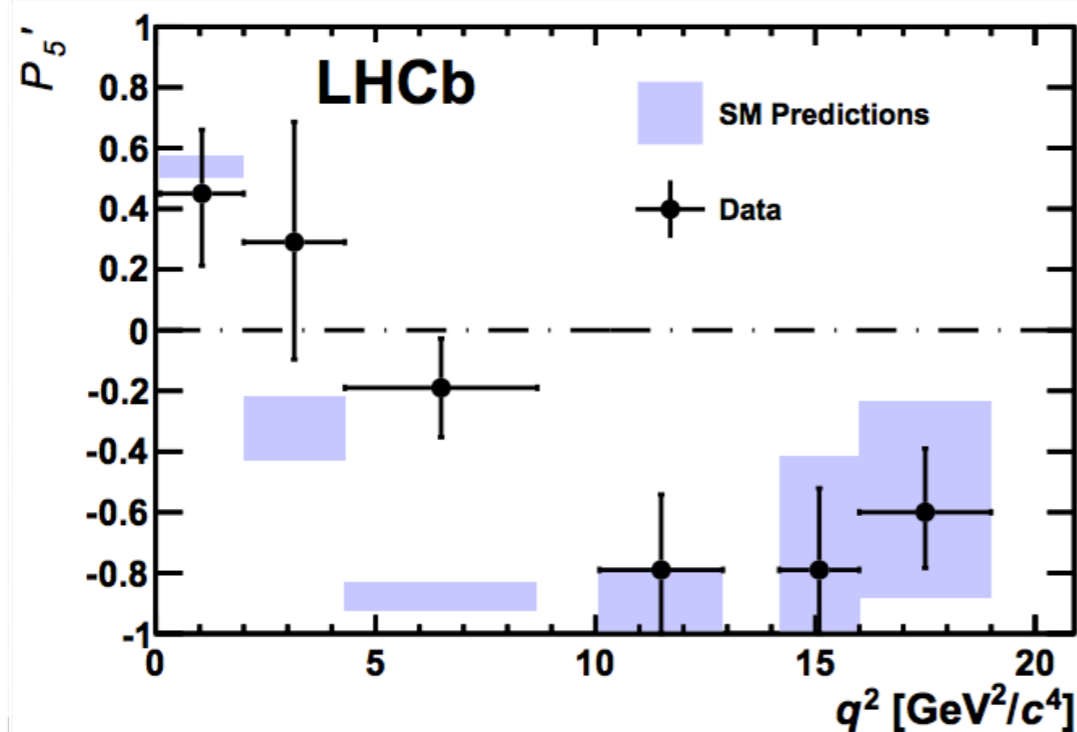
Analysis of 1fb^{-1}

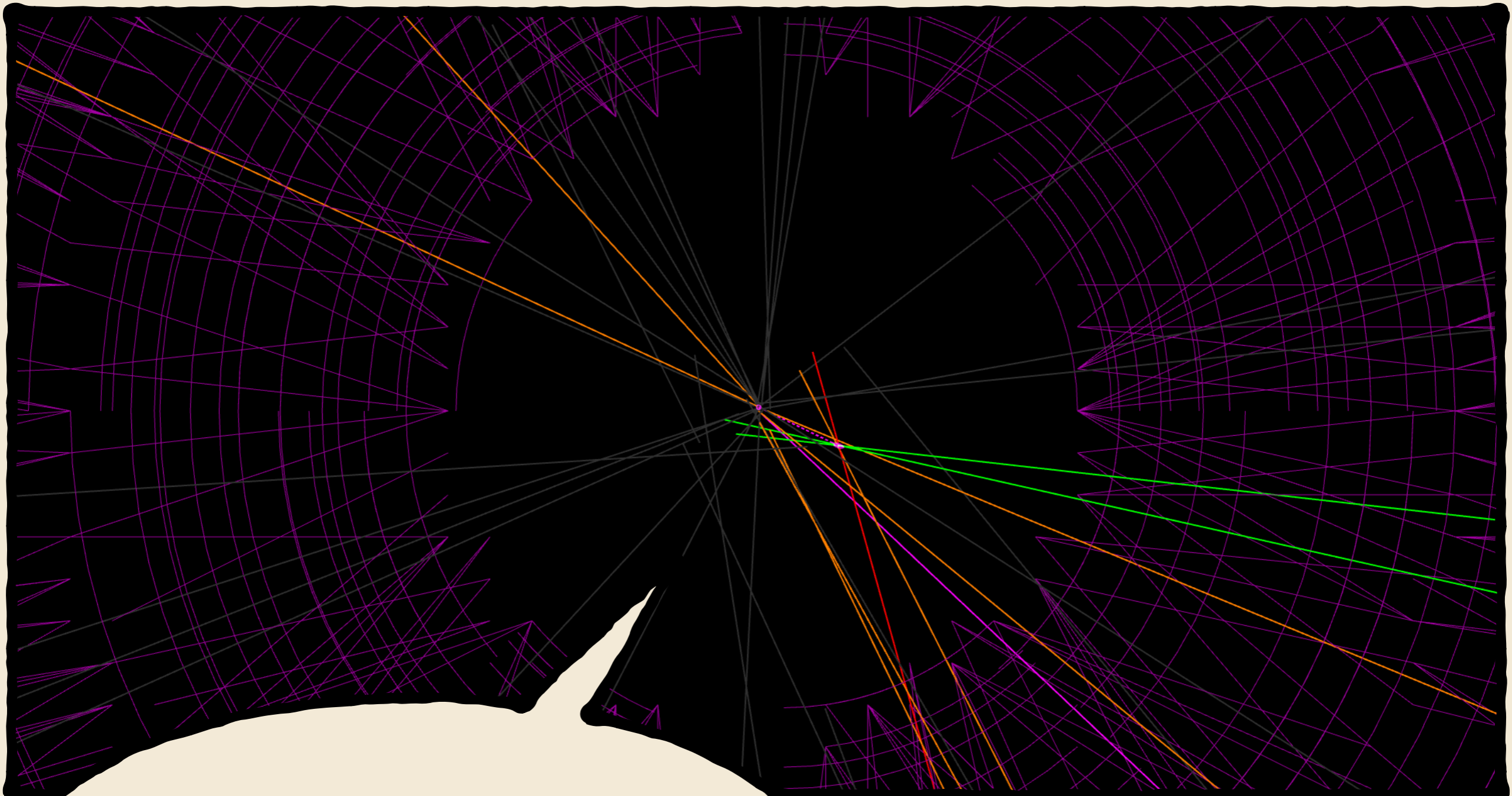
In the analysis of 1fb^{-1} we did not have enough data to fit the full Pdf, so we used "folding" of angles to simplify the Pdf

$$\begin{aligned} \phi &\rightarrow -\phi && \text{if } \phi < 0 \\ \theta_\ell &\rightarrow \pi - \theta_\ell && \text{if } \theta_\ell < \pi/2 \end{aligned}$$

LHCb Collaboration [JHEP 08 \(2013\) 131](#)
LHCb Collaboration [PRL 111 \(2013\) 191801](#)

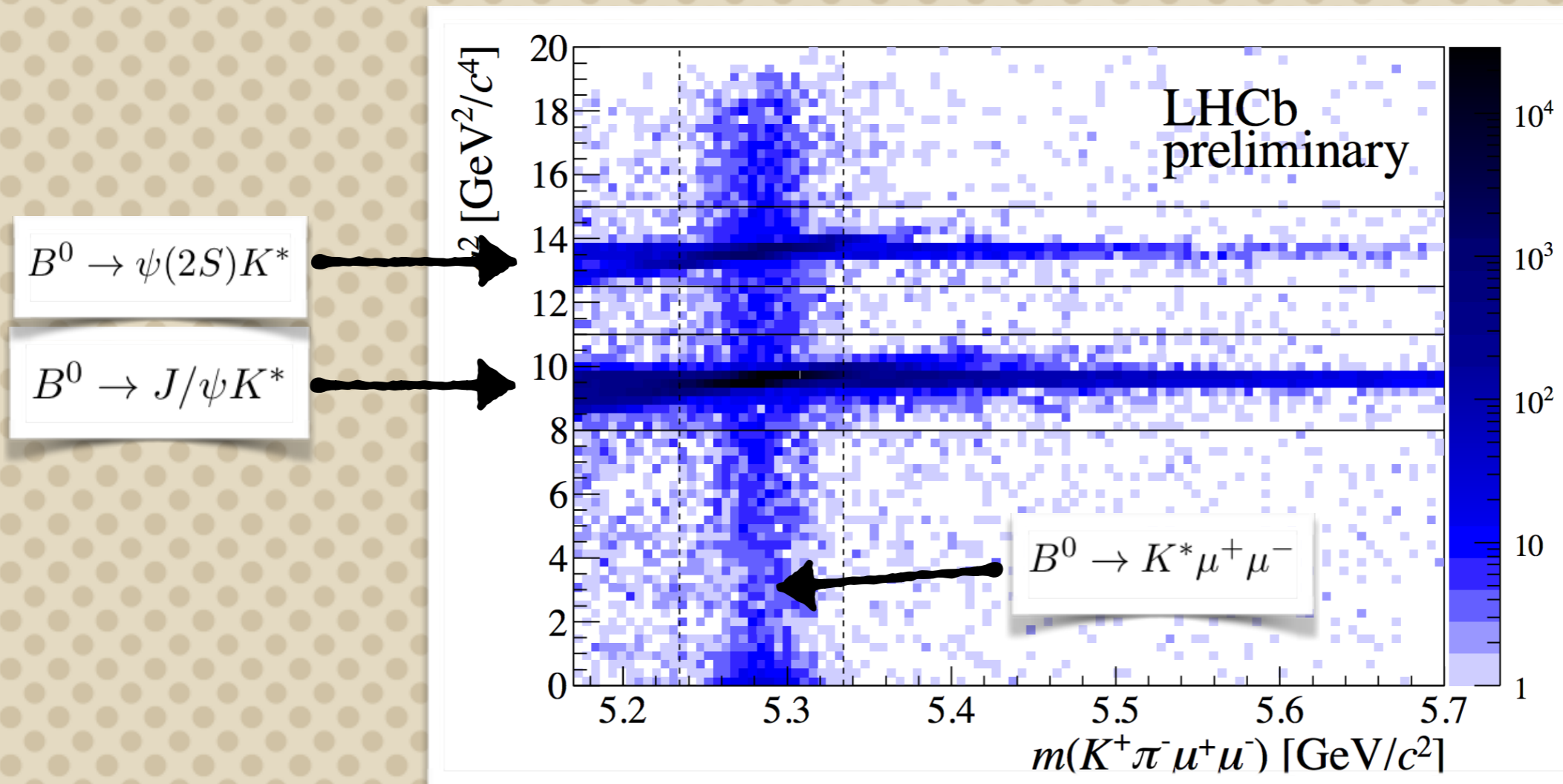
$$\frac{1}{\Gamma} \frac{d^3(\Gamma + \bar{\Gamma})}{d \cos \theta_\ell d \cos \theta_K d\phi} = \frac{9}{32\pi} \left[\frac{3}{4}(1 - F_L) \sin^2 \theta_K + F_L \cos^2 \theta_K + \frac{1}{4}(1 - F_L) \sin^2 \theta_K \cos 2\theta_\ell - F_L \cos^2 \theta_K \cos 2\theta_\ell + S_3 \sin^2 \theta_K \sin^2 \theta_\ell \cos 2\phi + \sqrt{F_L(1 - F_L)} P'_5 \sin 2\theta_K \sin \theta_\ell \cos \phi \right]$$





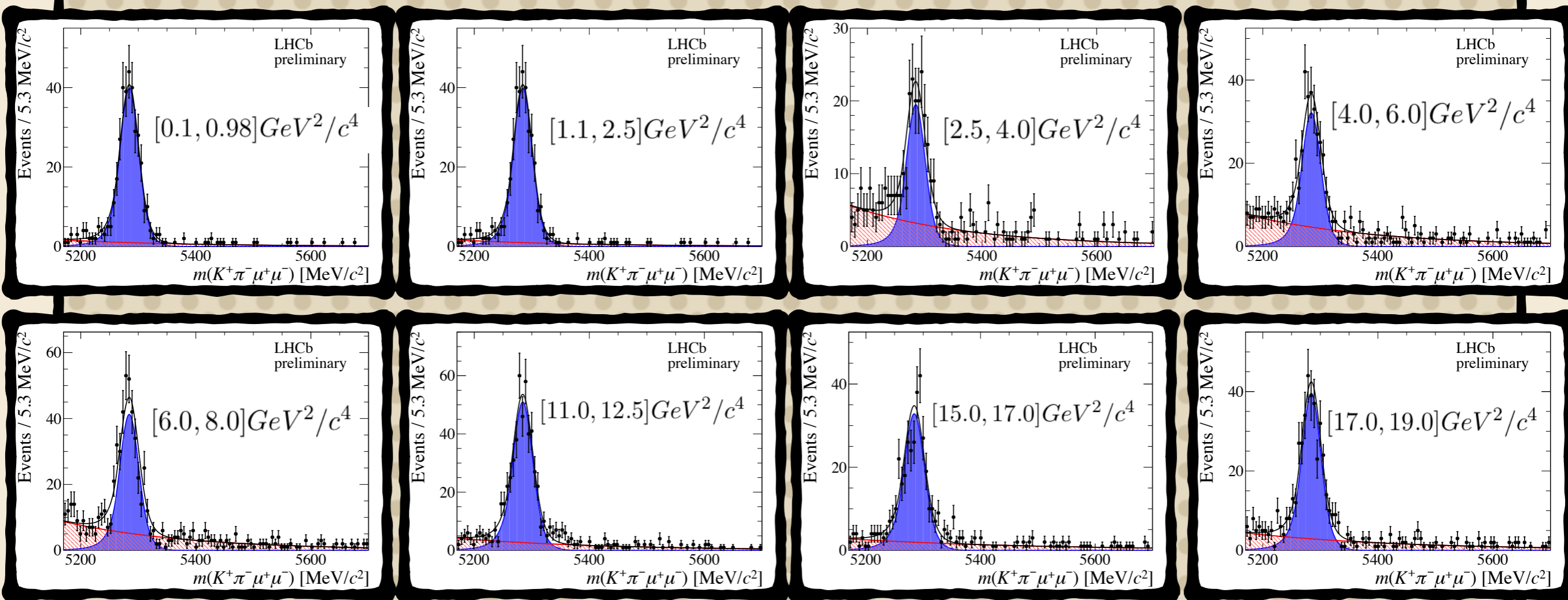
Analysis of $B_0 \rightarrow K^* \mu \mu$ (3 fb^{-1})

Signal region



- Signal selected with BDT which combines kinematic, geometric and PID criteria
- Veto charminium resonances
- Used of charmonia as control channels

Invariant Mass fit



- Total signal yield integrated in q^2 : 2398 ± 58 events
- Angular analysis performed in small q^2 bins is more sensitive to NP contributions
- High significance of the signal in all bins
- Independent angular and mass fits in each bins

Likelihood Fit

- Four dimensional fit of B-mass, angles $(\phi, \theta_\ell, \theta_K)$ and simultaneous fit of $m(K\pi)$ (background fraction shared)

$$\log \mathcal{L} = \sum_i \log \left[\epsilon(\vec{\Omega}, q^2) f_{\text{sig}} \mathcal{P}_{\text{sig}}(\vec{\Omega}) \mathcal{P}_{\text{sig}}(m_{K\pi\mu\mu}) + (1 - f_{\text{sig}}) \mathcal{P}_{\text{bkg}}(\vec{\Omega}) \mathcal{P}_{\text{bkg}}(m_{K\pi\mu\mu}) \right] + \sum_i \log \left[f_{\text{sig}} \mathcal{P}_{\text{sig}}(m_{K\pi}) + (1 - f_{\text{sig}}) \mathcal{P}_{\text{bkg}}(m_{K\pi}) \right]$$

- $\mathcal{P}_{\text{sig}}(\Omega) = \frac{d^3\Gamma}{d \cos \theta_\ell d \cos \theta_K d\phi}$ and $\epsilon(\Omega, q^2)$ is the signal efficiency
- $\mathcal{P}_{\text{bkg}}(\Omega)$ is modelled with three second order Chebychel polynomial and extracted from the sidebands
- $\mathcal{P}_{\text{bkg}}(m_{K\pi\mu\mu})$ is an esponential

Method of Moments

Use orthogonality of spherical harmonics to determine the coefficients

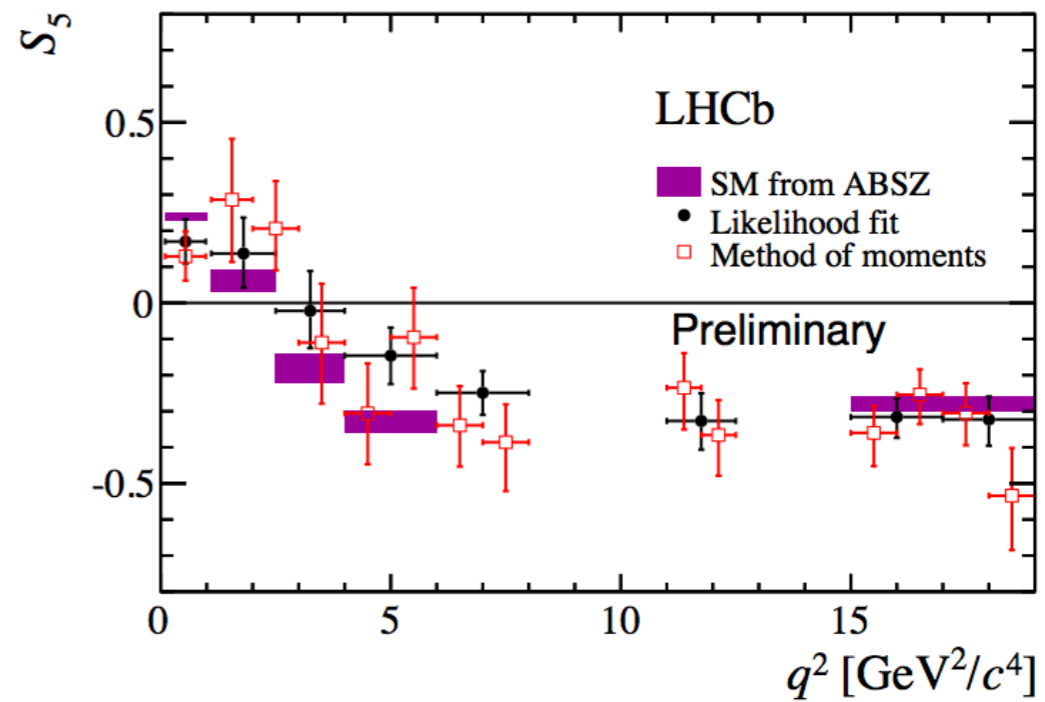
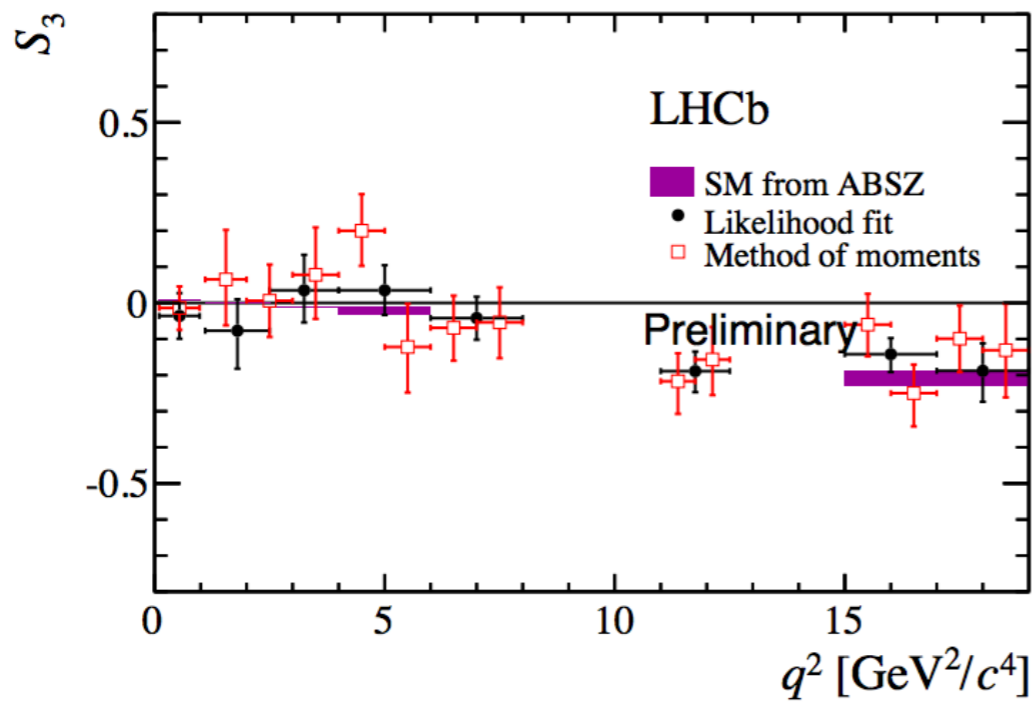
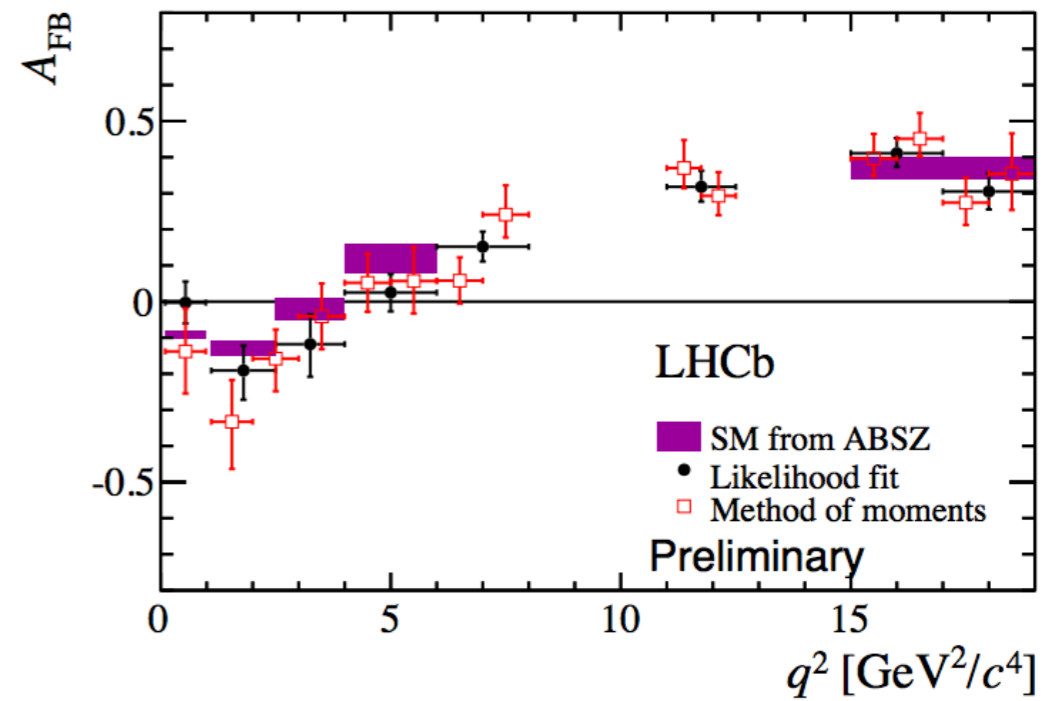
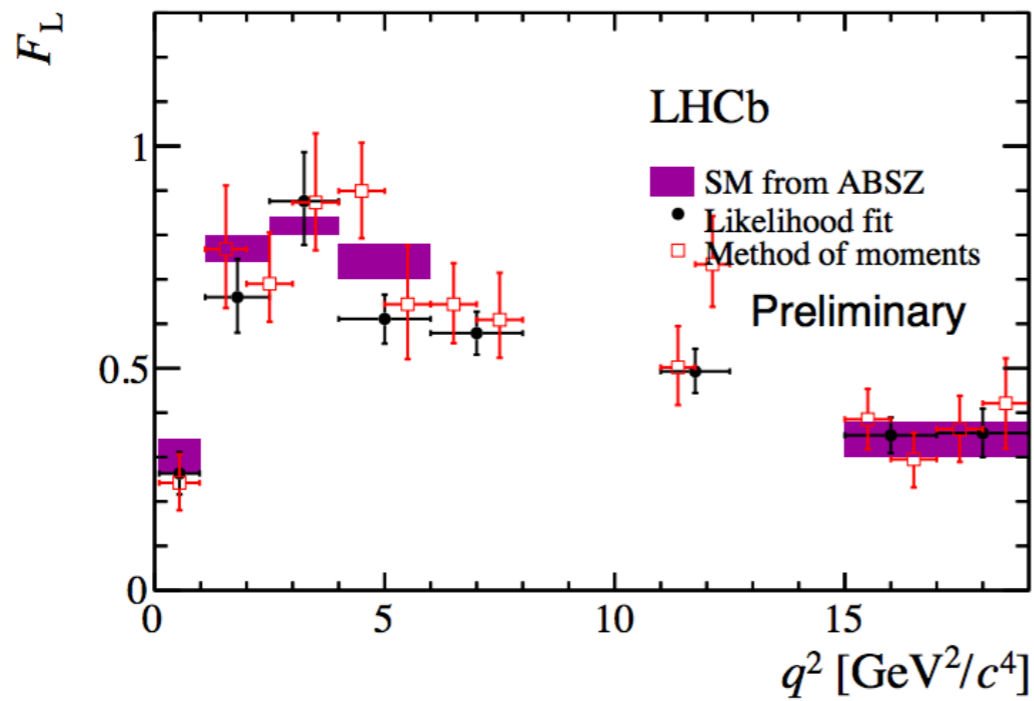
$$\int f_i(\vec{\Omega}) f_j(\vec{\Omega}) d\vec{\Omega} = \delta_{ij}$$

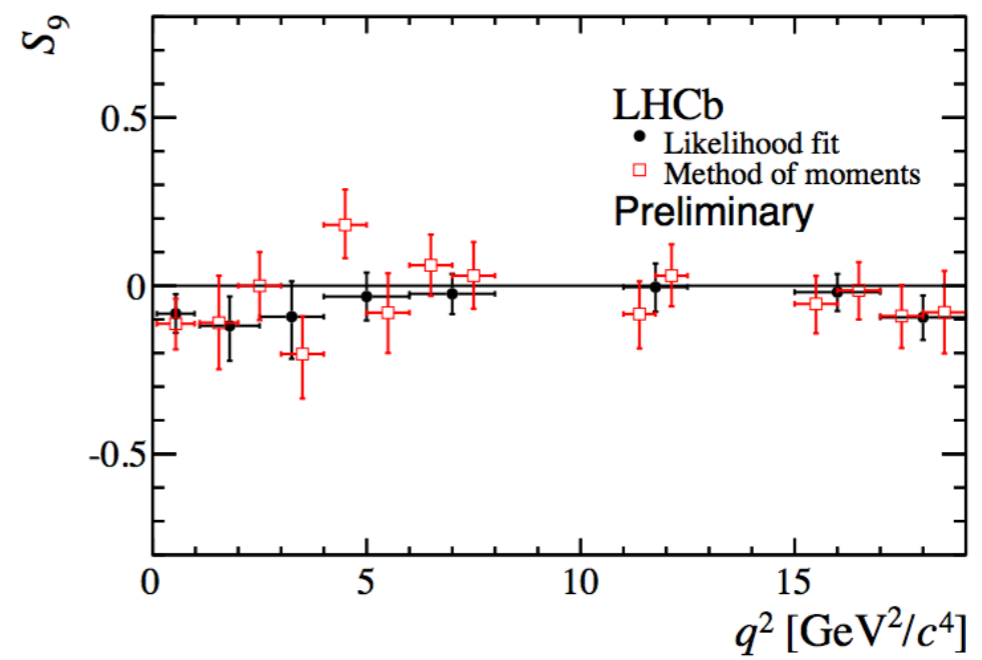
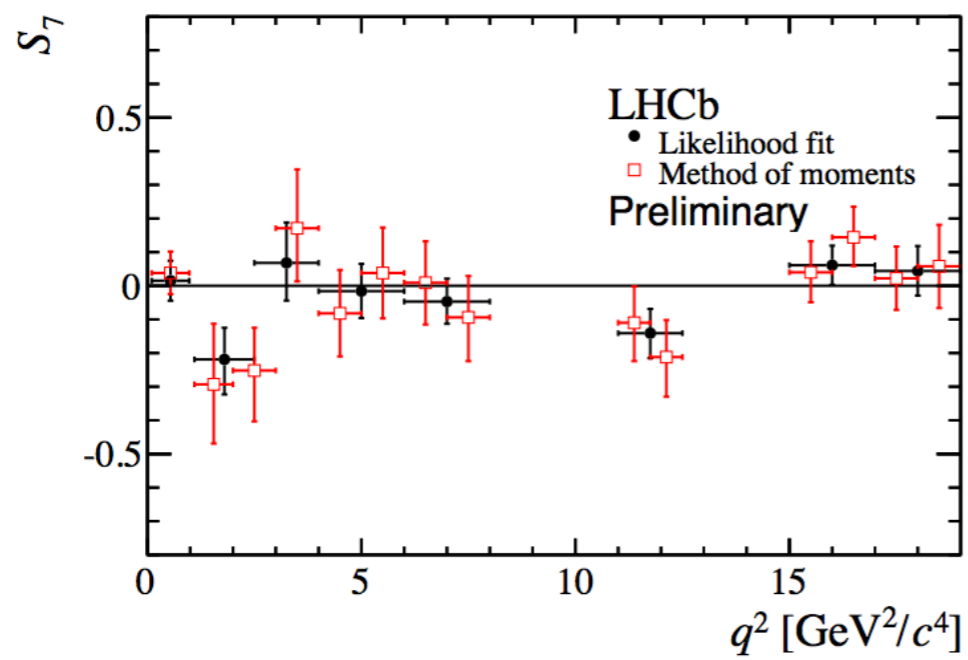
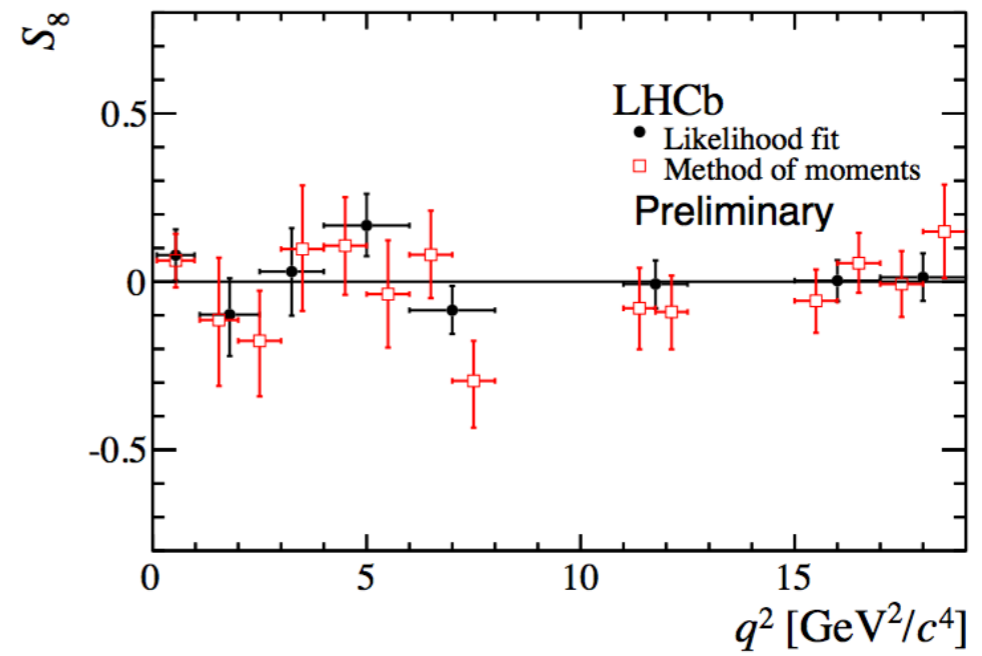
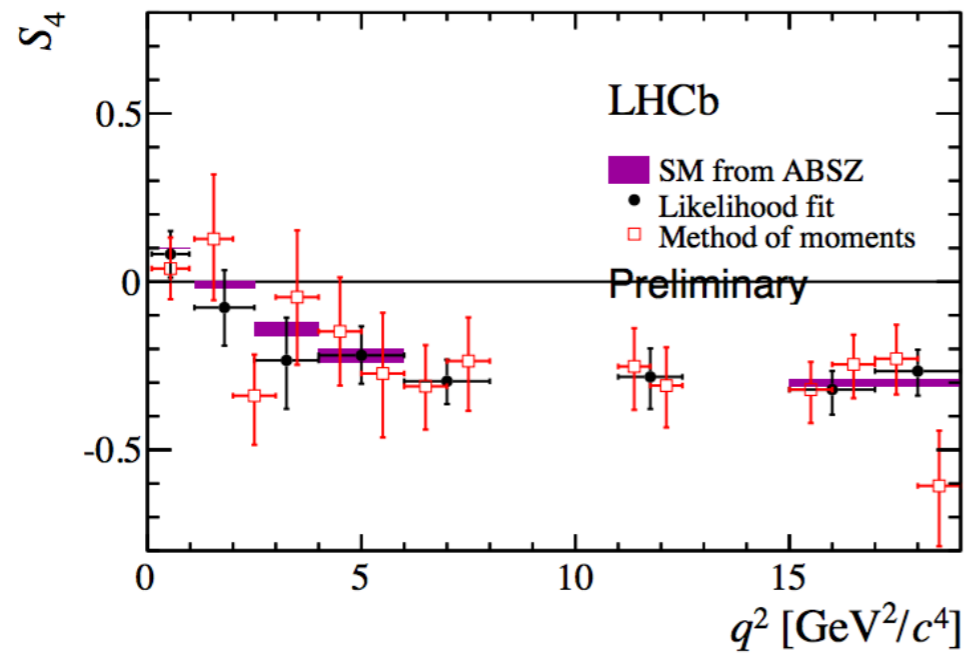
$$M_i = \int \left(\frac{1}{d(\Gamma + \bar{\Gamma})/dq^2} \right) \frac{d^3(\Gamma + \bar{\Gamma})}{d\vec{\Omega}} f_i(\vec{\Omega}) d\vec{\Omega}$$

We sample the angular distribution with our data, so the integral becomes a sum over data

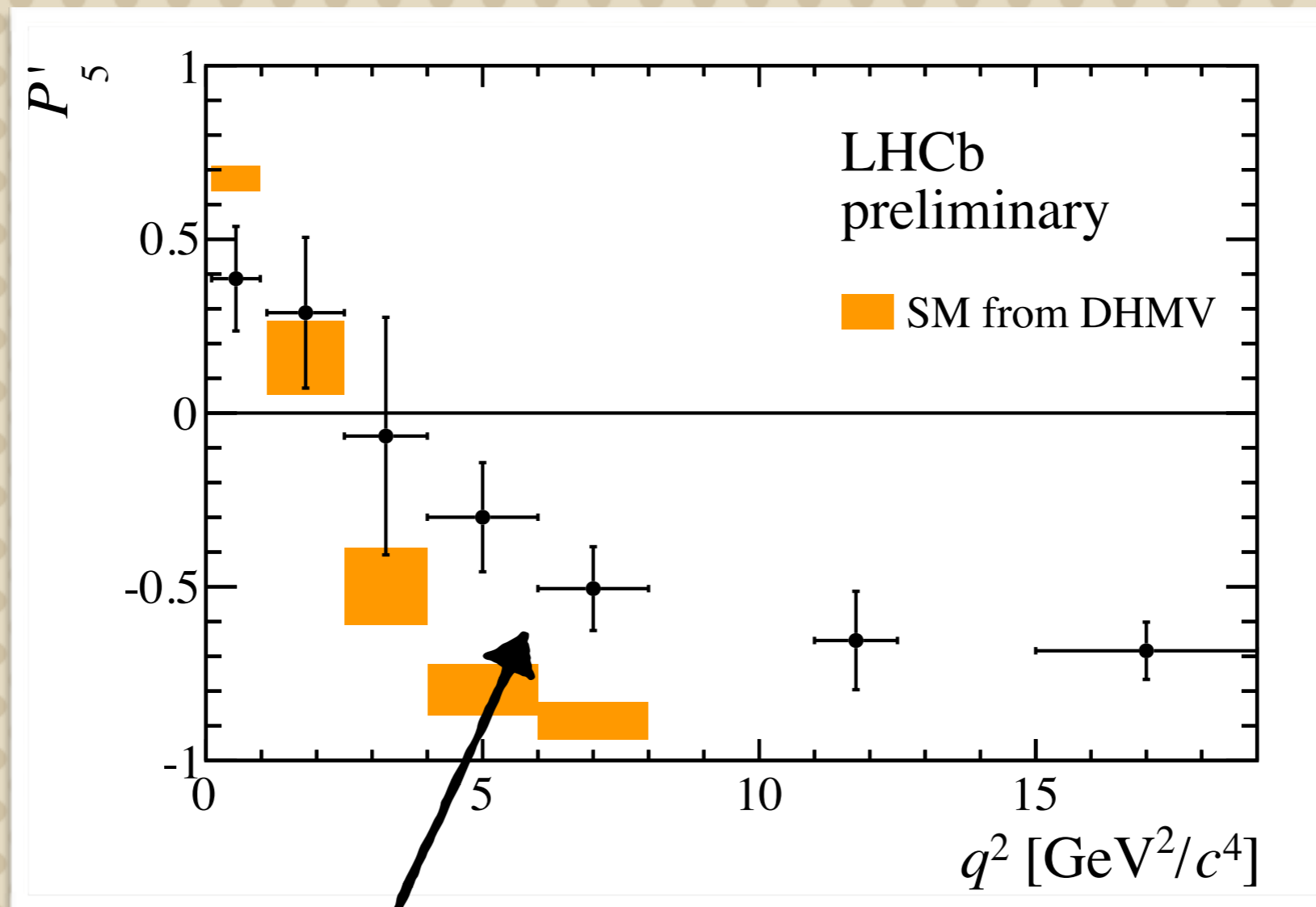
$$\widehat{M}_i = \frac{1}{\sum_e w_e} \sum_e w_e f_i(\vec{\Omega}_e)$$

The weights w_e accounts for the efficiency



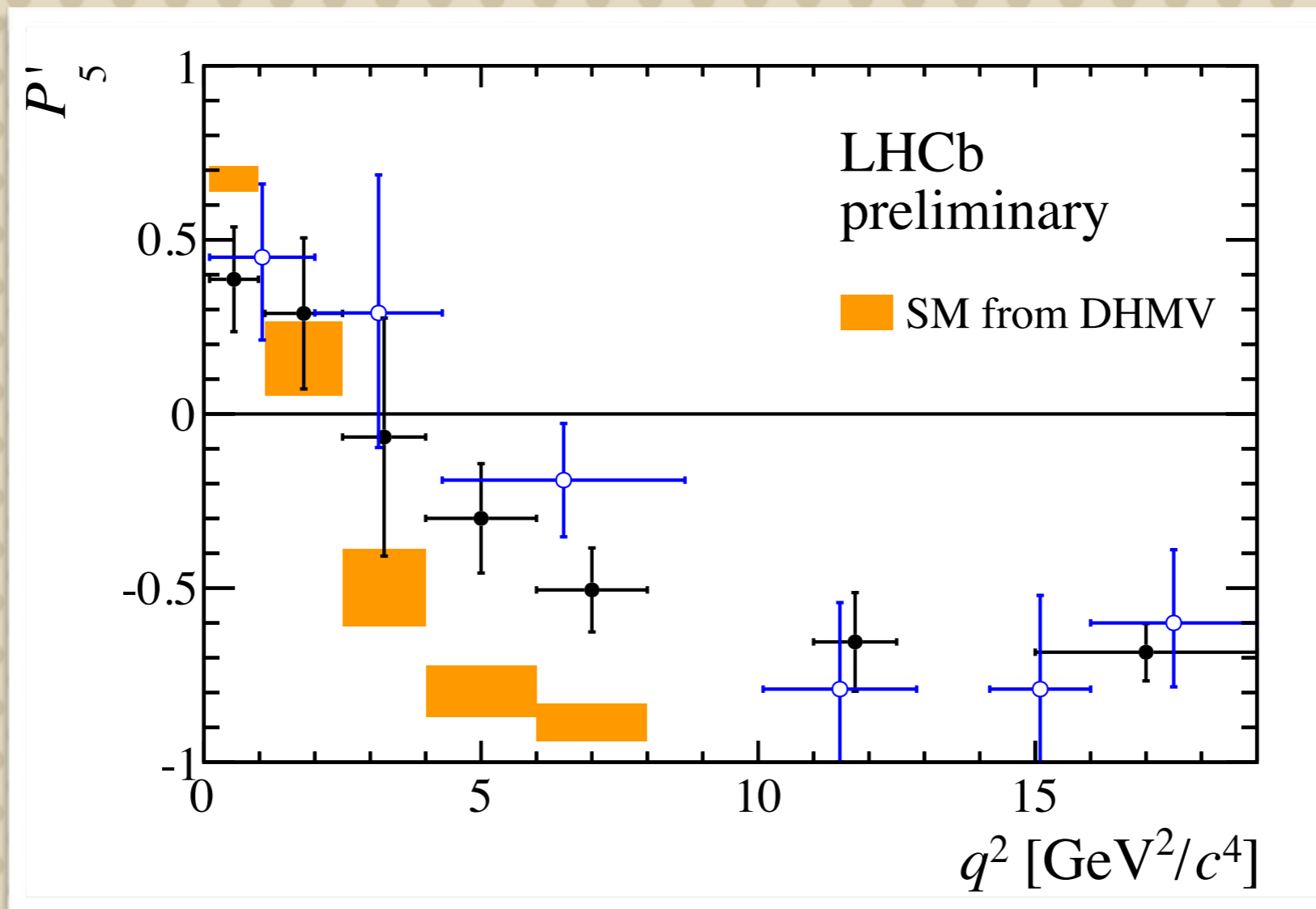


The $K^*\mu\mu$ anomaly persists



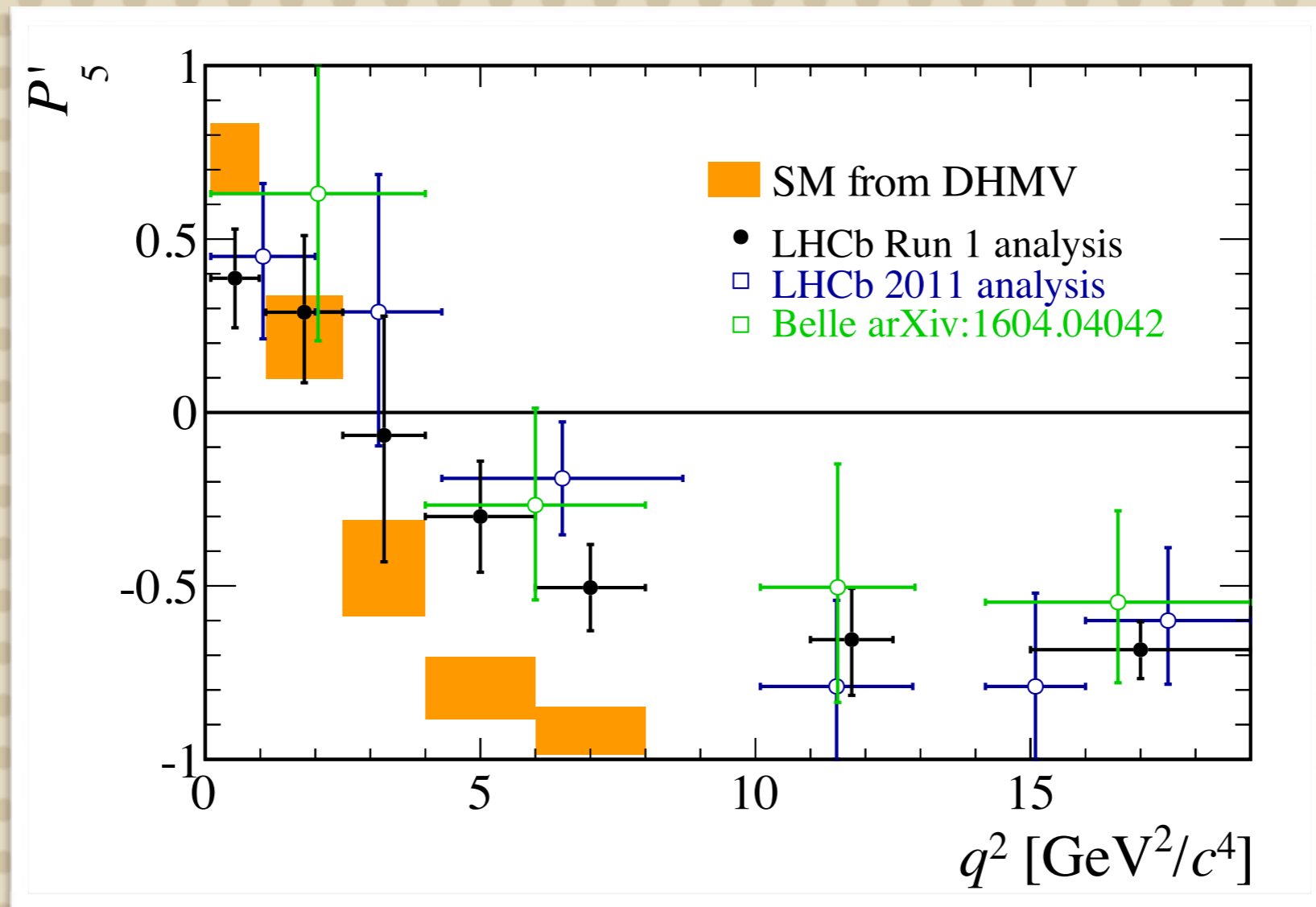
- Local discrepancy of about 3.0σ in each of these two bins

The $K^*\mu\mu$ anomaly persists

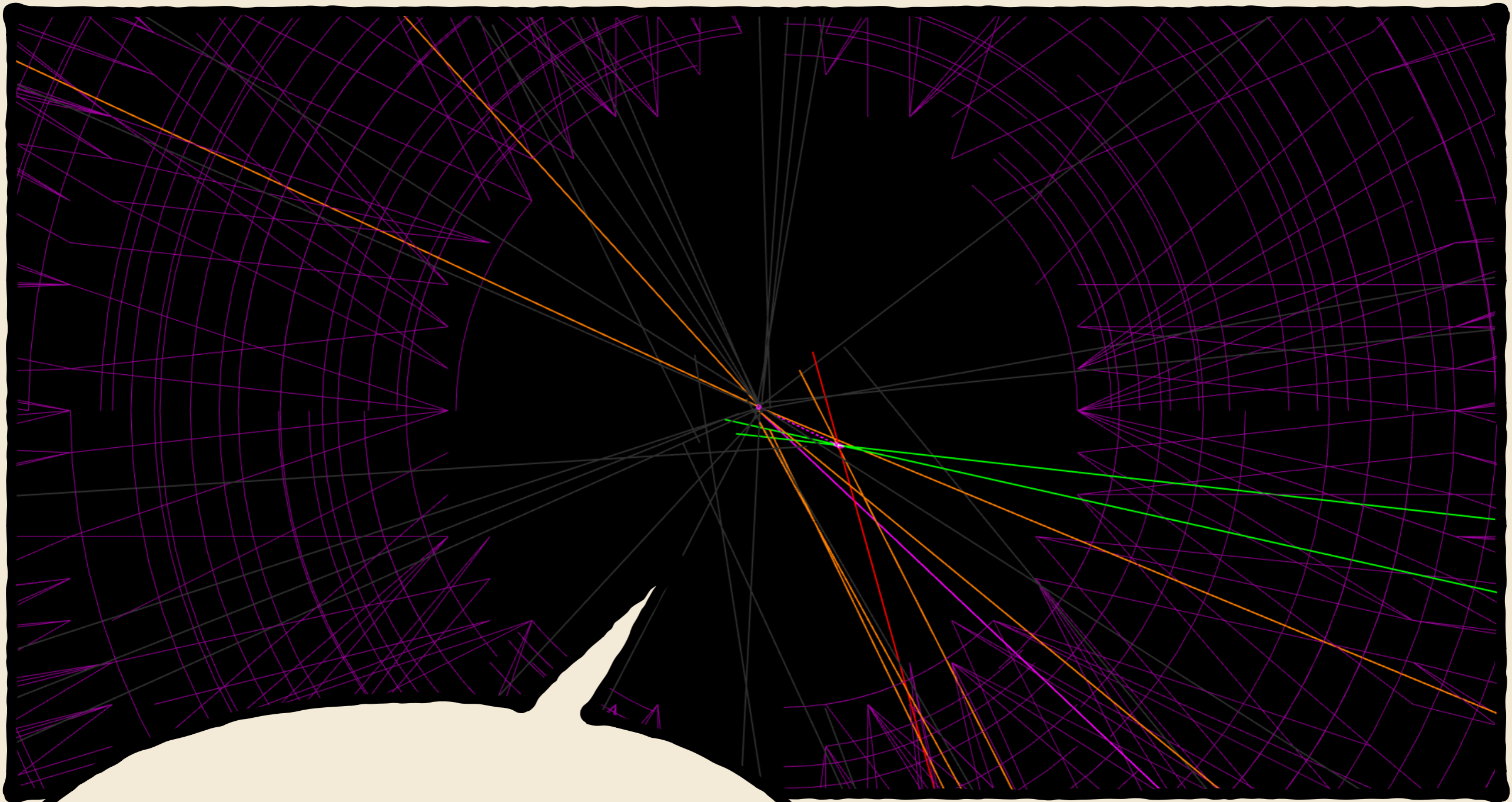


- Good agreement with the analysis of 1fb^{-1}

The $K^*_{\mu\mu}$ anomaly persists

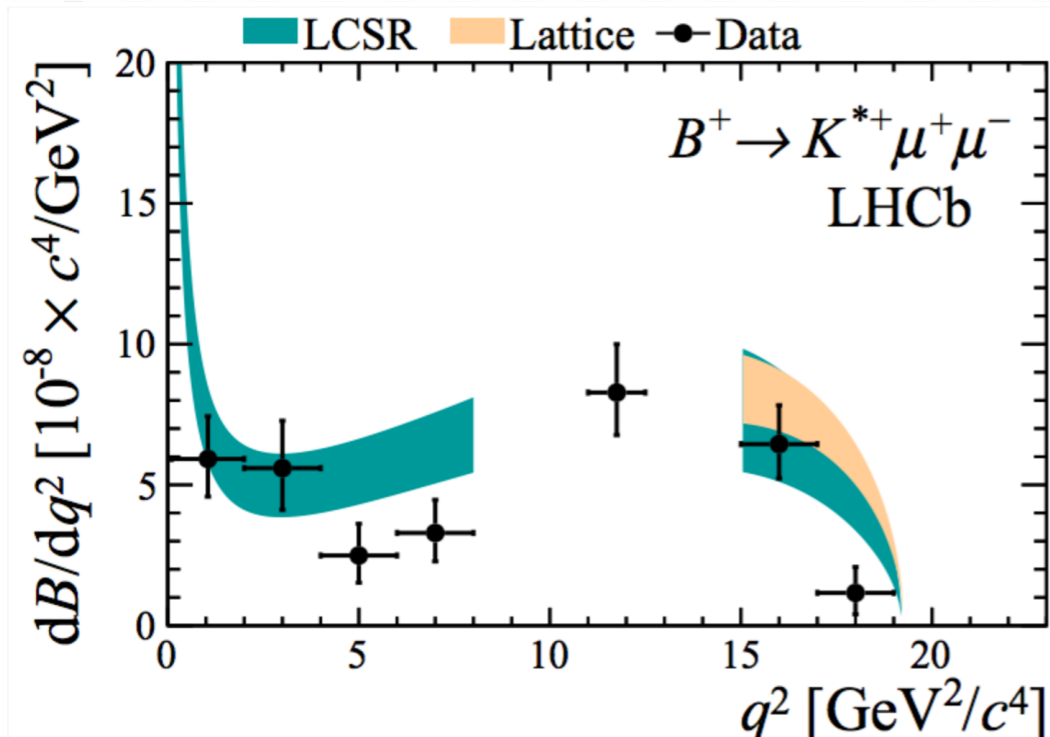
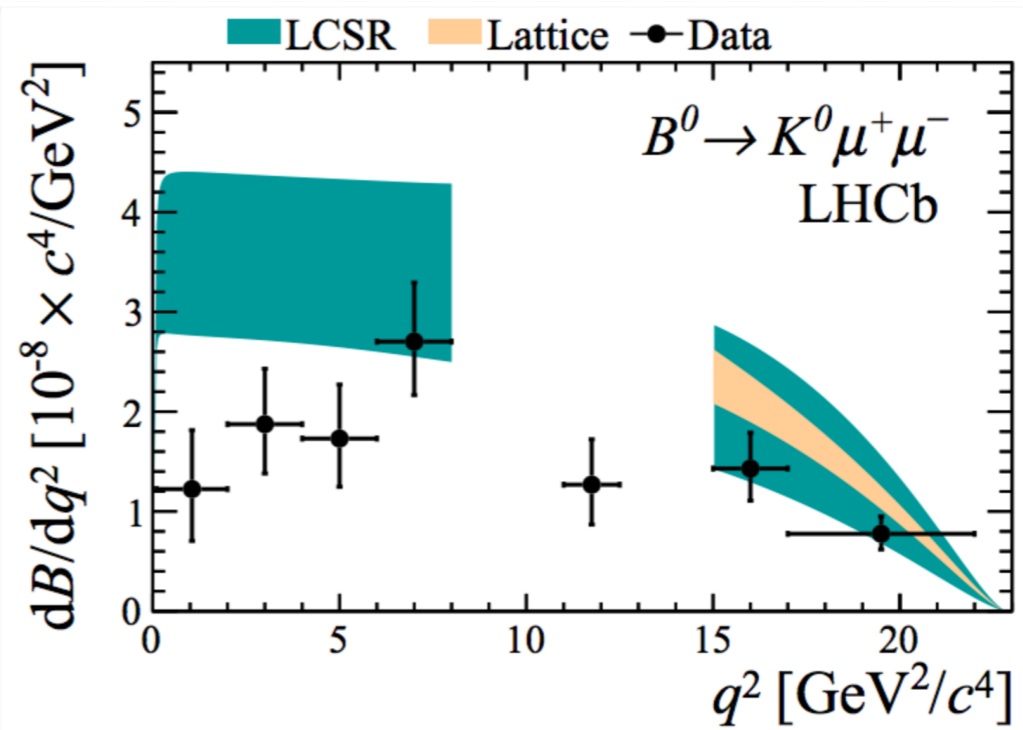
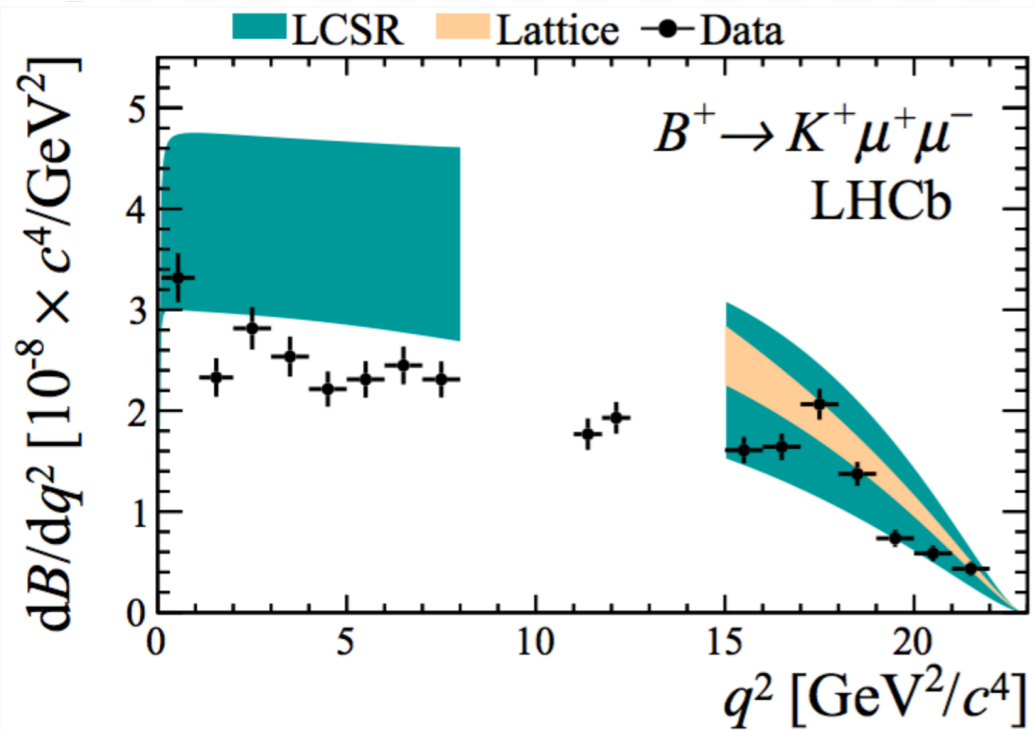


Very good agreement with the recent Belle measurement of P'_5



**A coherent
pattern?**

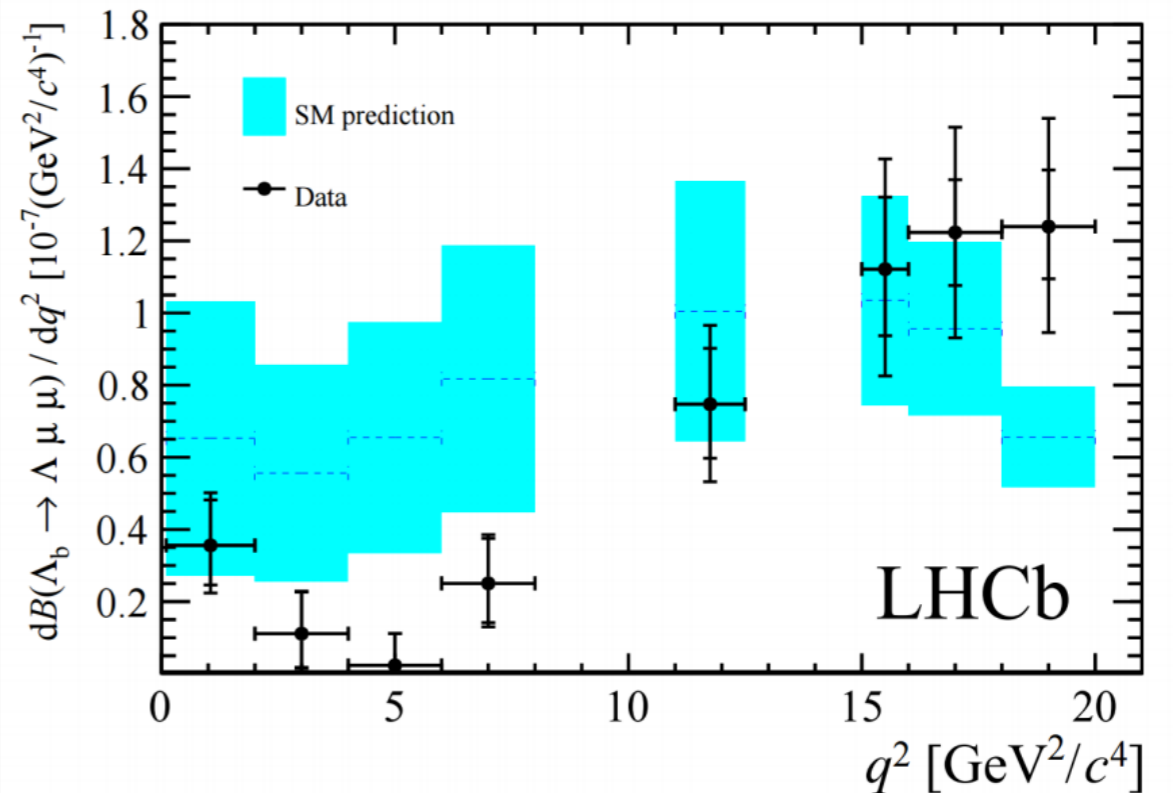
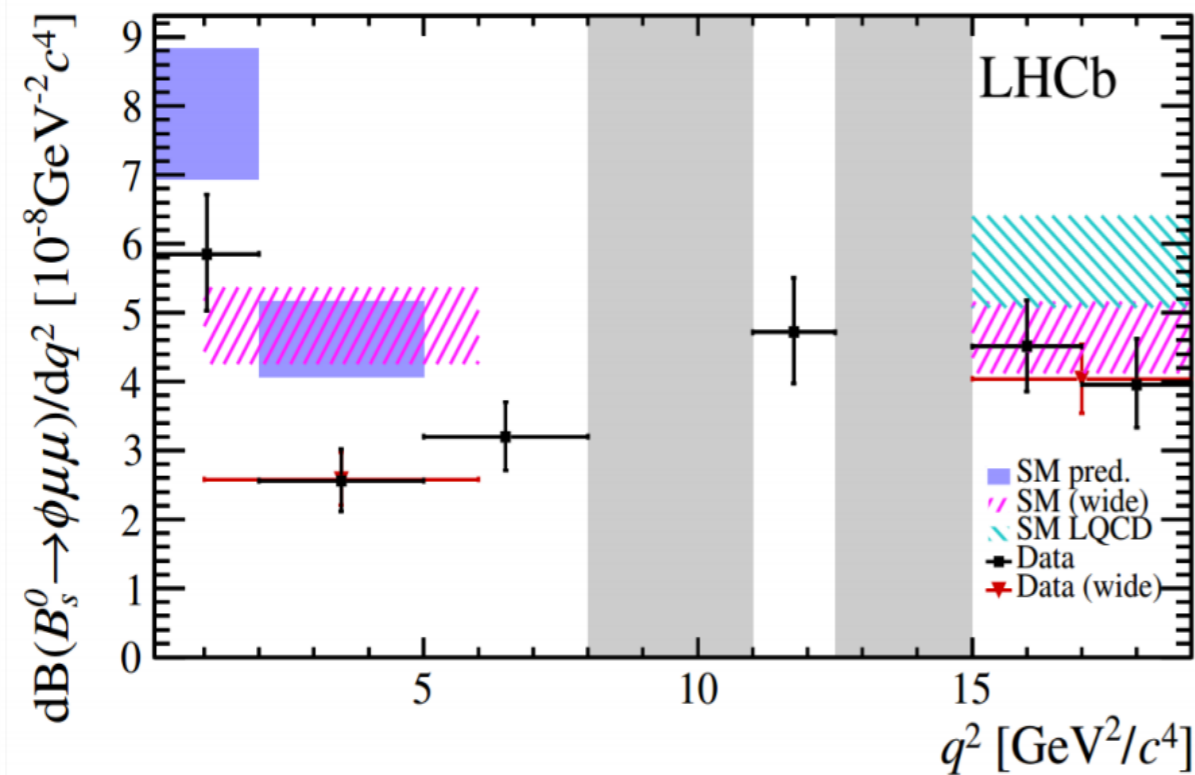
A coherent pattern?



LHCb Collaboration [JHEP 06 \(2014\) 133](#)

- All $b \rightarrow s \mu \mu$ branching ratios are measured to be lower than SM predictions
- All these measurements are numerically consistent with a reduced C_9 Wilson coefficient

A coherent pattern?

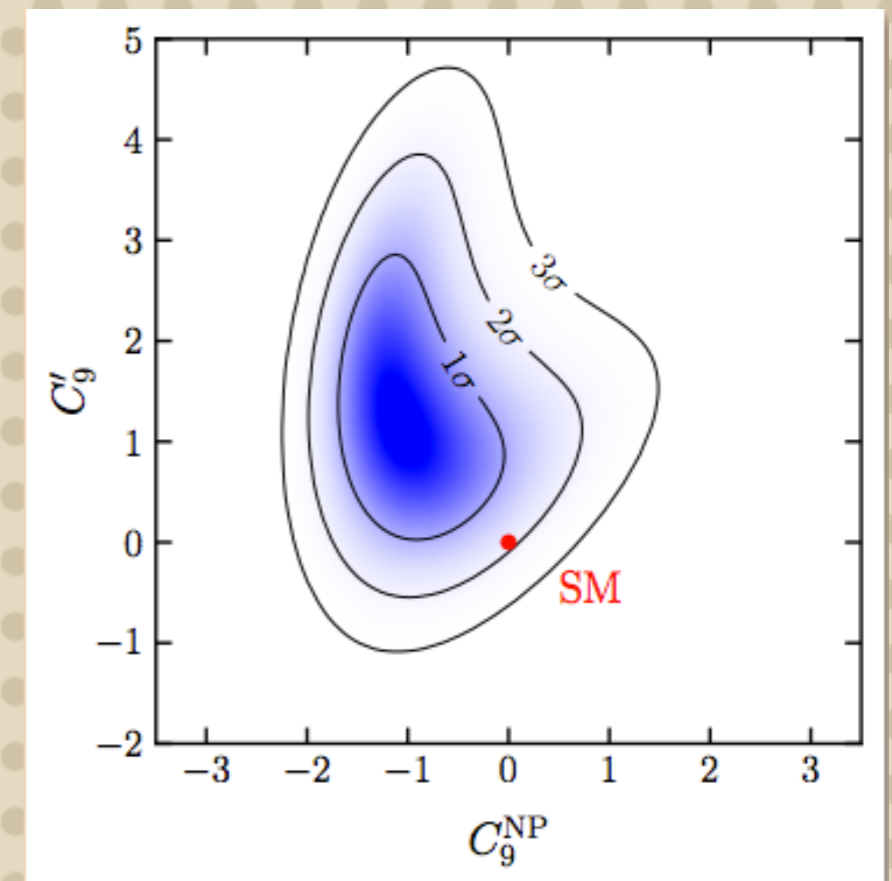
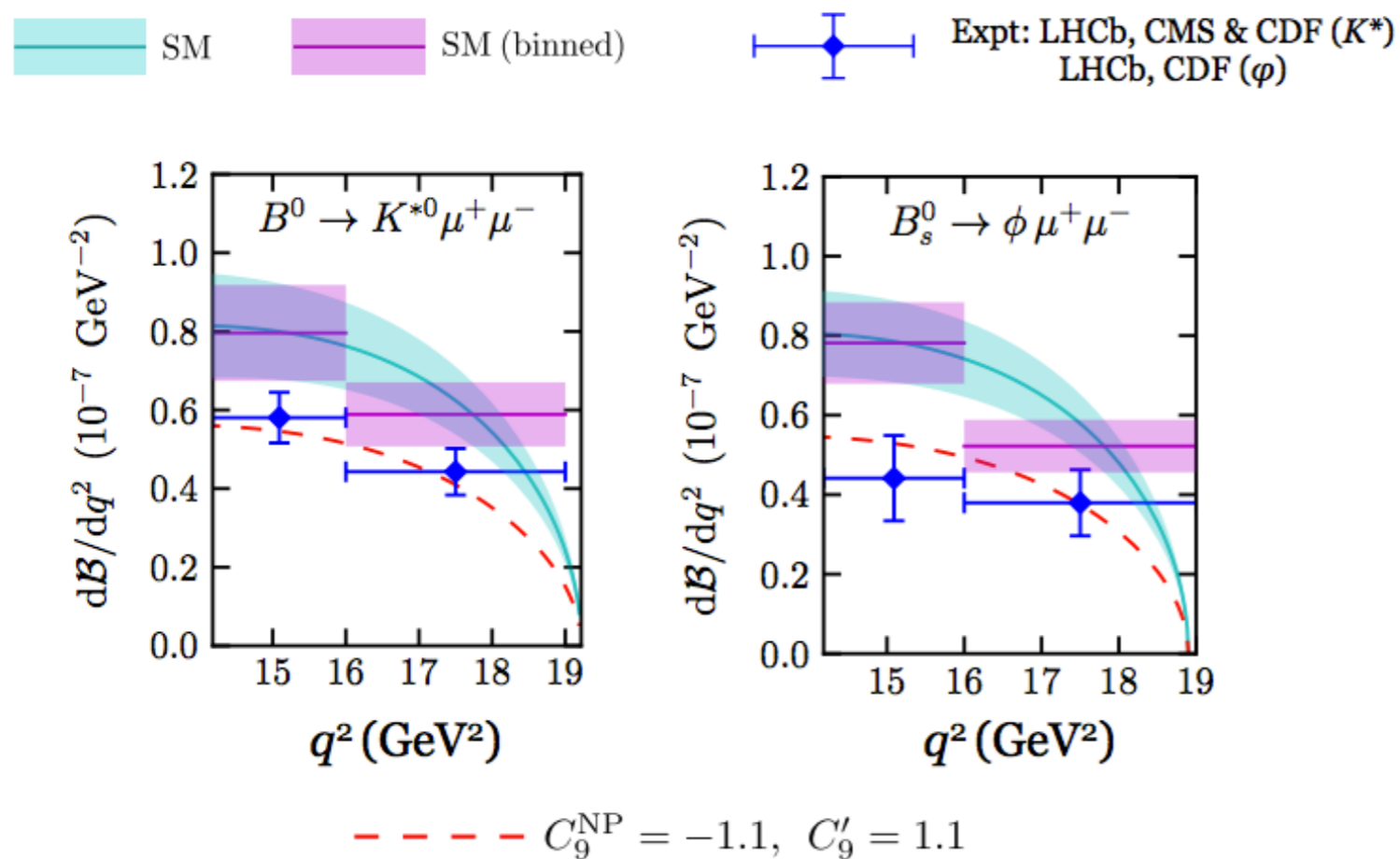


- All $b \rightarrow s \mu \mu$ branching ratios are measured to be lower than SM predictions
- All these measurements are numerically consistent with a reduced C_9 Wilson coefficient

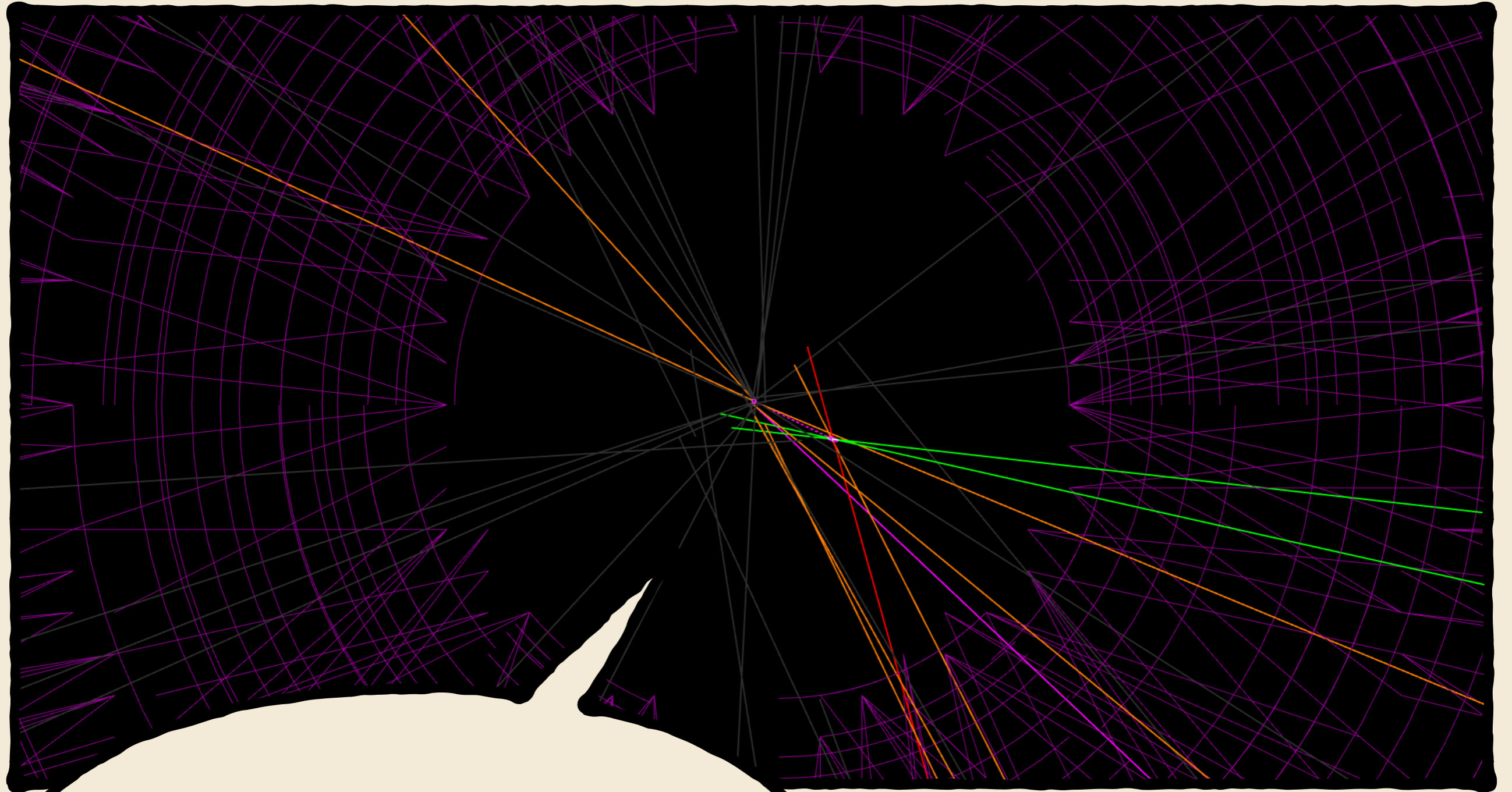
Larger than expected deviations (even in NP scenarios)

A coherent pattern?

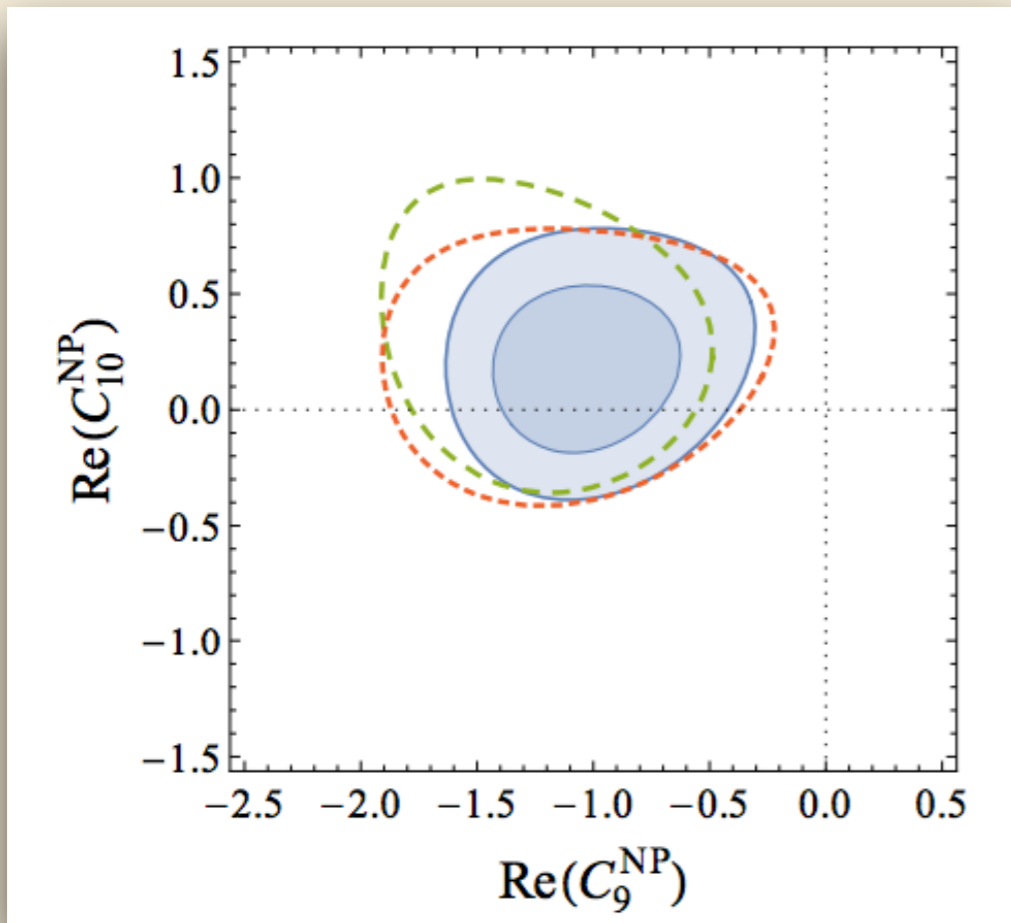
A reduced C_9 Wilson coefficient would be visible in a number of other observables, like branching ratios



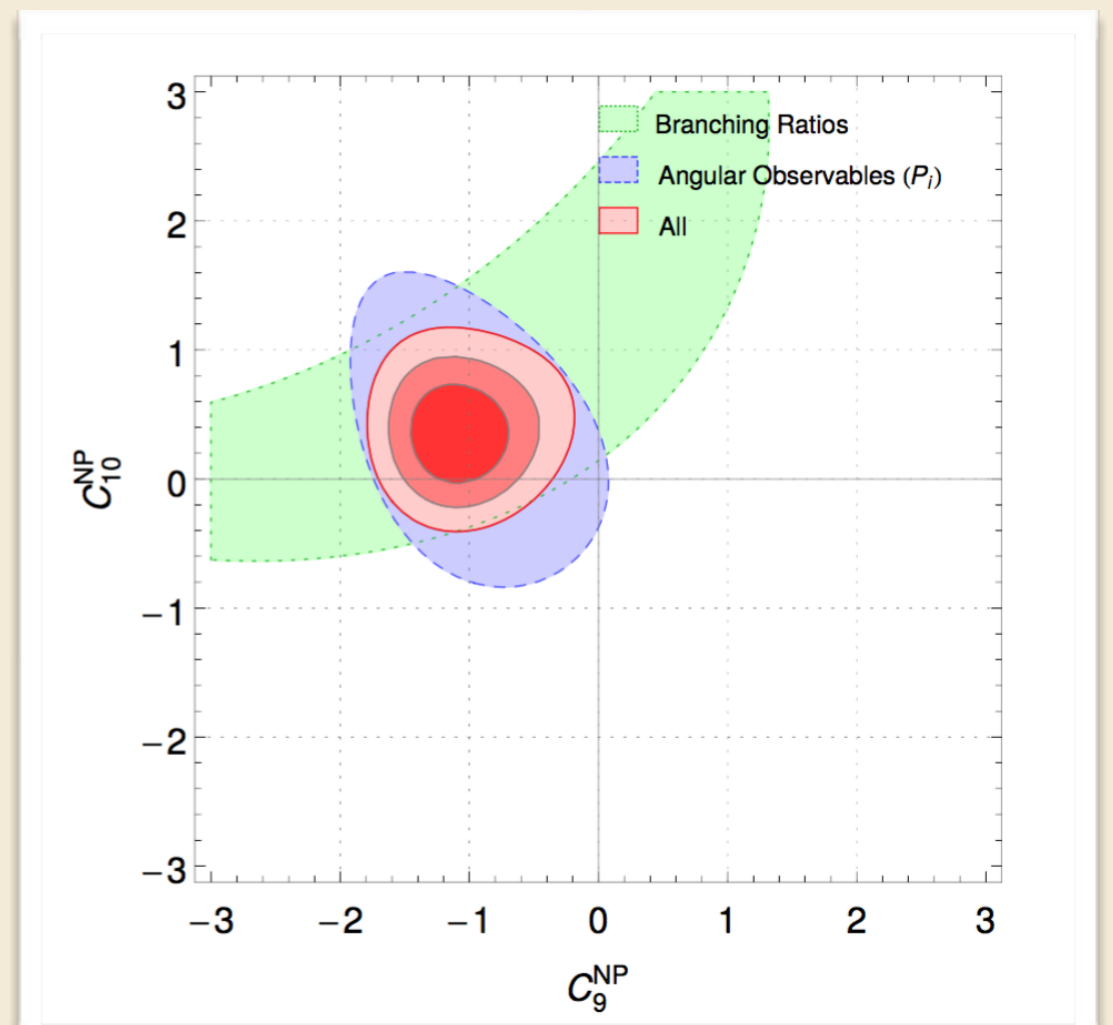
Wingate et al. Phys. Rev. Lett. **112** (2014) 212003
(high q^2 form factors from lattice QCD)



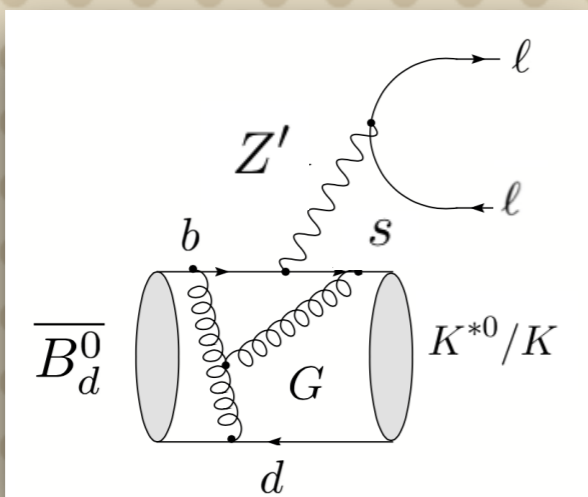
**Theory
Interpretation**



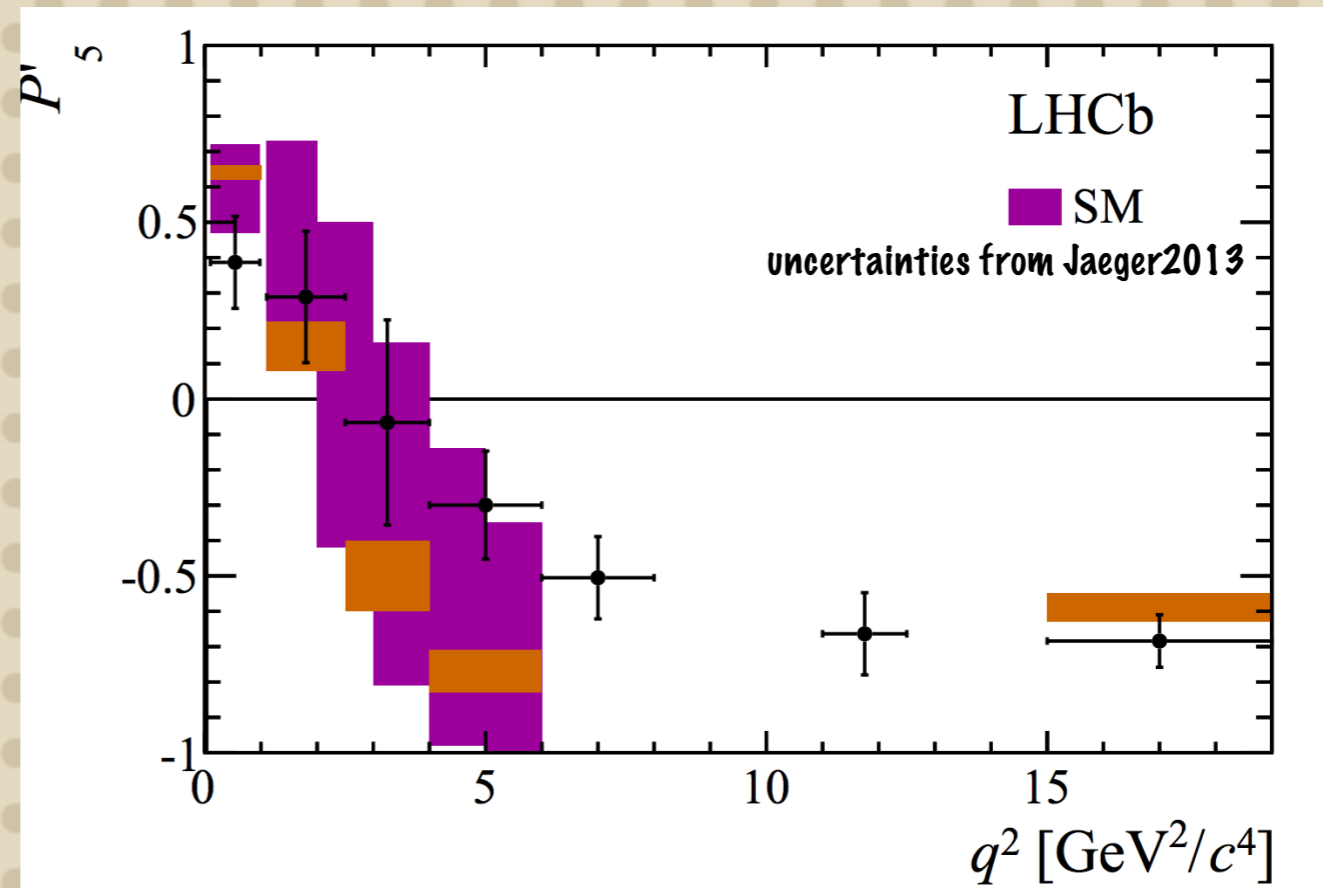
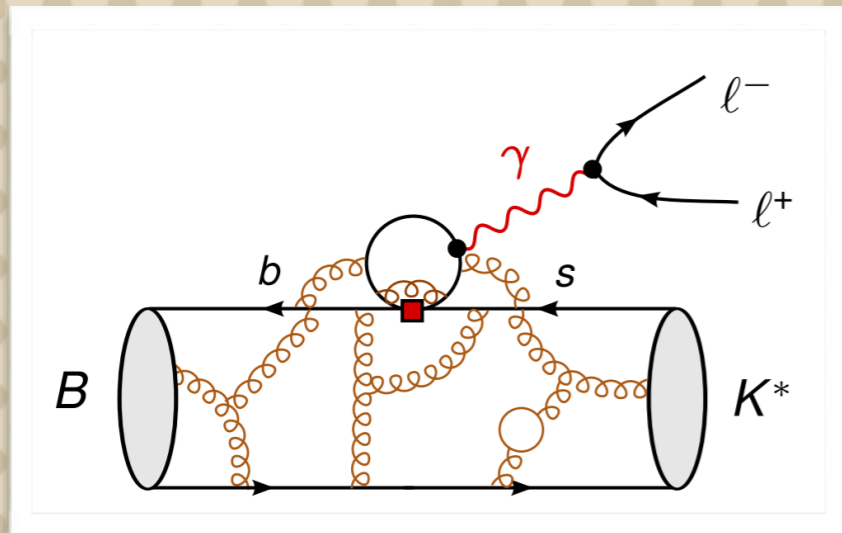
Tension with SM prediction when theory combine this measurements with many others



If it is a New Particle the best candidate seem to be a Z'

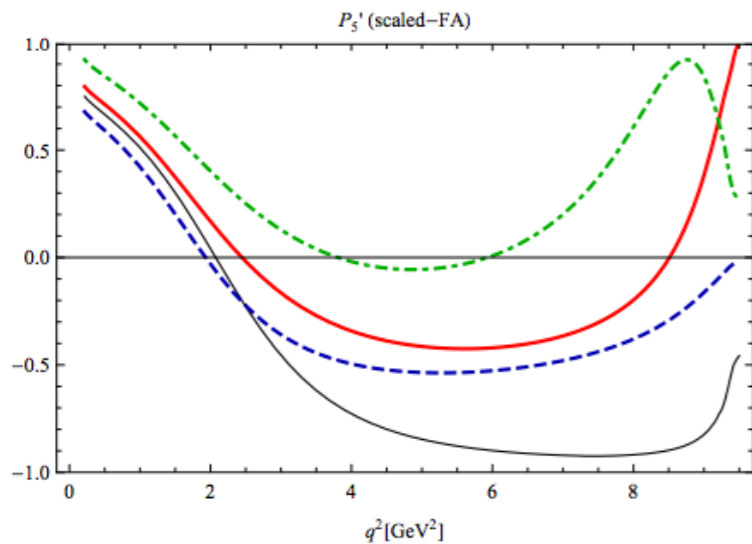


Charm loop effects?



- Non factorizable contribution could be large (Van Dyk 2013, Zwicky 2015, Silvestrini, Ciuchini 2016, ...)
- Charm loop photon mediated can give a C_9 -effect
- Possibility to explained with "large" charm loop contribution
- S. Jaeger pointed to possible (soft) form factors effects

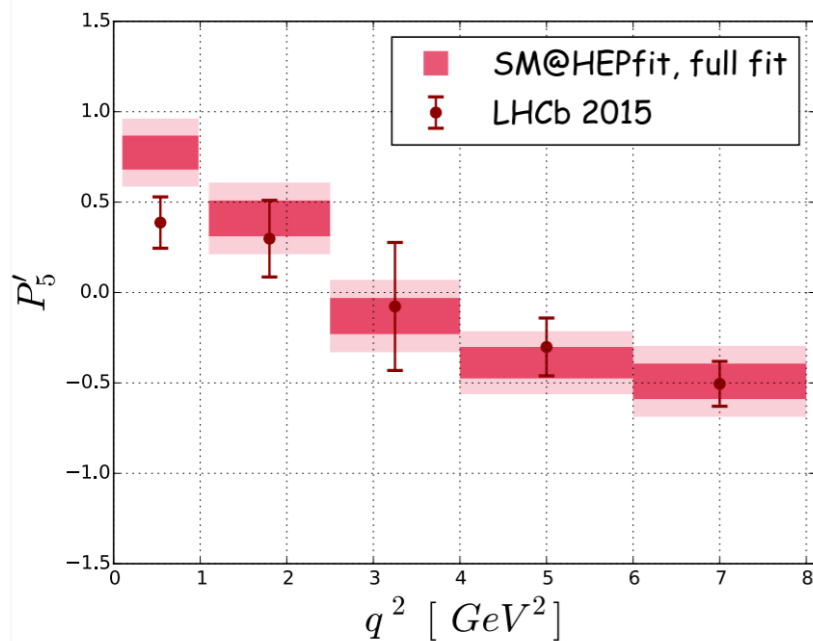
Charm loop effects?



Hadronic picture:

- Large effect from the tails of the $c\bar{c}$ resonances + open charm

Zwicky-Lyons 2015



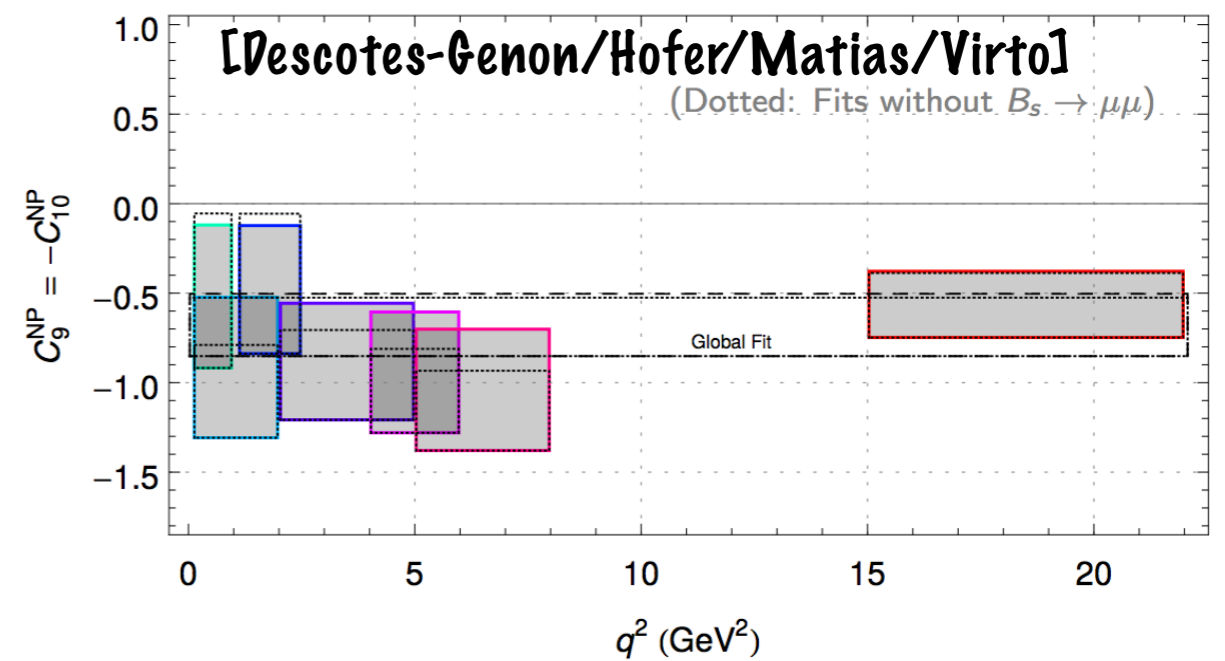
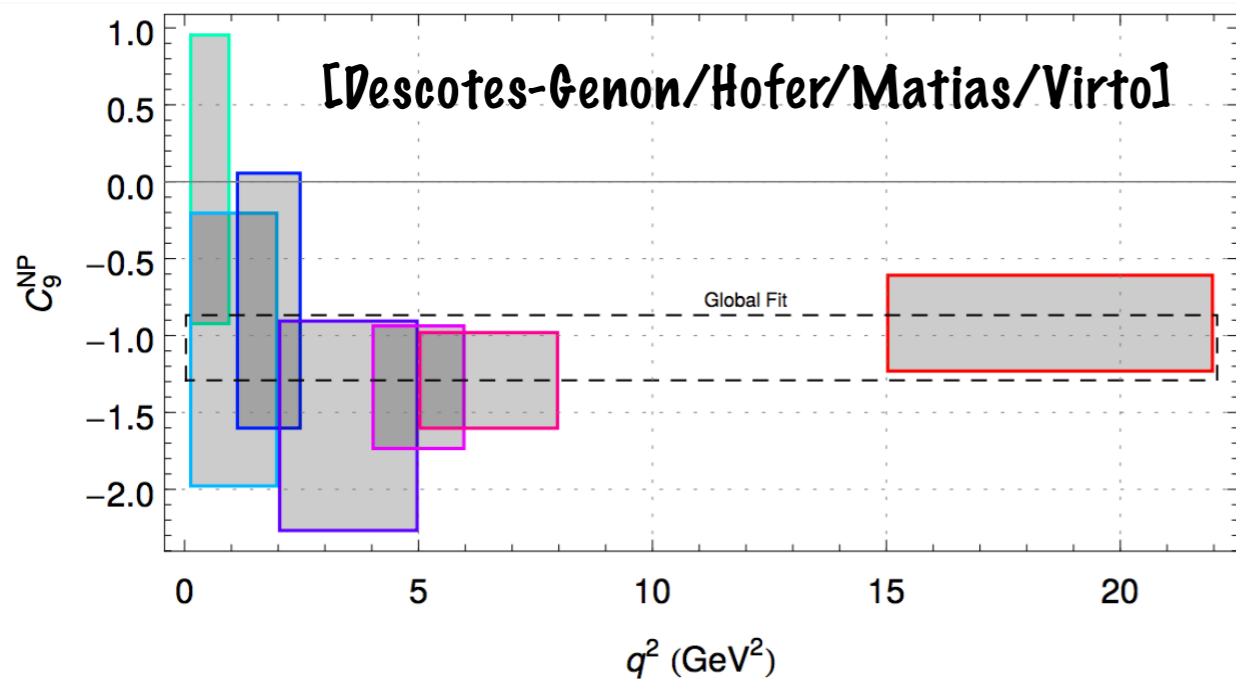
Partonic picture:

- Large effect from $c\bar{c}$ loop
- Adding an hadronic parameter to the fit it is possible to describe the anomaly

Silvestrini, Ciuchini et al., 2016

NP or hadronic effect?

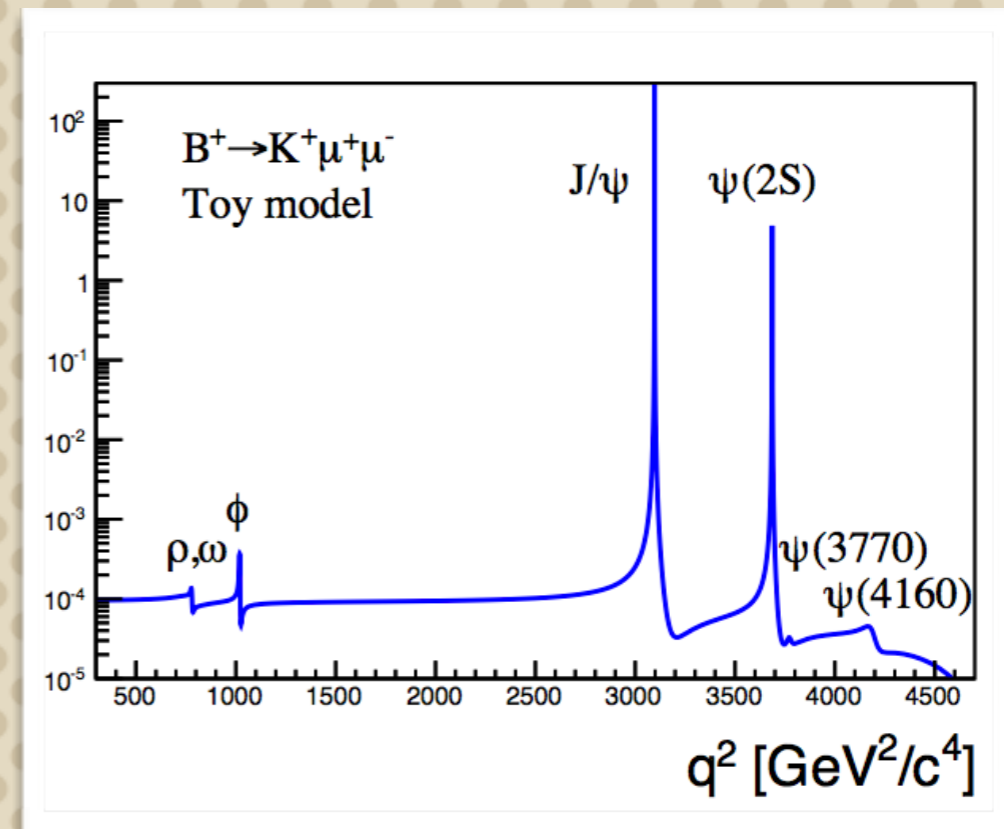
- NP is expected to be universal for all $b \rightarrow s \mu \mu$ transitions
- NP is expected to be q^2 independent



- For now we do not have evidence for process dependency or q^2 dependence
- Need more statistics

Trying to handle the ccb̄-loop

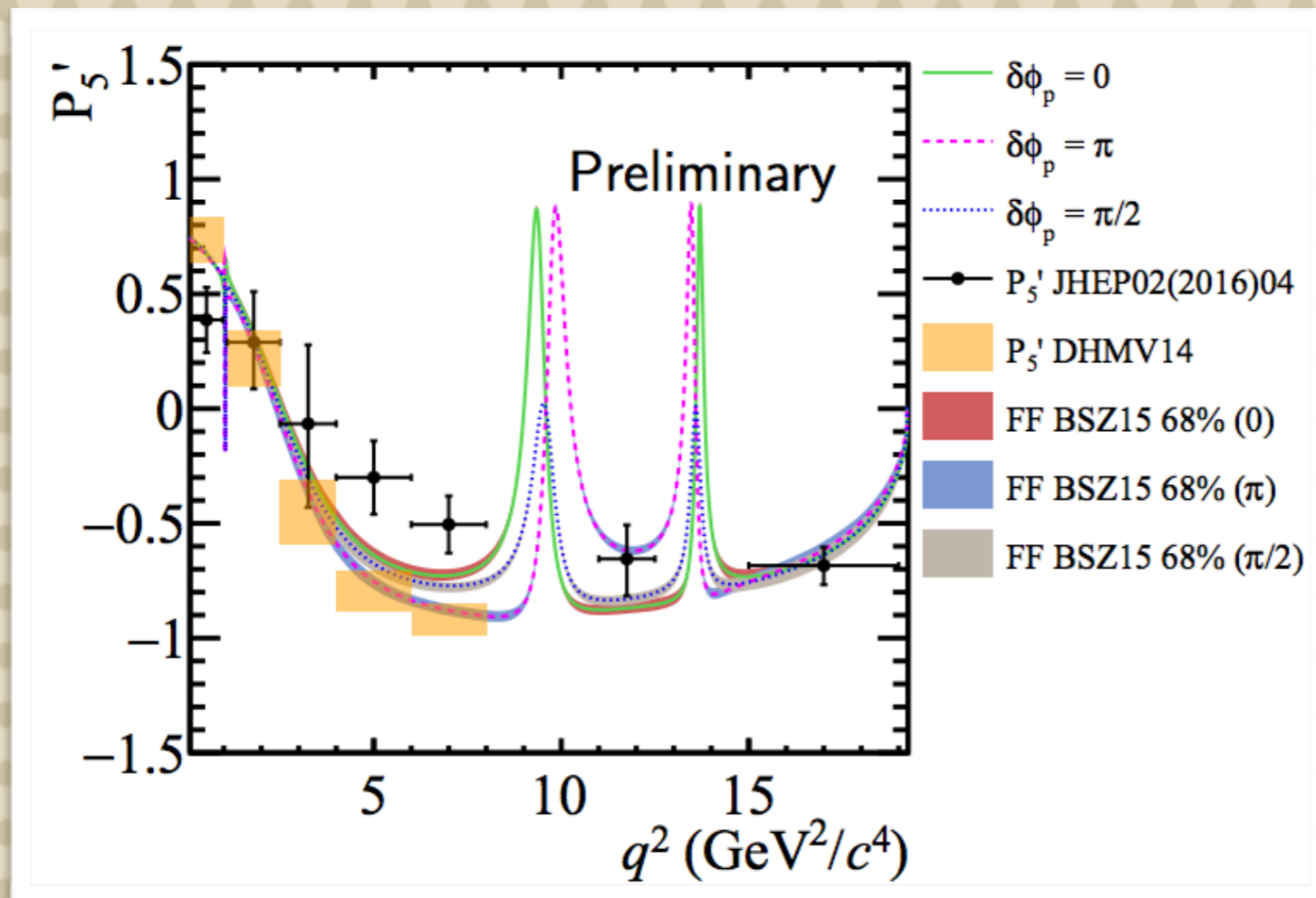
Decay	% of $B^+ \rightarrow K^+ \mu^+ \mu^-$
Penguin	0.6 %
$B^+ \rightarrow \rho K^+$	0.0003 %
$B^+ \rightarrow \omega K^+$	0.0006 %
$B^+ \rightarrow \phi K^+$	0.003 %
$B^+ \rightarrow J/\psi K^+$	92 %
$B^+ \rightarrow \psi(2S) K^+$	7.3 %
$B^+ \rightarrow \psi(3770) K^+$	0.007 %
$B^+ \rightarrow \psi(4040) K^+$	~ 0 %
$B^+ \rightarrow \psi(4160) K^+$	0.005 %
$B^+ \rightarrow \psi(4415) K^+$	~ 0 %



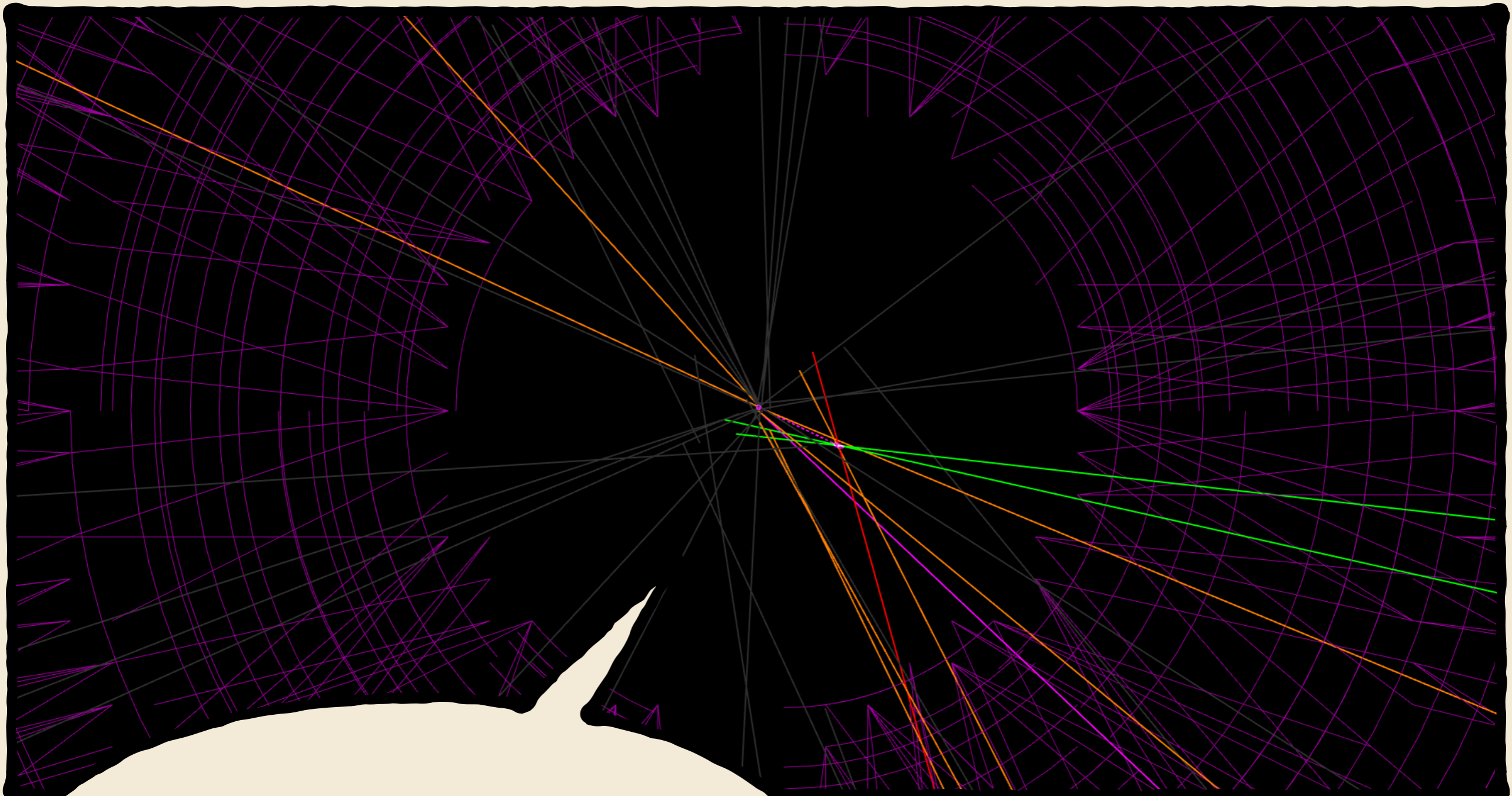
$$\frac{d\Gamma}{dq^2} = \frac{G_F^2 \alpha^2 |V_{tb} V_{ts}^*|^2}{27 \pi^5} |\mathbf{k}| \beta_+ \left\{ \frac{2}{3} |\mathbf{k}|^2 \beta_+^2 |C_{10}^{\text{eff}} f_+(q^2)|^2 + \frac{m_l^2 (M_B^2 - M_K^2)^2}{q^2 M_B^2} |C_{10}^{\text{eff}} f_0(q^2)|^2 \right. \\ \left. + |\mathbf{k}|^2 \left[1 - \frac{1}{3} \beta_+^2 \right] \left| C_9^{\text{eff}} f_+(q^2) + 2C_7^{\text{eff}} \frac{m_b + m_s}{M_B + M_K} f_T(q^2) \right|^2 \right\}$$

- Add all the resonances with BW and the try to fit for C_9

Trying to handle the $c\bar{c}$ -loop

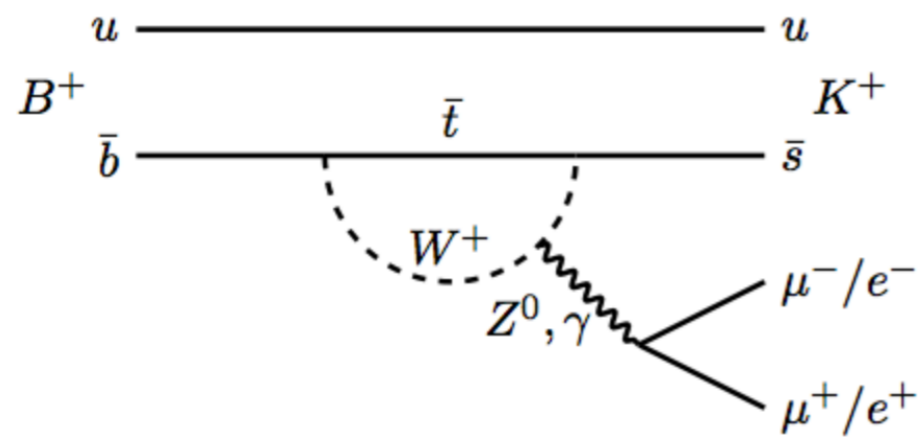


- Used SM predictions for $B^0 \rightarrow K^* \pi \pi$ with no charm loop
- Taking published measurements for the resonances
- Assuming the penguin pollution having small effect on the resonances
- Contribution from open charm missing



**Lepton Flavour
Universality (e/mu)**

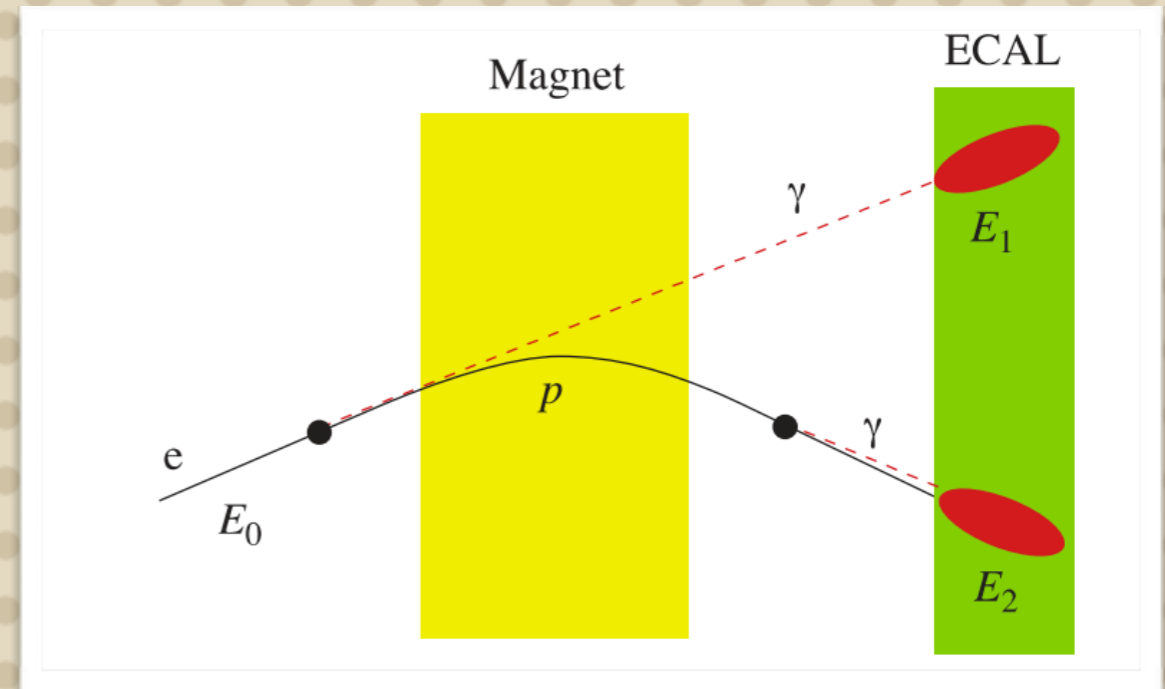
R_K Anomaly



$$R_K = \frac{\mathcal{B}(B^+ \rightarrow K^+ \mu^+ \mu^-)}{\mathcal{B}(B^+ \rightarrow K^+ e^+ e^-)}$$

$$R_K (\text{SM}) = 1.0003 \pm 0.0001$$

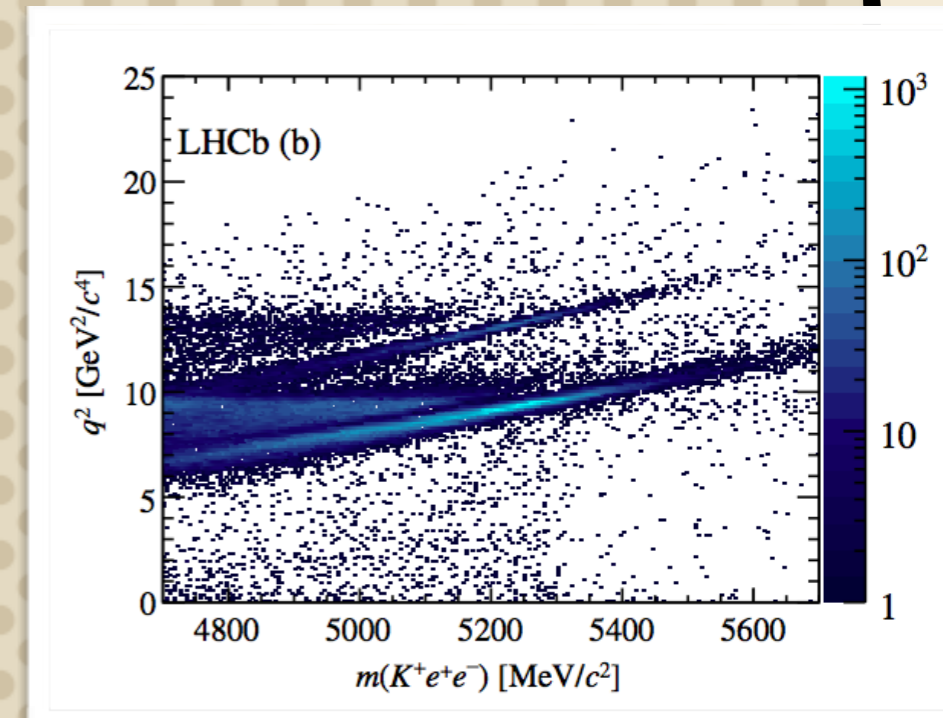
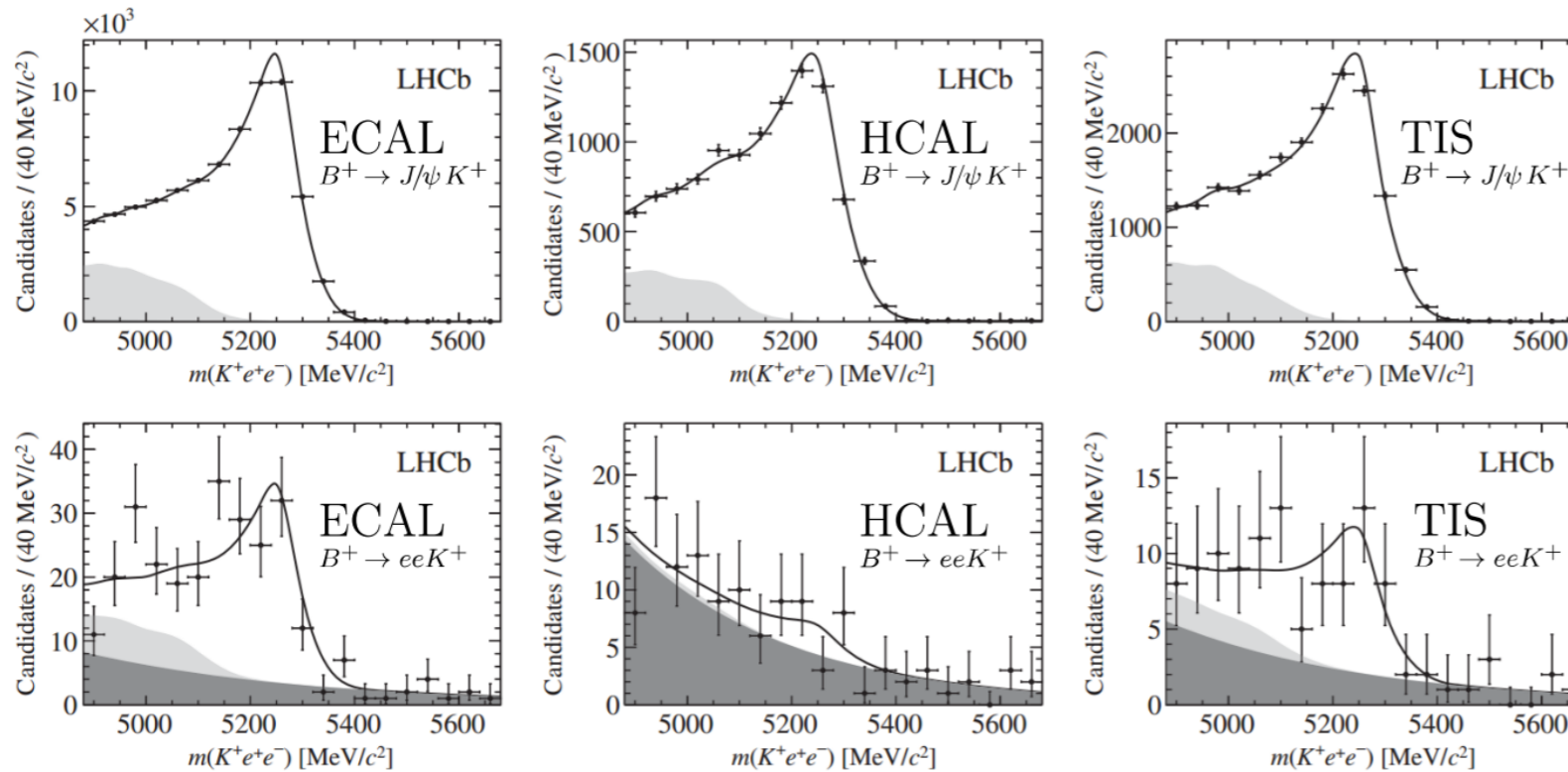
Bobeth et al., JHEP 12 (2007) 040



- Difficult bremsstrahlung recovery affects invariant mass resolution
- More complicated J/ψ veto
- Harder trigger, reconstruction, PID

R_K Anomaly

LHCb: PRD 113(2014).151601

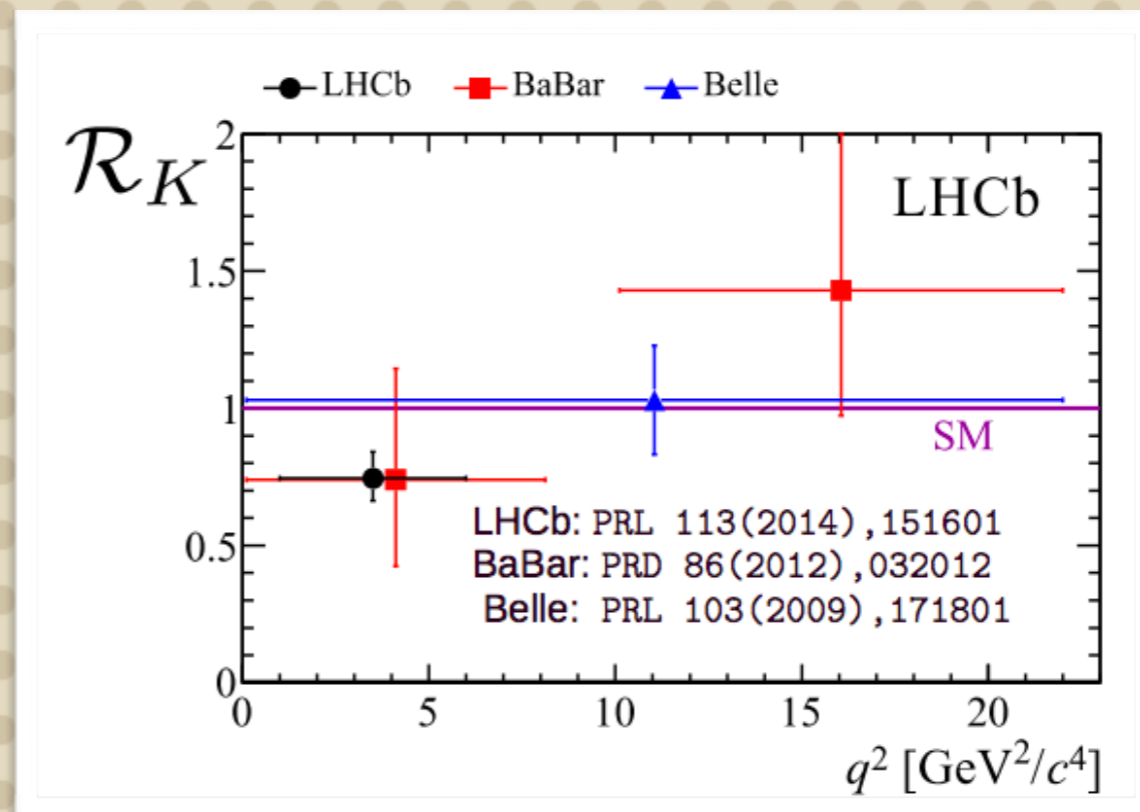
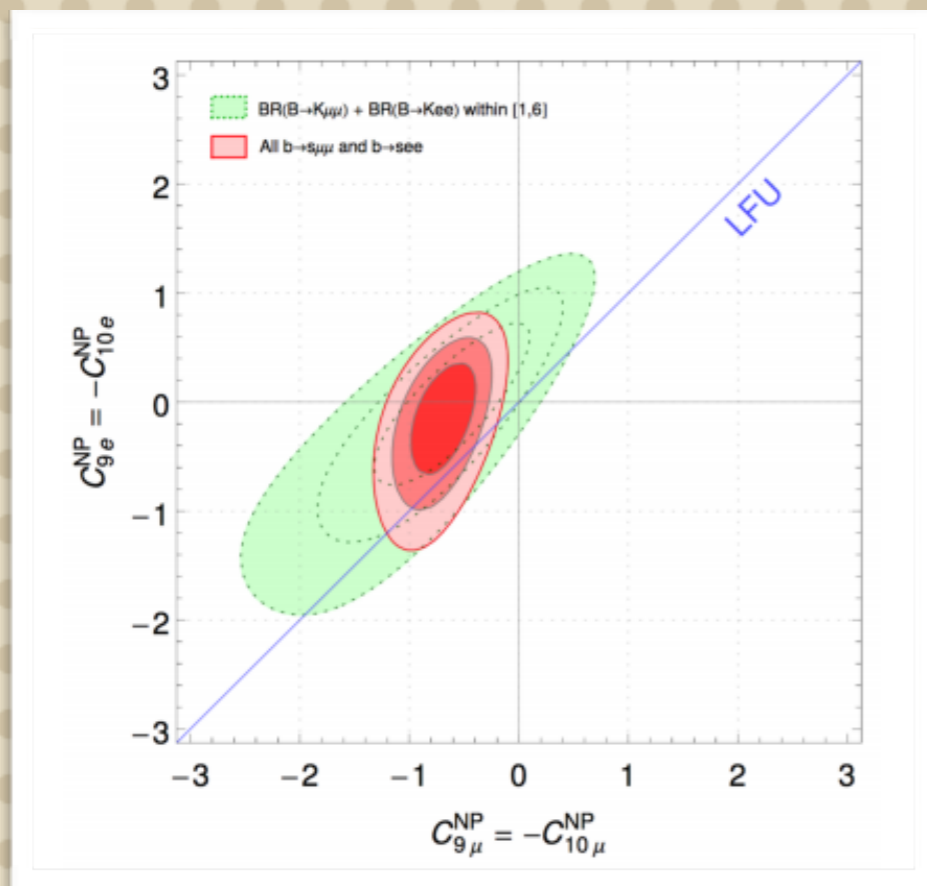


- Need to correct for q^2 migration, due to bremsstrahlung
- Total signal yield 264 events

$$\begin{aligned}
 \mathcal{R}_K &= \frac{\mathcal{B}(B^+ \rightarrow K^+ \mu^+ \mu^-)}{\mathcal{B}(B^+ \rightarrow K^+ J/\psi (\mu^+ \mu^-))} \frac{\mathcal{B}(B^+ \rightarrow K^+ J/\psi (e^+ e^-))}{\mathcal{B}(B^+ \rightarrow K^+ e^+ e^-)} = \\
 &= \frac{N_{K^+ \mu^+ \mu^-}}{N_{K^+ J/\psi (\mu^+ \mu^-)}} \frac{N_{K^+ J/\psi (e^+ e^-)}}{N_{K^+ e^+ e^-}} \frac{\epsilon_{K^+ J/\psi (\mu^+ \mu^-)}}{\epsilon_{K^+ \mu^+ \mu^-}} \frac{\epsilon_{K^+ e^+ e^-}}{\epsilon_{K^+ J/\psi (e^+ e^-)}} \\
 &\quad \rightarrow \text{cancel systematics}
 \end{aligned}$$

R_K Anomaly

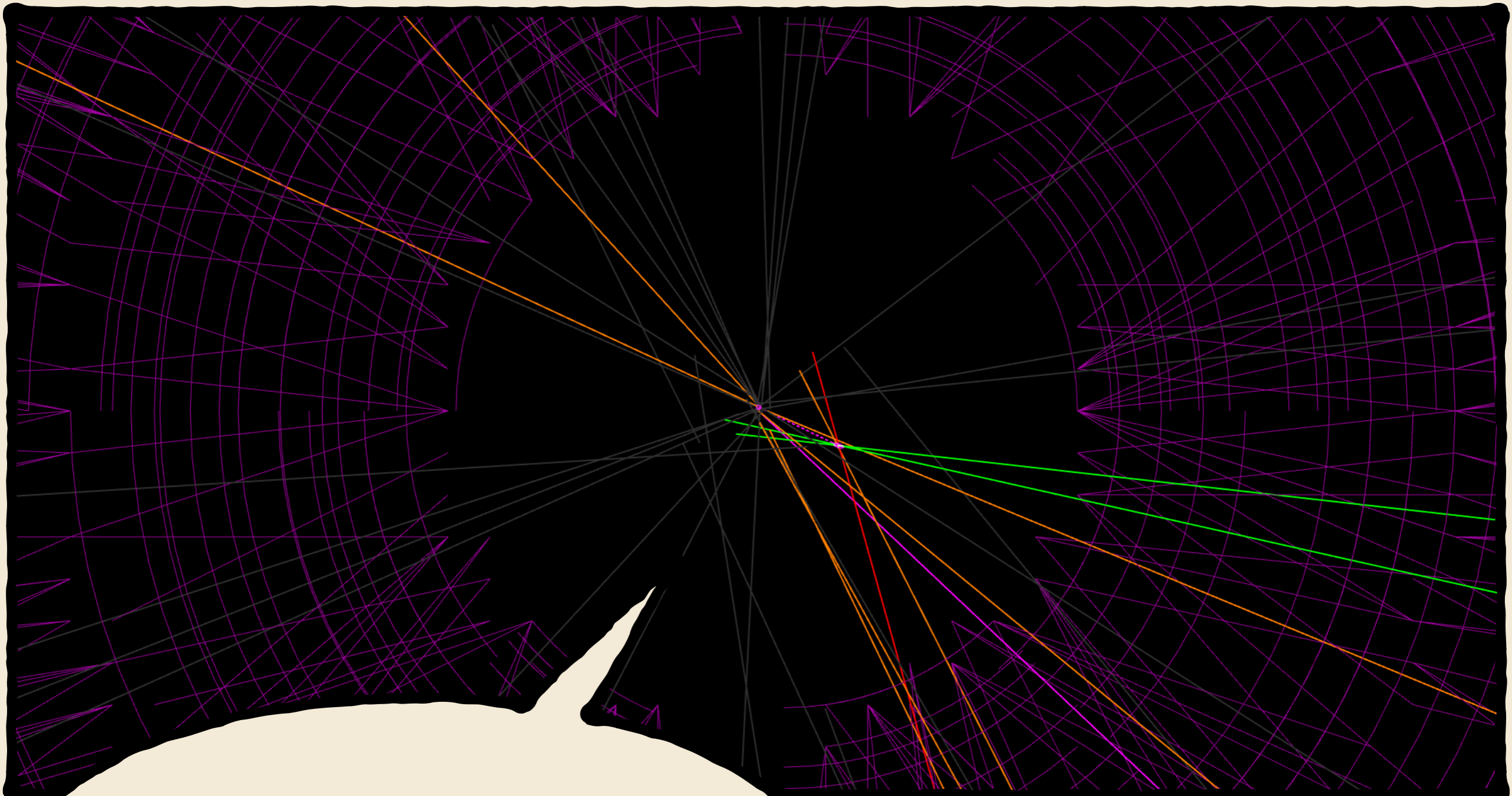
[Descotes-Genon/Hofer/Matias/Virto]



- Intriguing deficit in muon branching ratio compatible with the effect in $b \rightarrow smumu$ analyses (2.7 sigmas from SM)
- QCD uncertainties cancel out in the ratio
- Still statistically limited... need confirmation

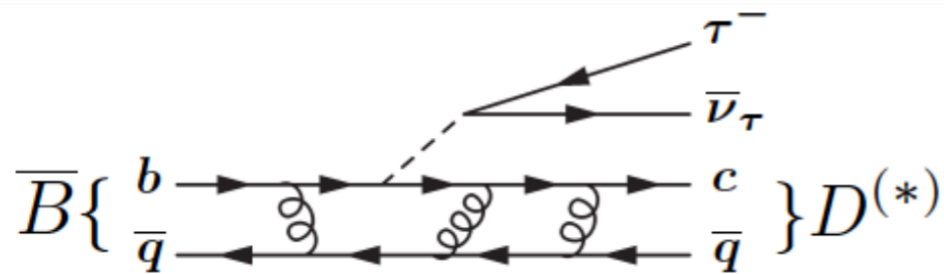
Future Measurements

- Measurement of LFU for $R_{K^*} = \text{BR}(B \rightarrow K^* e e) / \text{BR}(B \rightarrow K^* \mu \mu)$
- We can build asymmetries of angular observables, e.g. $R_{P5'}$ and R_{AFB} these are sensitive to C_9 and C_{10}
- Since we are studying LFU no reason to restrict to the $K^*(892)$, so we should test LFU in $B \rightarrow K \pi \ell \ell$ and $B^+ \rightarrow K^+ \pi \pi \ell \ell$
- We can test LFU in $L_b \rightarrow p K \ell \ell$



**Lepton Flavour
Universality (tau/mu)**

Semileptonic decays



$$\mathcal{R}(D^{(*)}) = \frac{\mathcal{B}(\bar{B} \rightarrow D^{(*)} \tau \nu)}{\mathcal{B}(\bar{B} \rightarrow D^{(*)} \ell \nu)} = \frac{\text{signal}}{\text{normalization}} \quad (\ell = e, \mu)$$

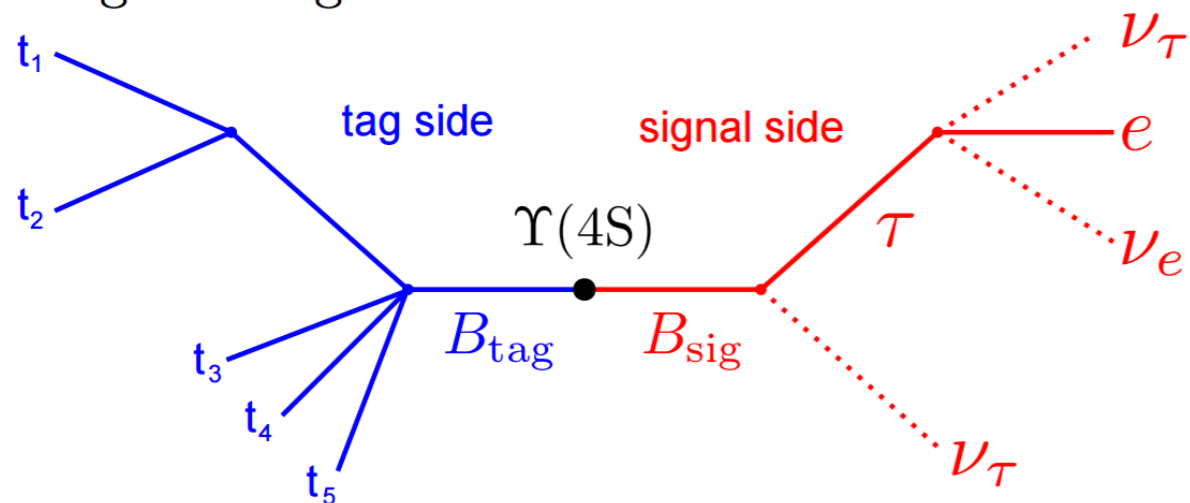
- B-factories measure $\tau \rightarrow e, \mu 2\nu$
- LHCb measures $\tau \rightarrow \mu 2\nu$

$$\frac{d\Gamma_\tau}{dq^2} = \frac{G_F^2 |V_{cb}|^2 |\mathbf{p}_{D^{(*)}}^*| q^2}{96\pi^3 m_B^2} \left(1 - \frac{m_\tau^2}{q^2}\right)^2 \left[(|H_+|^2 + |H_-|^2 + |H_0|^2) \left(1 + \frac{m_\tau^2}{2q^2}\right) + \frac{3m_\tau^2}{2q^2} |H_s|^2 \right]$$

- Since the D -meson is a scalar H_{\pm} vanish
- Amplitudes depend on 4 universal FFs extracted from data
- Four free parameters in the fit
- In the case of the e/μ H_s is suppressed by the mass, so this is only present in the channel with the tau (from HQET)

B-factory strategy

Tag- and signal-side of the full reconstruction



$$\mathcal{R}(D^{(*)}) \equiv \frac{\mathcal{B}(B \rightarrow D^{(*)} \tau \nu)}{\mathcal{B}(B \rightarrow D^{(*)} \ell \nu)} = \frac{\int_{m_\tau^2}^{q_{\max}^2} \frac{d\Gamma_\tau}{dq^2} dq^2}{\int_{m_\ell^2}^{q_{\max}^2} \frac{d\Gamma_\ell}{dq^2} dq^2}$$

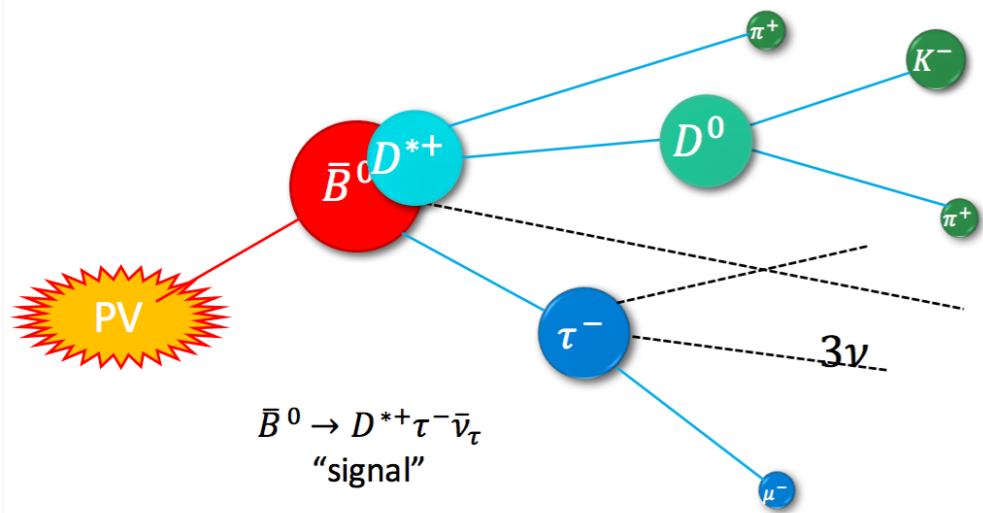
Hadronic tag analyses:

- Reconstruct tag B meson in all hadronic mode
- Precise knowledge of kinematic of missing system
- Kill background, but efficiency about 10^{-3}

Semileptonic analyses:

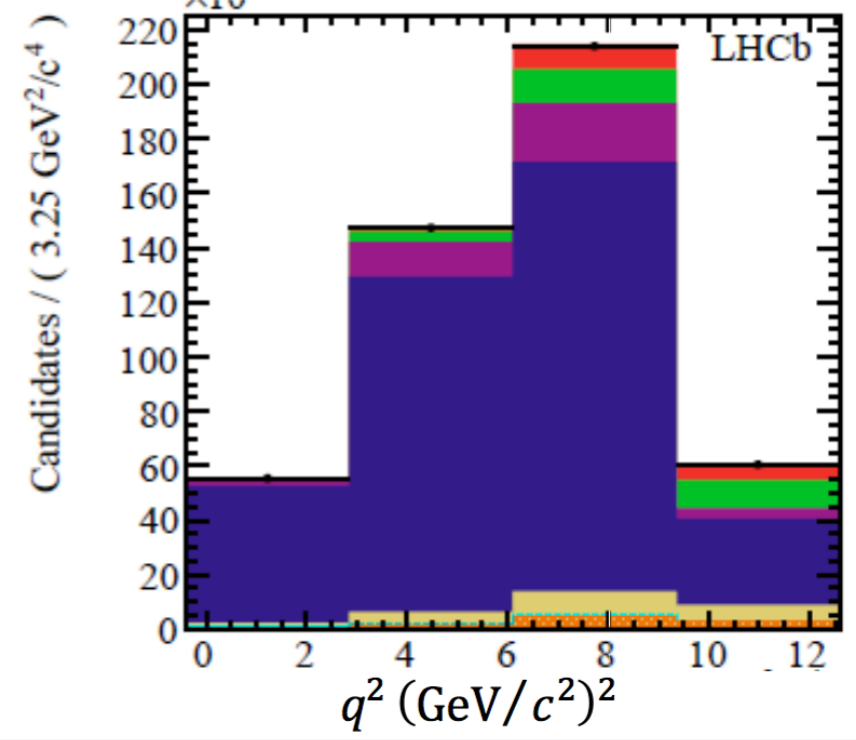
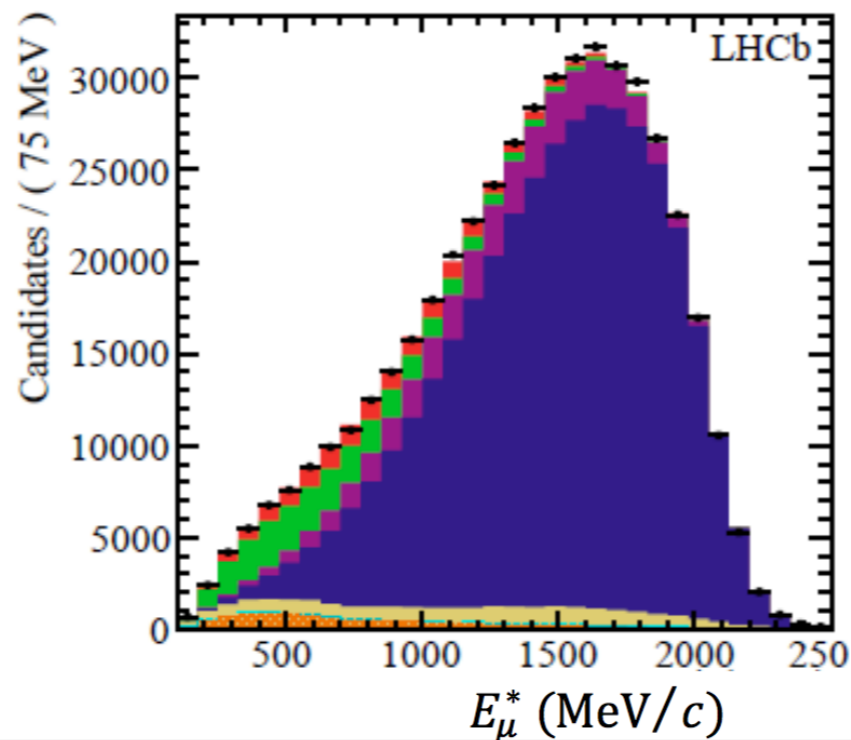
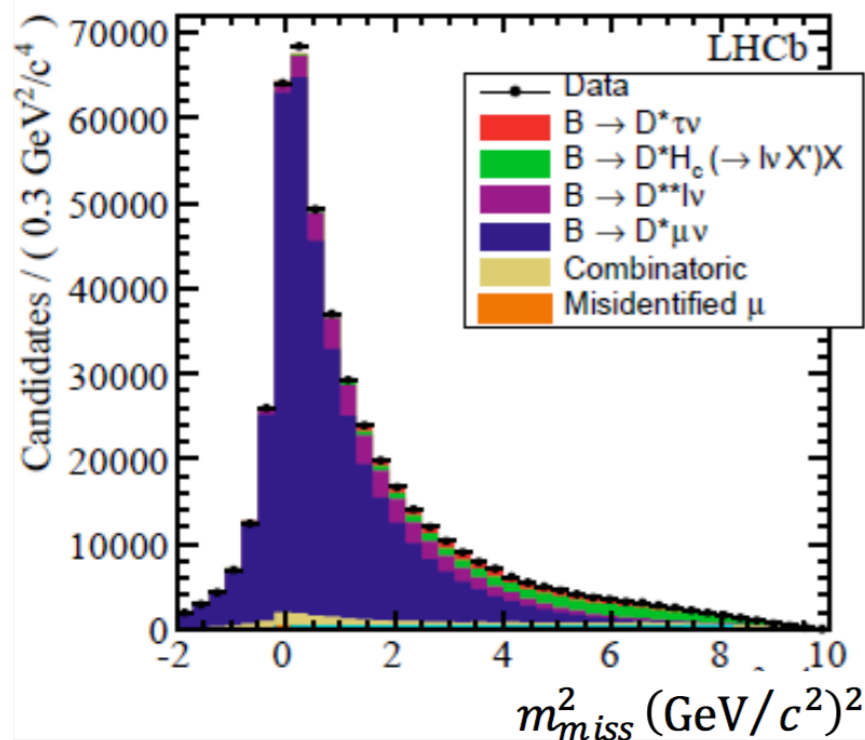
- Tag B-meson in semileptonic channel
- Selection: E_τ , missing mass and angle between D^{*l} and B

LHCb Strategy



$$(\gamma\beta_z)_{\bar{B}} = (\gamma\beta_z)_{D^* \mu} \Rightarrow (p_z)_{\bar{B}} = \frac{m_B}{m(D^* \mu)} (p_z)_{D^* \mu}$$

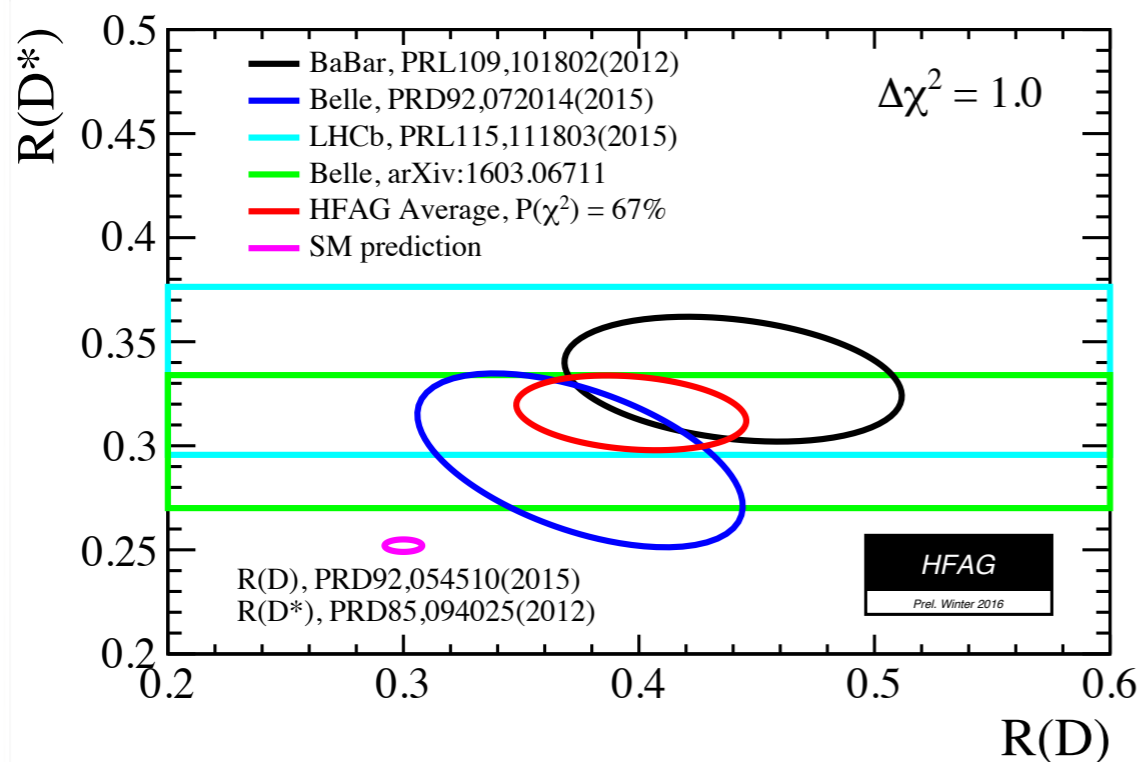
- B-direction given by PV-SV
- Full fit of the MM, E^* , q^2
- Muon, tau modes and bkg fit simultaneously



Results

From HFAG webpage

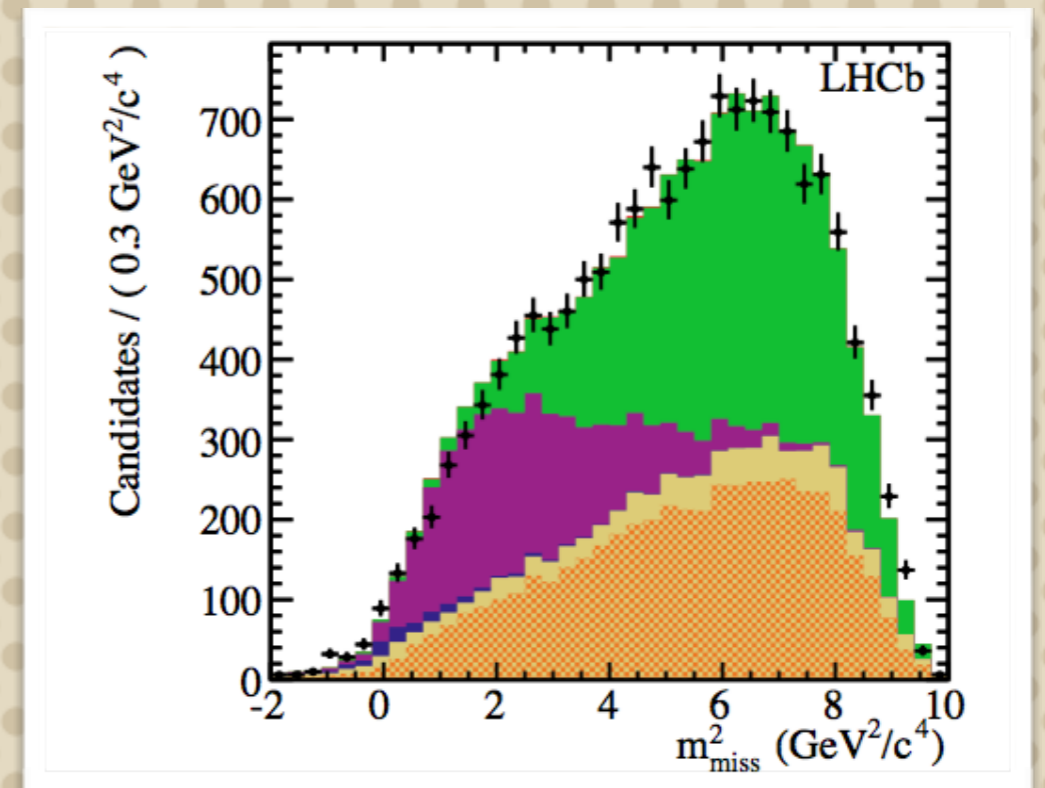
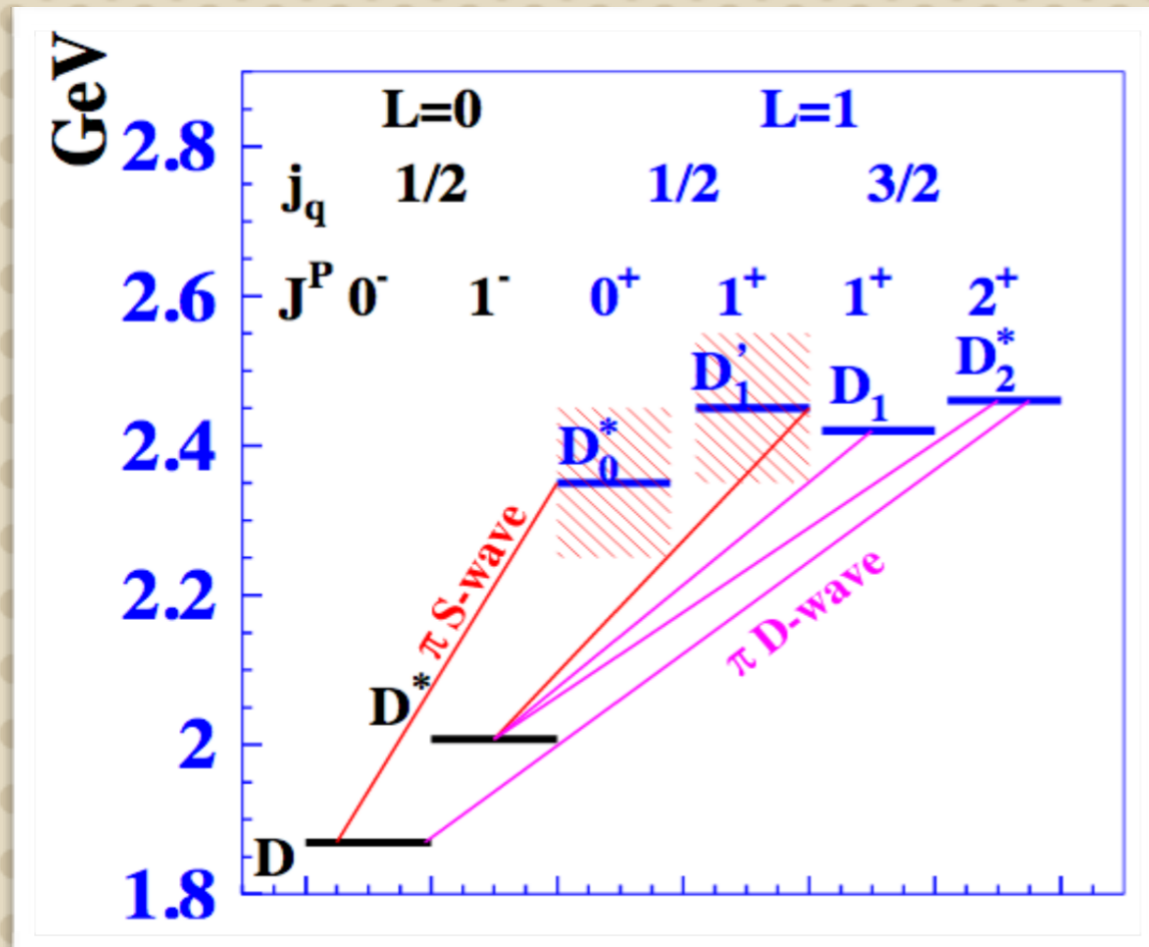
Experiment	R(D*)	R(D)	Rescaled Correlation (stat/syst/total)	Parameters	Remarks
BaBar	0.332 +/- 0.024 +/- 0.018	0.440 +/- 0.058 +/- 0.042	-0.45/-0.07/-0.27	input	Phys.Rev.Lett. 109,101802 (2012) [arXiv:1205.5442 [hep-ex]] Phys.Rev.D 88, 072012 (2013) [arXiv:1303.0571]
BELLE	0.293 +/- 0.038 +/- 0.015	0.375 +/- 0.064 +/- 0.026	-0.56/-0.11/-0.49	input	Phys.Rev.D 92, 072014 (2015) [arXiv:1507.03233 [hep-ex]]
BELLE	0.302 +/- 0.030 +/- 0.011	-	-	input	Preliminary at Moriond EW 2016 [arXiv:1603.06711 [hep-ex]]
LHCb	0.336 +/- 0.027 +/- 0.030	-	-	input	Phys.Rev.Lett.115,111803 (2015) [arXiv:1506.08614 [hep-ex]]
Average	0.316 +/- 0.016 +/- 0.010	0.397 +/- 0.040 +/- 0.028	-0.21	chi2/dof = 2.38/4 (CL = 0.67)	pdf png



Deviation of about 4sigmas wrt SM predictions!

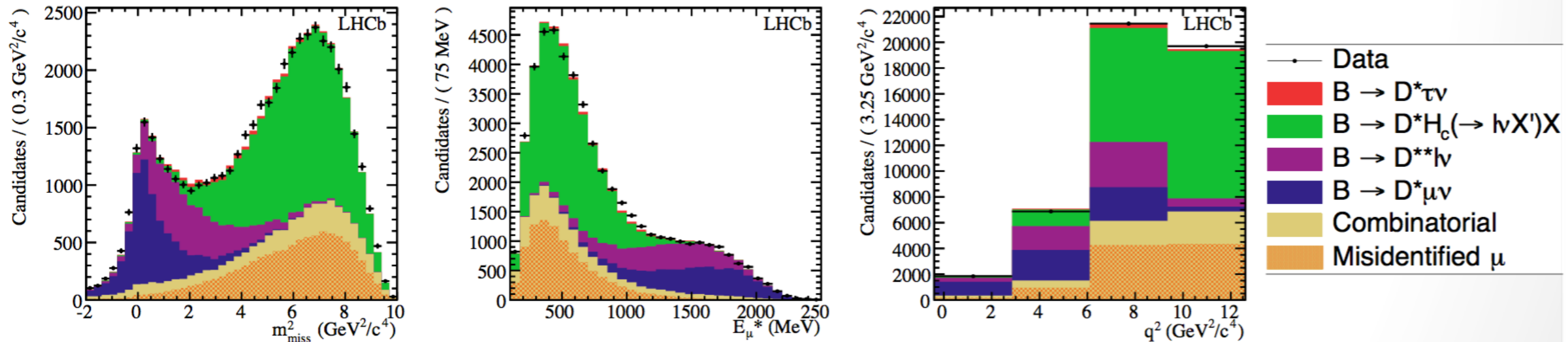
Experimental challenges

example $B \rightarrow D^* \pi \pi l \nu$



- Large contribution from excited D^{**} states
- Narrow states ($D_1^{(*)}$ and D_2^*) fit directly from data $B \rightarrow D^* \pi \pi l \nu$ used as a control sample
- Higher D^{**} excited states also fit from data and $B \rightarrow D \pi \pi l \nu$ used as a control channel

Double Charm Bkg



- As usual charm is a background for tau
- Bkg from $D_s \rightarrow \tau \nu$, $D \rightarrow K l \nu$ fit directly from data
- Control sample obtained reconstructing $B \rightarrow D^* K l \nu$

Future (LHCb) Prospects

- $R(D^*)$ measurement using tau $\rightarrow 3\pi$, advantage of knowing the decay vertex of the tau
- $L_b \rightarrow Lc^{(*)} \tau \nu$, cleaner because of the proton in the final state allows to constrain the double charm bkg
- $R(D^+)$ less feed down and large statistics
- Interesting to measure muon/tau universality for $b \rightarrow u$ transitions, e.g. using $L_b \rightarrow p \tau \nu$



Conclusions

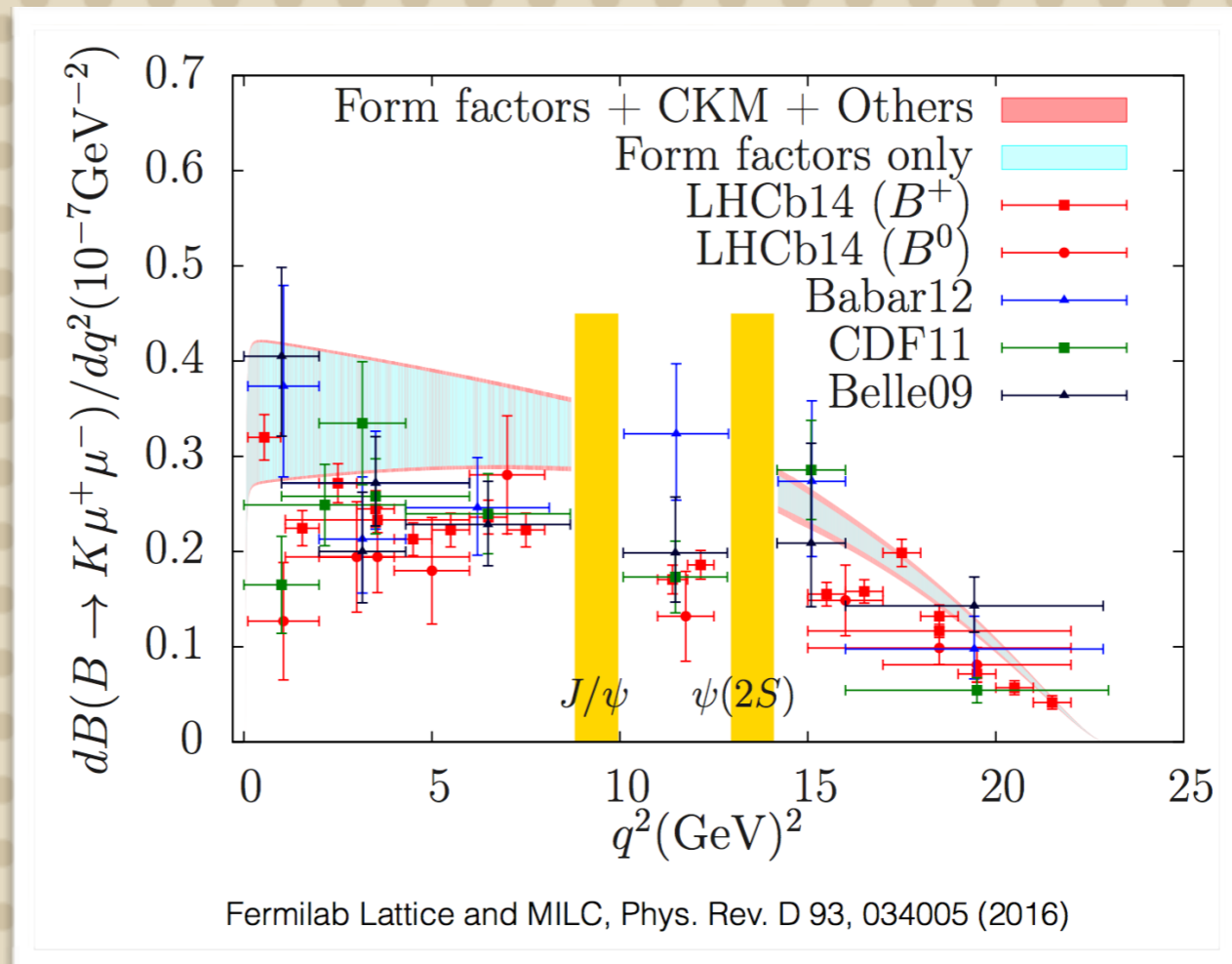
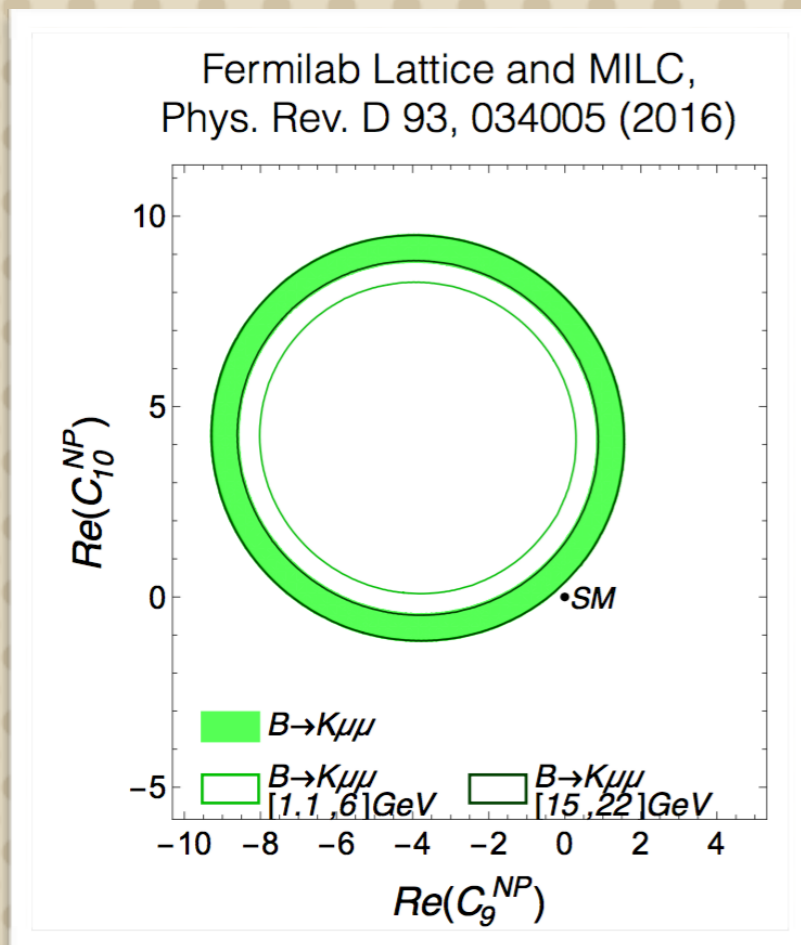
Conclusions

- There are intriguing anomalies in the flavour physics, maybe a coherent pattern
- Measurements of $b \rightarrow s \mu \mu$ transitions at LHCb show discrepancies wrt SM (modulo $c\bar{c}$ contributions, possible to determine this measuring $c\bar{c}$ resonances + open charm?)
- LFU deviations in R_K shows a discrepancy of 2.7 sigmas, many other measurements can confirm/disprove this deviation
- Significant deviations (about 4 sigmas) in tree level decays with taus in the final state (BaBar, Belle, LHCb), interesting to test LFU (μ/τ) in other tree decays

A hand-drawn speech bubble with a thick black outline. The background of the slide is a light beige color with a pattern of small, light brown dots. The speech bubble is white and contains the text "Backup slides" in a bold, black, sans-serif font. The speech bubble has a tail pointing towards the bottom right corner.

Backup slides

$B^+ \rightarrow K^+ \mu \mu$

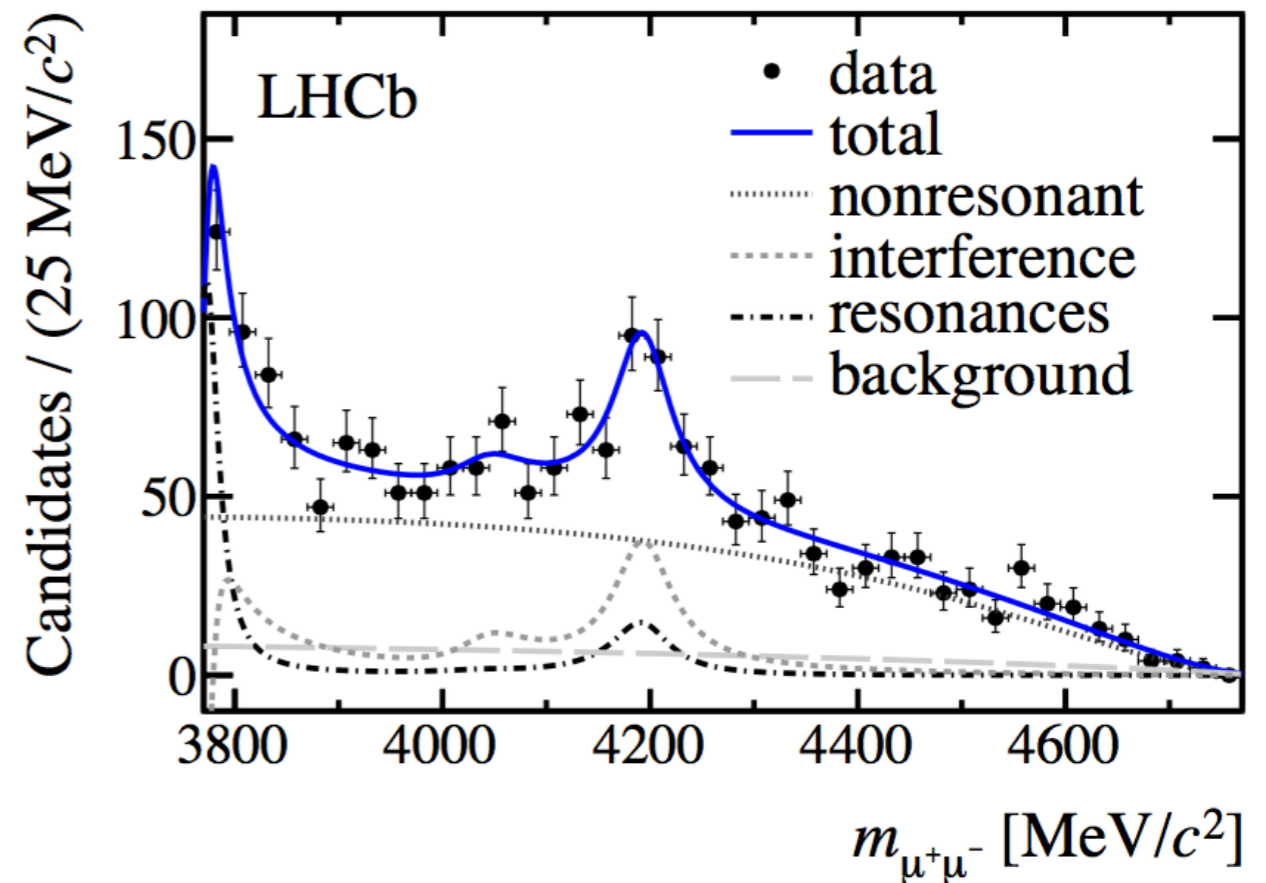
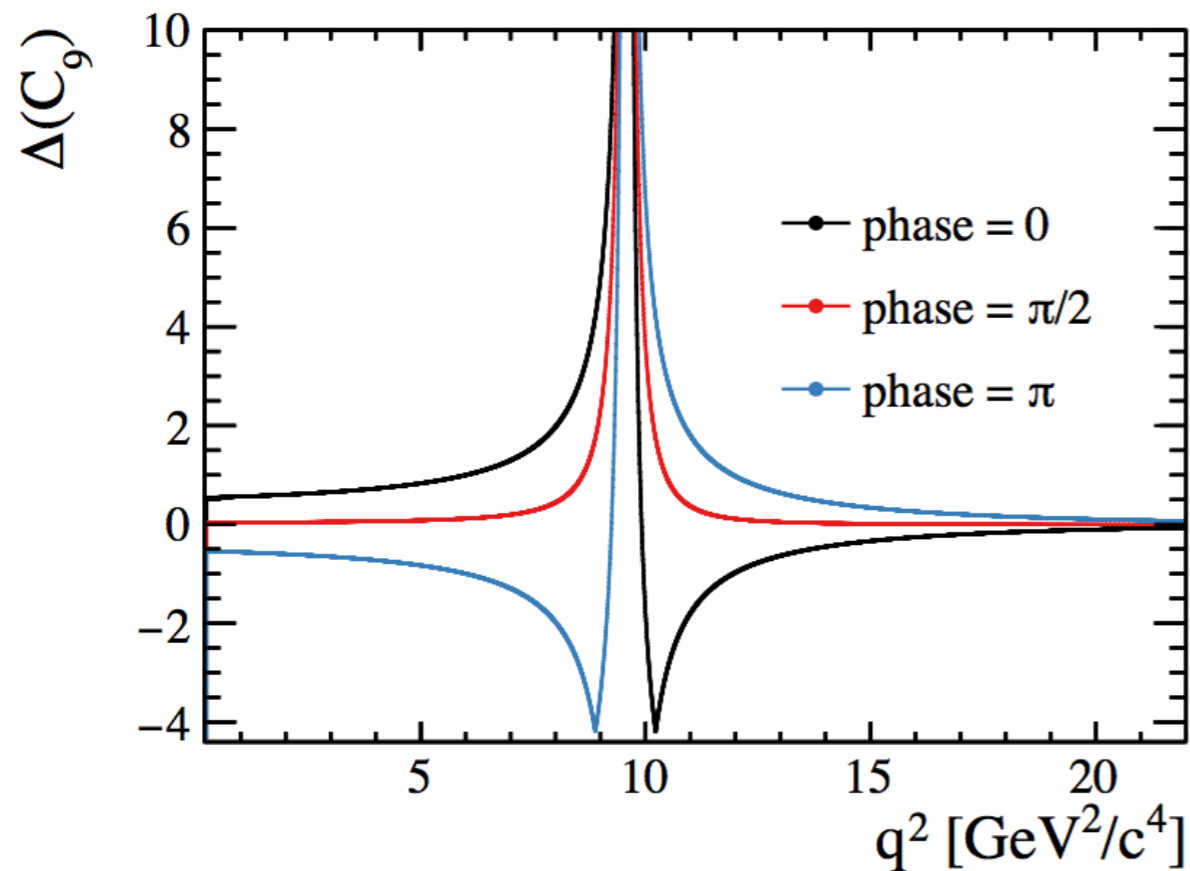


$$\frac{d\Gamma}{dq^2} = \frac{G_F^2 \alpha^2 |V_{tb} V_{ts}^*|^2}{27 \pi^5} |\mathbf{k}| \beta_+ \left\{ \frac{2}{3} |\mathbf{k}|^2 \beta_+^2 |C_{10}^{\text{eff}} f_+(q^2)|^2 + \frac{m_l^2 (M_B^2 - M_K^2)^2}{q^2 M_B^2} |C_{10}^{\text{eff}} f_0(q^2)|^2 \right. \\ \left. + |\mathbf{k}|^2 \left[1 - \frac{1}{3} \beta_+^2 \right] \left| C_9^{\text{eff}} f_+(q^2) + 2C_7^{\text{eff}} \frac{m_b + m_s}{M_B + M_K} f_T(q^2) \right|^2 \right\},$$

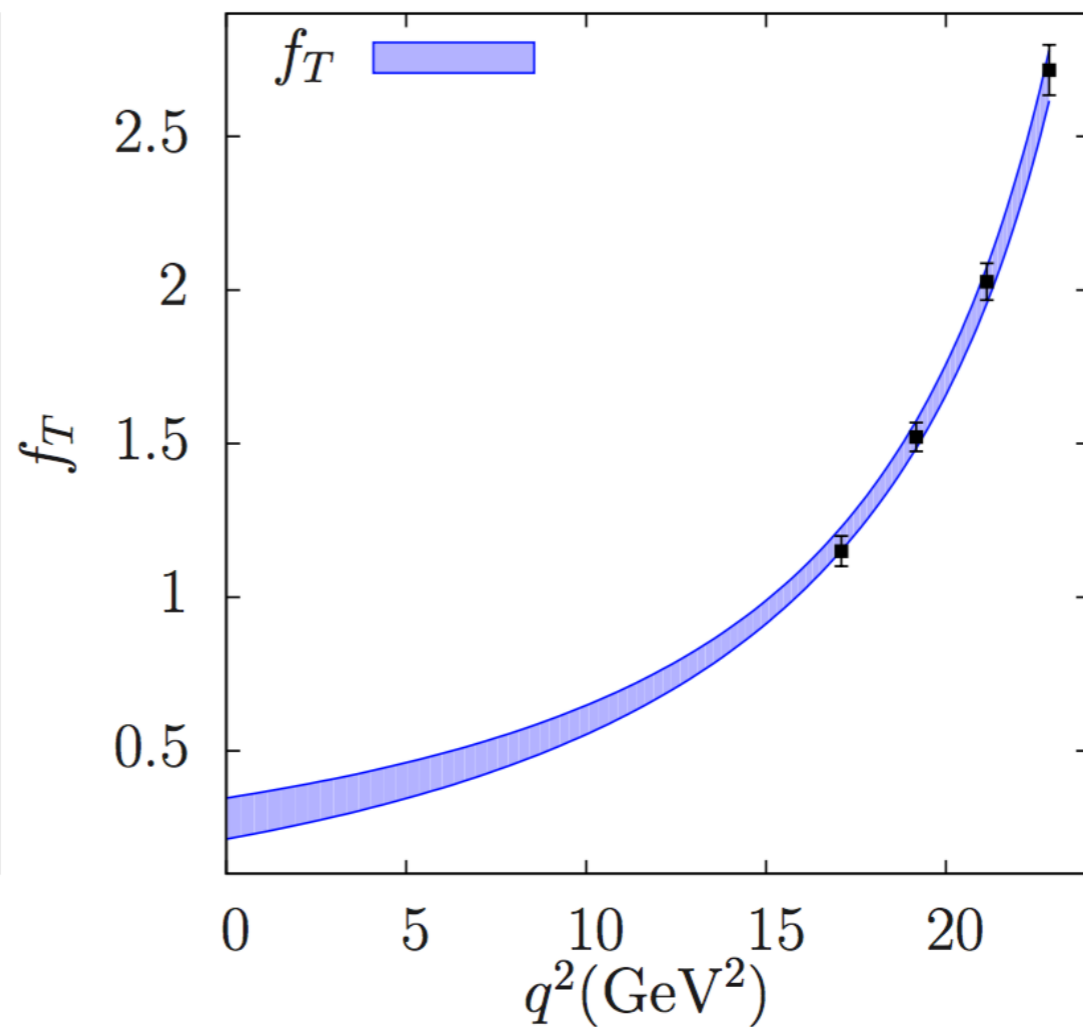
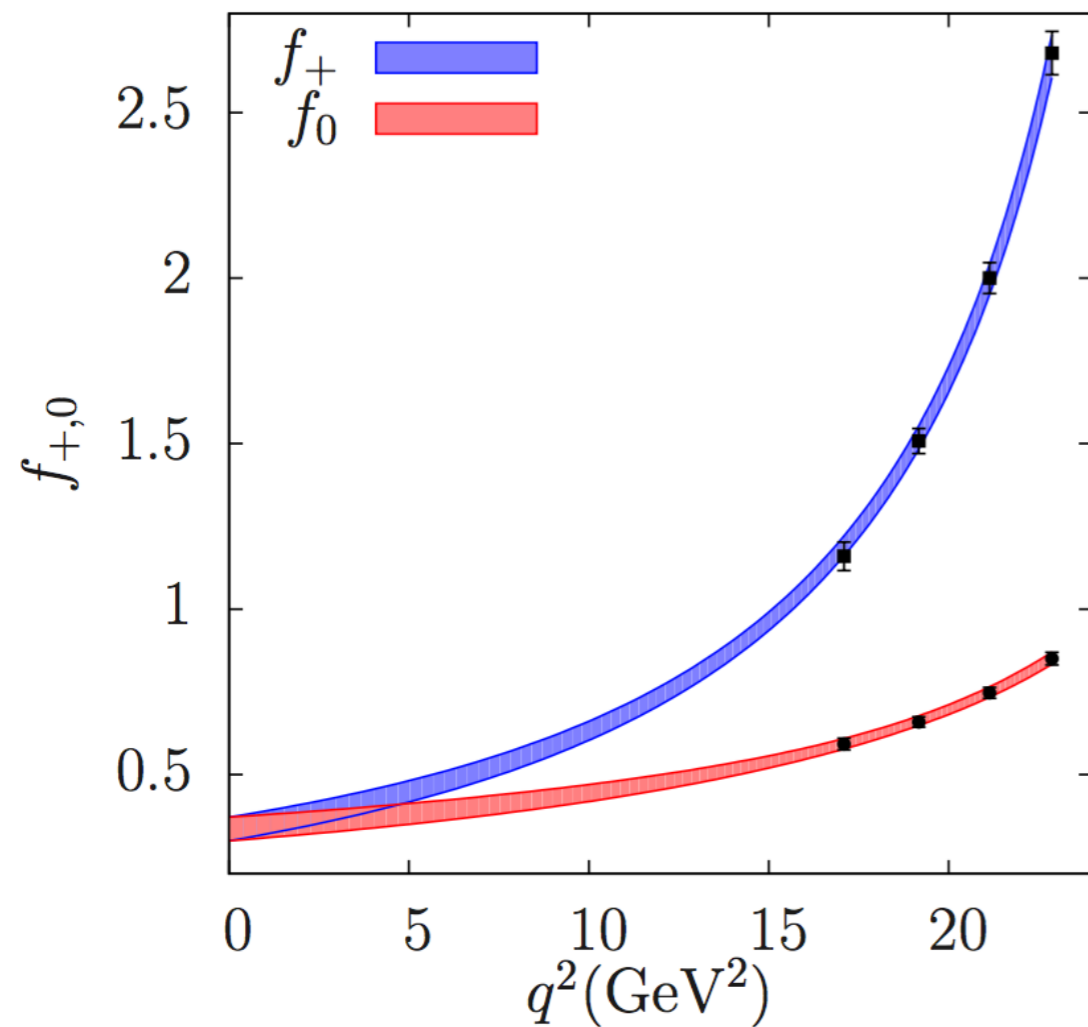
Equation from Fermilab Lattice and MILC, Phys. Rev. D 93, 025026

$B^+ \rightarrow K^+ \mu\mu$

Effect of interference between the $B \rightarrow J\psi K$ and the rare mode $B \rightarrow K\mu\mu$ on DC_9

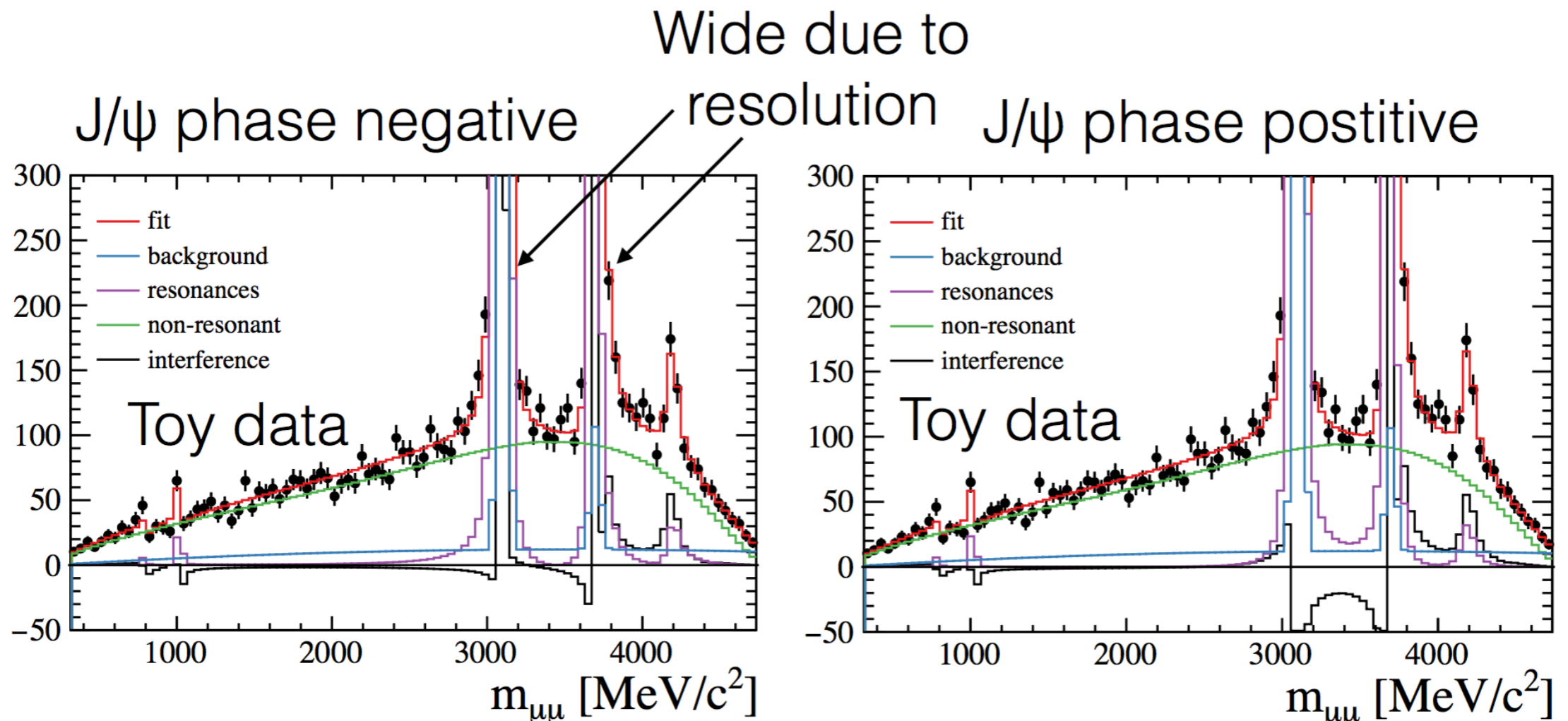


$B^+ \rightarrow K^+ \pi \pi$



Fermilab Lattice and MILC, Phys. Rev. D 93, 025026

$B^+ \rightarrow K^+ \mu\mu$



Uncertainty on phase is about 0.1rad with four minima.
Ambiguities whether J/ ψ or $\psi(2S)$ phase is negative/positive.

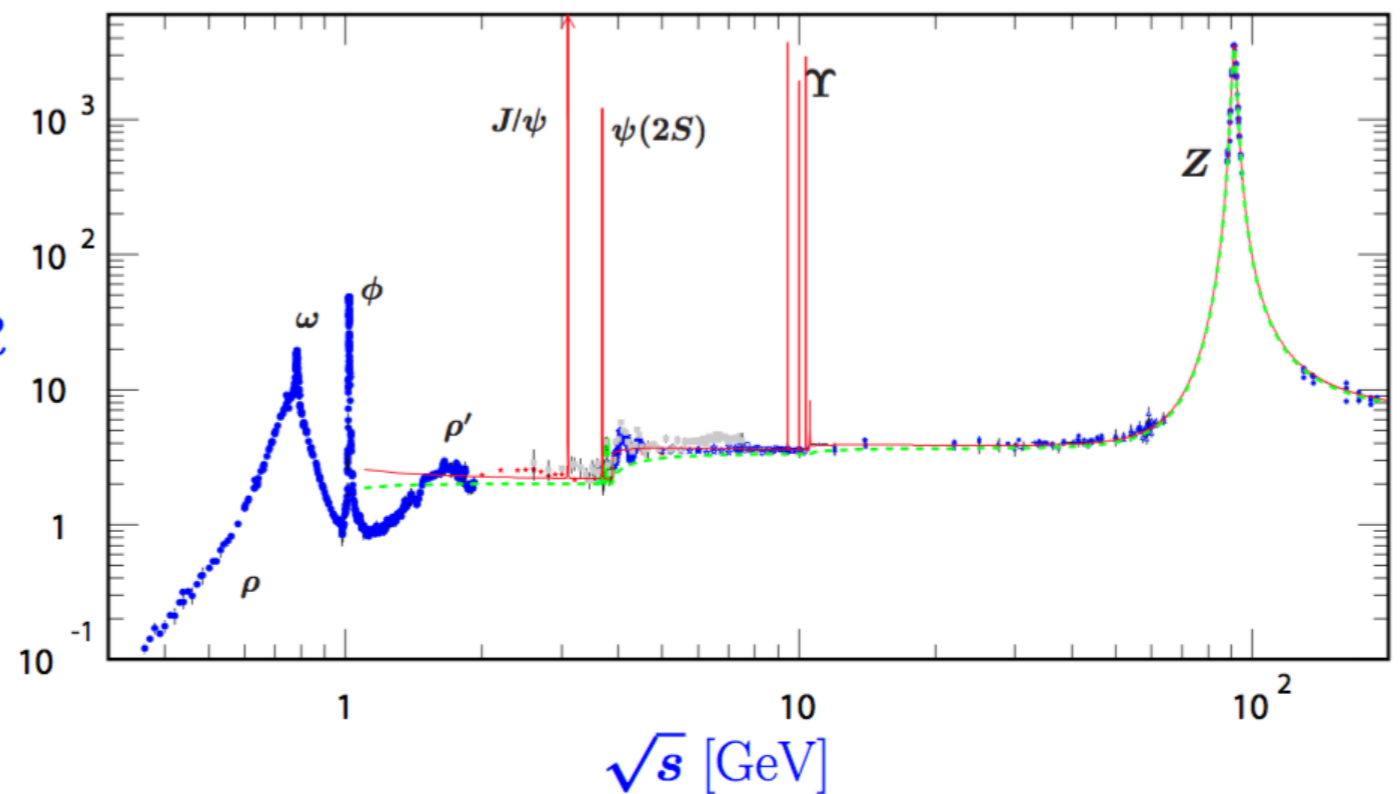
$B^+ \rightarrow K^+ \pi \pi$

- What about additional broad contributions such as $\rho'/\omega'/\phi'$?
- We cannot fit for this as there is literally an infinite number.

$$R = \frac{\sigma(e^+e^- \rightarrow \text{hadrons})}{\sigma(e^+e^- \rightarrow \mu^+\mu^-)}$$

R

- The nominal fit ignores these contributions.



B \rightarrow K* mm

- ▶ Introduce relativistic Breit-Wigner to each C_9^{eff} term of each transversity amplitude with relative phase and magnitude $\chi_{0,\parallel,\perp}, \eta_{0,\parallel,\perp}$ (common for L and R)
- ▶ Fit for the angular and q^2 distribution across full q^2 range, to determine $\chi_{0,\parallel,\perp}$ and $\eta_{0,\parallel,\perp}$
 - ▷ Relations between amplitudes explicitly encoded \rightarrow no redundant information

$$A_{\perp}^{L(R)} = N\sqrt{2\lambda} \left\{ [(C_9^{\text{eff}} + C_9^{\prime\text{eff}}) \mp (C_{10}^{\text{eff}} + C_{10}^{\prime\text{eff}})] \frac{V(q^2)}{m_B + m_{K^*}} + \frac{2m_b}{q^2} (C_7^{\text{eff}} + C_7^{\prime\text{eff}}) T_1(q^2) \right\}$$

$$A_{\parallel}^{L(R)} = -N\sqrt{2}(m_B^2 - m_{K^*}^2) \left\{ [(C_9^{\text{eff}} - C_9^{\prime\text{eff}}) \mp (C_{10}^{\text{eff}} - C_{10}^{\prime\text{eff}})] \frac{A_1(q^2)}{m_B - m_{K^*}} + \frac{2m_b}{q^2} (C_7^{\text{eff}} - C_7^{\prime\text{eff}}) T_2(q^2) \right\}$$

$$A_0^{L(R)} = -\frac{N}{2m_{K^*}\sqrt{q^2}} \left\{ [(C_9^{\text{eff}} - C_9^{\prime\text{eff}}) \mp (C_{10}^{\text{eff}} - C_{10}^{\prime\text{eff}})] [(m_B^2 - m_{K^*}^2 - q^2)(m_B + m_{K^*}) A_1(q^2) - \lambda \frac{A_2(q^2)}{m_B + m_{K^*}}] \right. \\ \left. + 2m_b (C_7^{\text{eff}} - C_7^{\prime\text{eff}}) [(m_B^2 + 3m_{K^*}^2 - q^2) T_2(q^2) - \frac{\lambda}{m_B^2 - m_{K^*}^2} T_3(q^2)] \right\}$$

$B \rightarrow K^* \mu \mu$

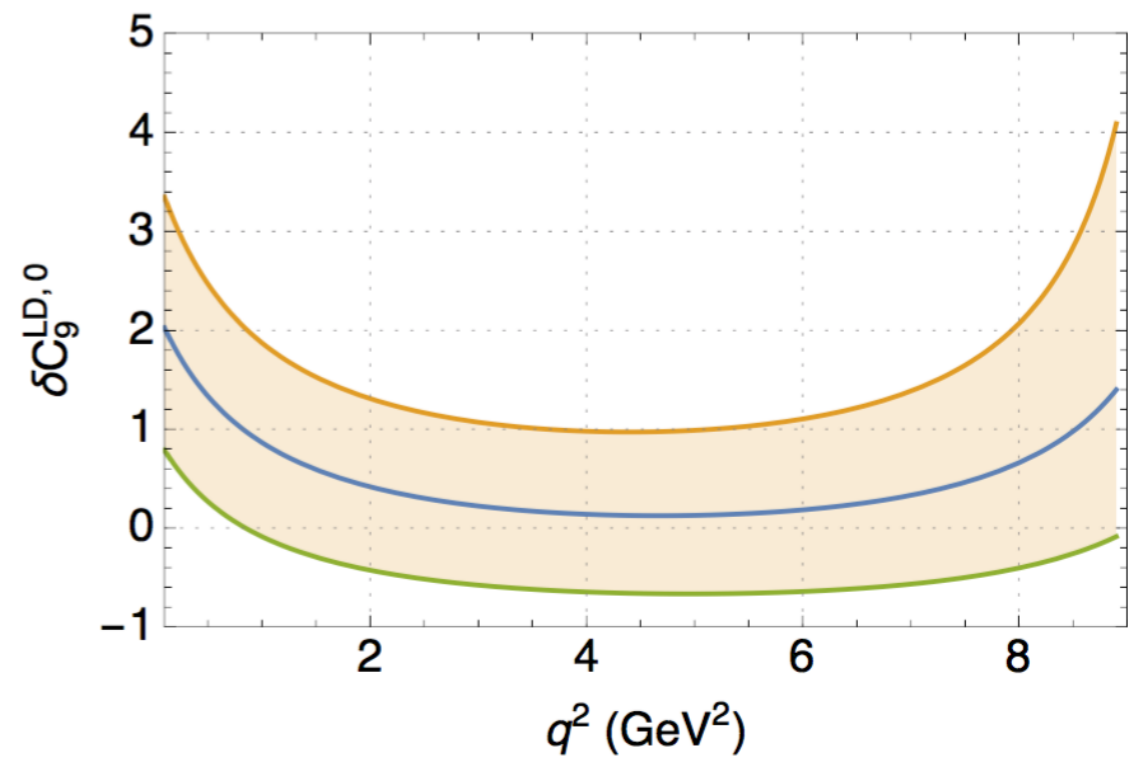
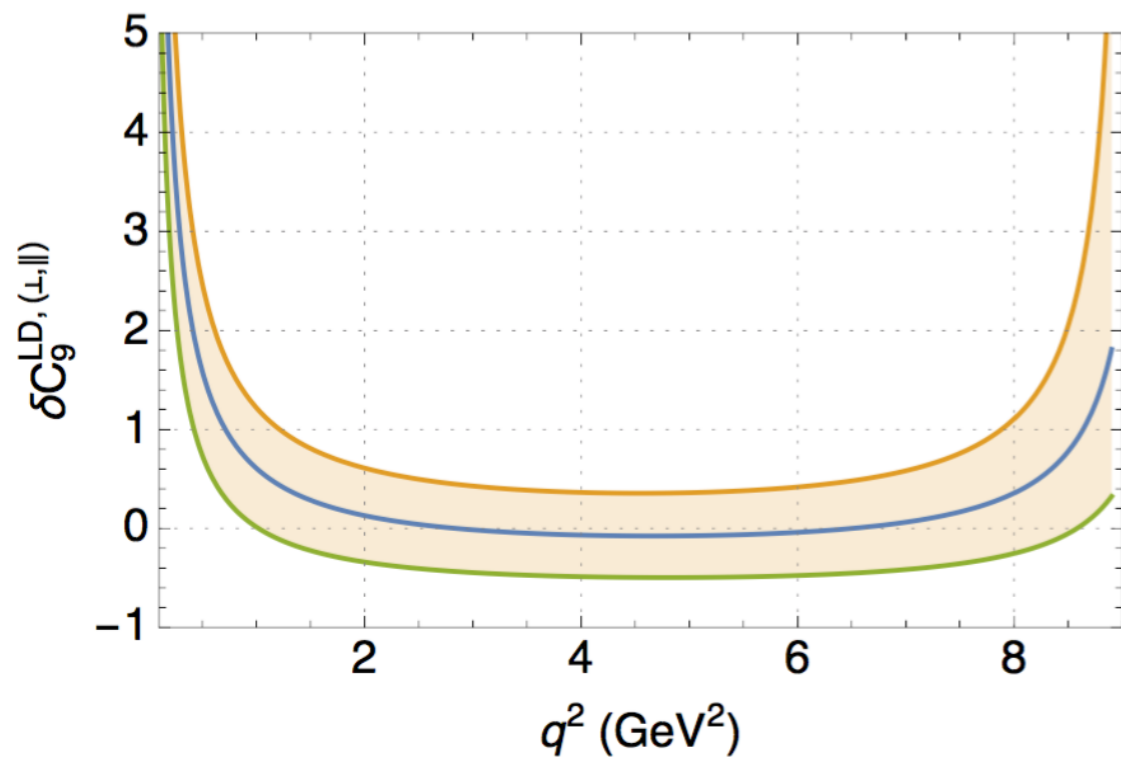
- ▶ Angular analyses of $B^0 \rightarrow J/\psi K^{*0}$, $B^0 \rightarrow \psi(2S)K^{*0}$ and $B^0 \rightarrow \phi K^{*0}$ determine relative magnitudes and phases between transversity amplitudes of the decay LHCb[PRD88,052002(2013)], Belle[PRD88,074026(2013)], LHCb[JHEP1405(2014)069] e.g.
 - ▷ $|A_{\perp}^{J/\psi}|^2 = 0.20 \pm 0.01$, $|A_{\parallel}^{J/\psi}|^2 = 0.23 \pm 0.01$,
 $\delta_{\perp}^{J/\psi} = 2.94 \pm 0.03$, $\delta_{\parallel}^{J/\psi} = -2.94 \pm 0.04$,
- ▶ Combined with branching fraction measurements from PDG, we can estimate $\chi_{0,\parallel,\perp}$ and $\eta_{0,\parallel,\perp}$ up to a single overall phase difference with the penguin mode ($\delta\phi_p$) for each resonance
- ▶ The naive assumption is made that the effect of the penguin contribution within the resonant regions has a small effect on the relative magnitude and phases of the resonant amplitudes

c cbar loop

$$\delta C_9^{\text{LD},(\perp,\parallel)}(q^2) = \frac{a^{(\perp,\parallel)} + b^{(\perp,\parallel)} q^2 [c^{(\perp,\parallel)} - q^2]}{b^{(\perp,\parallel)} q^2 [c^{(\perp,\parallel)} - q^2]}$$

$$\delta C_9^{\text{LD},0}(q^2) = \frac{a^0 + b^0 [q^2 + s_0] [c^0 - q^2]}{b^0 [q^2 + s_0] [c^0 - q^2]}$$

We vary s_i independently in the range $[-1, 1]$ (only $s_i = 1$ in KMPW).



c cbar loop

$$\mathcal{H}_{\text{eff}}^{\Delta B=1} = \mathcal{H}_{\text{eff}}^{\text{sl}} + \mathcal{H}_{\text{eff}}^{\text{had}}$$

- NNLO matching and evolution of Wilson coefficients for Q_{1-10}

- 7 Form Factors from LCSRs

$$F^{(i)}(q^2) = \sum_k \alpha_k^{(i)} \frac{[z(q^2) - z(0)]^k}{1 - (q/m_R^{(i)})^2} +$$

19 x 19 correlation matrix

A.Bharucha, D.M.Straub
and **R.Zwicky** arXiv:1503.05534

- Hard gluon exchanges from QCD factorization

S.W.Bosch and **G.Buchalla**
arXiv:0106081

M.Beneke, T.Feldmann
and **D.Seidel** arXiv:0106067

- Soft gluon exchanges ($u\bar{u}$, $c\bar{c}$ loops, Q_{8g} and WA)

$$h_\lambda(q^2) = h_\lambda^{(0)} + h_\lambda^{(1)} q^2 + h_\lambda^{(2)} q^4$$

by M.Valli

c cbar loop

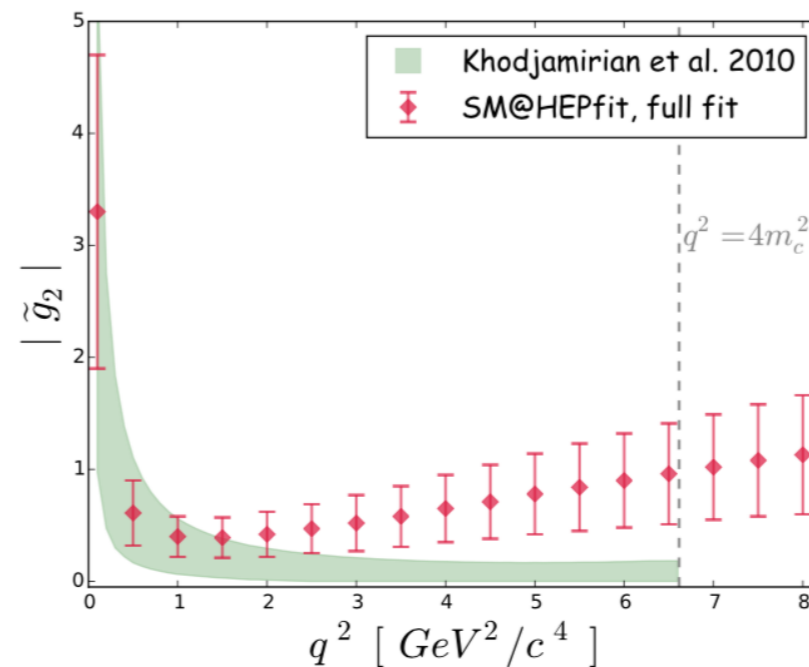
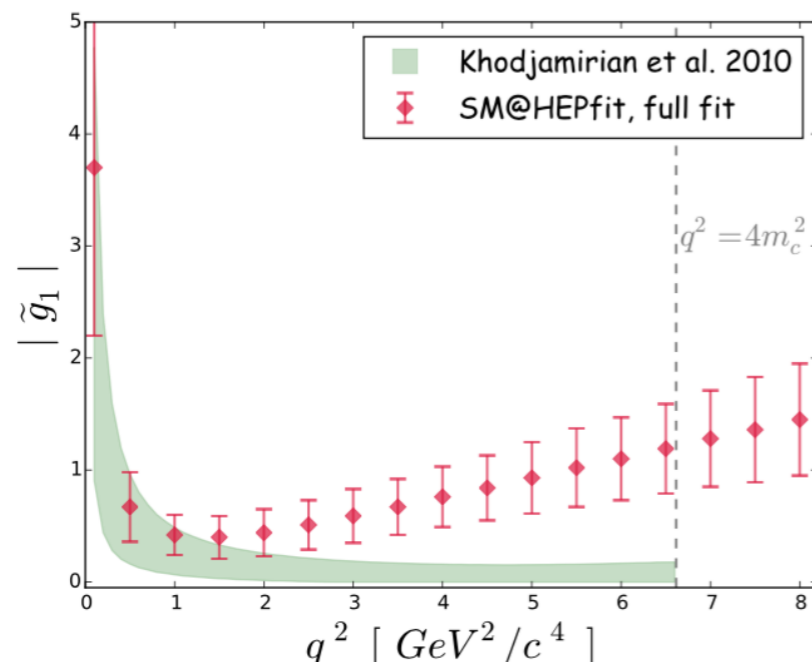
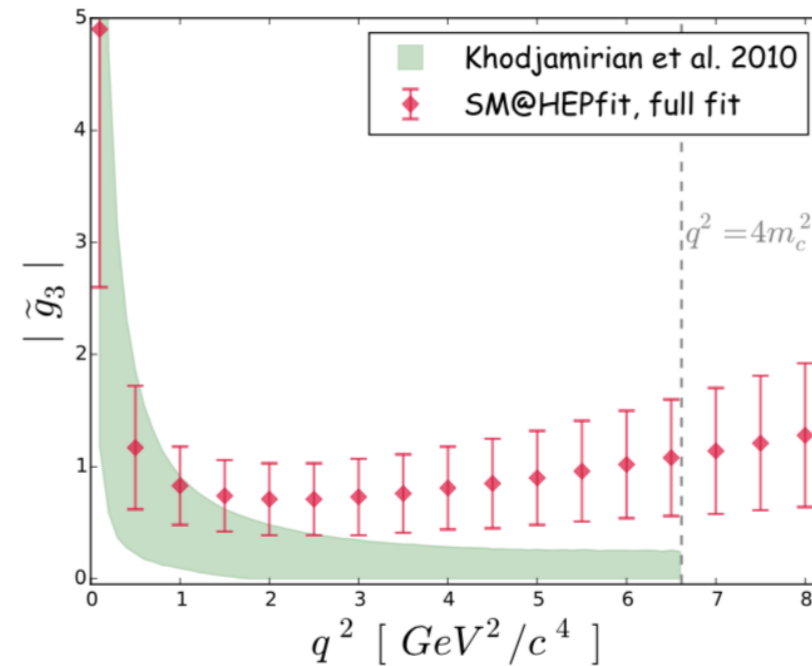
EXTRACTING THE NON-PERTURBATIVE
HADRONIC CONTRIBUTION

$$\tilde{g} \equiv \Delta C_9^{(\text{non pert.})} / (2C_1)$$

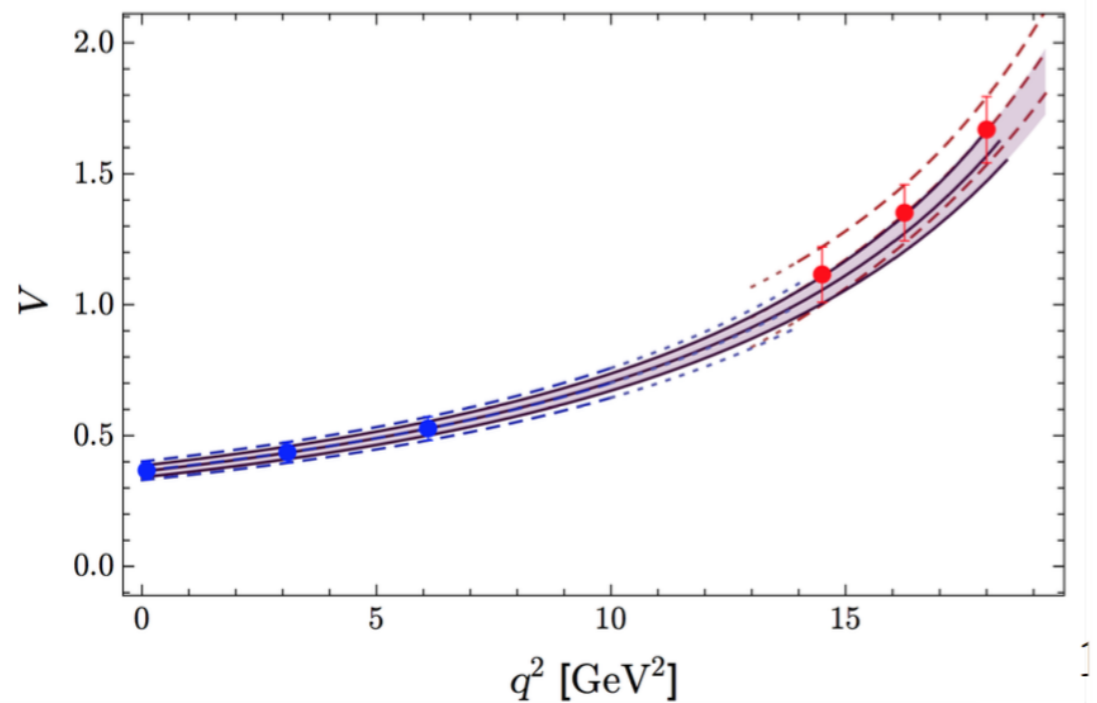
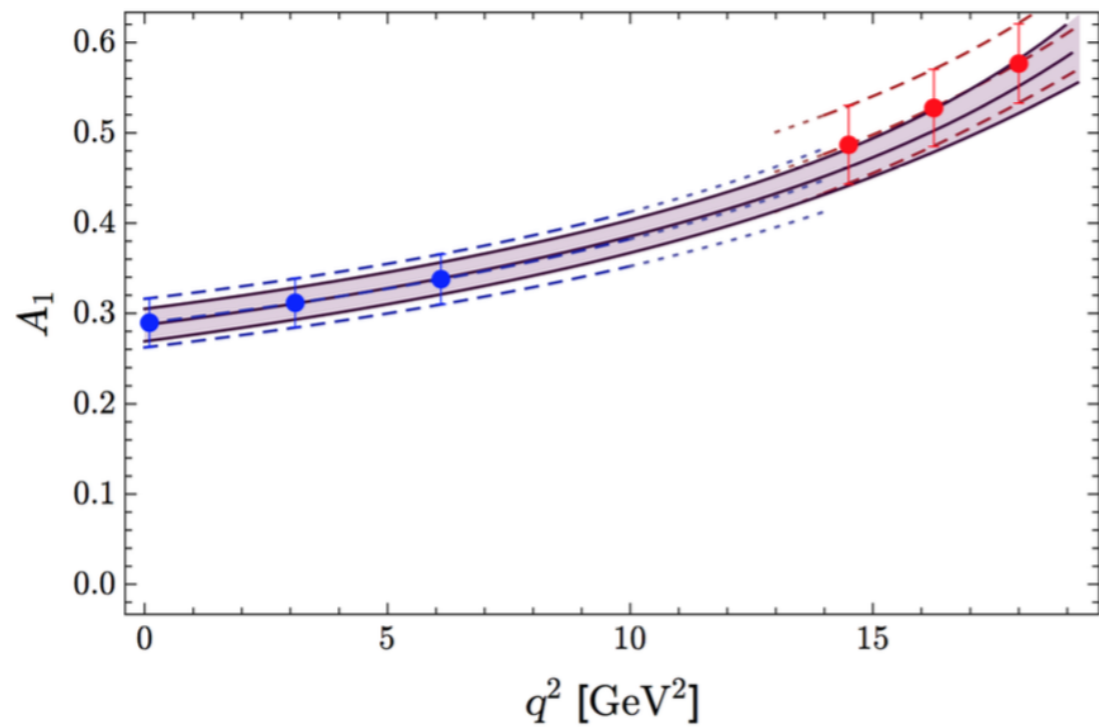
see arXiv:1006.4945

DISCLAIMER

NP contribution in C_7 and/or C_9 cannot
reproduce such a q^2 behaviour



c cbar loop

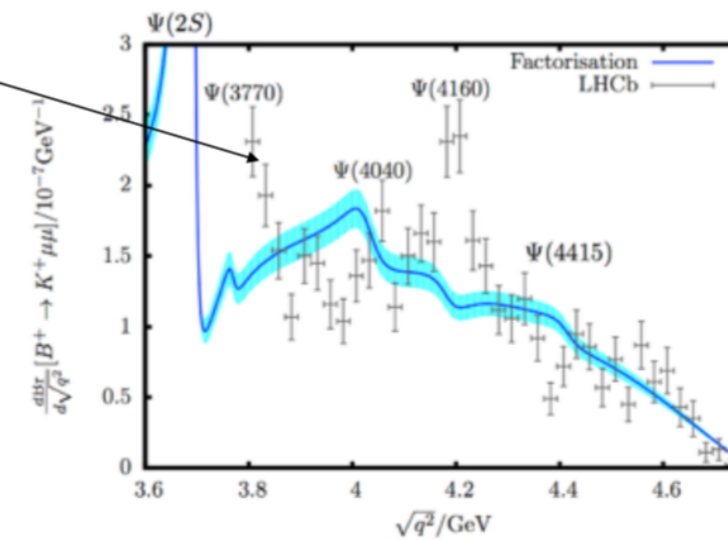
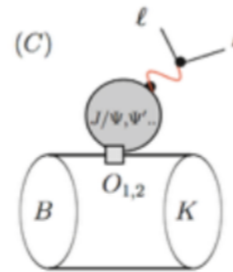
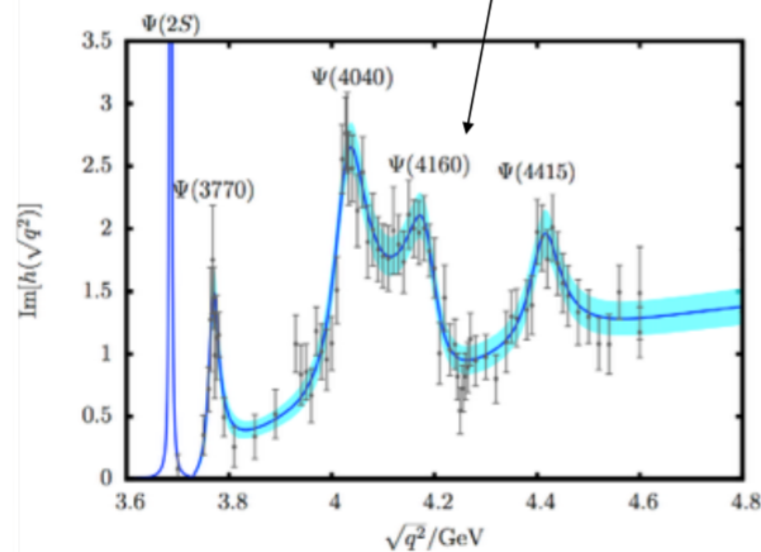


$$\begin{aligned}
 A_{\perp L,R} &= N\sqrt{2}\lambda^{1/2} \left[[(C_9 + C'_9) \mp (C_{10} + C'_{10})] \frac{V(q^2)}{m_B + m_{K^*}} \right. \\
 &\quad \left. + \frac{2m_b}{q^2}(C_7 + C'_7)T_1(q^2) \right], \\
 A_{\parallel L,R} &= -N\sqrt{2}(m_B^2 - m_{K^*}^2) \left[[(C_9 - C'_9) \mp (C_{10} - C'_{10})] \frac{A_1(q^2)}{m_B - m_{K^*}} \right. \\
 &\quad \left. + \frac{2m_b}{q^2}(C_7 - C'_7)T_2(q^2) \right], \\
 A_{0L,R} &= -\frac{N}{2m_{K^*}\sqrt{q^2}} \left\{ [(C_9 - C'_9) \mp (C_{10} - C'_{10})] \right. \\
 &\quad \times \left[(m_B^2 - m_{K^*}^2 - q^2)(m_B + m_{K^*})A_1(q^2) - \lambda \frac{A_2(q^2)}{m_B + m_{K^*}} \right] \\
 &\quad \left. + 2m_b(C_7 - C'_7) \left[(m_B^2 + 3m_{K^*}^2 - q^2)T_2(q^2) - \frac{\lambda}{m_B^2 - m_{K^*}^2}T_3(q^2) \right] \right\},
 \end{aligned}$$

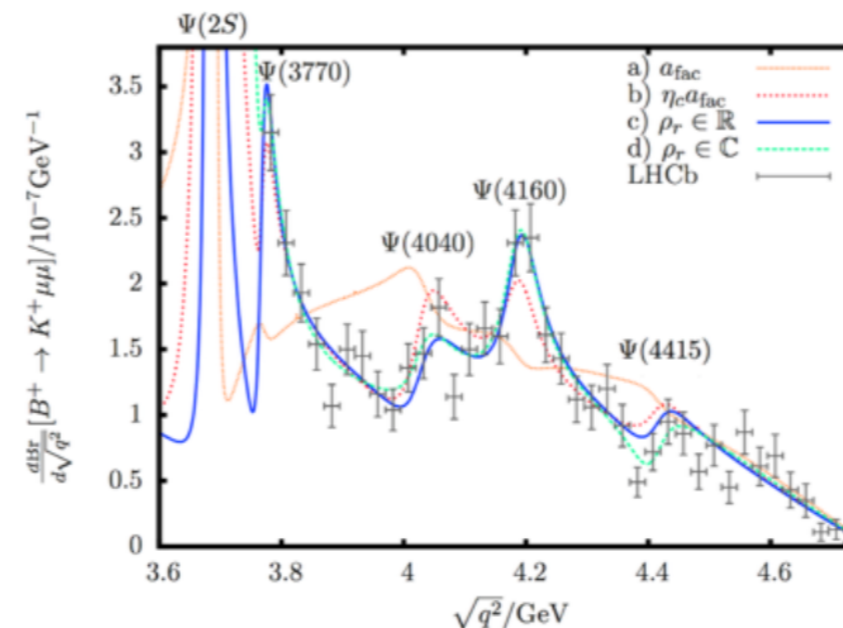
c cbar loop

Lyon RZ 1406.0566

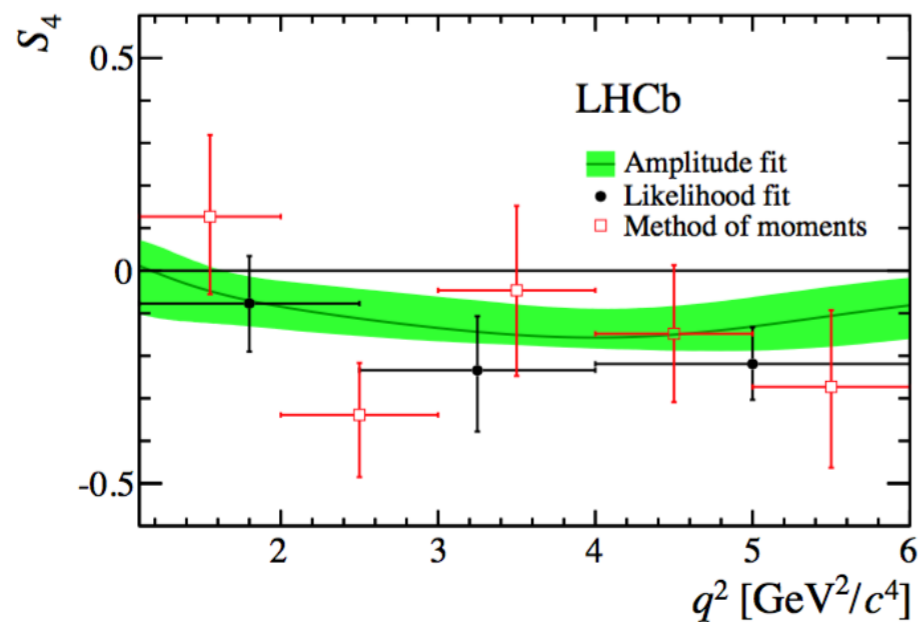
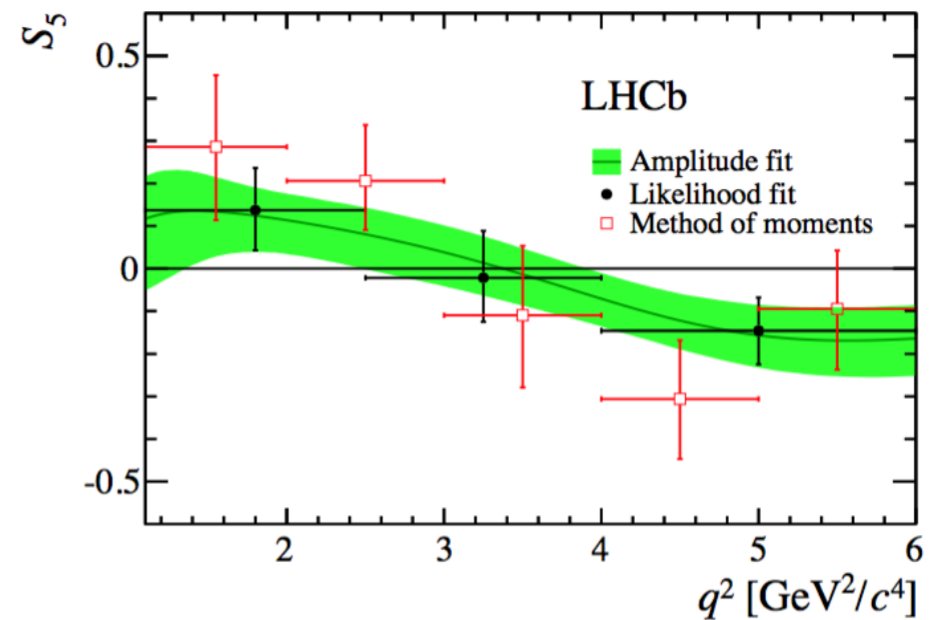
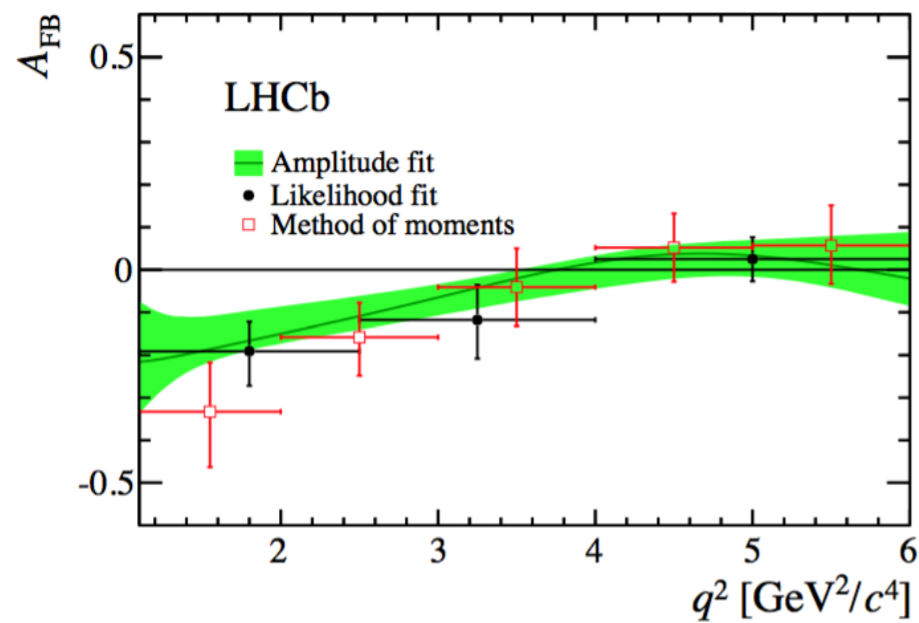
- Using a fit to BES-II data $e^+e^- \rightarrow$ hadrons able to check status of “naive” factorisation at high q^2 in $B \rightarrow K\ell\ell$



height of resonances in naive fac. by factor $\sim(-2.5)$ fits the data well



Amplitude analysis



Zero crossing points:

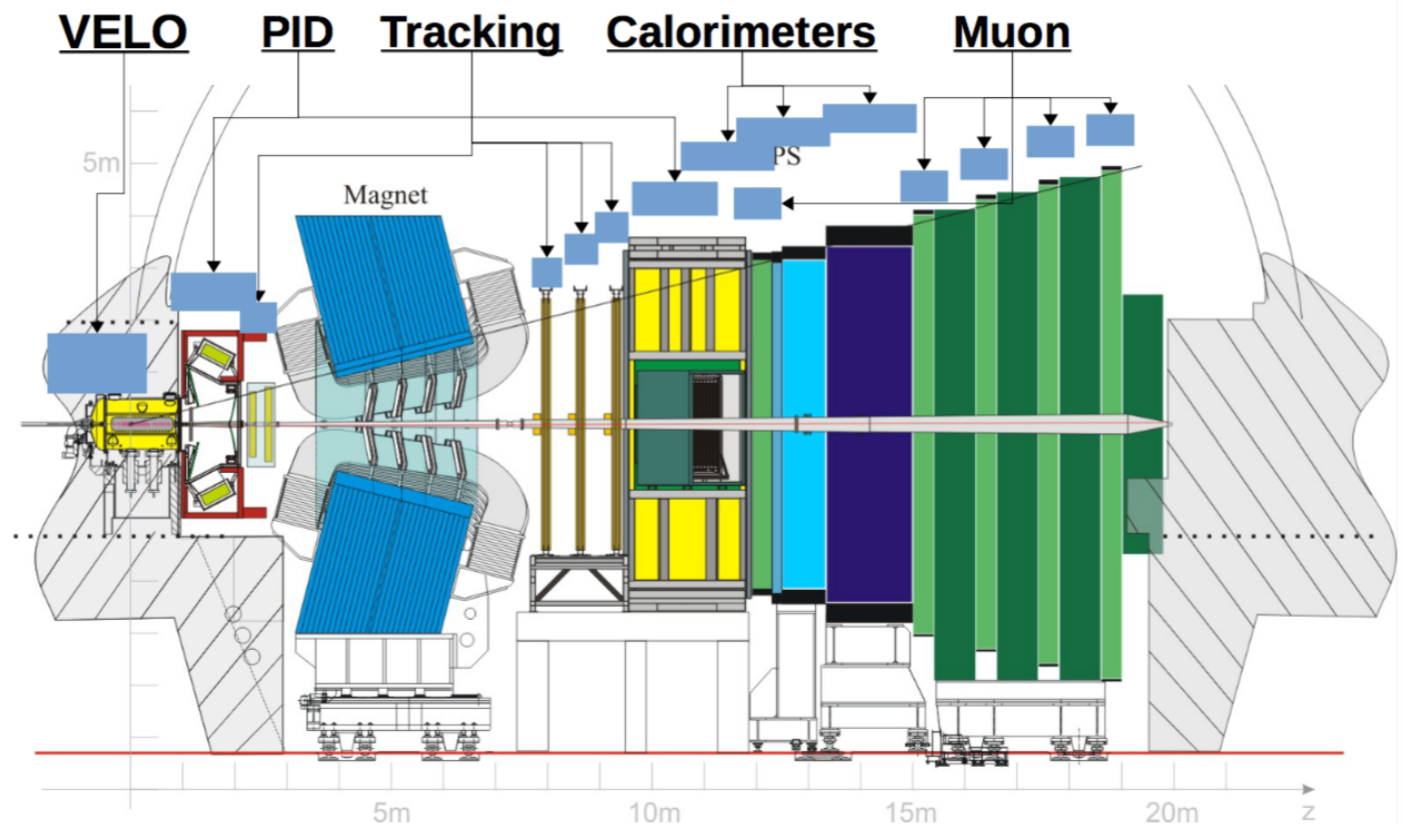
$$q_0(S_4) < 2.65 \quad \text{at } 95\% \text{ CL}$$

$$q_0(S_5) \in [2.49, 3.95] \quad \text{at } 68\% \text{ CL}$$

$$q_0(A_{FB}) \in [3.40, 4.87] \quad \text{at } 68\% \text{ CL}$$

LHCb

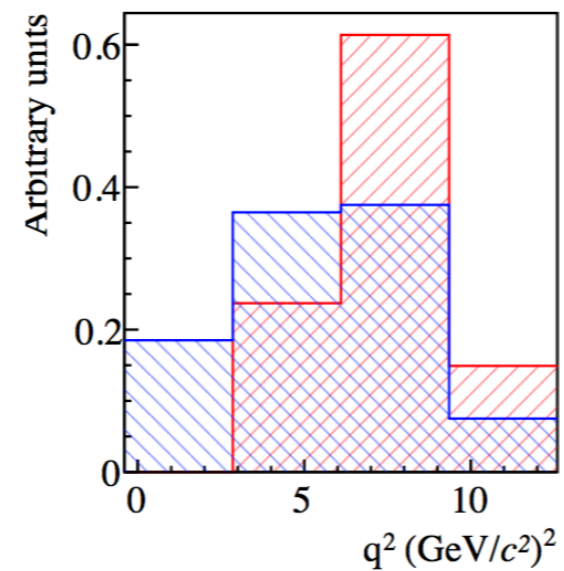
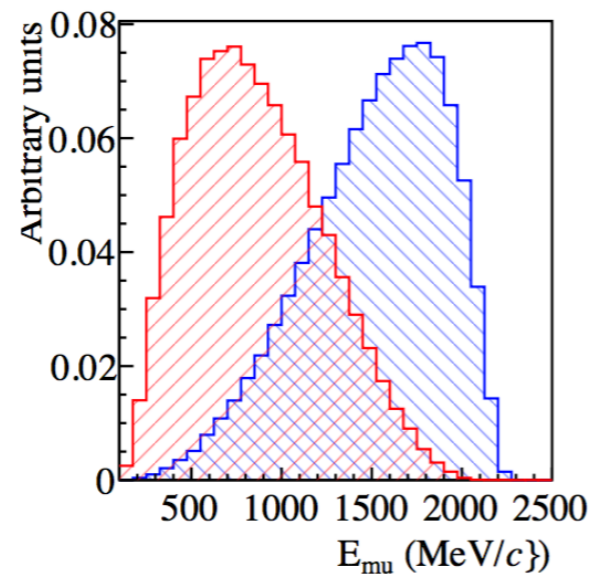
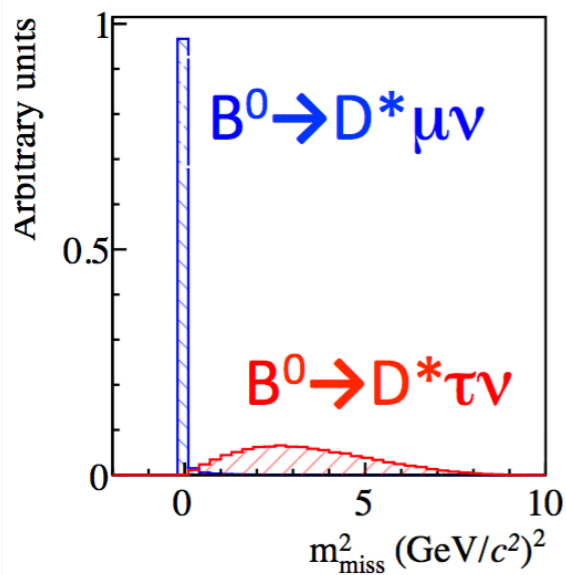
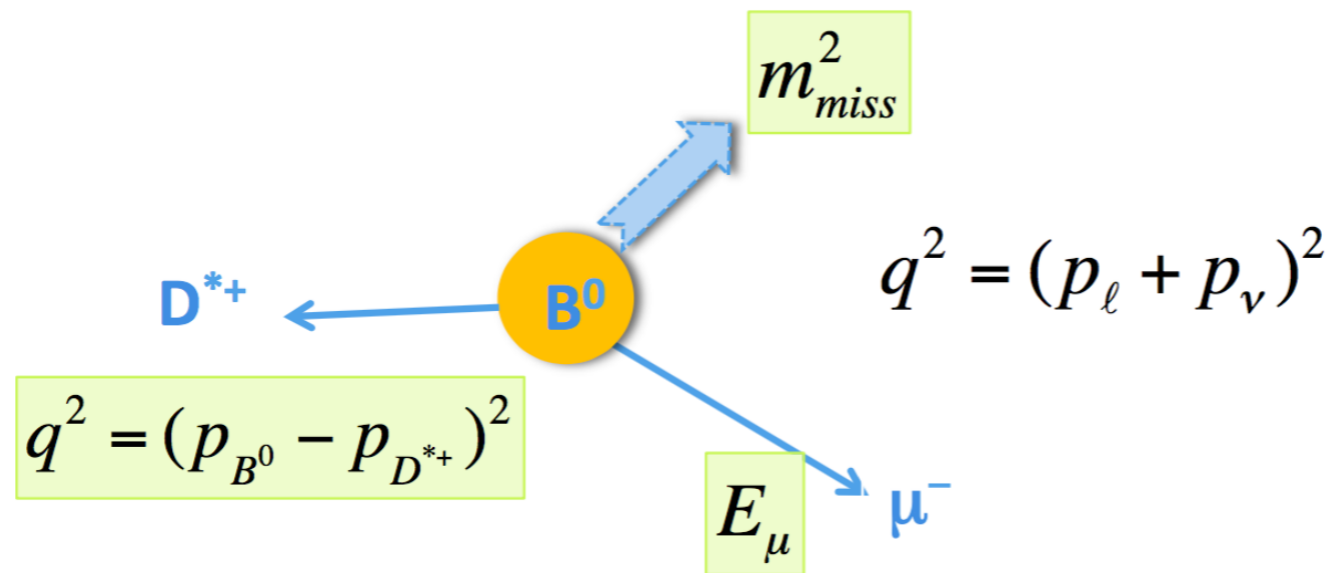
- **VELO**: $\sigma_{\text{IP}}^{\text{trk}} \sim 20 \mu\text{m}$ for $p_{\text{T}}^{\text{trk}} > 2 \text{ GeV}/c$
- **PID**: by 2 dedicated RICH detectors:
 $\pi/K/p$ separation in range 2 - 100 GeV/c
- **Tracking** stations and 4 Tm magnet:
excellent mass resolution ($7\text{-}20 \text{ MeV}/c^2$)
- **Calorimeters**: high-granularity,
ECAL for e^{\pm}/γ and HCAL for hadrons
 - Used for hardware trigger
- **Muon** system: high muon ID
 - Used for hardware trigger
- **Trigger** at low- p_{T} $\sim 20 \text{ MHz} \rightarrow 5 \text{ kHz}$
 - Hardware and then software



- 3 fb^{-1} collected in LHC Run 1 at 7-8 TeV

$B \rightarrow D^* \tau \nu$

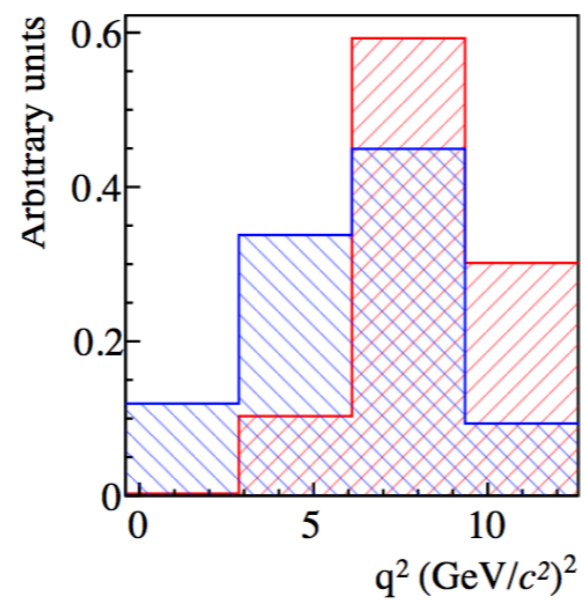
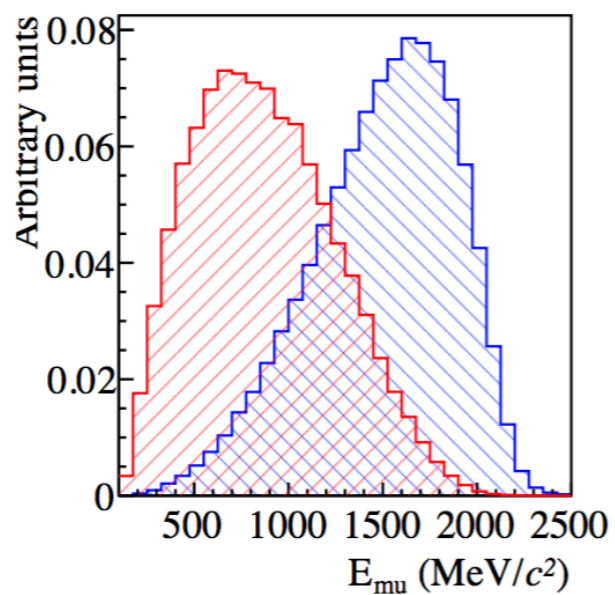
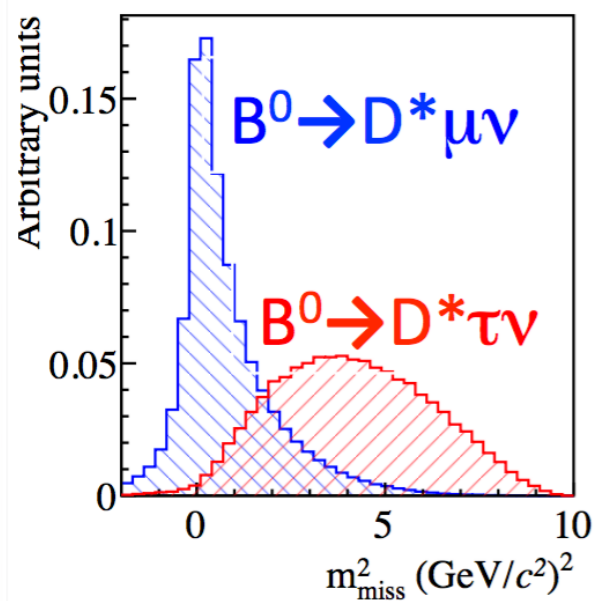
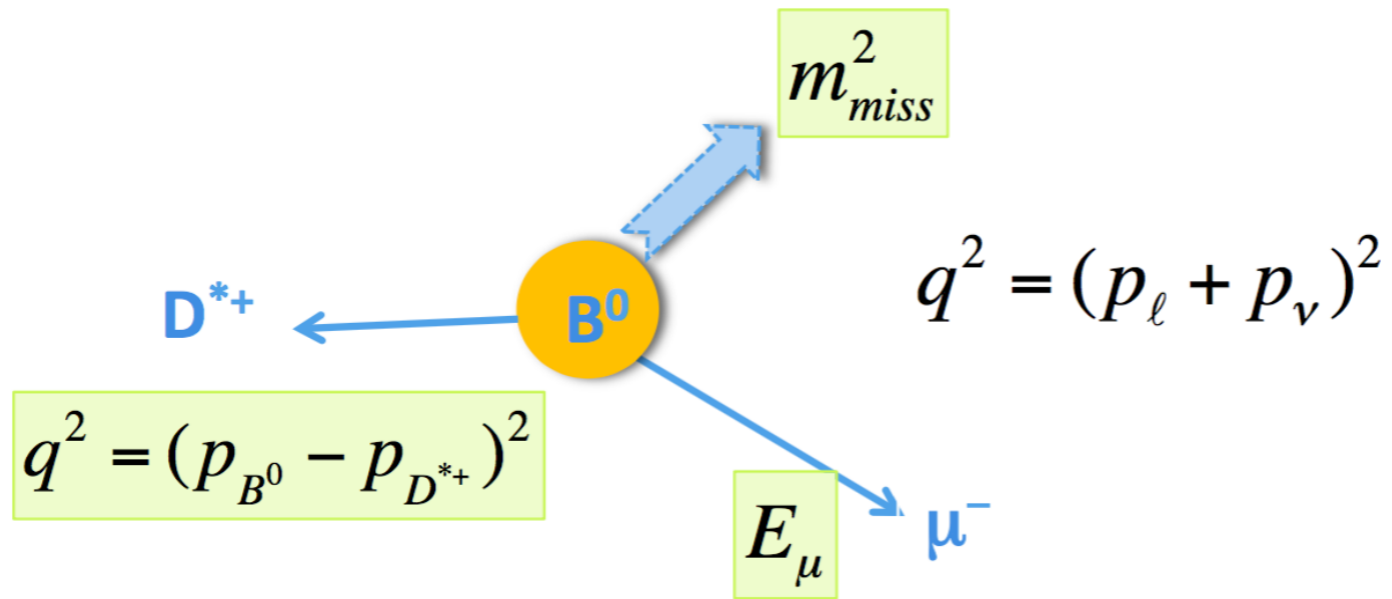
- 3 key kinematic variables computed in the B rest frame



LHCb
simulation

MC truth

$B \rightarrow D^* \tau \nu$

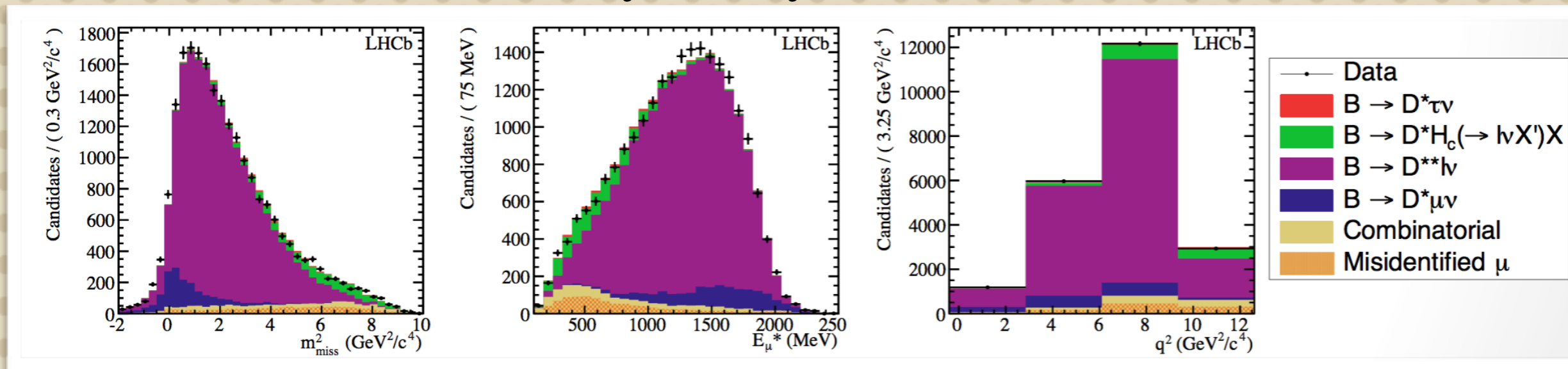


LHCb
simulation

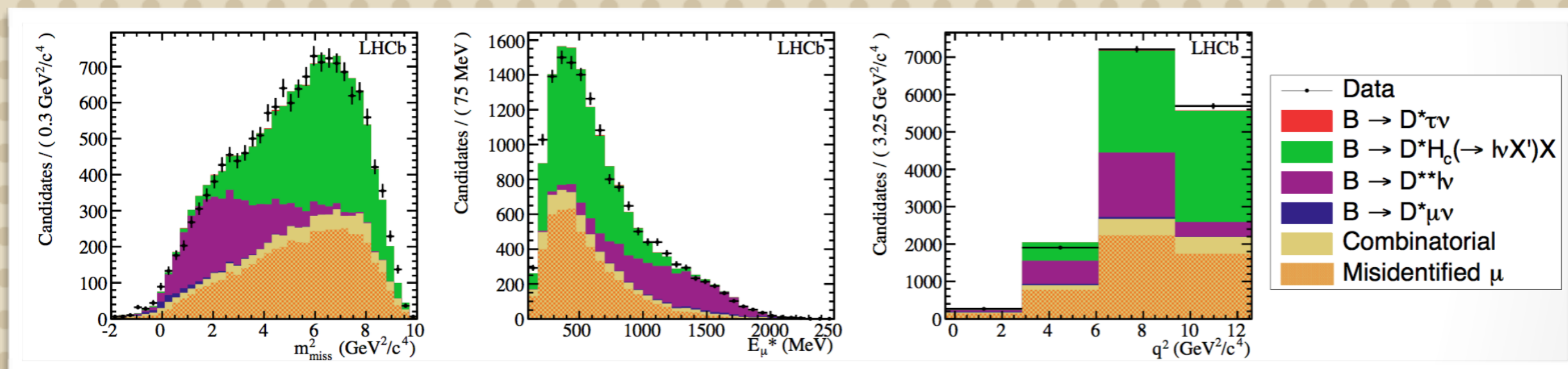
approximate
B rest frame

$B \rightarrow D^* \tau \nu$

- Fit to the control sample " $D^* \pi l$ "

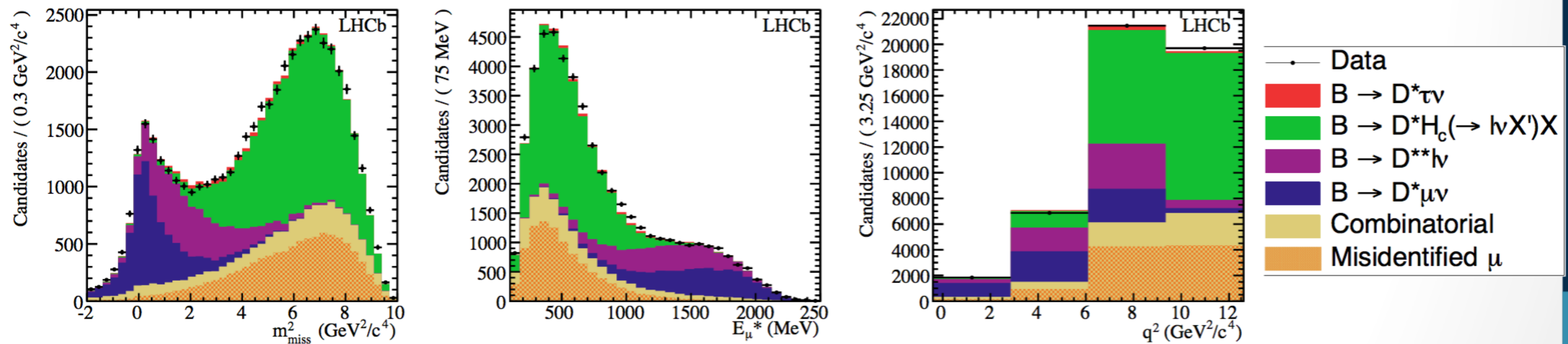


- Fit to the control sample " $D^* \pi \pi l$ "



$B \rightarrow D^* \tau \nu$

- Fit to the control sample " $D^* K l$ "



- Similar simulated sample for $B \rightarrow D D_s$ with $D_s \rightarrow \tau \nu$

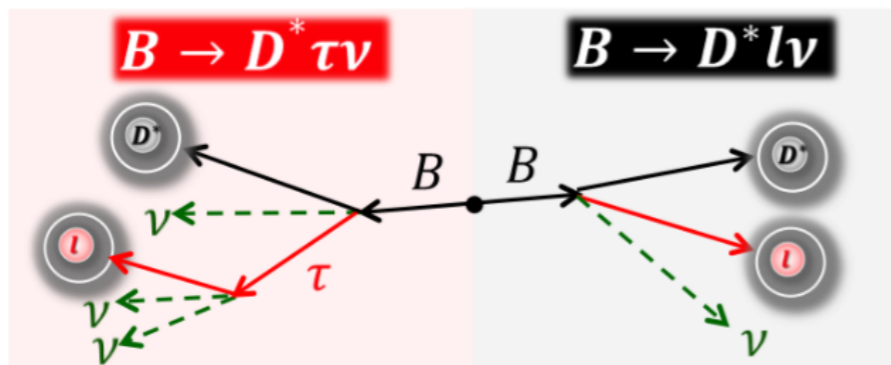
$B \rightarrow D^* \tau \nu$

Model uncertainties	Absolute size ($\times 10^{-2}$)
Simulated sample size	2.0
Misidentified μ template shape	1.6
$\bar{B}^0 \rightarrow D^{*+}(\tau^-/\mu^-)\bar{\nu}$ form factors	0.6
$\bar{B} \rightarrow D^{*+}H_c(\rightarrow \mu\nu X')X$ shape corrections	0.5
$\mathcal{B}(\bar{B} \rightarrow D^{**}\tau^-\bar{\nu}_\tau)/\mathcal{B}(\bar{B} \rightarrow D^{**}\mu^-\bar{\nu}_\mu)$	0.5
$\bar{B} \rightarrow D^{**}(\rightarrow D^*\pi\pi)\mu\nu$ shape corrections	0.4
Corrections to simulation	0.4
Combinatorial background shape	0.3
$\bar{B} \rightarrow D^{**}(\rightarrow D^{*+}\pi)\mu^-\bar{\nu}_\mu$ form factors	0.3
$\bar{B} \rightarrow D^{*+}(D_s \rightarrow \tau\nu)X$ fraction	0.1
Total model uncertainty	2.8
Normalization uncertainties	Absolute size ($\times 10^{-2}$)
Simulated sample size	0.6
Hardware trigger efficiency	0.6
Particle identification efficiencies	0.3
Form-factors	0.2
$\mathcal{B}(\tau^- \rightarrow \mu^-\bar{\nu}_\mu\nu_\tau)$	< 0.1
Total normalization uncertainty	0.9
Total systematic uncertainty	3.0

Background
modelling;
depends
on control
sample size

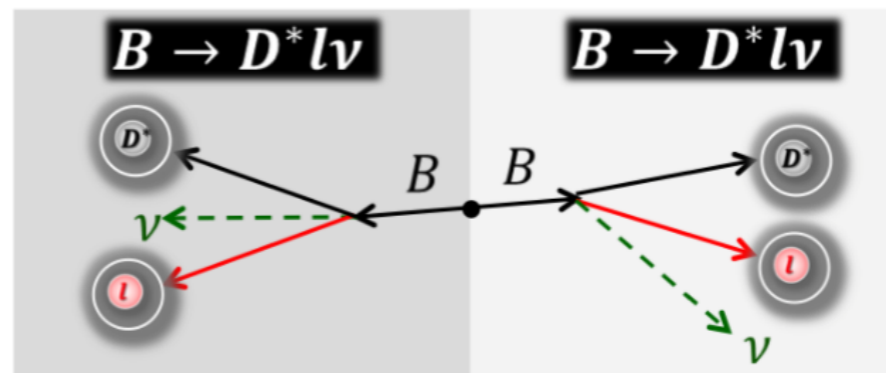
$B \rightarrow D^* \tau \nu$

Semitauonic signal-side decay and semileptonic tag-side.



Numerator in $\mathcal{R}(D^*)$

Normalization events are double semileptonic decays.



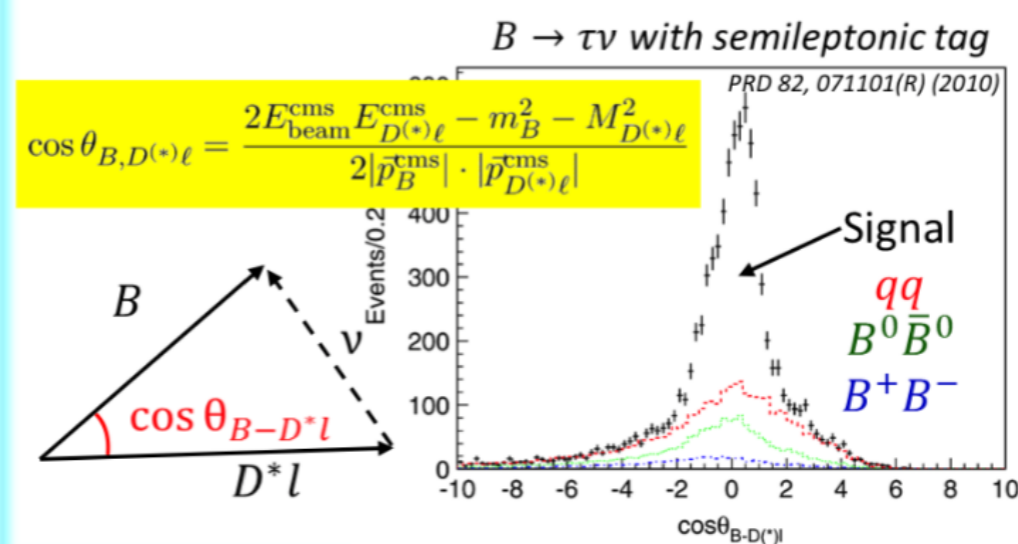
Denominator in $\mathcal{R}(D^*)$

D^* reconstruction:

- ▶ $D^{*+} \rightarrow D^0 \pi^+, D^+ \pi^0$ ($\sim 100\%$)
- D^0 : 10 modes ($\sim 37\%$)
- D^+ : 5 modes ($\sim 22\%$)

Tag semileptonic B -decay: Combine D^{*+} and oppositely-charged lepton candidates and calculate the cosine of the angle between the B momentum and the D^*l in the $\Upsilon(4S)$ frame.

\Rightarrow



✓ tag candidates: $\cos \theta_{B-D^*\ell} \in [-1, 1]$

Image credits: Y. Sato (Nagoya)

$B \rightarrow D^* \tau \nu$

Sources	$\mathcal{R}(D^*)$ [%]		
	$\ell^{\text{sig}} = e, \mu$	$\ell^{\text{sig}} = e$	$\ell^{\text{sig}} = \mu$
MC statistics for PDF shape	2.2%	2.5%	3.9%
PDF shape of the normalization	+1.1% -0.0%	+2.1% -0.0%	+2.8% -0.0%
PDF shape of $B \rightarrow D^{**} \ell \nu_\ell$	+1.0% -1.7%	+0.7% -1.3%	+2.2% -3.3%
PDF shape and yields of fake $D^{(*)}$	1.4%	1.6%	1.6%
PDF shape and yields of $B \rightarrow X_c D^*$	1.1%	1.2%	1.1%
Reconstruction efficiency ratio $\varepsilon_{\text{norm}}/\varepsilon_{\text{sig}}$	1.2%	1.5%	1.9%
Modeling of semileptonic decay $\mathcal{B}(\tau^- \rightarrow \ell^- \bar{\nu}_\ell \nu_\tau)$	0.2%	0.2%	0.3%
Total systematic uncertainties	+3.4% -3.5%	+4.1% -3.7%	+5.9% -5.8%

B \rightarrow D* tau v

$$w \equiv v_B \cdot v_{D^*} = \frac{m_B^2 + m_{D^*}^2 - q^2}{2m_{D^*}m_B}.$$

$$\begin{aligned} H_{\pm}(q^2) &= (m_B + m_{D^*})A_1(q^2) \mp \frac{2m_B}{m_B + m_{D^*}} |\mathbf{p}_{D^*}^*| V(q^2), \\ H_0(q^2) &= \frac{-1}{2m_{D^*} \sqrt{q^2}} \left[\frac{4m_B^2 |\mathbf{p}_{D^*}^*|^2}{m_B + m_{D^*}} A_2(q^2) \right. \\ &\quad \left. - (m_B^2 - m_{D^*}^2 - q^2)(m_B + m_{D^*}) A_1(q^2) \right], \\ H_s(q^2) &= \frac{2m_B |\mathbf{p}_{D^*}^*|}{\sqrt{q^2}} A_0(q^2). \end{aligned} \quad (10)$$

$$\begin{aligned} h_{A_1}(w) &= h_{A_1}(1) [1 - 8\rho_{D^*}^2 z(w) + (53\rho_{D^*}^2 - 15)z(w)^2 \\ &\quad - (231\rho_{D^*}^2 - 91)z(w)^3], \\ R_1(w) &= R_1(1) - 0.12(w - 1) + 0.05(w - 1)^2, \\ R_2(w) &= R_2(1) + 0.11(w - 1) - 0.06(w - 1)^2, \\ R_0(w) &= R_0(1) - 0.11(w - 1) + 0.01(w - 1)^2. \end{aligned}$$

$$\begin{aligned} A_1(w) &= \frac{w + 1}{2} r_{D^*} h_{A_1}(w), & A_0(w) &= \frac{R_0(w)}{r_{D^*}} h_{A_1}(w), \\ A_2(w) &= \frac{R_2(w)}{r_{D^*}} h_{A_1}(w), & V(w) &= \frac{R_1(w)}{r_{D^*}} h_{A_1}(w), \end{aligned}$$

$$\begin{aligned} \rho_{D^*}^2 &= 1.207 \pm 0.028, & C(\rho_{D^*}^2, R_1(1)) &= 0.566, \\ R_1(1) &= 1.401 \pm 0.033, & C(\rho_{D^*}^2, R_2(1)) &= -0.807, \\ R_2(1) &= 0.854 \pm 0.020, & C(R_1(1), R_2(1)) &= -0.758. \end{aligned}$$

$h_{A_1}(1)$ drops out in the ratio and R_0 affects only H_s so must be determined from lattice

Analysis of $1fb^{-1}$

In the analysis of $1fb^{-1}$ we did not have enough data to fit the full Pdf, so we used "folding" of angles to simplify the Pdf

by doing $\phi \rightarrow \phi + \pi$ if $\phi < 0$

$$\frac{1}{\Gamma} \frac{d^3(\Gamma + \bar{\Gamma})}{d \cos \theta_\ell d \cos \theta_K d\phi} = \frac{9}{32\pi} \left[\frac{3}{4}(1 - F_L) \sin^2 \theta_K + F_L \cos^2 \theta_K + \frac{1}{4}(1 - F_L) \sin^2 \theta_K \cos 2\theta_\ell \right. \\ \left. - F_L \cos^2 \theta_K \cos 2\theta_\ell + S_3 \sin^2 \theta_K \sin^2 \theta_\ell \cos 2\phi + \frac{1}{2}(1 - F_L) A_T^{Re} \sin^2 \theta_K \cos \theta_\ell \right. \\ \left. + S_9 \sin^2 \theta_K \sin^2 \theta_\ell \sin 2\phi \right]$$

by doing

$$\phi \rightarrow -\phi \quad \text{if } \phi < 0$$

$$\theta_\ell \rightarrow \pi - \theta_\ell \quad \text{if } \theta_\ell < \pi/2$$

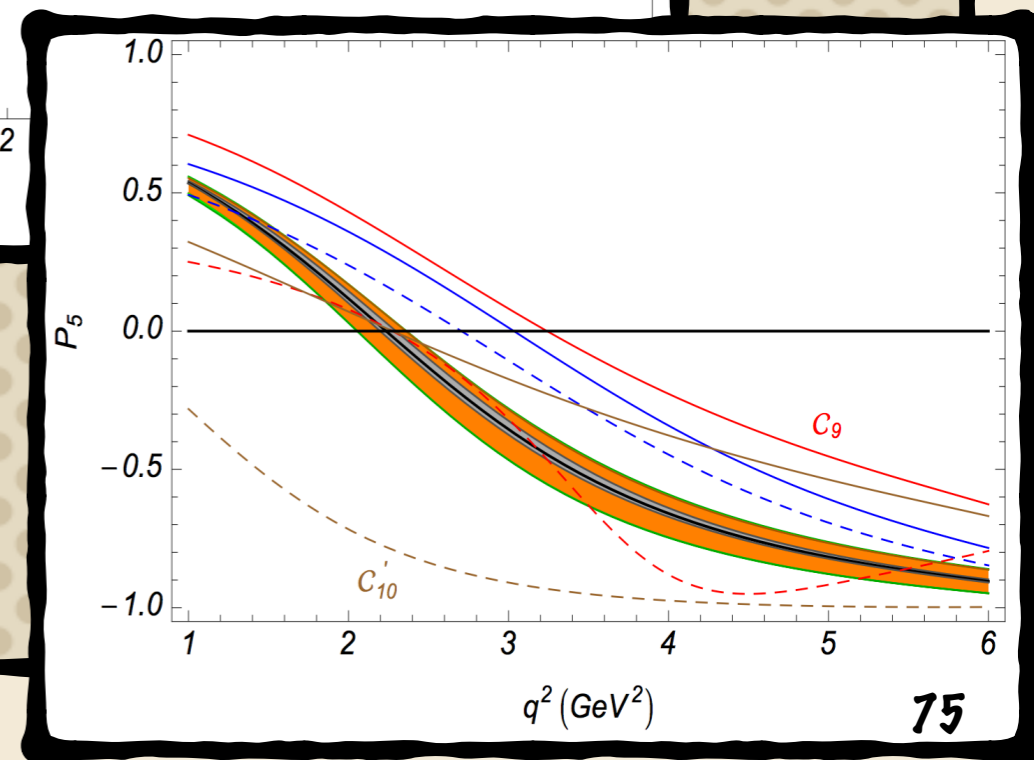
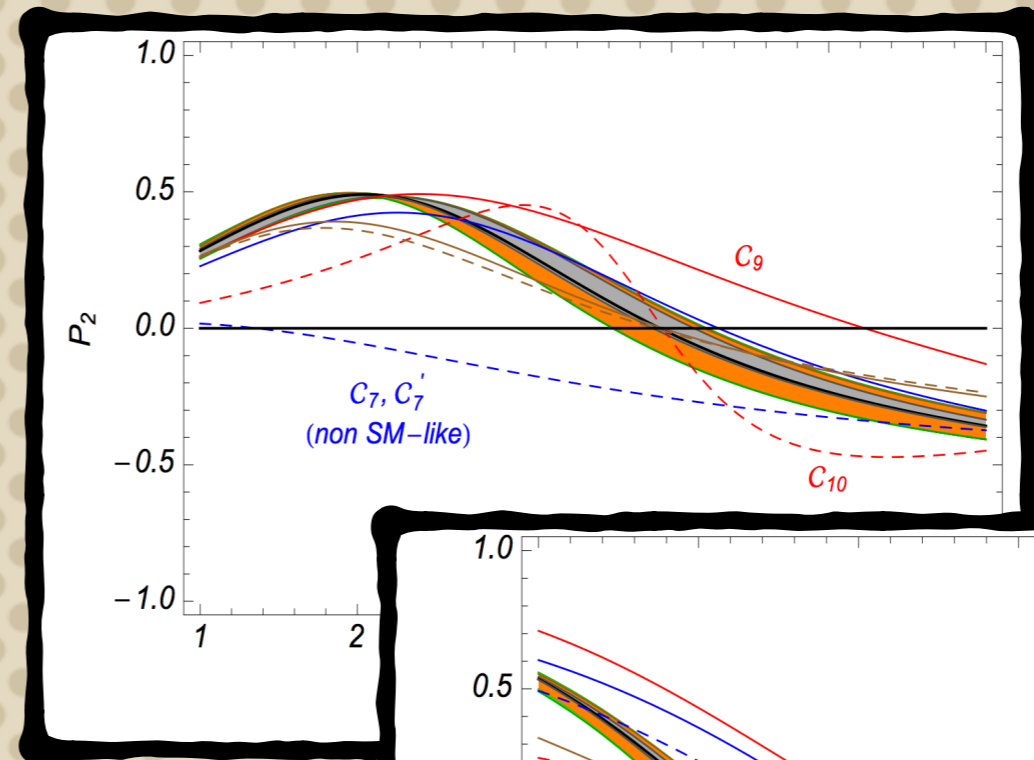
Folding for all other
observables in the backup

$$\frac{1}{\Gamma} \frac{d^3(\Gamma + \bar{\Gamma})}{d \cos \theta_\ell d \cos \theta_K d\phi} = \frac{9}{32\pi} \left[\frac{3}{4}(1 - F_L) \sin^2 \theta_K + F_L \cos^2 \theta_K + \frac{1}{4}(1 - F_L) \sin^2 \theta_K \cos 2\theta_\ell \right. \\ \left. - F_L \cos^2 \theta_K \cos 2\theta_\ell + S_3 \sin^2 \theta_K \sin^2 \theta_\ell \cos 2\phi + \sqrt{F_L(1 - F_L)} P_5' \sin 2\theta_K \sin \theta_\ell \cos \phi \right]$$

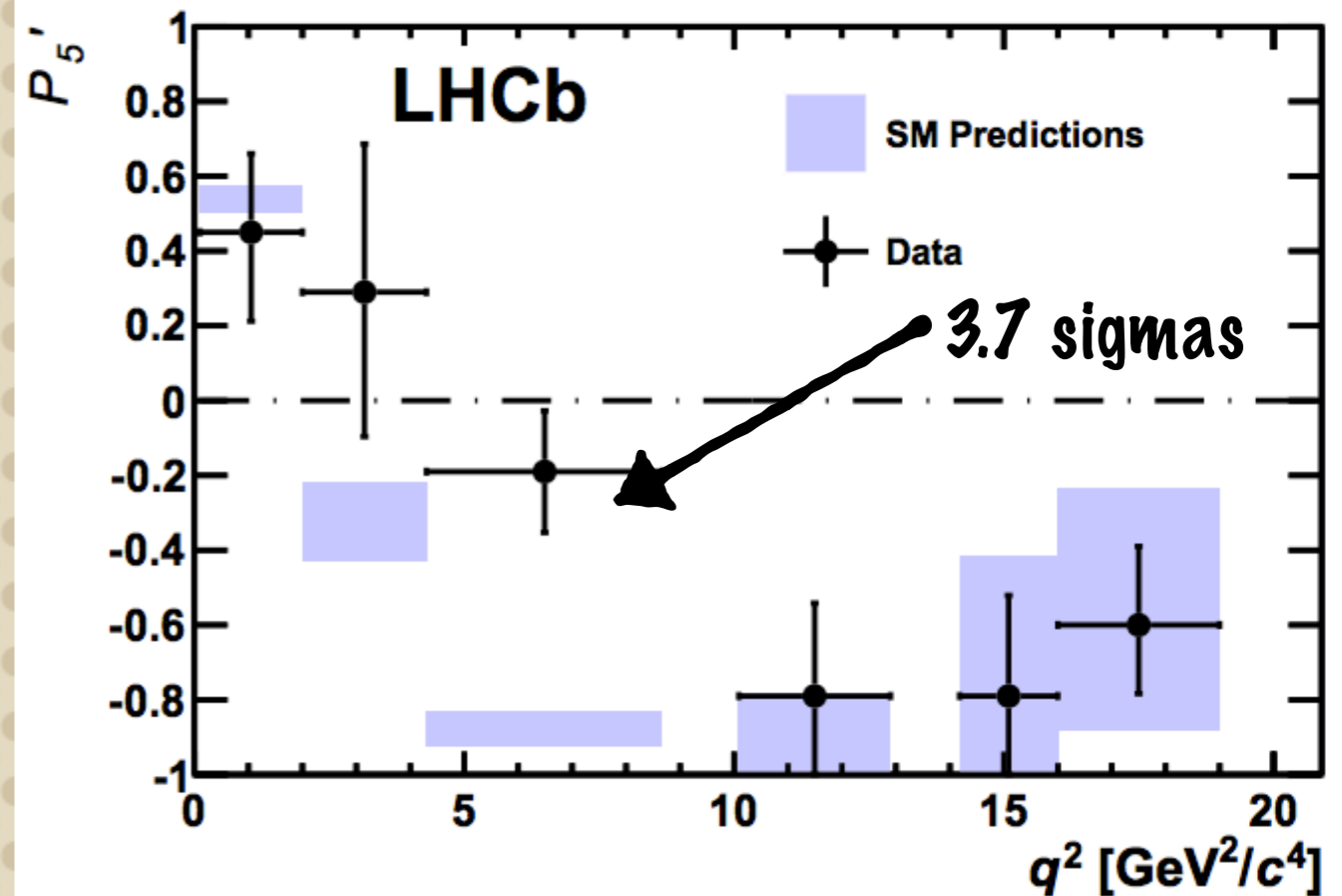
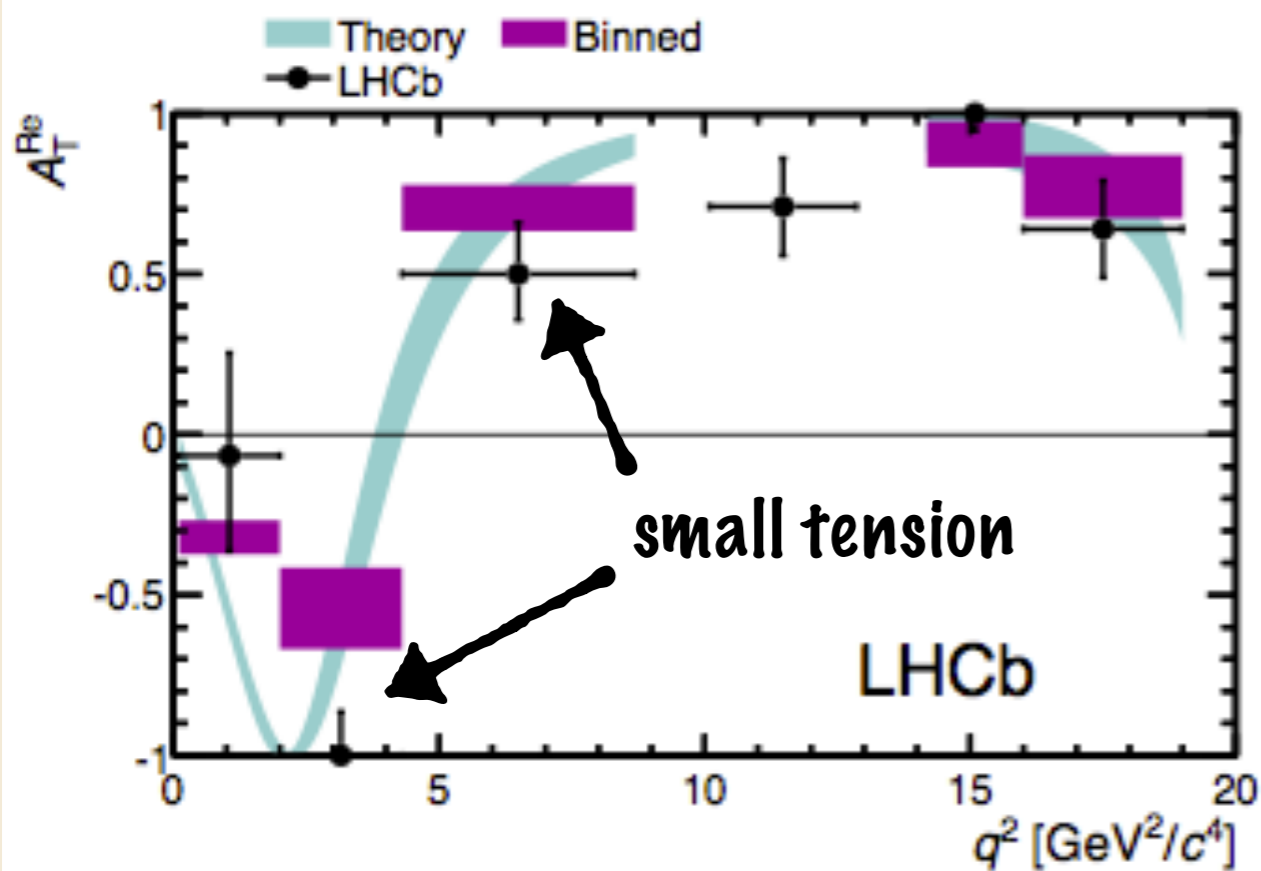
Introduction

- The number of degrees of freedom are $3 \times 2 \times 2 = 12$
- However there are 4 symmetries of the angular distributions, so there are 8 independent observables
- The maximum number of "clean" observables is 6

$$\begin{aligned}
 P_1 &= A_T^{(2)} = \frac{2S_3}{(1-F_L)} = \frac{A_{\perp}^{L2} - A_{\parallel}^{L2}}{A_{\parallel}^2 + A_{\perp}^2} + L \rightarrow R \\
 P_2 &= 2A_T^{Re} = \frac{2A_{FB}}{3(1-F_L)} \propto \frac{\Re(A_{\perp}^{L*} A_{\parallel}^L)}{A_{\parallel}^2 + A_{\perp}^2} - L \rightarrow R \\
 P_3 &= \frac{S_9}{(1-F_L)} = \frac{\Im(A_{\perp}^{L*} A_{\parallel}^L)}{A_{\parallel}^2 + A_{\perp}^2} - L \rightarrow R \\
 P'_4 &= \frac{S_4}{\sqrt{F_L(1-F_L)}} \propto \frac{\Re(A_0^{L*} A_{\parallel}^L)}{\sqrt{|A_0|^2 |A_{\parallel}|^2}} + L \rightarrow R \\
 P'_5 &= \frac{S_5}{\sqrt{F_L(1-F_L)}} \propto \frac{\Re(A_0^{L*} A_{\perp}^L)}{\sqrt{|A_{\perp}|^2 |A_0|^2}} - L \rightarrow R \\
 P'_6 &= \frac{S_7}{\sqrt{F_L(1-F_L)}} \propto \frac{\Im(A_0^{L*} A_{\parallel}^L)}{\sqrt{|A_{\parallel}|^2 |A_0|^2}} + L \rightarrow R
 \end{aligned}$$



Result of $1fb^{-1}$ analysis

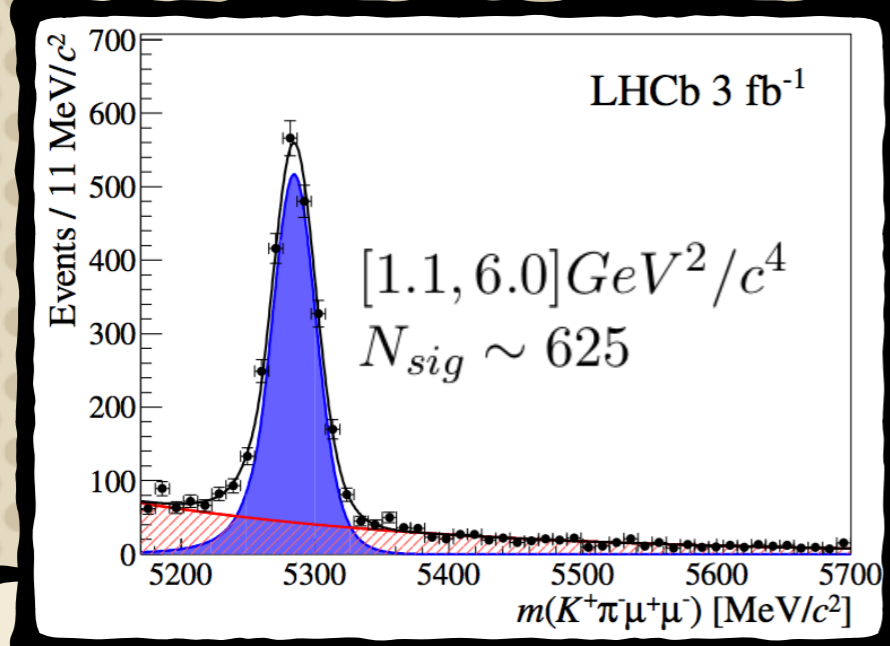
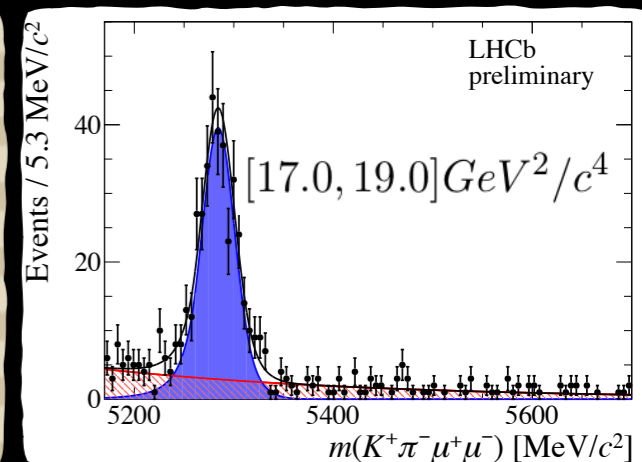
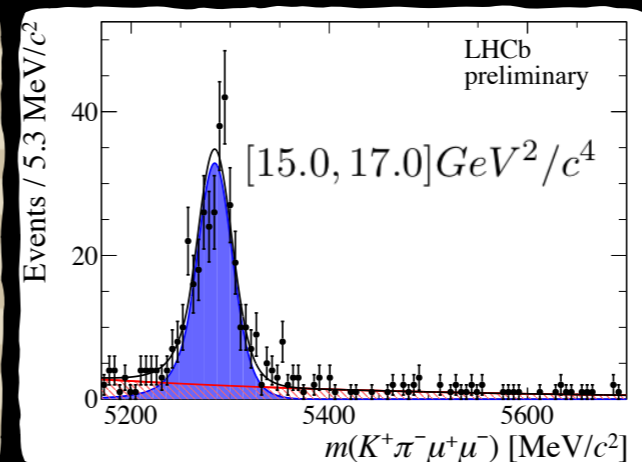
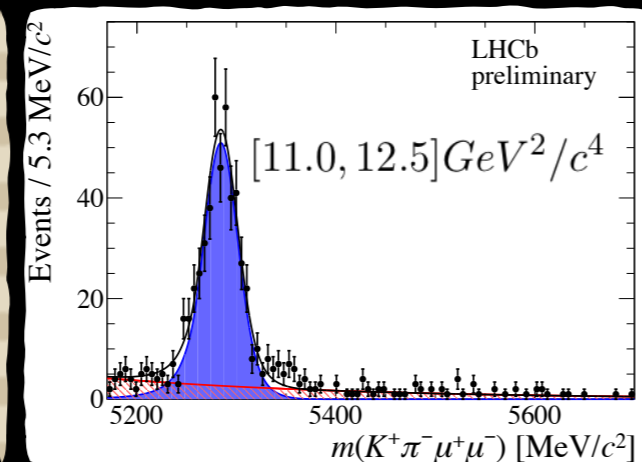
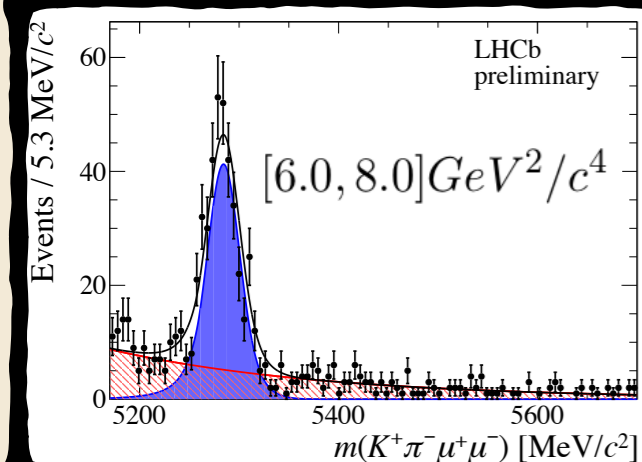
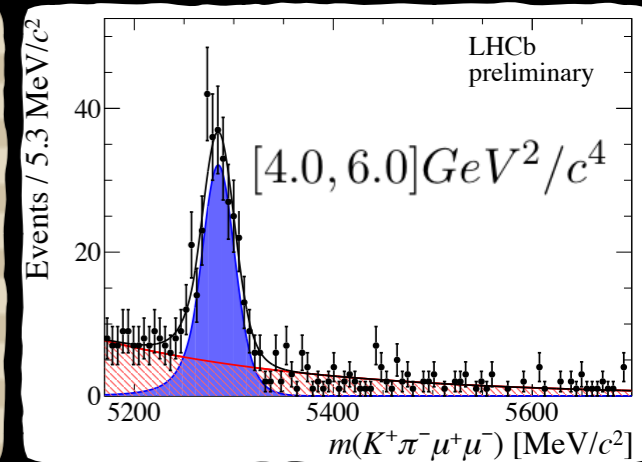
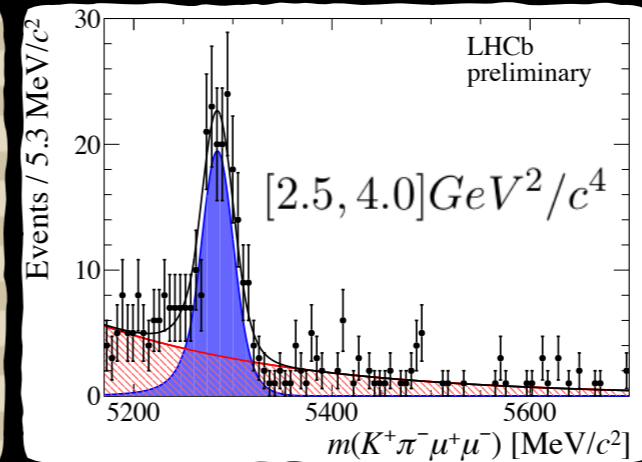
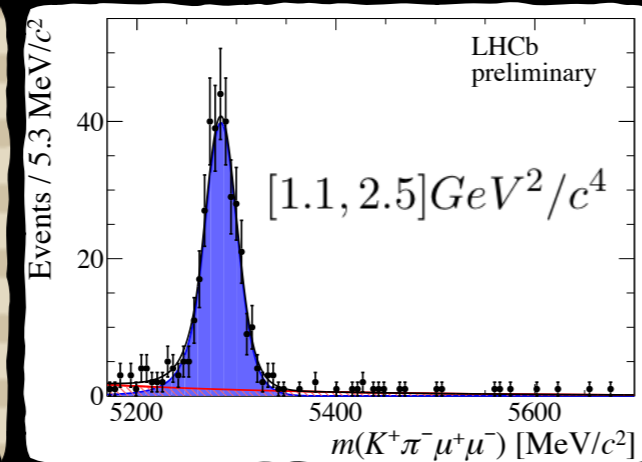
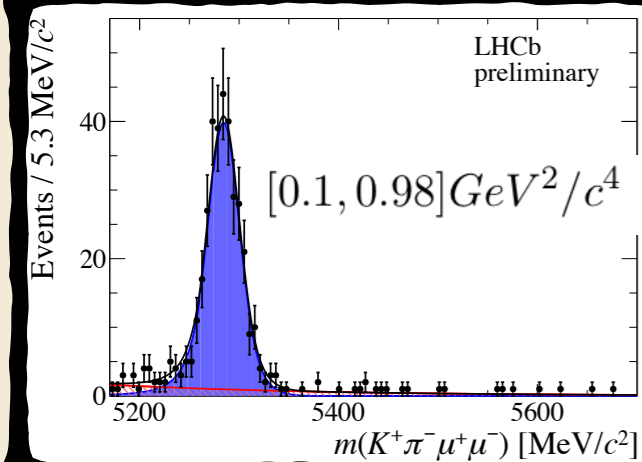


- Evident local discrepancy in the low q^2 region of P_5'
- Other observables visually in agreement with SM predictions

LHCb Collaboration [JHEP 08 \(2013\) 131](#)

LHCb Collaboration [Phys. Rev. Lett. 111 \(2013\) 191801](#)

Invariant Mass fit



$q^2 [GeV^2]$	signal yield	background yield
$[0.1, 0.98]$	339.1 ± 19.6	58.9 ± 10.3
$[1.1, 2.5]$	179.7 ± 15.4	124.4 ± 13.5
$[2.5, 4.0]$	165.4 ± 15.9	206.6 ± 17.1
$[4.0, 6.0]$	279.5 ± 20.2	300.4 ± 20.7
$[6.0, 8.0]$	344.3 ± 22.1	344.8 ± 22.1
$[11.0, 12.5]$	329.8 ± 21.0	212.1 ± 18.0
$[15.0, 17.0]$	449.2 ± 23.8	189.8 ± 17.5
$[17.0, 19.0]$	299.9 ± 19.8	144.1 ± 15.3

Amplitudes

The lepton system can be in a RH or LH state

$$A_{\perp}^{L,R} \propto [(C_9^{eff} + C_9^{eff'}) \mp (C_{10}^{eff} + C_{10}^{eff'}) \frac{V(q^2)}{m_B + m_{K^*}} + \frac{2m_b}{q^2} (C_7^{eff} + C_7^{eff'}) T_1(q^2)]$$

$$A_{\parallel}^{L,R} \propto [(C_9^{eff} - C_9^{eff'}) \mp (C_{10}^{eff} - C_{10}^{eff'}) \frac{A_1(q^2)}{m_B + m_{K^*}} + \frac{2m_b}{q^2} (C_7^{eff} - C_7^{eff'}) T_2(q^2)]$$

$$A_0^{L,R} \propto [(C_9^{eff} - C_9^{eff'}) \mp (C_{10}^{eff} - C_{10}^{eff'})] \times [(m_B^2 - m_{K^*}^2 - q^2)(m_B + m_{K^*} A_1(q^2) - \lambda \frac{A_2(q^2)}{m_B + m_{K^*}})] + 2m_b (C_7^{eff} + C_7^{eff'}) [(m_B^2 + 3m_{K^*}^2 - q^2) T_2(q^2) - \frac{\lambda}{m_B^2 - m_{K^*}^2} T_3(q^2)]$$

Amplitudes

The quark current can be either V-A or V+A

$$A_{\perp}^{L,R} \propto [(C_9^{eff} + C_9^{eff'}) \mp (C_{10}^{eff} + C_{10}^{eff'})] \frac{V(q^2)}{m_B + m_{K^*}} + \frac{2m_b}{q^2} (C_7^{eff} + C_7^{eff'}) T_1(q^2)$$

$$A_{\parallel}^{L,R} \propto [(C_9^{eff} - C_9^{eff'}) \mp (C_{10}^{eff} - C_{10}^{eff'})] \frac{A_1(q^2)}{m_B + m_{K^*}} + \frac{2m_b}{q^2} (C_7^{eff} - C_7^{eff'}) T_2(q^2)$$

$$A_0^{L,R} \propto [(C_9^{eff} - C_9^{eff'}) \mp (C_{10}^{eff} - C_{10}^{eff'})] \times [(m_B^2 - m_{K^*}^2 - q^2)(m_B + m_{K^*} A_1(q^2) - \lambda \frac{A_2(q^2)}{m_B + m_{K^*}})] + 2m_b (C_7^{eff} + C_7^{eff'}) [(m_B^2 + 3m_{K^*}^2 - q^2) T_2(q^2) - \frac{\lambda}{m_B^2 - m_{K^*}^2} T_3(q^2)]$$

Amplitudes

We have six different form factors

$$A_{\perp}^{L,R} \propto [(C_9^{eff} + C_9^{eff'}) \mp (C_{10}^{eff} + C_{10}^{eff'})] \frac{V(q^2)}{m_B + m_{K^*}} + \frac{2m_b}{q^2} (C_7^{eff} + C_7^{eff'}) T_1(q^2)$$

$$A_{\parallel}^{L,R} \propto [(C_9^{eff} - C_9^{eff'}) \mp (C_{10}^{eff} - C_{10}^{eff'})] \frac{A_1(q^2)}{m_B + m_{K^*}} + \frac{2m_b}{q^2} (C_7^{eff} - C_7^{eff'}) T_2(q^2)$$

$$A_0^{L,R} \propto [(C_9^{eff} - C_9^{eff'}) \mp (C_{10}^{eff} - C_{10}^{eff'})] \times [(m_B^2 - m_{K^*}^2 - q^2)(m_B + m_{K^*} A_1(q^2) - \lambda \frac{A_2(q^2)}{m_B + m_{K^*}})] + \\ 2m_b (C_7^{eff} + C_7^{eff'}) [(m_B^2 + 3m_{K^*}^2 - q^2) T_2(q^2) - \frac{\lambda}{m_B^2 - m_{K^*}^2} T_3(q^2)]$$

Amplitudes

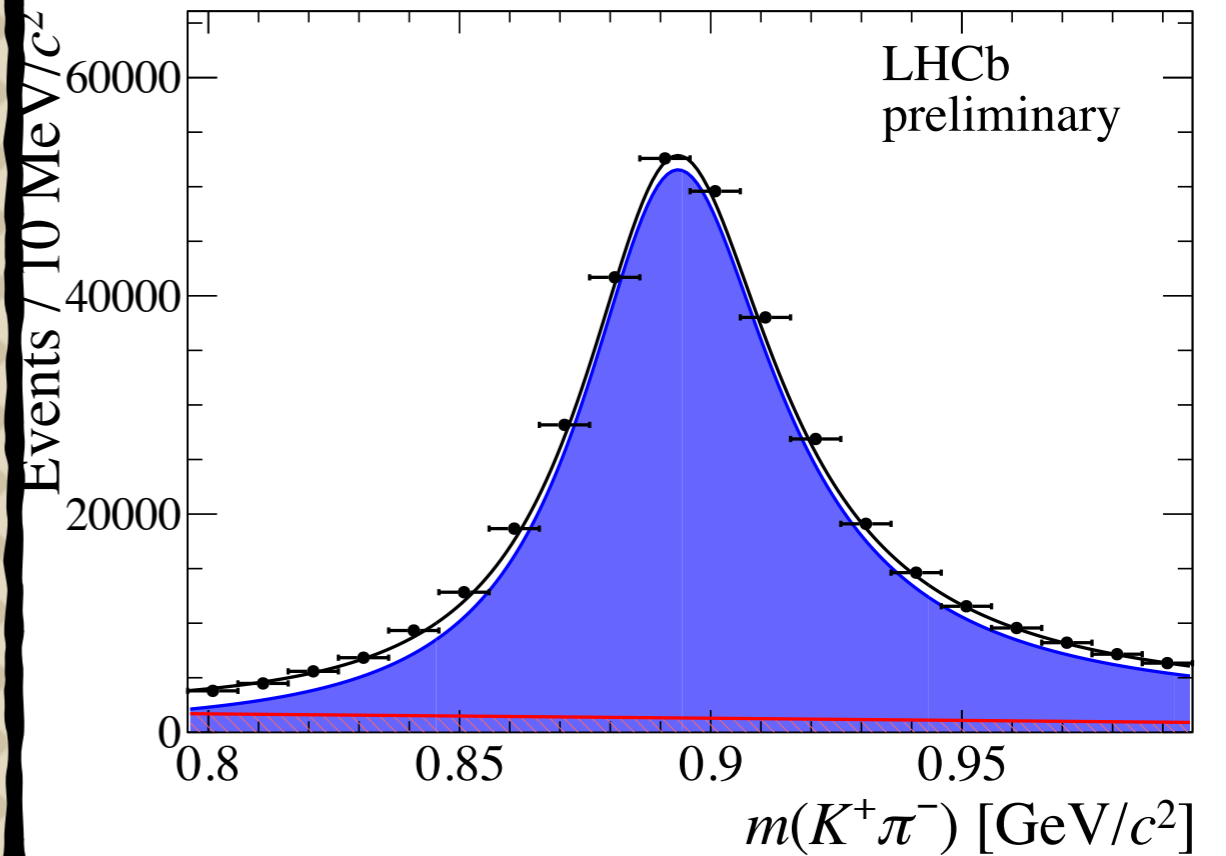
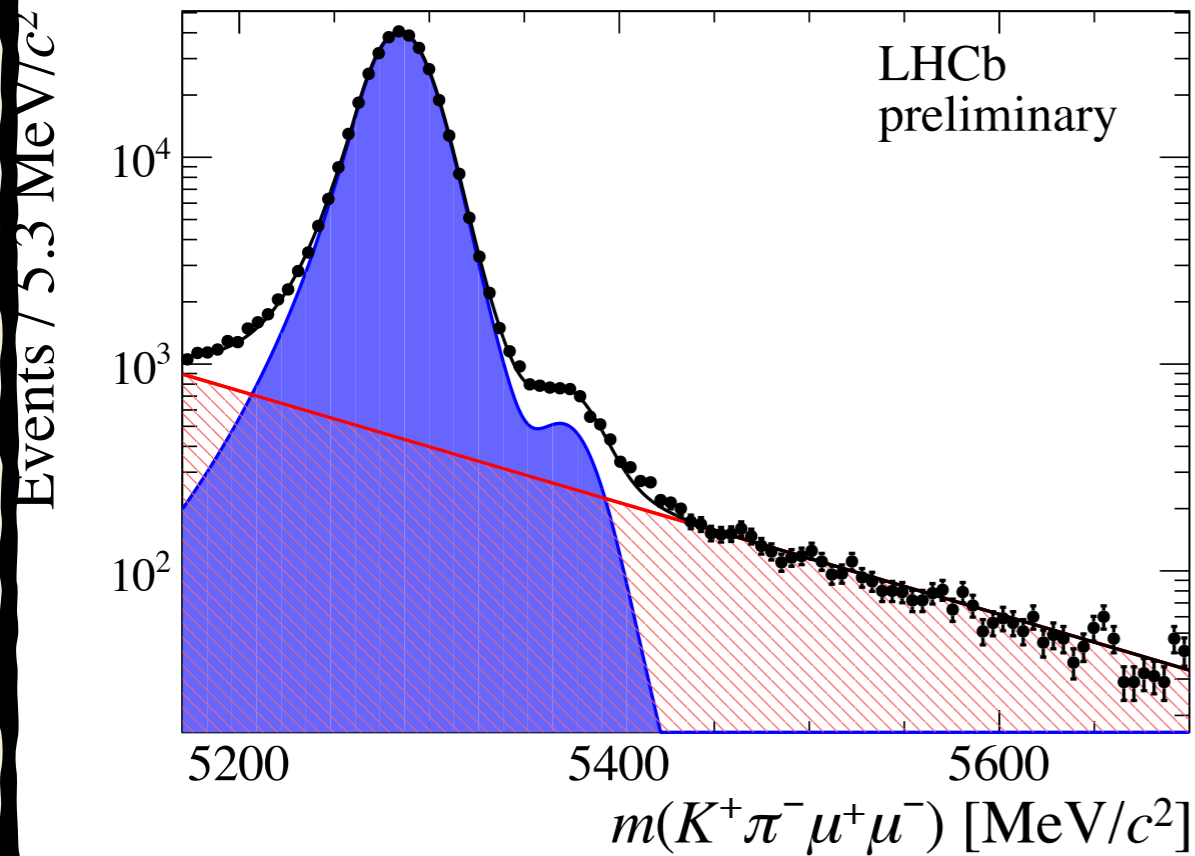
And six (complex) Wilson coefficients: $C_7^{(\prime)}$, $C_9^{(\prime)}$ and $C_{10}^{(\prime)}$

$$A_{\perp}^{L,R} \propto [(C_9^{eff} + C_9^{eff'}) \mp (C_{10}^{eff} + C_{10}^{eff'})] \frac{V(q^2)}{m_B + m_{K^*}} + \frac{2m_b}{q^2} (C_7^{eff} + C_7^{eff'}) T_1(q^2)$$

$$A_{\parallel}^{L,R} \propto [(C_9^{eff} - C_9^{eff'}) \mp (C_{10}^{eff} - C_{10}^{eff'})] \frac{A_1(q^2)}{m_B + m_{K^*}} + \frac{2m_b}{q^2} (C_7^{eff} - C_7^{eff'}) T_2(q^2)$$

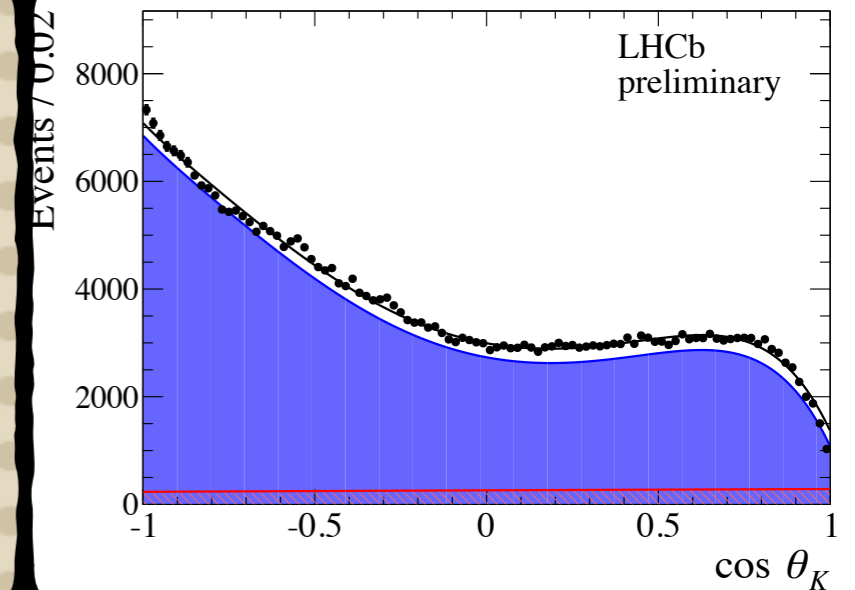
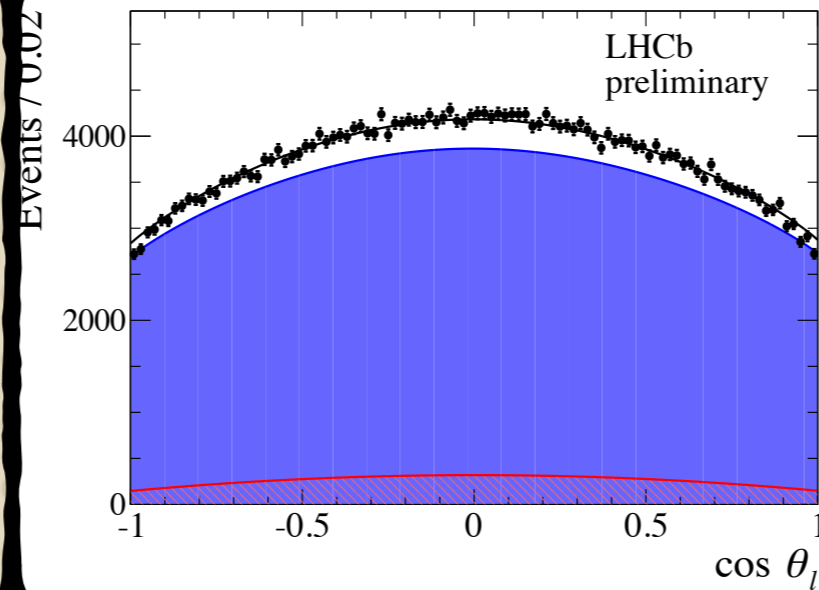
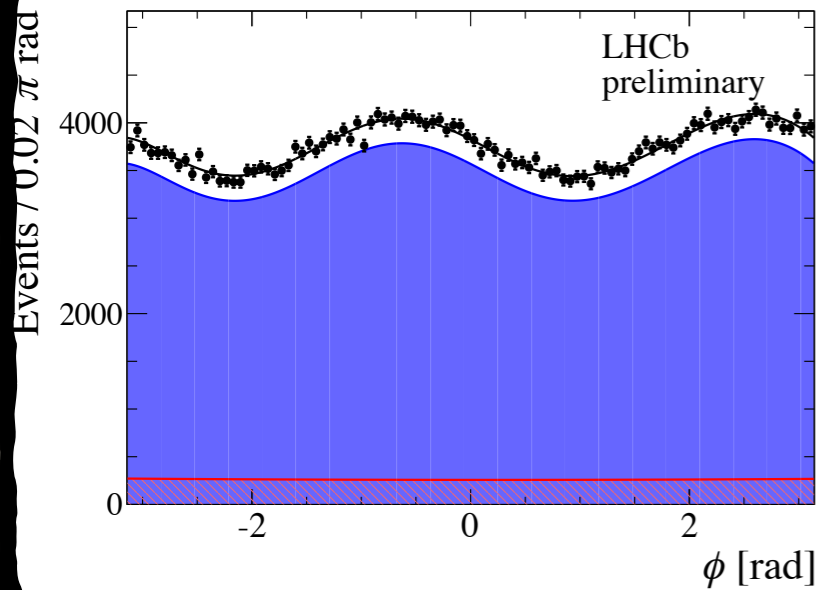
$$A_0^{L,R} \propto [(C_9^{eff} - C_9^{eff'}) \mp (C_{10}^{eff} - C_{10}^{eff'})] \times [(m_B^2 - m_{K^*}^2 - q^2)(m_B + m_{K^*} A_1(q^2) - \lambda \frac{A_2(q^2)}{m_B + m_{K^*}})] + 2m_b (C_7^{eff} + C_7^{eff'}) [(m_B^2 + 3m_{K^*}^2 - q^2) T_2(q^2) - \frac{\lambda}{m_B^2 - m_{K^*}^2} T_3(q^2)]$$

Control Channel

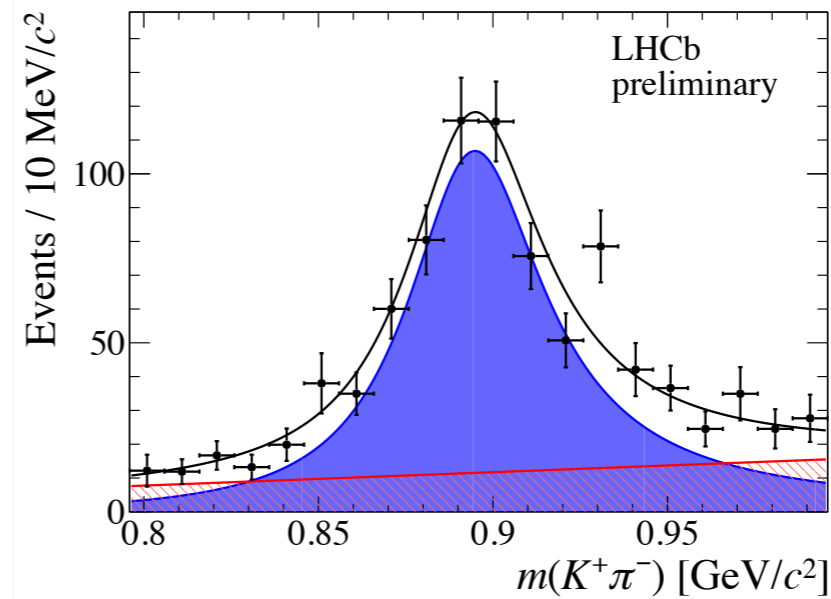
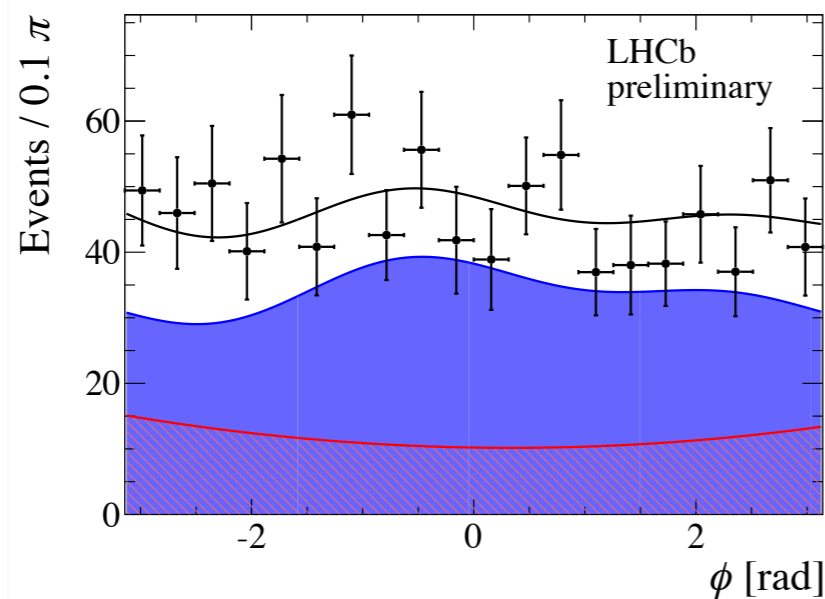
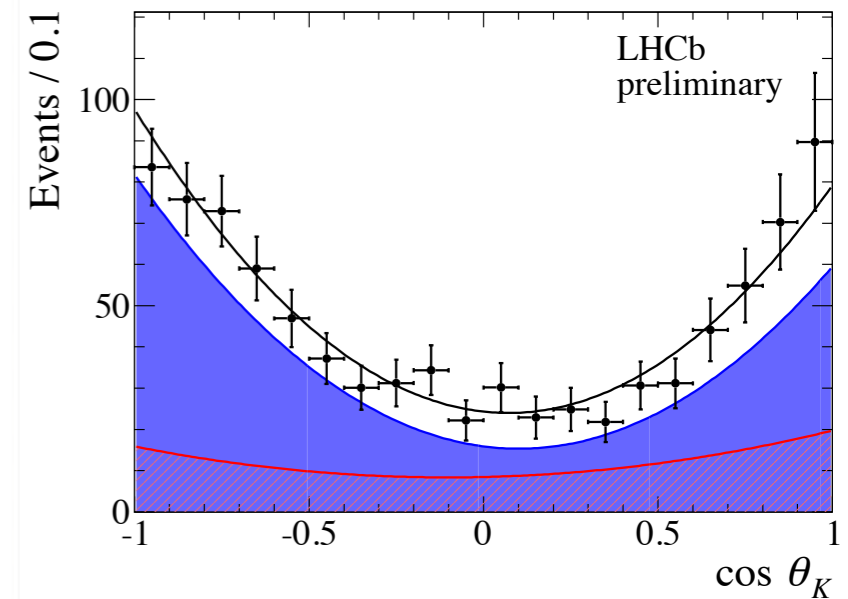
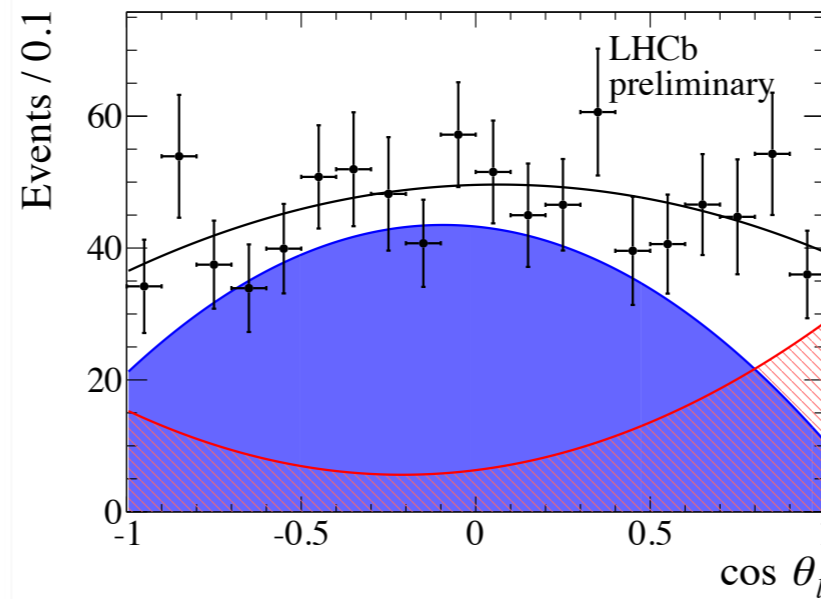
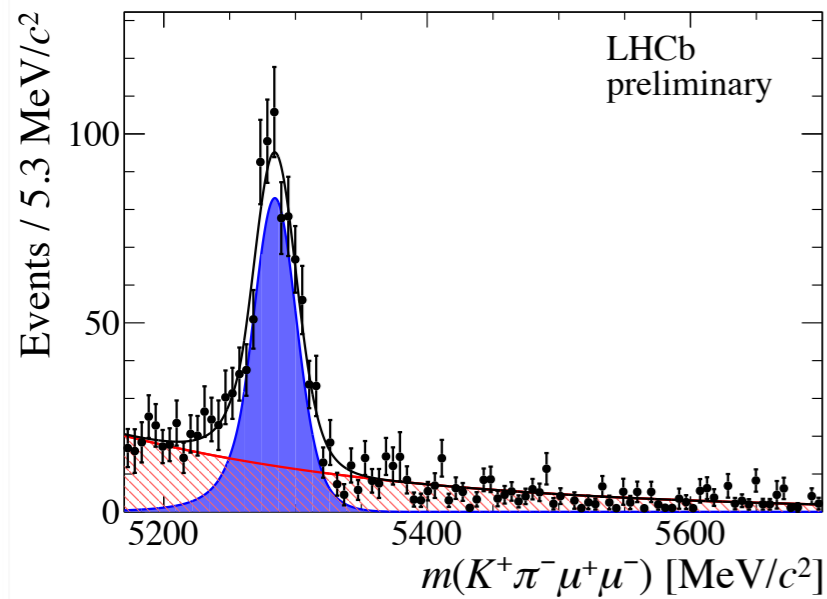


- High statistics control channel ($\sim 300K$ events)

Control Channel



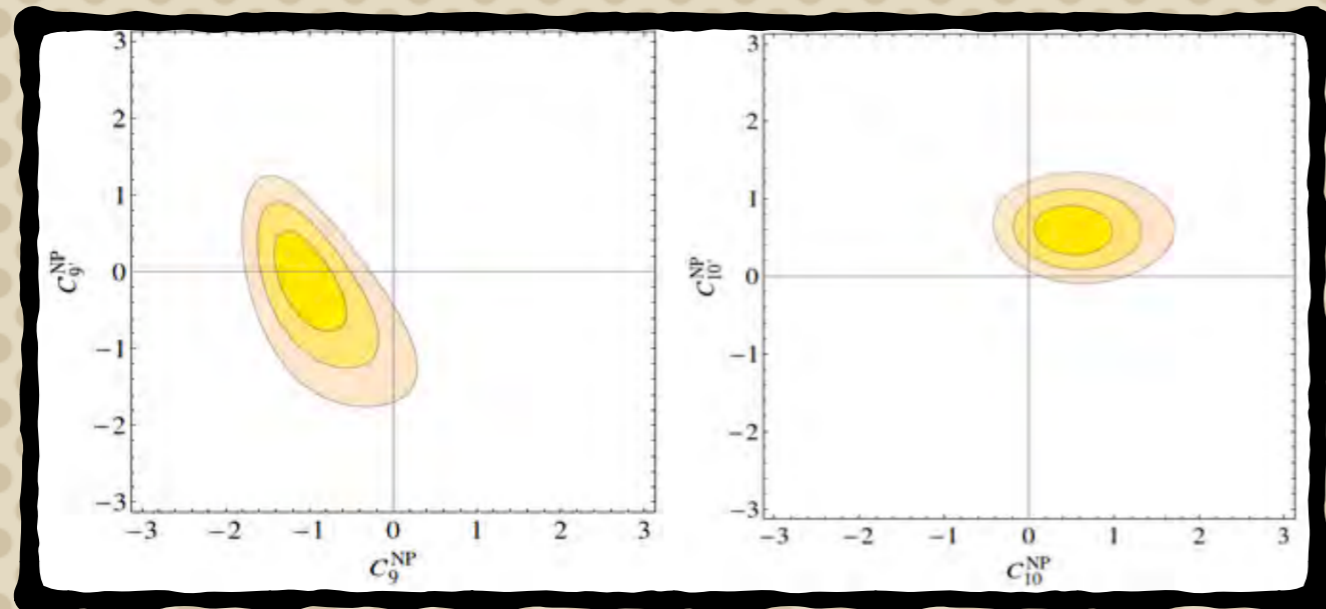
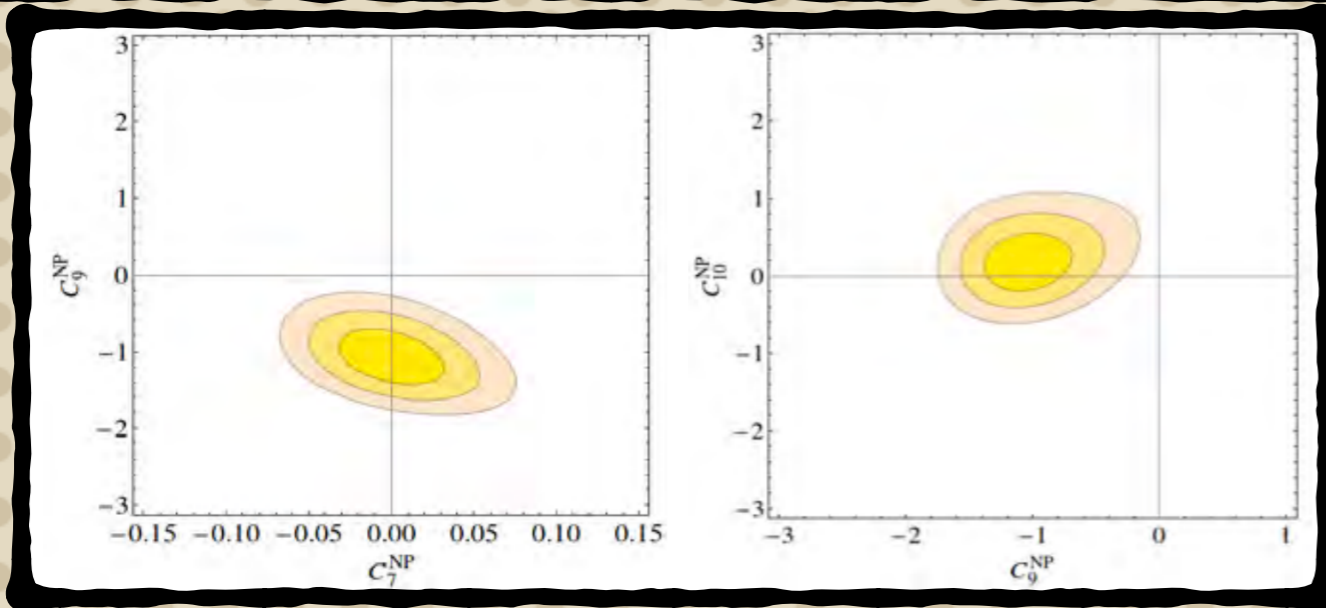
- Results in very good agreement with existing measurement of $B^0 \rightarrow J/\psi K^*$ (**PRD 88, 052002 (2013)**)
- Allows to check overall strategy, in particular allowed to spot small mismodelling (solved) in the angular acceptance
- Overall procedure also tested with high statistics MC



- Events in $1.1 < q^2 < 6.0 \text{ GeV}^2$
- $4D + 1D$ fit of B-meson invariant mass and the three angles $(\theta_\ell, \theta_K, \phi) + m_{K\pi}$
- Fit in $m_{K\pi}$ used to determine the S-wave fraction (see backup)
- Acceptance corrections incorporated in the Pdf, using a range of control channels + MC simulation

First theory reactions

- J. Matias performed a preliminary fit of Wilson coefficients (Moriond EW)

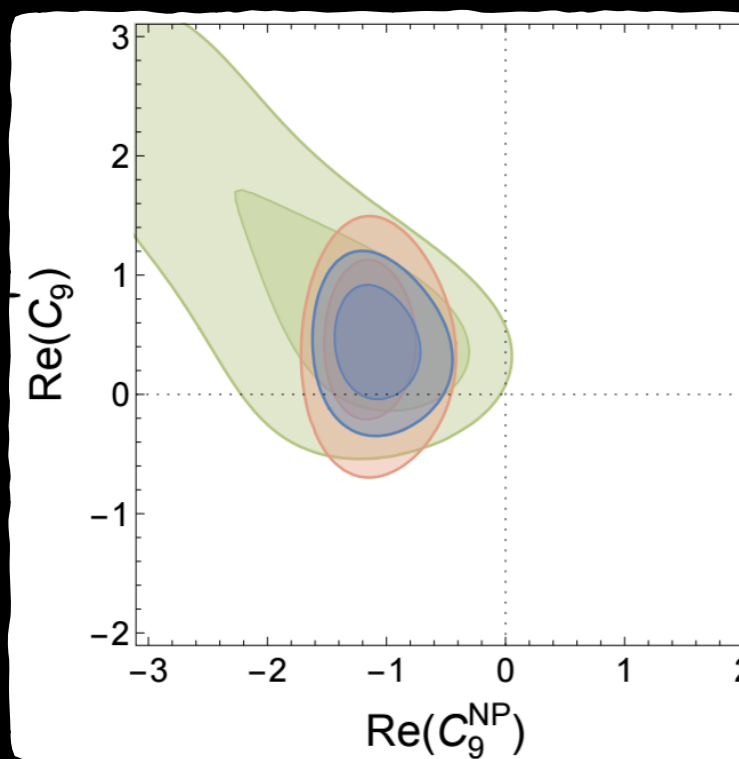
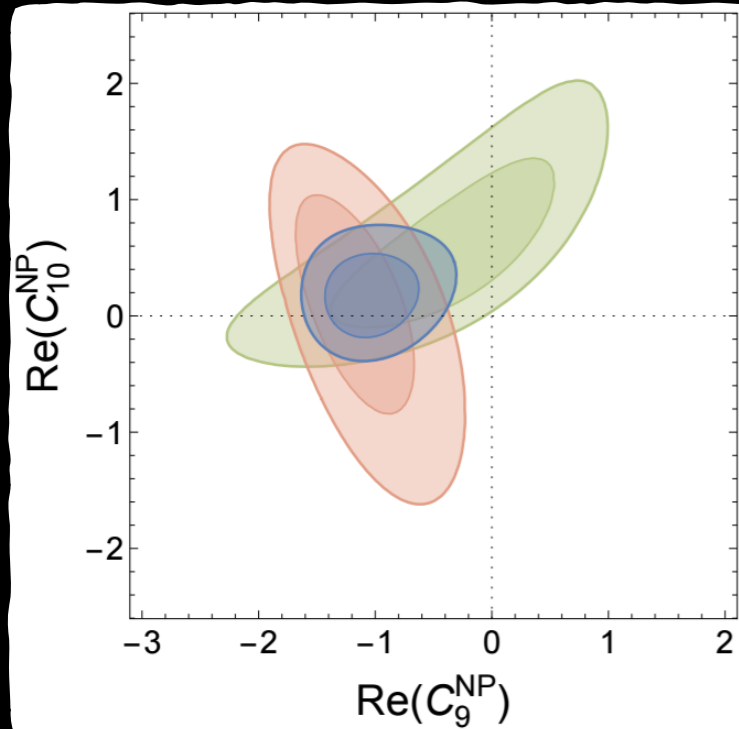


Hypothesis	Best fit	pull
$C_9^{\text{NP}} = -C_{10}^{\text{NP}}$	-0.62	4.0
$C_9^{\text{NP}} = C_{10}^{\text{NP}}$	-0.37	1.7
$C'_9 = C'_{10}$	0.32	1.3
$C_9^{\text{NP}} = C'_9$	-0.67	4.3
$C'_9 = -C'_{10}$	-0.42	3.6

Hypothesis	Best fit	pull
C_9^{NP}	-1.1	4.6
C_{10}^{NP}	0.62	2.4
C'_9	-1.0	3.4
C'_{10}	0.61	3.3

Relevant Observables included: $B \rightarrow K^* \mu^+ \mu^-$ ($P_{1,2}, P'_{4,5,6,8}, F_L$ in all 5 large-recoil + low-recoil), $B^+ \rightarrow K^+ \mu^+ \mu^-$ and $B^0 \rightarrow K^0 \mu^+ \mu^-$, $\mathcal{B}_{B \rightarrow X_s \gamma}$, $\mathcal{B}_{B \rightarrow X_s \mu^+ \mu^-}$, $\mathcal{B}_{B_S \rightarrow \mu^+ \mu^-}$, $A_I(B \rightarrow K^* \gamma)$, $S_{K^* \gamma}$

First theory reactions



- D. Straub performed a preliminary fit of Wilson coefficients (Moriond EW)

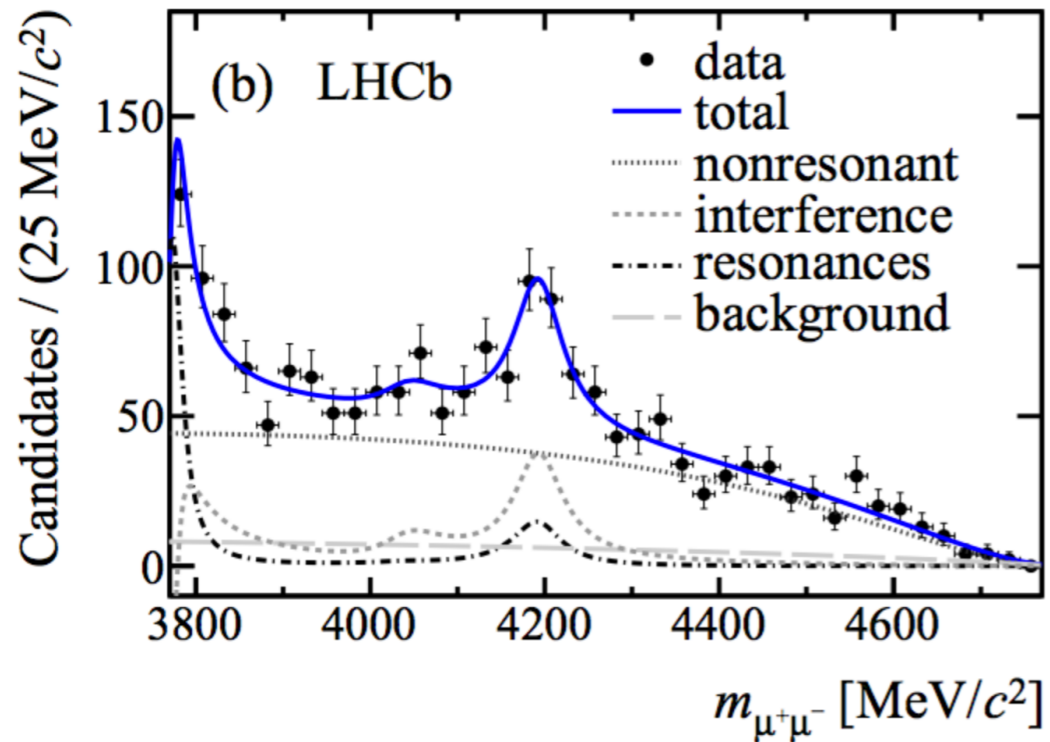
- ▶ Angular observables in $\bar{B}^0 \rightarrow K^{*0} \mu^+ \mu^-$
- ▶ (Differential) branching ratios of
 - ▶ $\bar{B}^0 \rightarrow \bar{K}^{*0} \mu^+ \mu^-$, $B^- \rightarrow K^{*-} \mu^+ \mu^-$, $\bar{B}^0 \rightarrow \bar{K}^{*0} \mu^+ \mu^-$, $B^- \rightarrow K^- \mu^+ \mu^-$, $B_s \rightarrow \phi \mu^+ \mu^-$, $B_s \rightarrow \mu^+ \mu^-$, $\bar{B}^0 \rightarrow \bar{K}^{*0} \gamma$, $B^- \rightarrow K^{*-} \gamma$, $B \rightarrow X_s \gamma$, $B \rightarrow X_s \mu^+ \mu^-$.

Coeff.	best fit	1σ	2σ	$\sqrt{\chi_{\text{b.f.}}^2 - \chi_{\text{SM}}^2}$	p [%]
C_7^{NP}	-0.04	[-0.07, -0.01]	[-0.10, 0.02]	1.42	2.4
C_7'	0.01	[-0.04, 0.07]	[-0.10, 0.12]	0.24	1.8
C_9^{NP}	-1.07	[-1.32, -0.81]	[-1.54, -0.53]	3.70	11.3
C_9'	0.21	[-0.04, 0.46]	[-0.29, 0.70]	0.84	2.0
C_{10}^{NP}	0.50	[0.24, 0.78]	[-0.01, 1.08]	1.97	3.2
C_{10}'	-0.16	[-0.34, 0.02]	[-0.52, 0.21]	0.87	2.0
$C_9^{\text{NP}} = C_{10}^{\text{NP}}$	-0.22	[-0.44, 0.03]	[-0.64, 0.33]	0.89	2.0
$C_9^{\text{NP}} = -C_{10}^{\text{NP}}$	-0.53	[-0.71, -0.35]	[-0.91, -0.18]	3.13	7.1
$C_9' = C_{10}'$	-0.10	[-0.36, 0.17]	[-0.64, 0.43]	0.36	1.8
$C_9' = -C_{10}'$	0.11	[-0.01, 0.22]	[-0.12, 0.33]	0.93	2.0

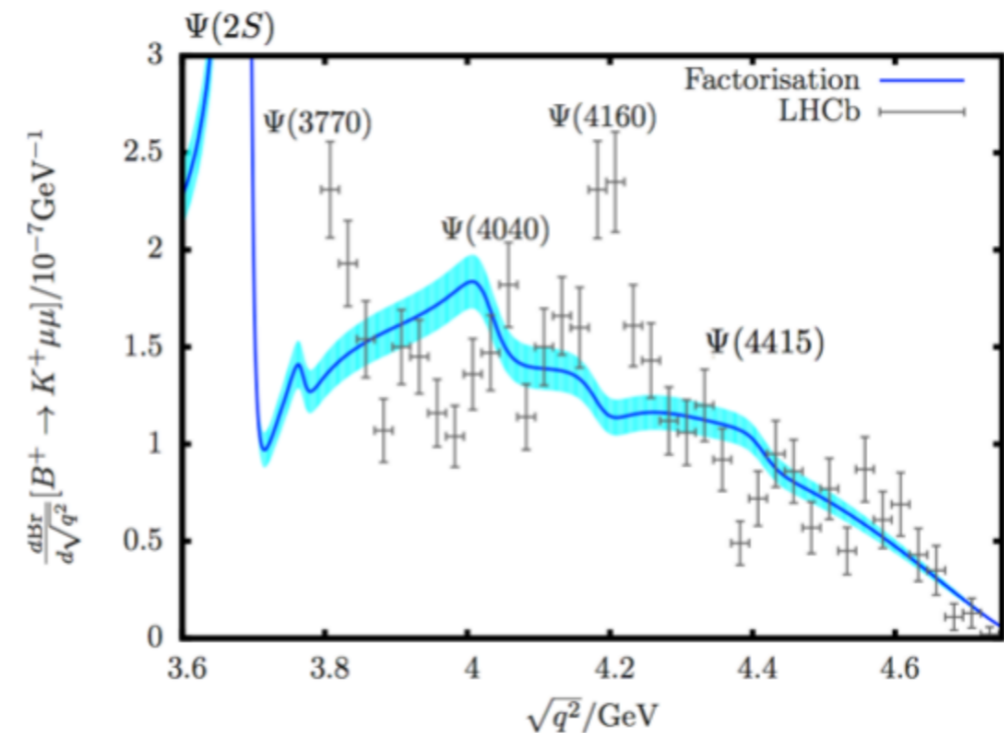
Green: all branching ratios | Red: $B \rightarrow K^* \mu^+ \mu^-$ angular observables | Blue: Global fit

Charm loop effects?

- LHCb has evidence of resonance structures in the high q^2 region of $B^+ \rightarrow K^+ \mu^+ \mu^-$
- First observation of $B^+ \rightarrow K^+ \psi(4160)(\rightarrow \mu^+ \mu^-)$



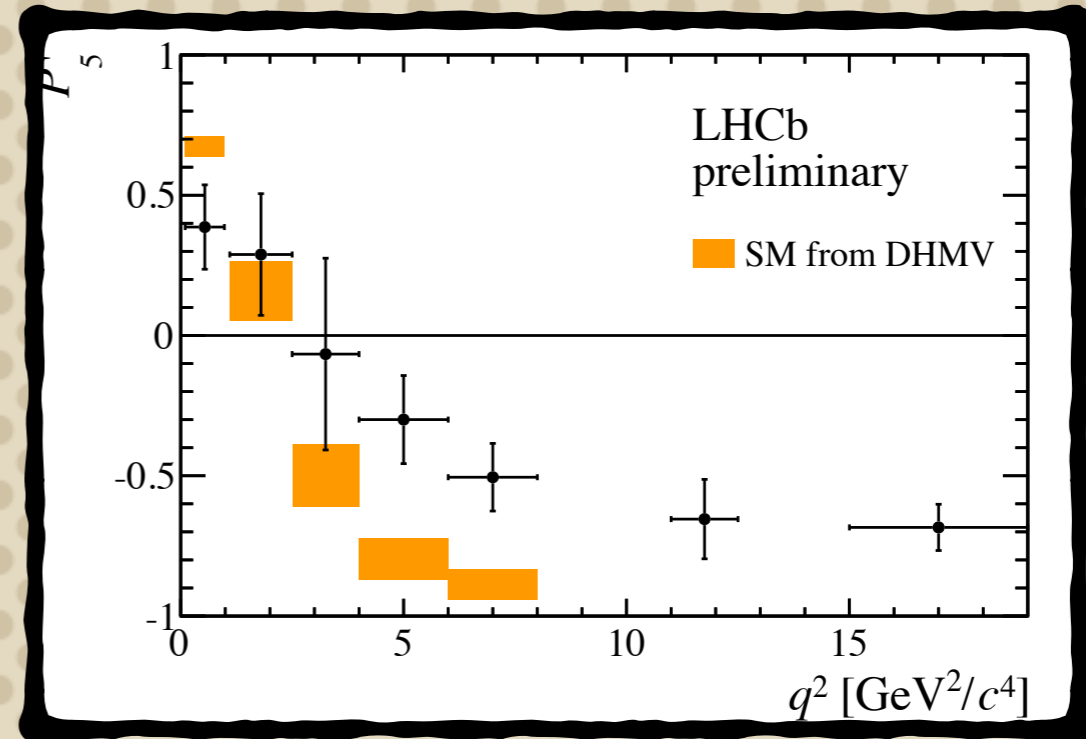
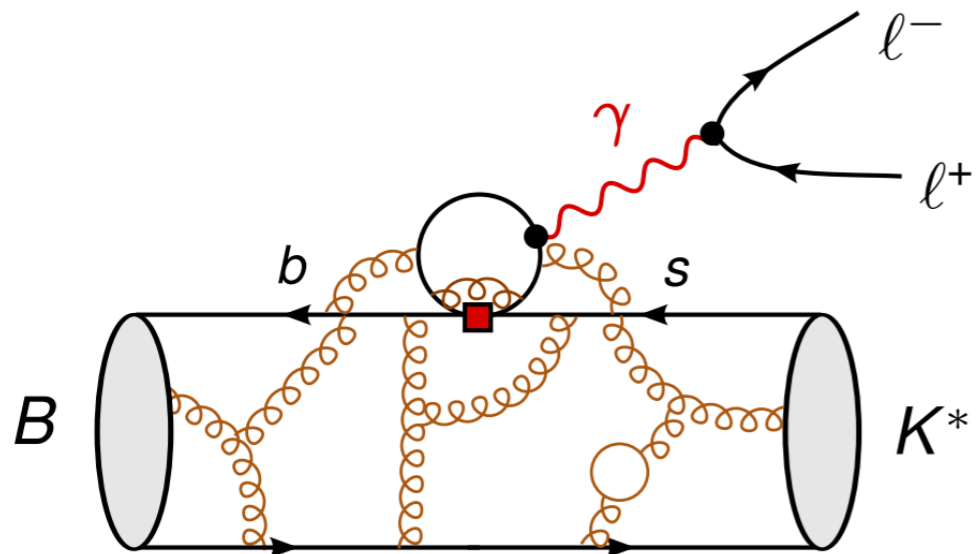
Extrapolation from BESII assuming QCD factorisation



Lyons and Zwicky [arXiv:1406.0566](https://arxiv.org/abs/1406.0566)

Resonance structure at high q^2 failure of factorisation

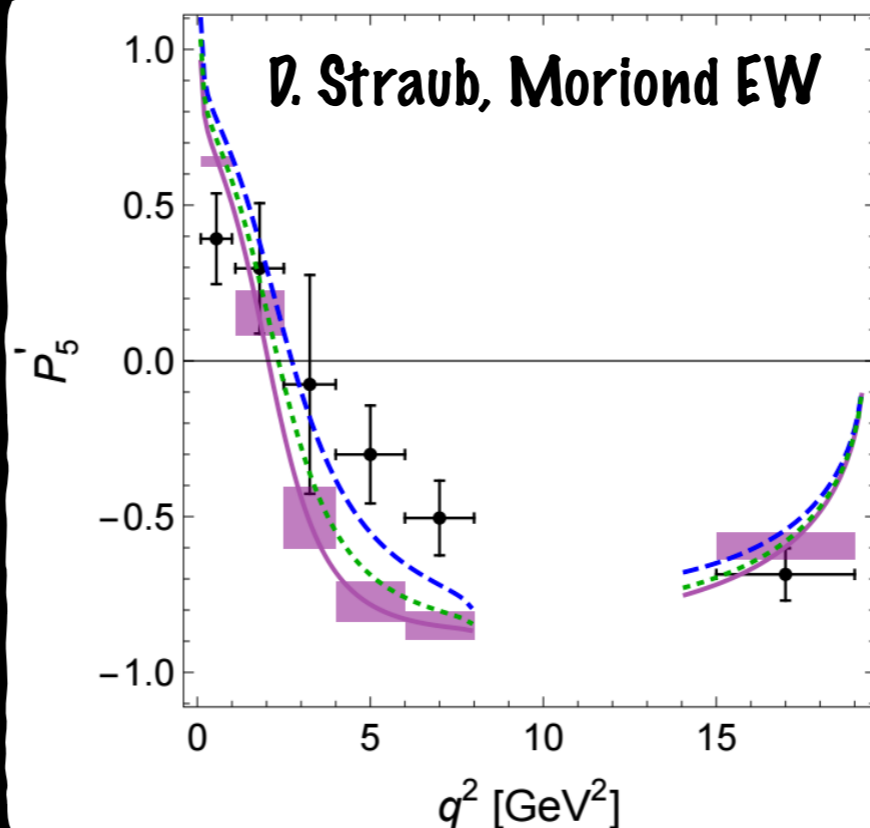
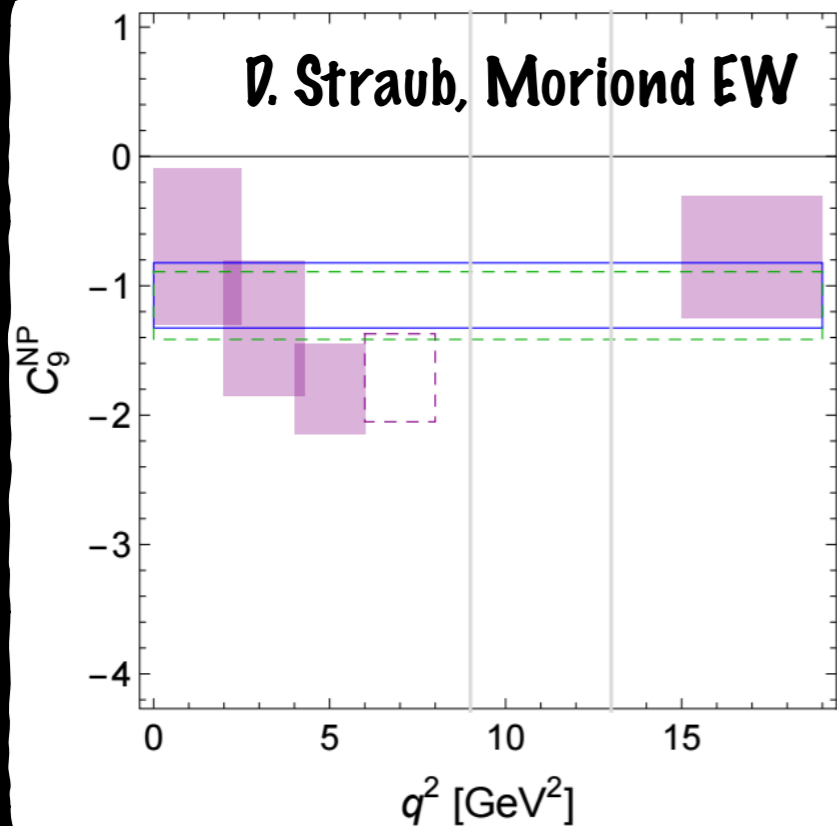
Charm loop effects?



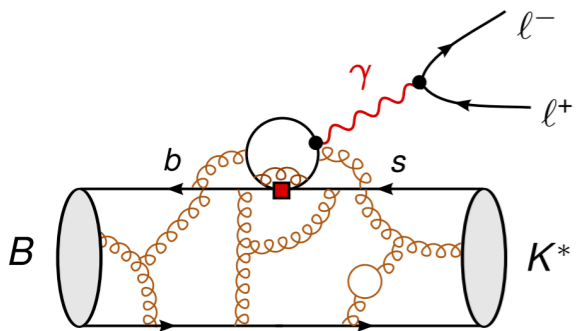
- Charm loop photon mediated can give an effect similar to C_9
- P_5' anomaly close to J/ψ
- Possibility to explained with anomalously large charm loop

q^2 dependence different in NP and hadronic effects

First theory reactions

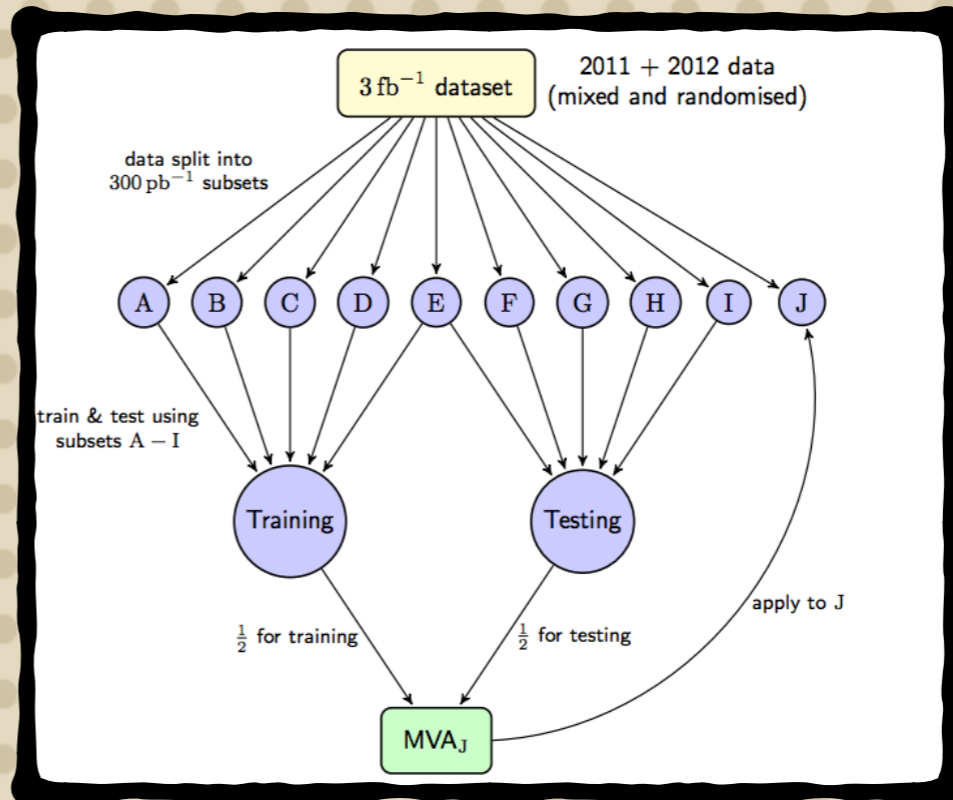
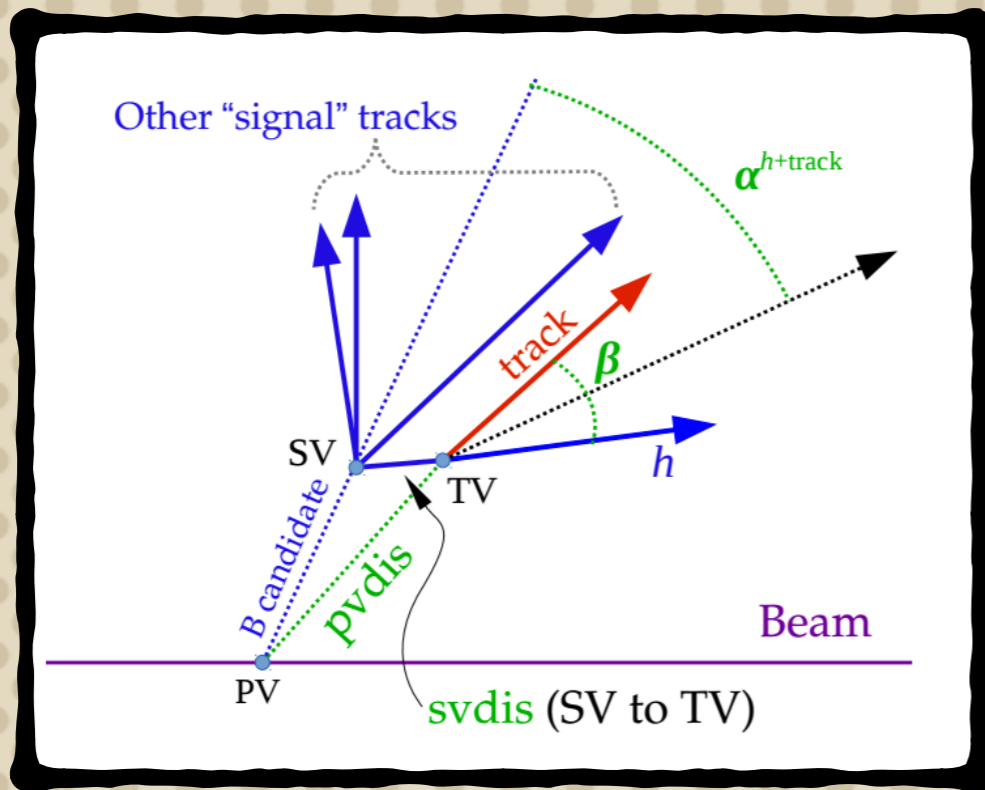


- ▶ **Blue dashed:**
 $C_9^{\text{NP}} = -1.1$ fits best at intermediate q^2
- ▶ **Green dotted:**
 $C_9^{\text{NP}} = -C_{10}^{\text{NP}} = -0.55$ fits slightly better in first and last bin



- Still possible that such effect comes from anomalously large charm loop effects
- NP and QCD have a different q^2 dependence (need more data)

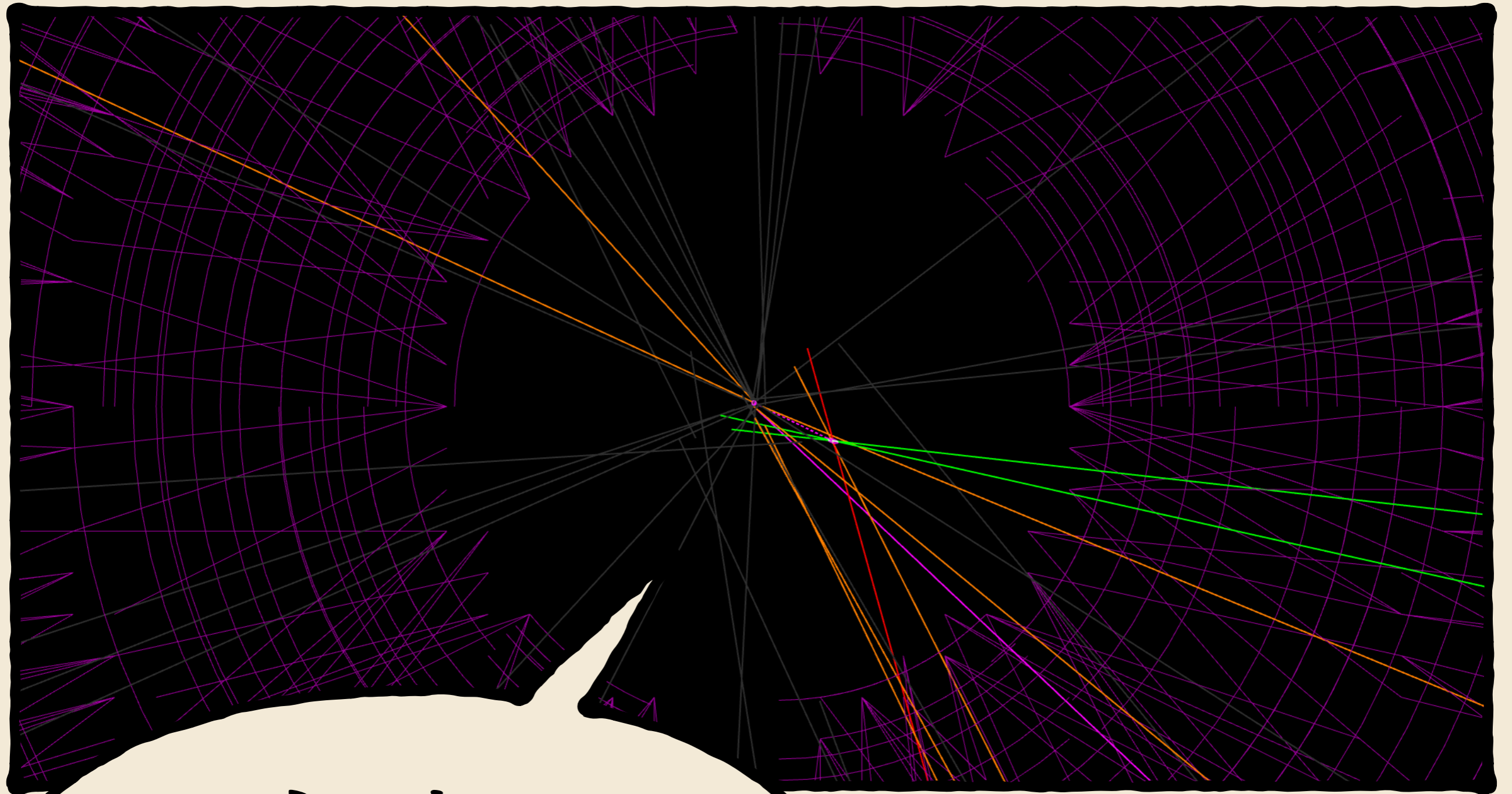
Selection



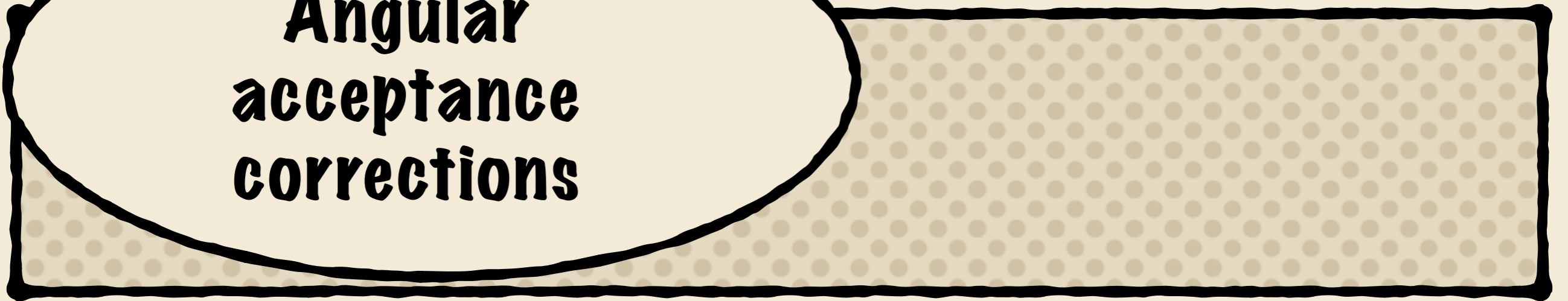
- Train of the BDT performed using $B^0 \rightarrow J\psi K^*$ as proxy for the signal
 - Kinematic variables: $p(B)$, $p_T(B)$, $K\pi\mu\mu$ vertex quality, $\tau(B)$ and pointing to PV
 - Particle identification
 - Track isolation
- The upper side of the signal is used for background using k-Folding
 - Split data in 10 samples
 - For each sample a BDT is optimized on 9/10 of the statistics and then applied to the 1/10
 - We have 10 different BDTs with the same observables
 - No overtraining, improved performances because used large statistics in the train

Peaking Backgrounds

- Vetoed charmonia resonances ($B^0 \rightarrow J/\psi K^*$, $B^0 \rightarrow \psi(2S)K^*$) by binning in q^2
- Final state radiation of charmonia resonances vetoed by B invariant mass cut
- We see evidence of $B^0 \rightarrow \phi K^*$, excluded by the cut $[0.98, 1.1]\text{GeV}^2/c^4$
- Several other peaking backgrounds identified: $\Lambda_b \rightarrow pK\mu\mu$, $B_s \rightarrow \phi\mu\mu$, $B^+ \rightarrow K^+\mu\mu$ and $B^+ \rightarrow K^{*+}\mu\mu$
- After peaking background vetos dominant contribution $\Lambda_b \rightarrow pK\mu\mu$ at about 1% level (systematics assigned)
- Also vetoed events with $K - \pi$, $K - \mu$ or $\pi - mu$ swap (for signal and control channel)



**Angular
acceptance
corrections**



Corrections of angular acceptance

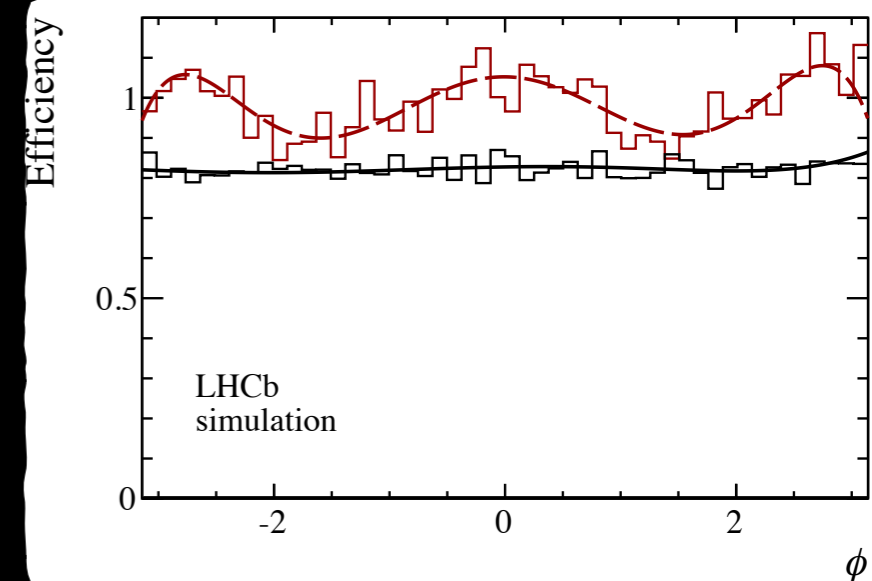
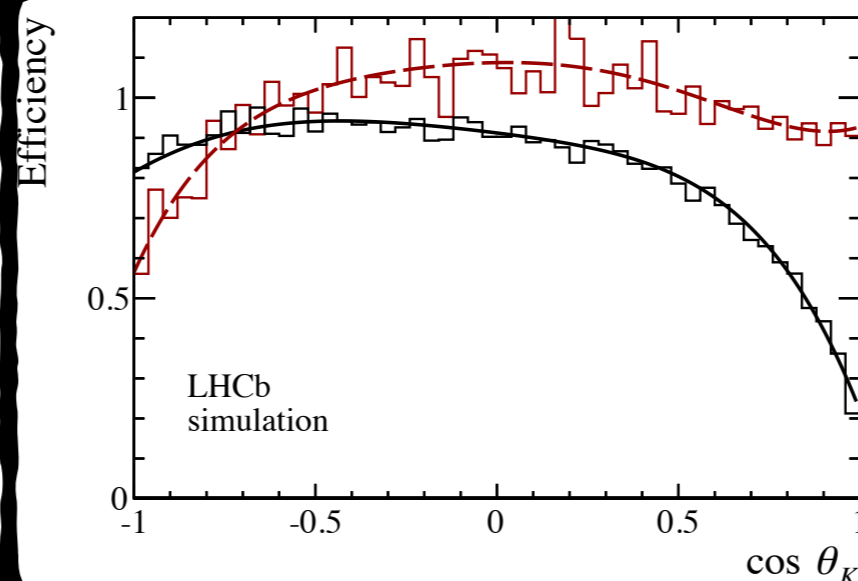
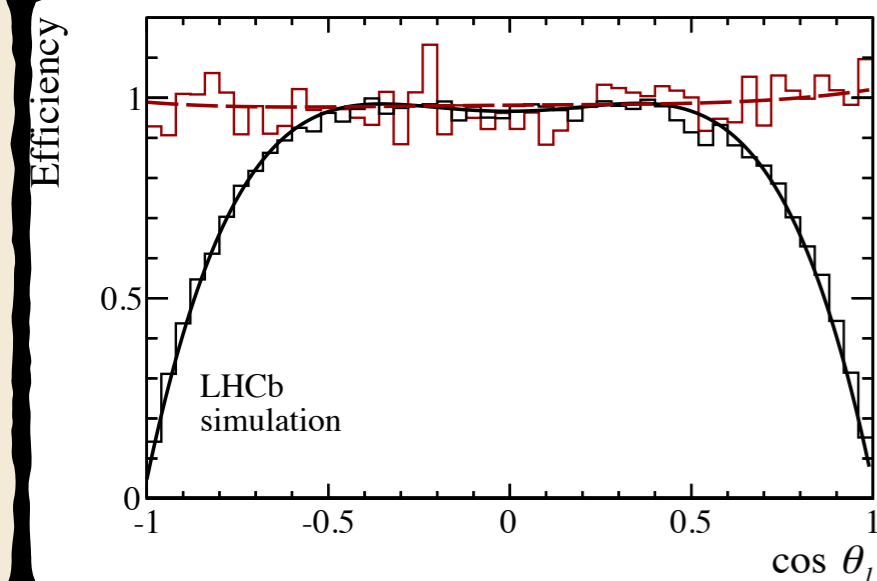
- Determine the angular efficiency from a principal moment analysis of phase-space $B^0 \rightarrow K^{*0} \mu^+ \mu^-$ MC
 - Re-weighting events to correct for data-MC differences and to remove the phase-space q^2 dependence.
- Efficiency in 4D is given by

$$\varepsilon(\cos \theta_\ell, \cos \theta_K, \phi, q^2) = \sum_{klmn} c_{klmn} P_k(\cos \theta_\ell) P_l(\cos \theta_K) P_m(\phi) P_n(q^2)$$

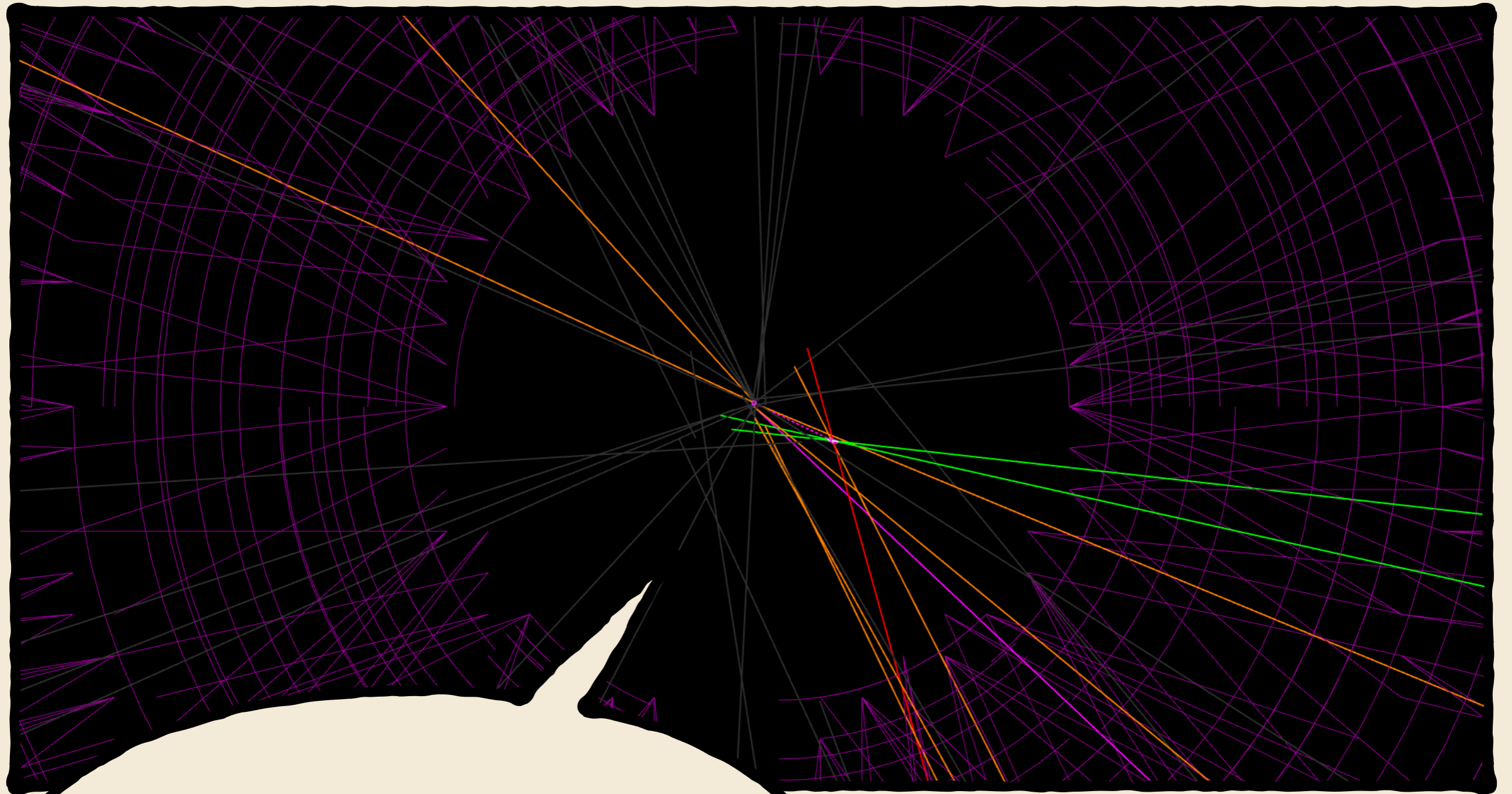
where $P_i(x)$ are Legendre polynomials of order i .

- We use polynomials up-to orders 6, 5, 6, 7 for $\cos \theta_K$, $\cos \theta_\ell$, ϕ and q^2 , respectively.

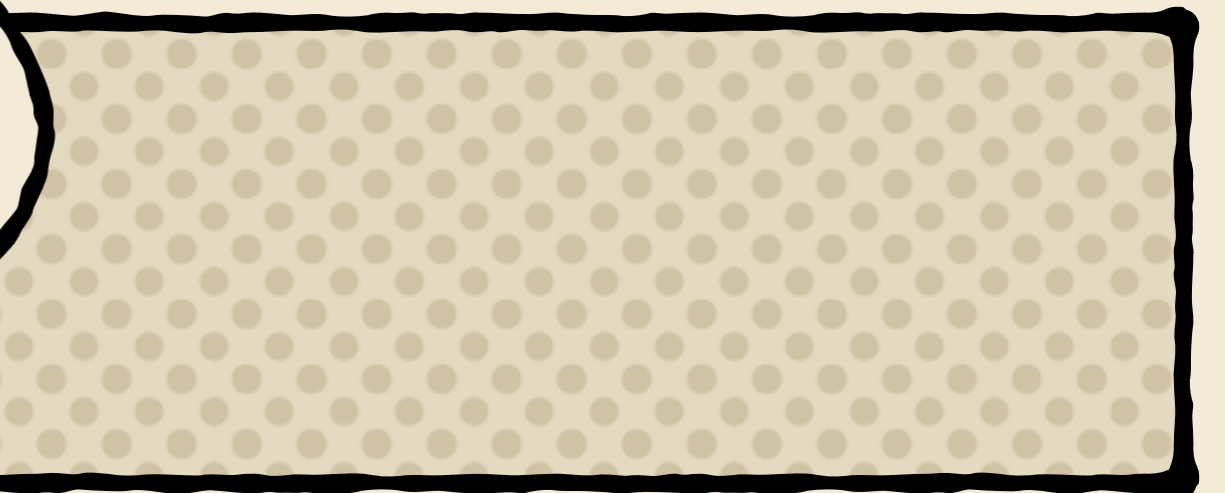
Acceptance Correction



- High statistics phase space MC used to extract the efficiency as a function of angles and q^2
- Acceptance for $18.0 < q^2 < 19.0 \text{ GeV}^2/c^4$ (red) and for $0.1 < q^2 < 0.98 \text{ GeV}^2/c^4$ (black)
- No factorization in the angles assumed
- Very good description of the efficiency by our polynomial model



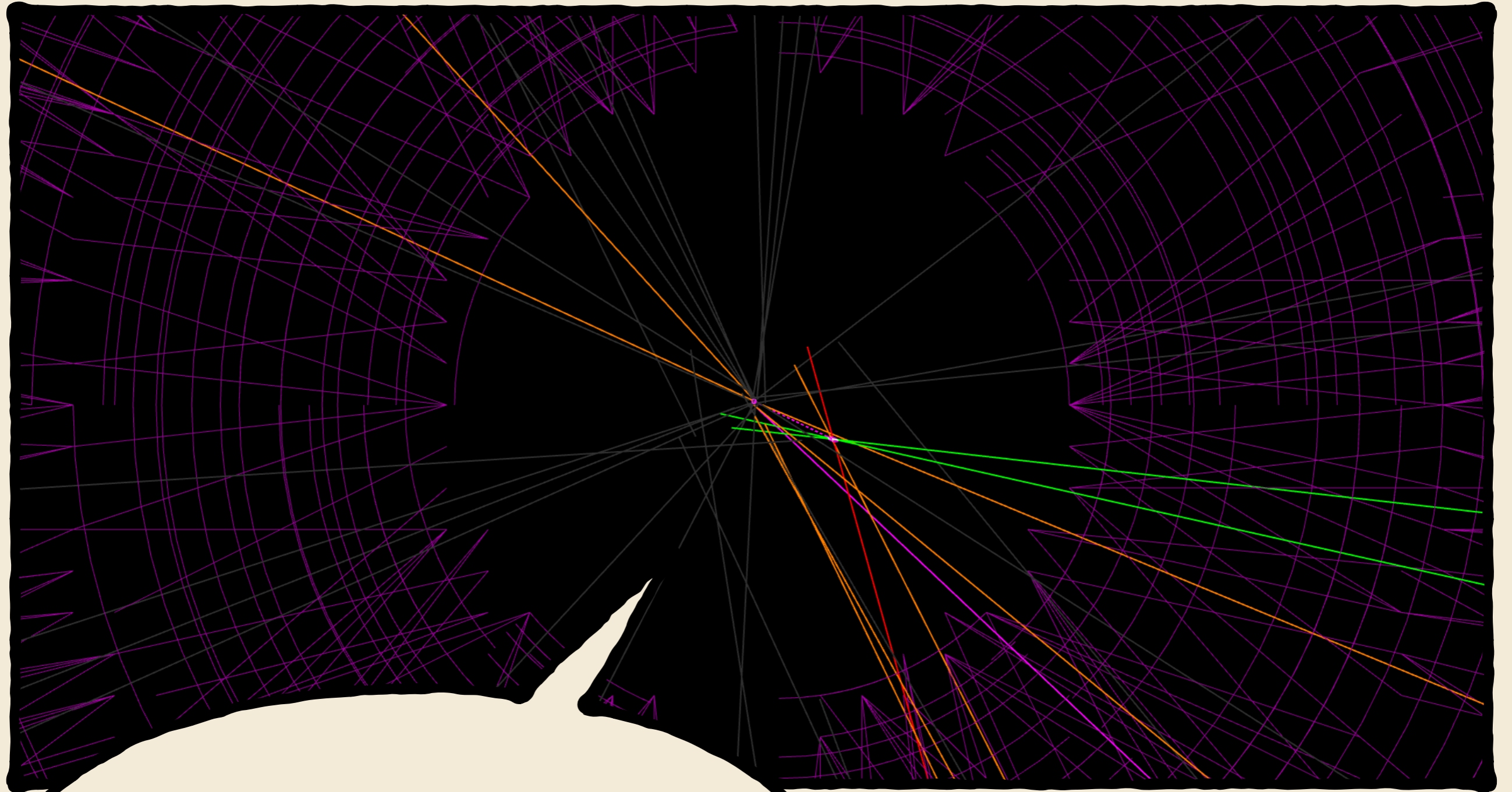
Systematics



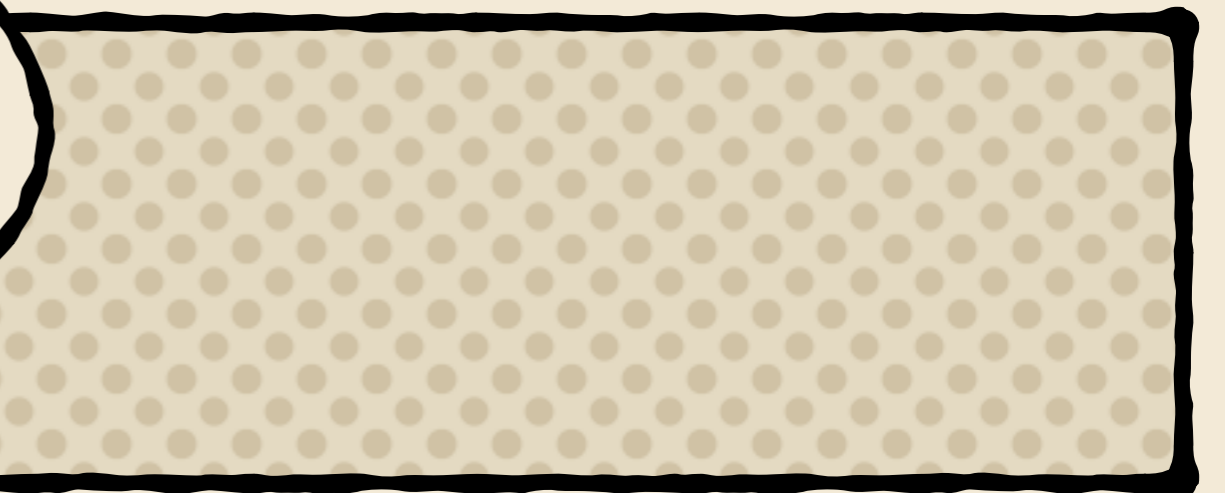
Systematics

σ	$0.1 < q^2 < 0.98 \text{ GeV}^2/c^4$							
	F_L	S_3	S_4	S_5	A_{FB}	S_7	S_8	S_9
$\sigma_{\text{stat.}}$	0.0440	0.0614	0.0659	0.0575	0.0564	0.0585	0.0739	0.0582
π reweighting	0.0139	0.0010	0.0005	0.0030	0.0003	0.0003	0.0000	0.0001
K reweighting	0.0035	0.0010	0.0003	0.0010	0.0008	0.0002	0.0001	0.0001
$p_T(B^0)$ reweighting	0.0009	0.0002	0.0003	0.0004	0.0003	0.0000	0.0001	0.0000
$\chi_{V_{tx}}^2$ reweighting	0.0019	0.0001	0.0019	0.0004	0.0019	0.0002	0.0000	0.0001
N_{tracks} reweighting	0.0010	0.0000	0.0005	0.0003	0.0022	0.0001	0.0002	0.0000
higher order acc.	0.0037	0.0007	0.0042	0.0162	0.0004	0.0036	0.0003	0.0017
$\epsilon(q^2)$	0.0070	0.0031	0.0051	0.0009	0.0008	0.0058	0.0012	0.0029
peaking bkg.	0.0024	0.0019	0.0008	0.0037	0.0018	0.0015	0.0017	0.0014
angular bkg. model	0.0003	0.0010	0.0007	0.0002	0.0001	0.0001	0.0000	0.0006
sig. mass	0.0009	0.0001	0.0000	0.0008	0.0005	0.0000	0.0000	0.0000
$m_{K\pi}$ isobar	0.0002	0.0000	0.0001	0.0004	0.0001	0.0000	0.0000	0.0000
$m_{K\pi}$ bkg.	0.0004	0.0000	0.0003	0.0009	0.0003	0.0001	0.0000	0.0000
$m_{K\pi}$ eff.	0.0007	0.0008	0.0025	0.0011	0.0005	0.0019	0.0033	0.0009
acc. stat.	0.0028	0.0041	0.0042	0.0045	0.0040	0.0038	0.0044	0.0038
$\sigma_{\text{syst.}}$	0.0170	0.0058	0.0085	0.0176	0.0055	0.0082	0.0058	0.0054

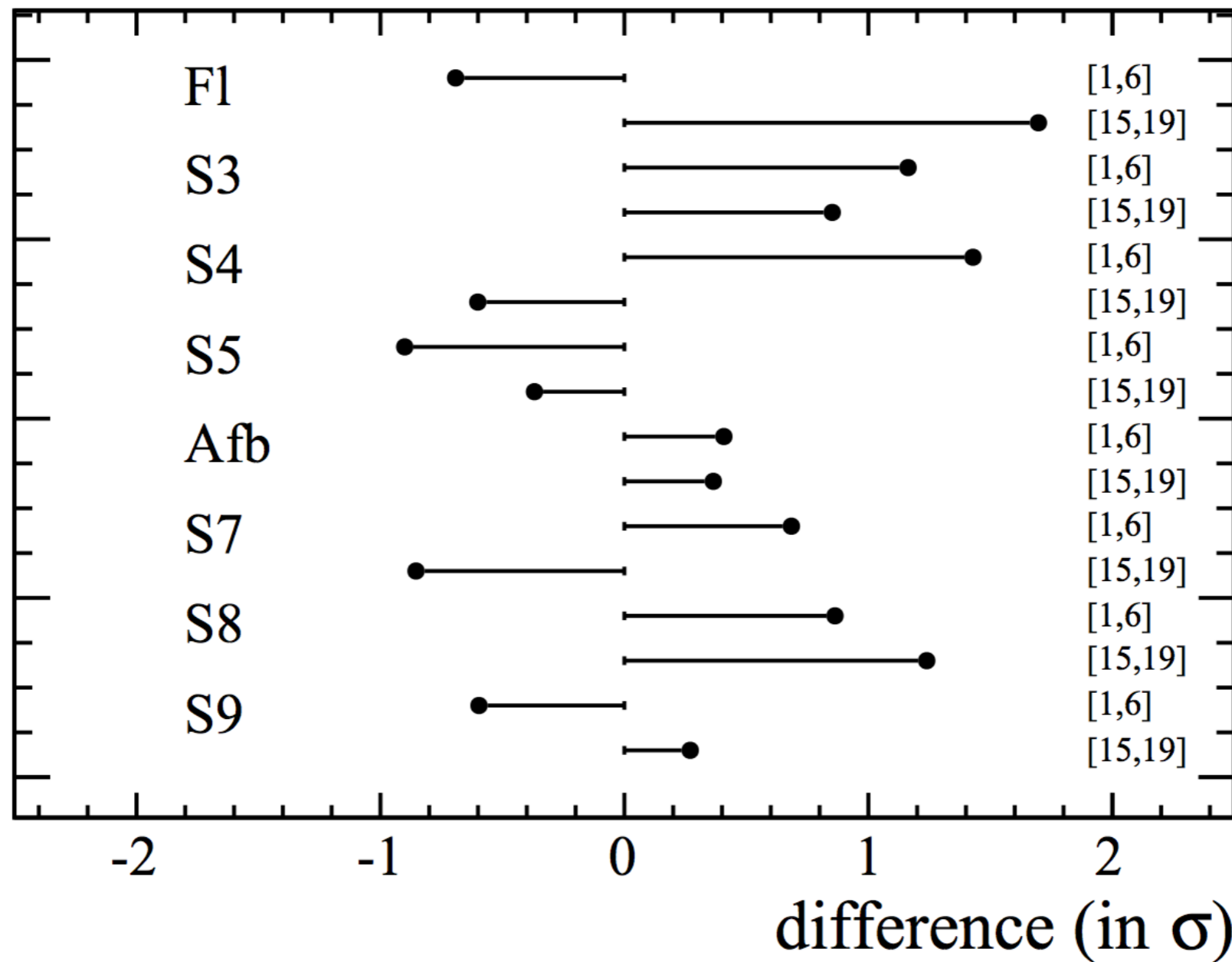
- Systematics small compared to statistical error
- Larger systematics form uncertainty on the acceptance correction



Cross checks

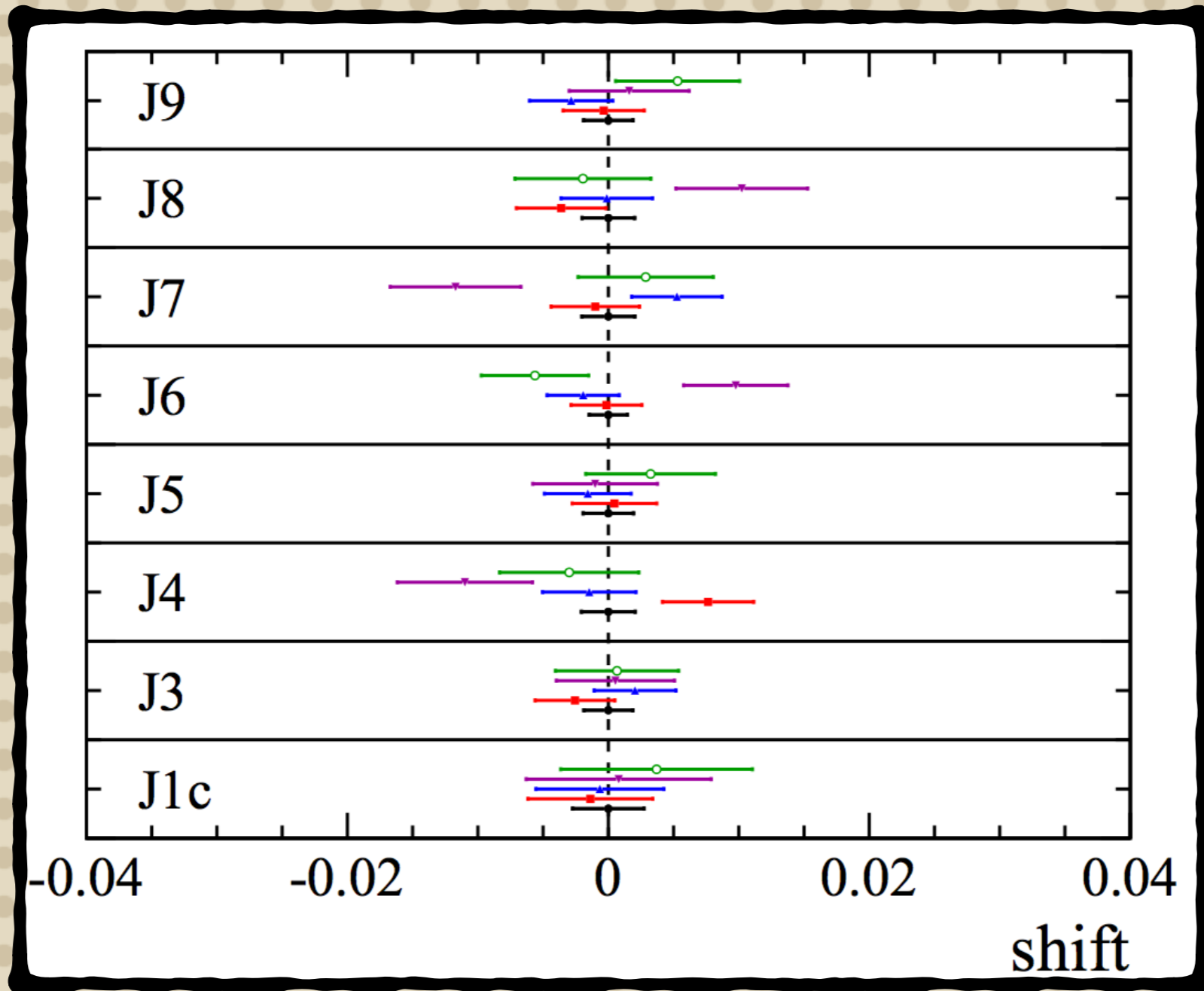


Magnet Polarity



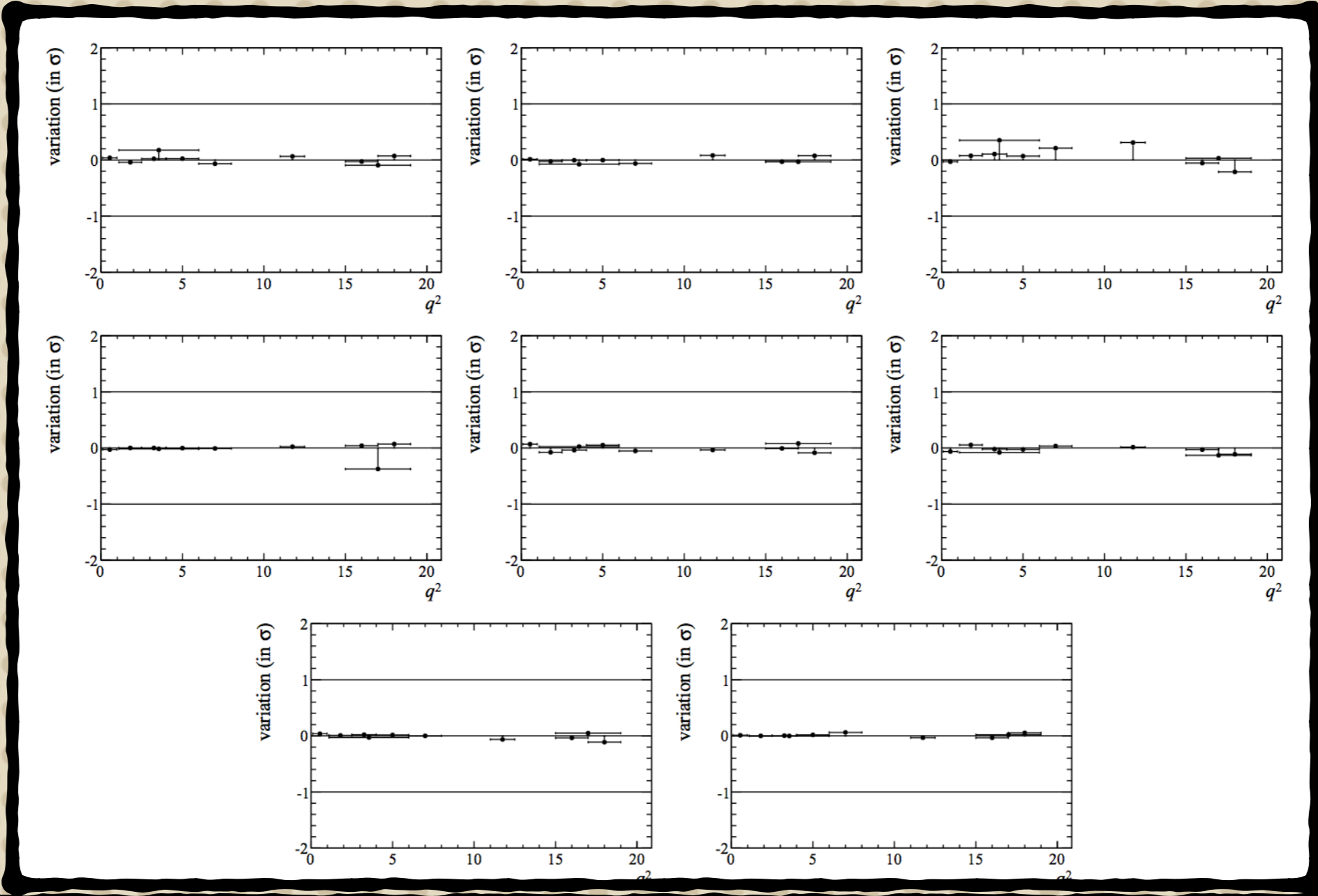
- We split the samples for two different magnet polarities and look at the statistical compatibility of the observables in the two samples
- Same cross check done for other detector variables (e.g. azimuthal angle, B momentum, ...)

Cross check with control channel

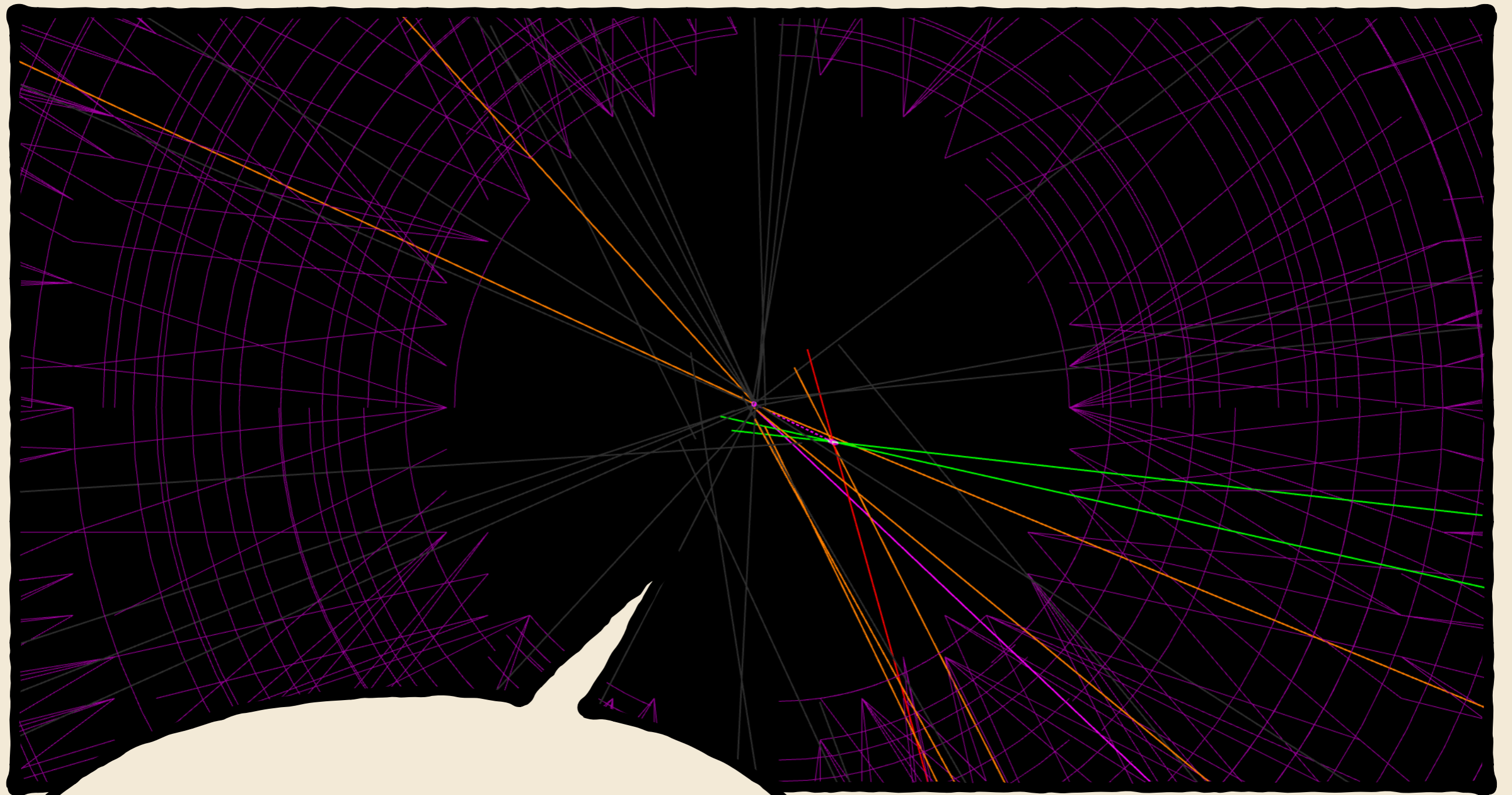


B^0 2012 only, \bar{B}^0 2012 only, B^0 2011 only, \bar{B}^0 2011 only

Check using higher order acceptance



- Increased the order of the polynomial used for the acceptance and looked at the difference
- Systematic uncertainty evaluated with high statistics toys



**S wave
contribution**

S-wave

- The decay $B^0 \rightarrow K\pi\mu^+\mu^-$, where the $K\pi$ system is in a spin 0 configuration (S-wave) has a different angular distribution from the signal (P-wave state)
- This comes mainly from the left tail of the resonance $K^{*0}(1430)$

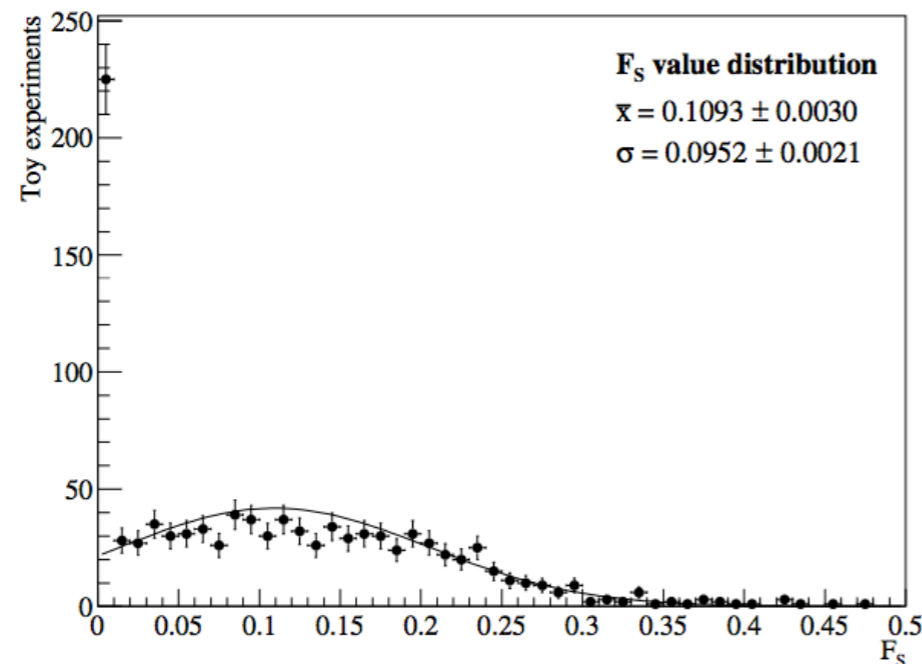
$$\frac{1}{d(\Gamma + \bar{\Gamma})/dq^2} \frac{d(\Gamma + \bar{\Gamma})}{d\cos\theta_\ell d\cos\theta_K d\phi} \Big|_{S+P} = (1 - F_S) \frac{1}{d(\Gamma + \bar{\Gamma})/dq^2} \frac{d(\Gamma + \bar{\Gamma})}{d\cos\theta_\ell d\cos\theta_K d\phi} \Big|_P + \frac{3}{16\pi} [F_S \sin^2 \theta_\ell + S_{S1} \sin^2 \theta_\ell \cos \theta_K + S_{S2} \sin 2\theta_\ell \sin \theta_K \cos \phi + S_{S3} \sin \theta_\ell \sin \theta_K \cos \phi + S_{S4} \sin \theta_\ell \sin \theta_K \sin \phi + S_{S5} \sin 2\theta_\ell \sin \theta_K \sin \phi].$$

- Additional parameters:
 - F_S : S-wave fraction
 - S_{Si} are the interference terms between the amplitude A_{00} and the P-wave amplitudes
- S_{si} are nuisance parameters
- F_s dilutes the P-wave observables

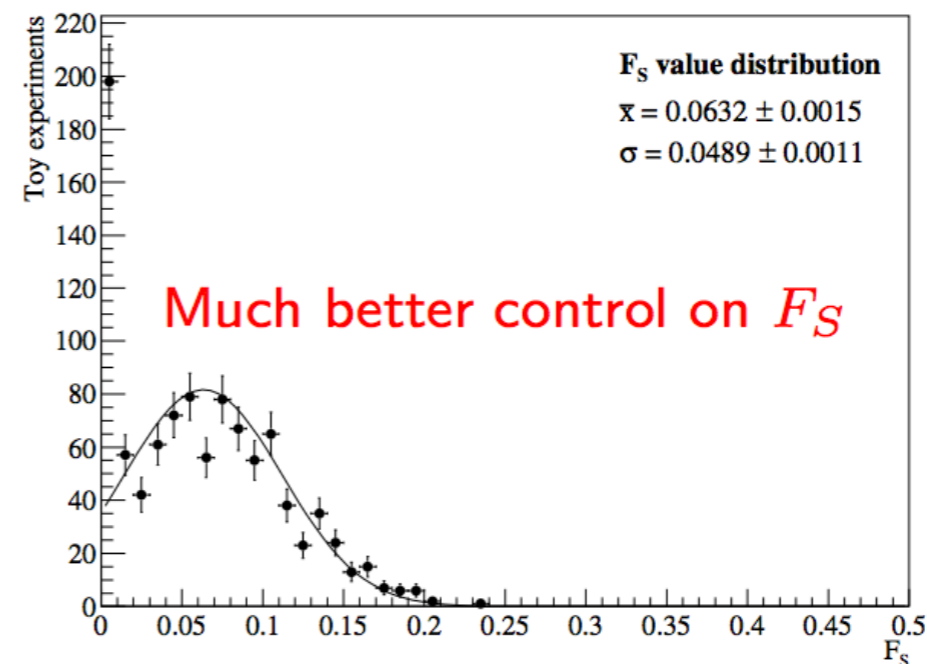
S-wave

- 4D+1 fit gives an improved sensitivity
 - The $m(K\pi)$ mass is fit simultaneously
 - Shared parameters F_S and the fraction of background from the sidebands of the B-mass
- Relativistic BW for the P-wave
- LASS $m(K\pi)$ model for the S-wave
- linear shape for the background

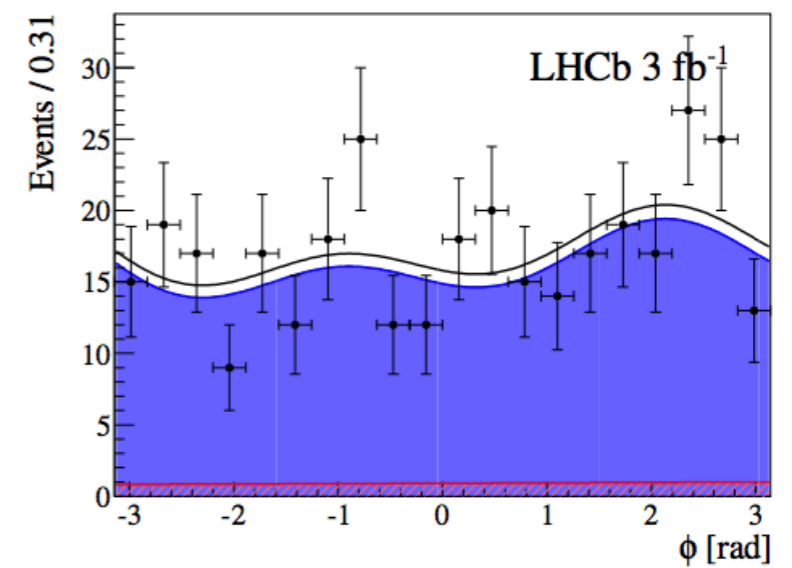
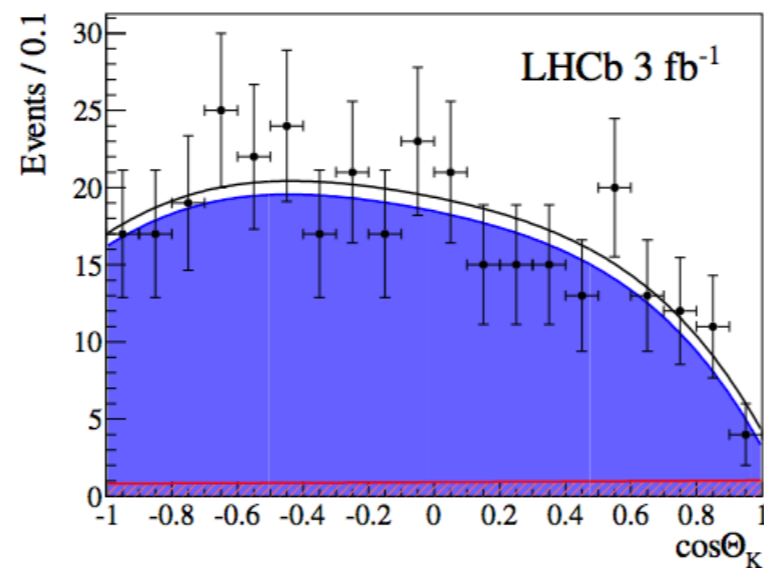
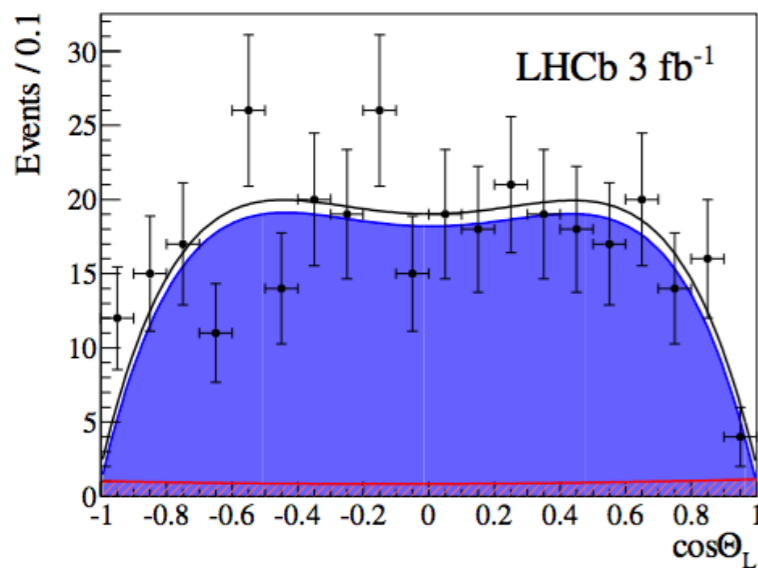
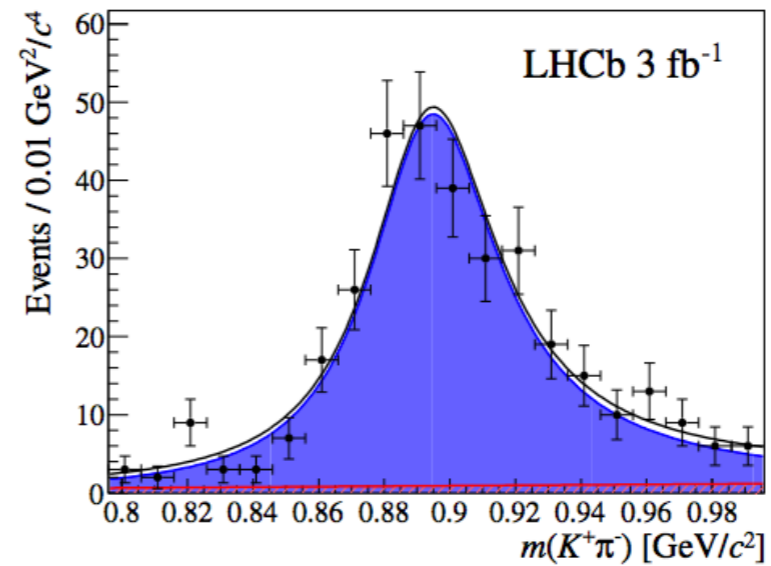
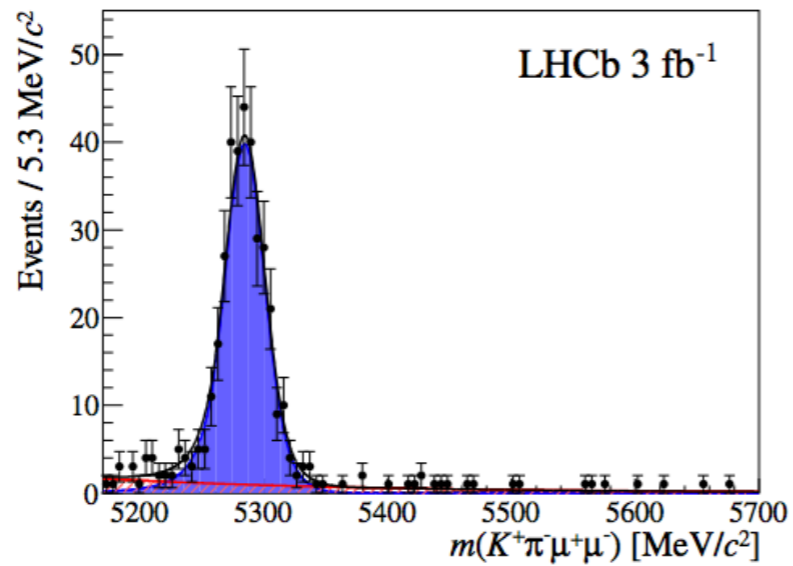
4D fit



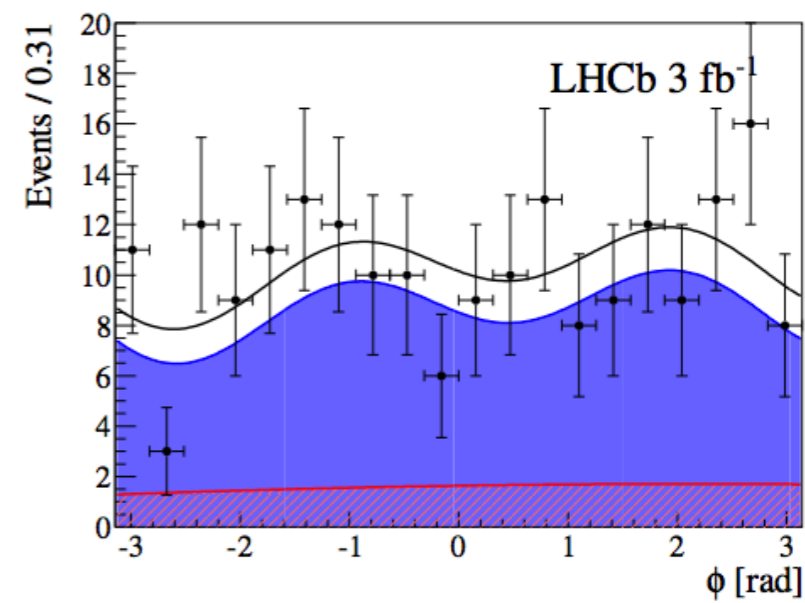
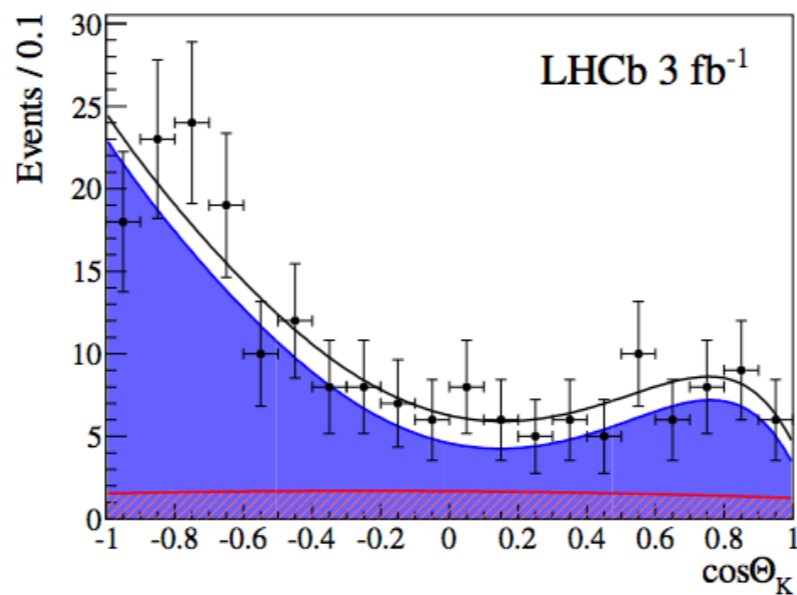
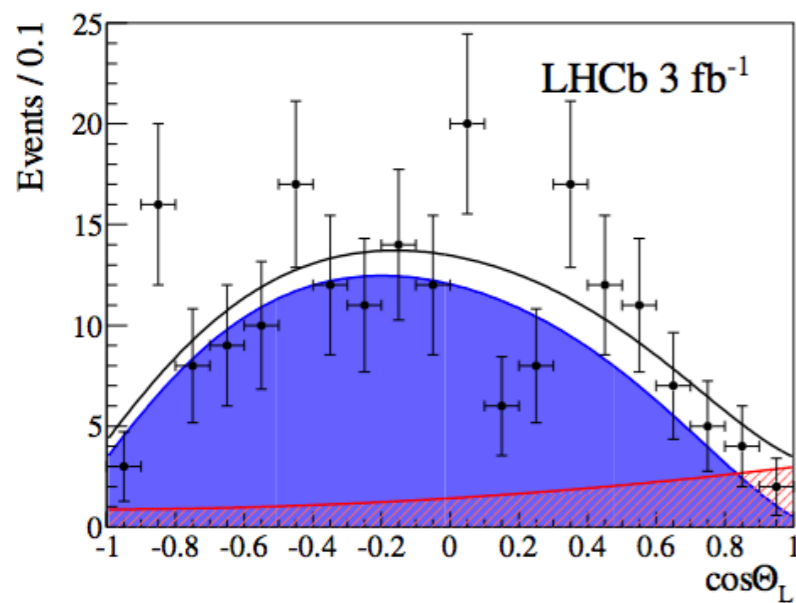
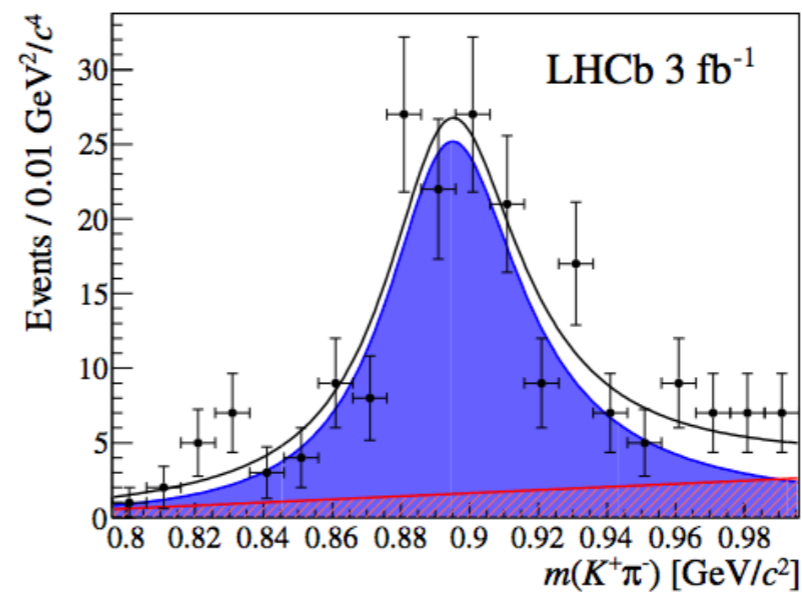
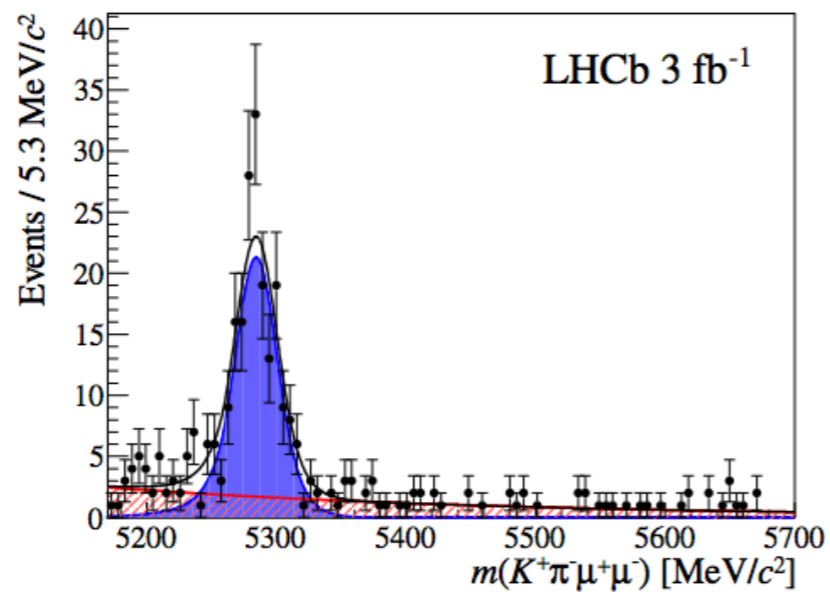
4D+1D fit



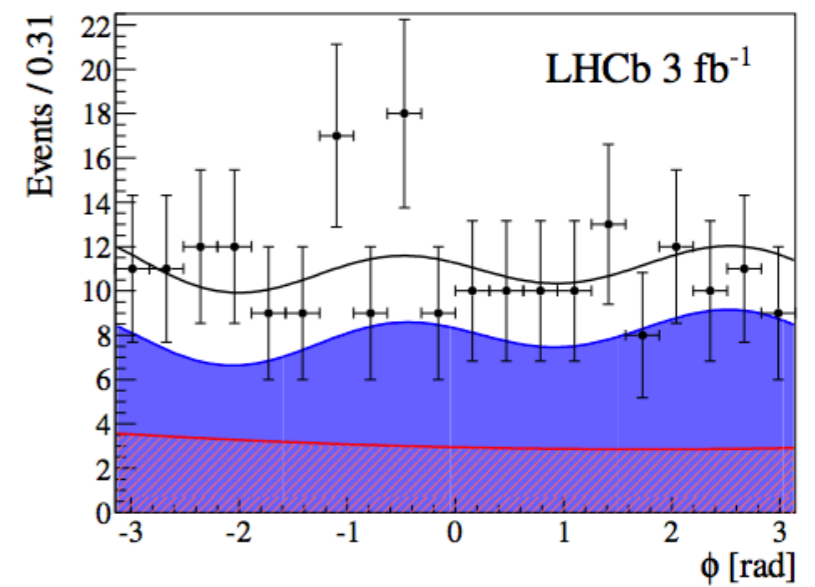
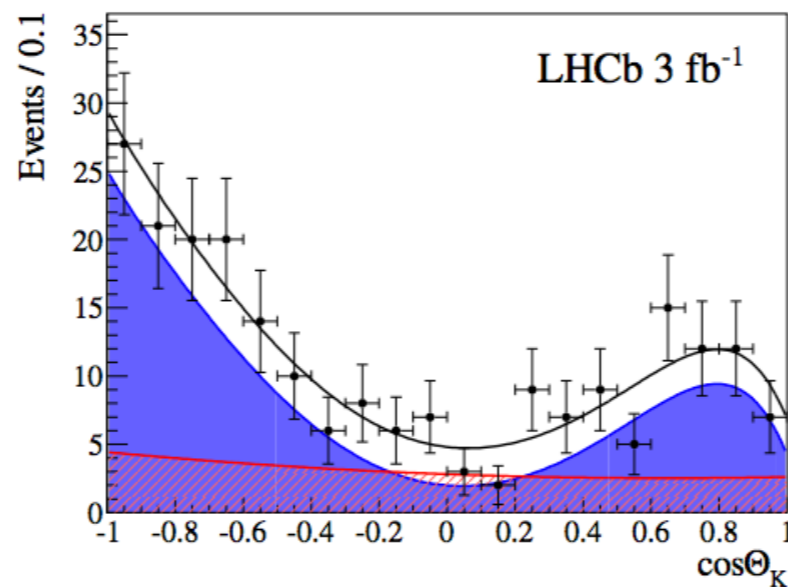
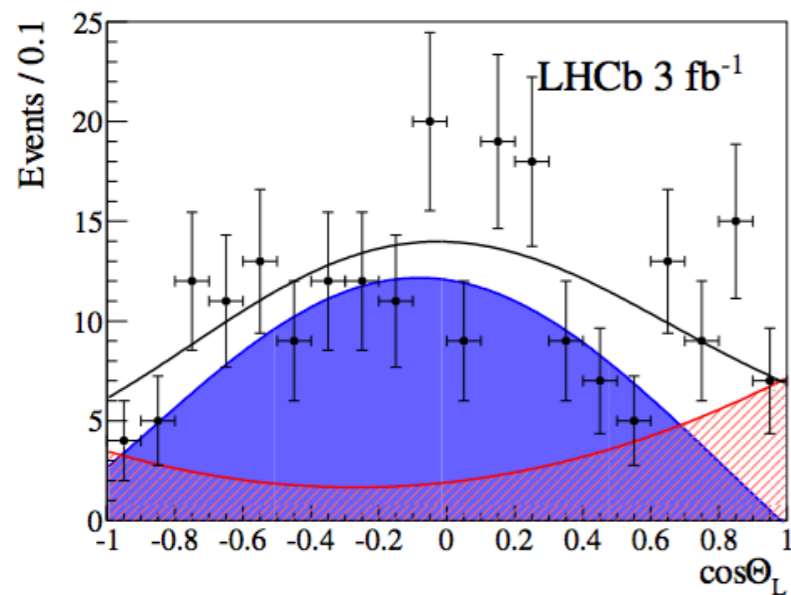
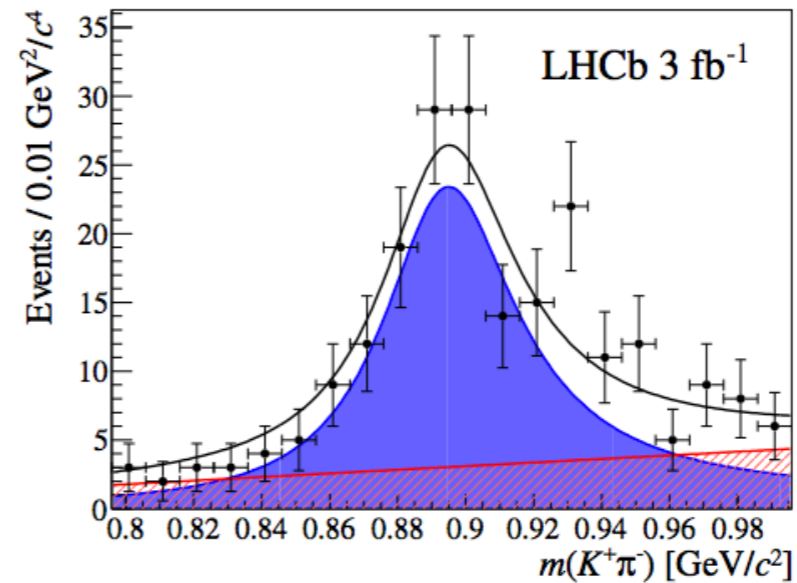
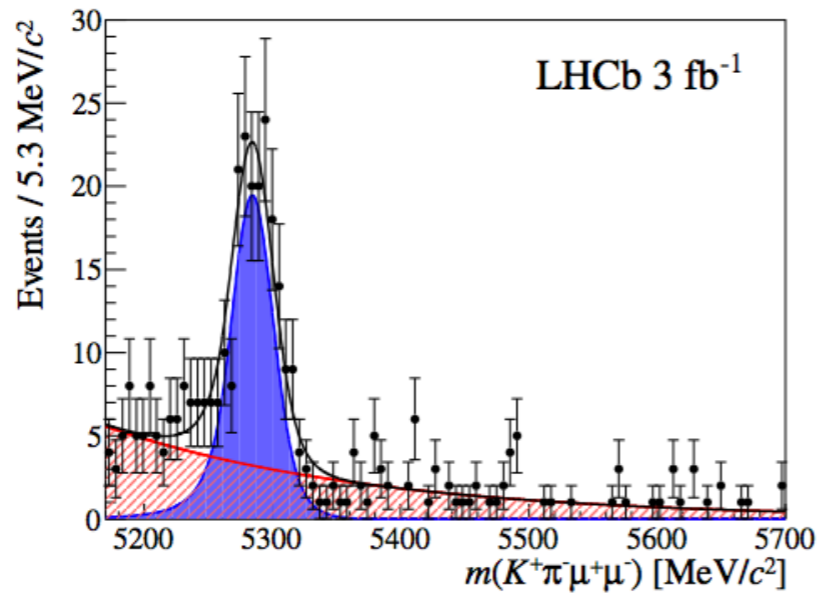
$$0.1 < q^2 < 0.98 \text{ GeV}^2/c^4$$



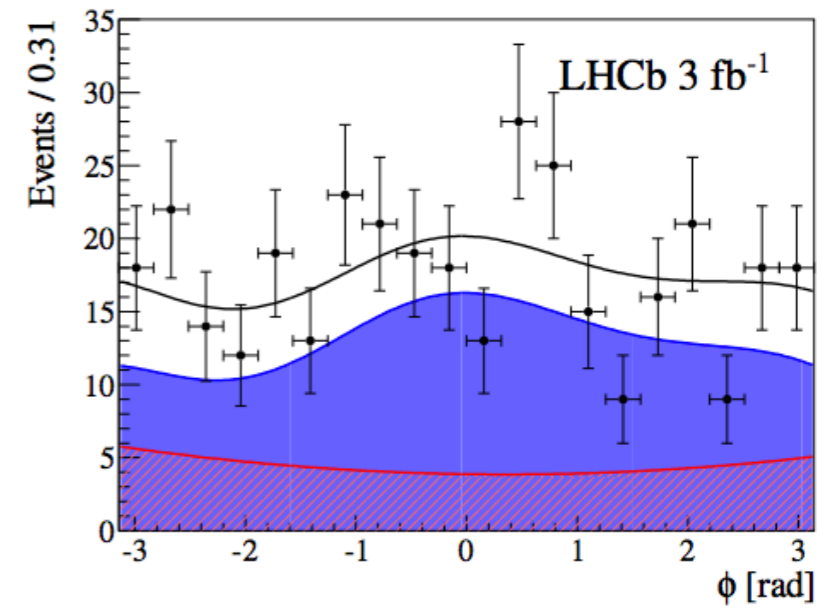
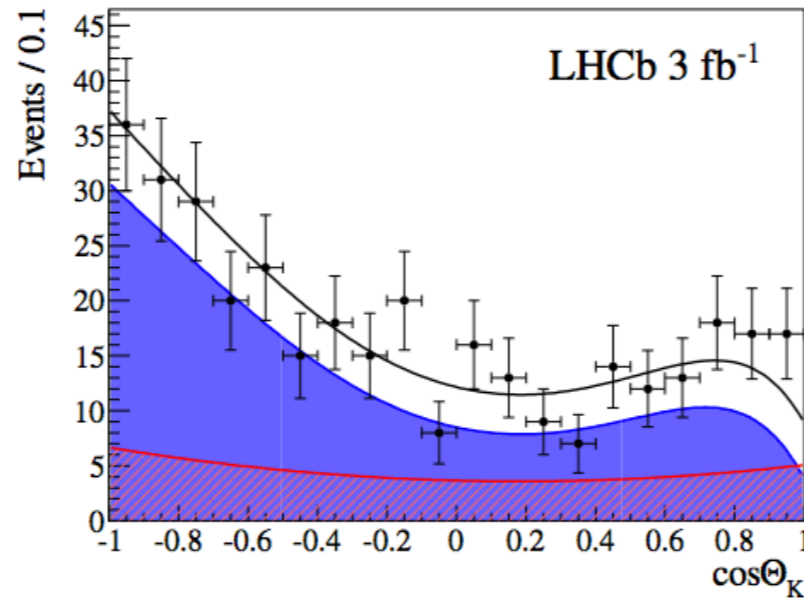
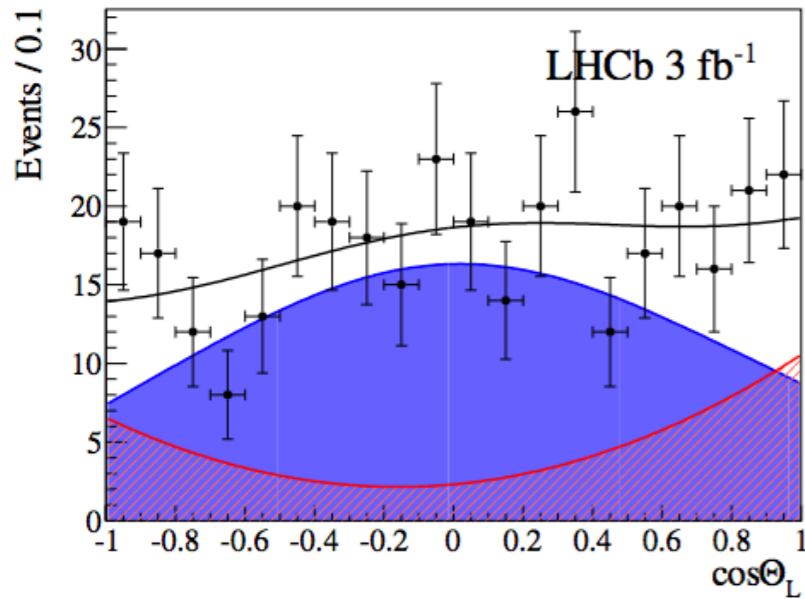
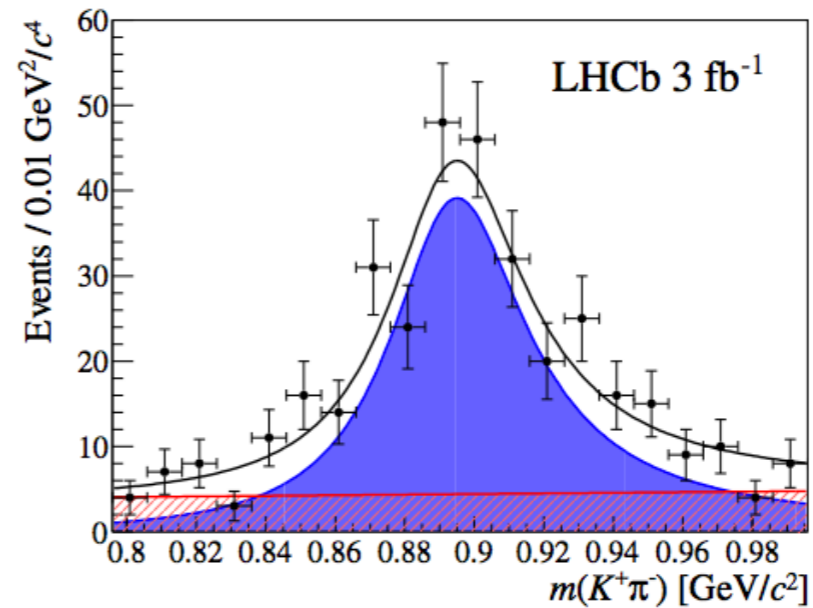
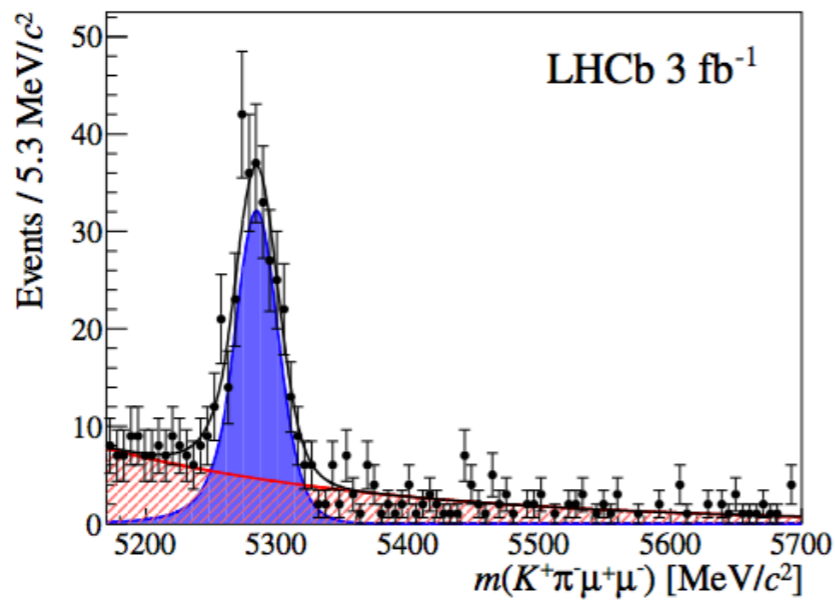
$$1.1 < q^2 < 2.5 \text{ GeV}^2/c^4$$



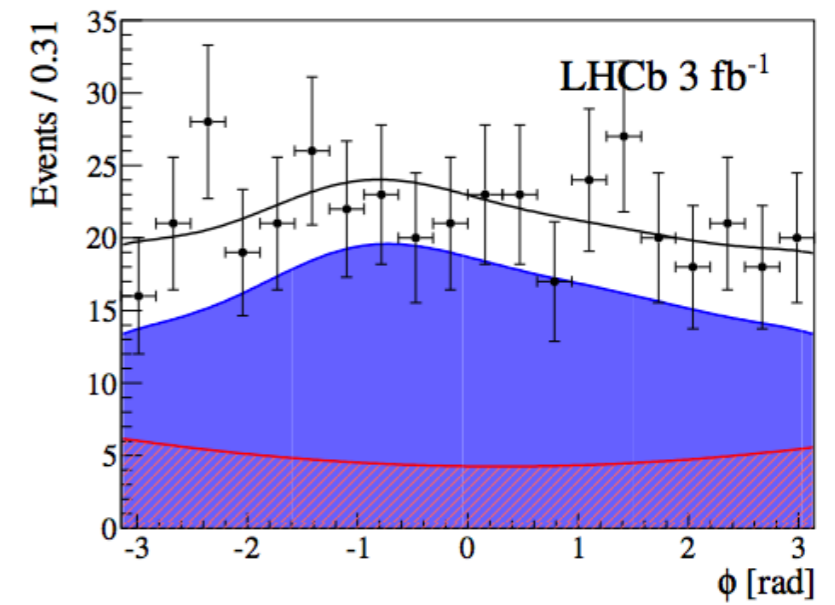
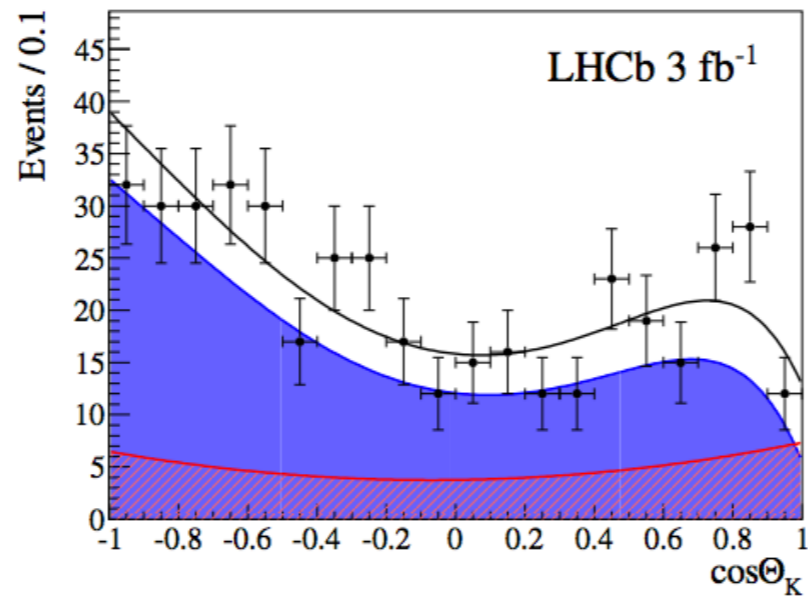
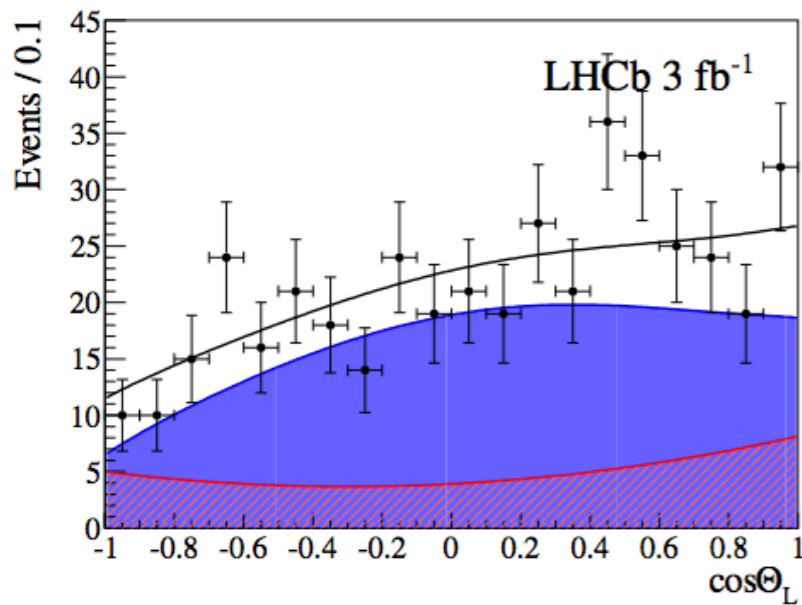
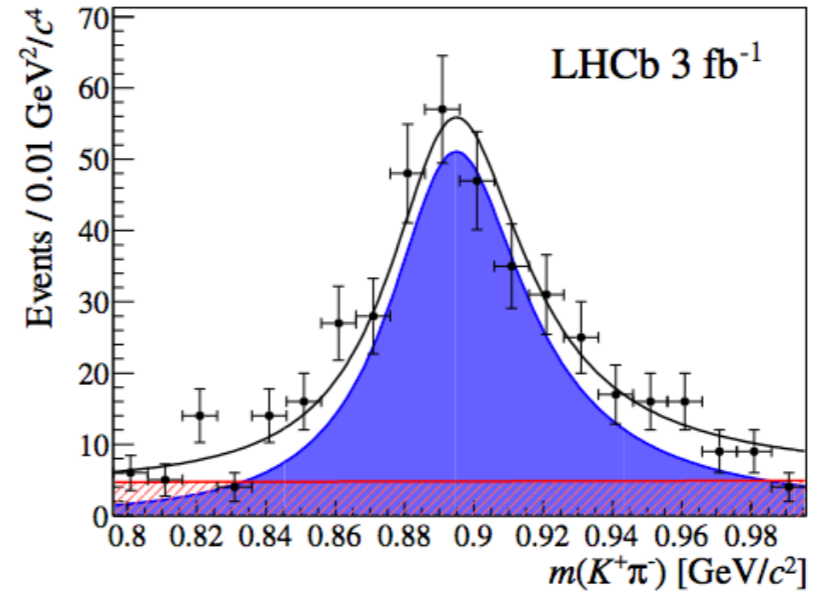
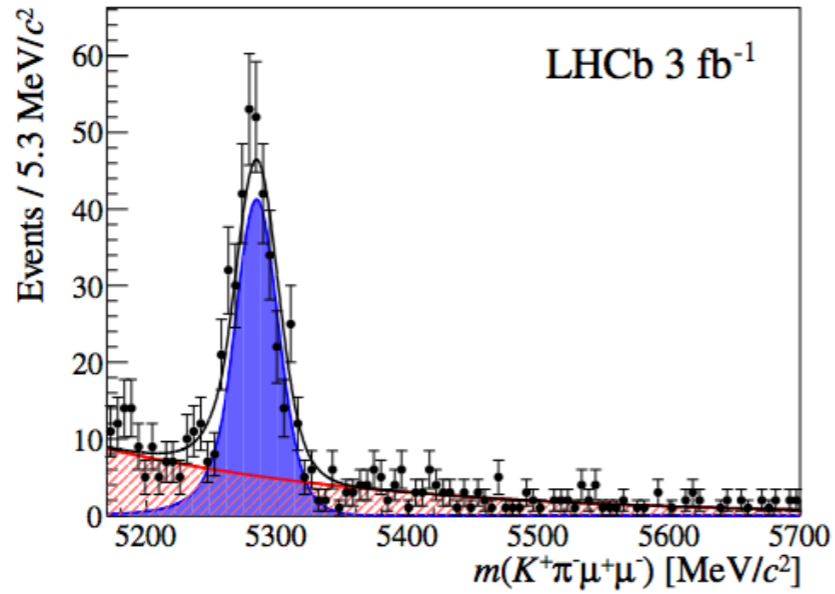
$2.5 < q^2 < 4.0 \text{ GeV}^2/c^4$



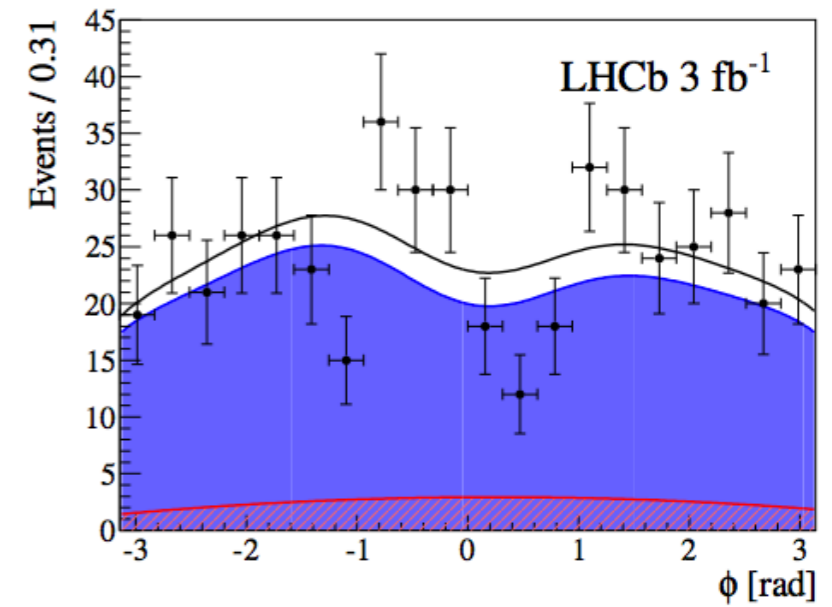
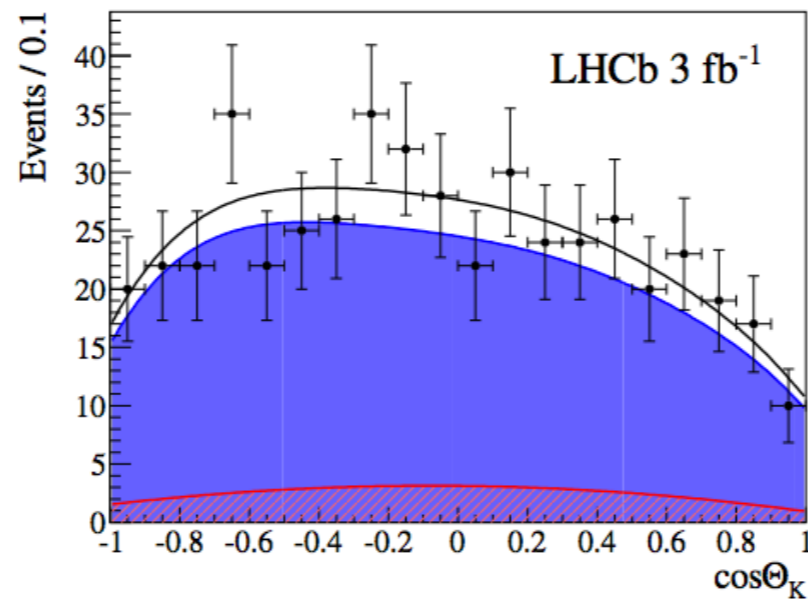
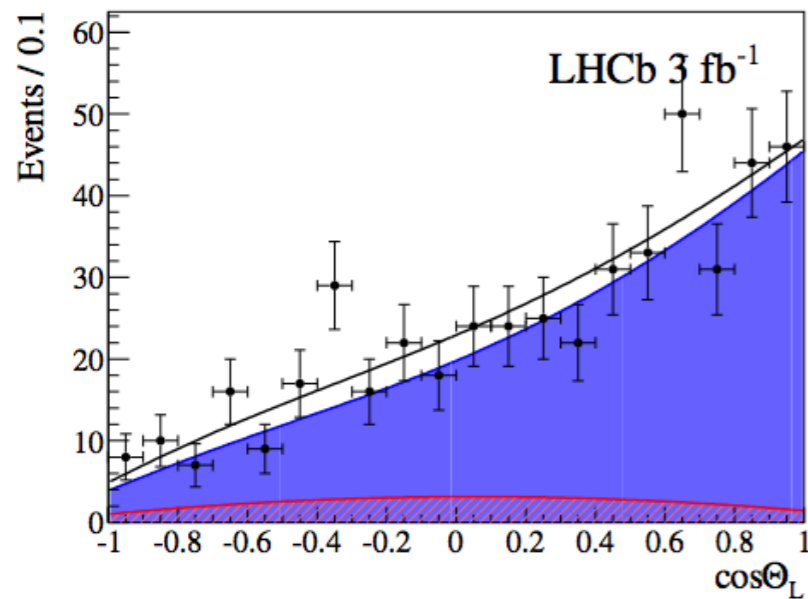
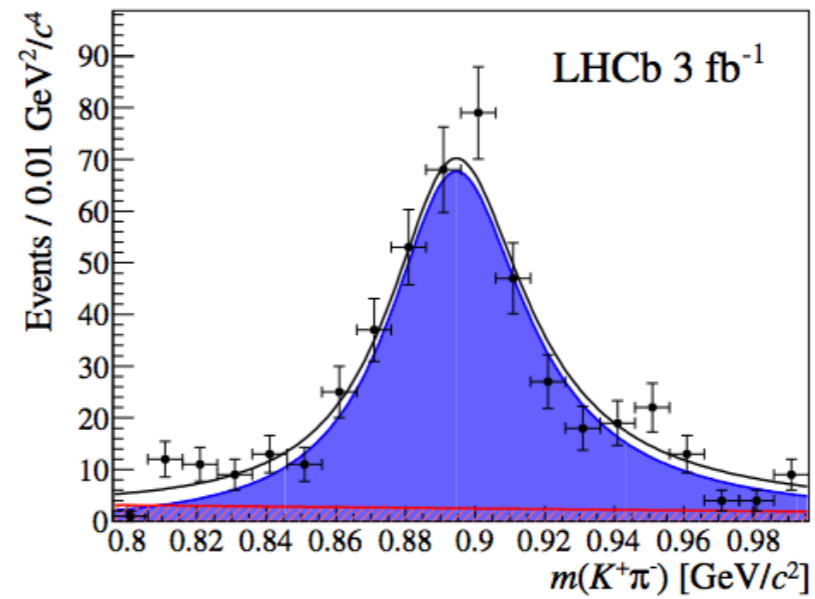
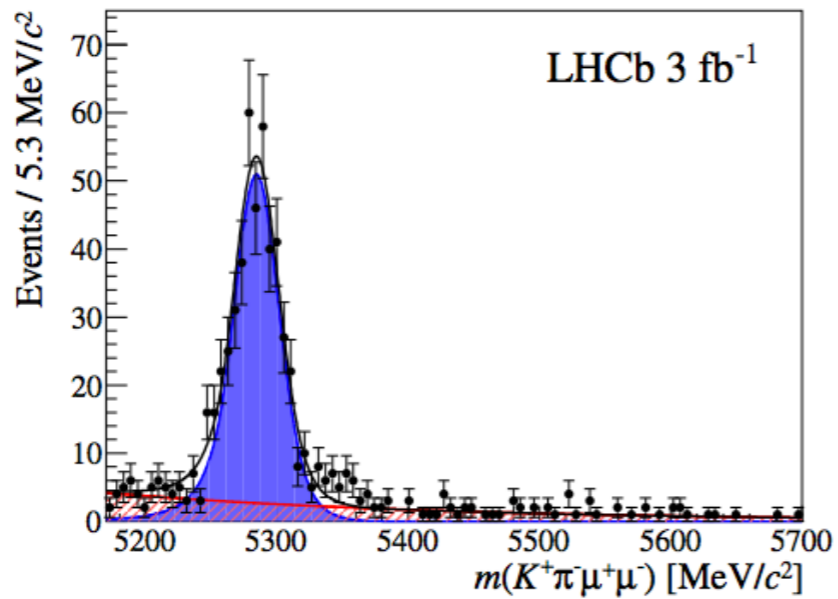
$4.0 < q^2 < 6.0 \text{ GeV}^2/c^4$



$6.0 < q^2 < 8.0 \text{ GeV}^2/c^4$



$11.0 < q^2 < 12.5 \text{ GeV}^2/c^4$



$$15.0 < q^2 < 19.0 \text{ GeV}^2/c^4$$

